THE CONCENTRATION AND DISTRIBUTION OF TRACE ELEMENTS IN OTOLITHS COLLECTED FROM FISH FROM EDEN LAKE, NORTHERN MANITOBA: A LINK BETWEEN THE LACUSTRINE FAUNA AND REGIONAL GEOCHEMISTRY

By

KAREN H. MATHERS

A Thesis
Submitted to the Faculty of Graduate Studies
in Partial Fulfillment of the Requirements
for the Degree of

MASTER OF SCIENCE

Department of Geological Sciences
University of Manitoba
Winnipeg, Manitoba

National Library of Canada
Acquisitions and Bibliographic Services
395 Wellington Street
Ottawa ON K1A 0N4
Canada

Bibliothèque nationale du Canada
Acquisitions et services bibliographiques
395, rue Wellington
Ottawa ON K1A 0N4
Canada

Your file Votre référence

Our file Notre référence

0-612-45093-7

Canada

THE UNIVERSITY OF MANITOBA

FACULTY OF GRADUATE STUDIES

*****

COPYRIGHT PERMISSION PAGE

The Concentration and Distribution of Trace Elements in Otoliths Collected from Fish from Eden Lake, Northern Manitoba: A Link between the Lacustrine Fauna and Regional Geochemistry

BY

Karen H. Mathers

A Thesis/Practicum submitted to the Faculty of Graduate Studies of The University of Manitoba in partial fulfillment of the requirements of the degree of

Master of Science

Abstract

This work is a baseline study of the relationship between the fish fauna at Eden Lake and the surrounding rocks. A broad suite of trace elements is incorporated into the otoliths of fish in their natural habitat where the only source of these trace elements is the local geology.

Otoliths are calcified structures found in the inner ear of teleost fish and are composed of alternating layers of aragonite and protein. The layers are thought to be deposited annually as the otoliths and fish grow and are not resorbed, thereby containing a complete chemical record of the fish's environment throughout its life.

Eden Lake is underlain by the Eden Lake Complex. The Eden Lake Complex is a monzonitic intrusion associated with pegmatite veins containing rare element-bearing minerals such as britholite, allanite and titanite. These minerals show distinct textures suggesting trace elements are being leached and liberated to the environment. Radiometric and biogeochemical surveys of the Eden Lake area have detected a surplus of trace element abundances in the lake and vegetation.

REE and other trace elements, such as Sr, Zn, Mn, Fe, Ba, U, Th and F can all substitute in carbonate minerals and many of these elements have been detected in otoliths taken from different species of Eden Lake fish. Cathodoluminescence microscopy found both yellow-green luminescence and red luminescence within the otoliths. The luminescence observed shows a complex zoned distribution of trace elements that corresponds with the annular structure of the otoliths.

A combination of LAM-ICP-MS, PIXE, SPM and image analysis determined the concentrations (in ppm) and distribution of the trace elements across the otoliths of different species. No trends appear to exist between the element concentrations detected in each species and their capture location; the elements detected and their concentrations within each species appear to be a regional signature, and are not strictly related to proximity to the Complex. The luminescence is attributed to the fluctuating Mn concentrations in the otoliths, which was likely incorporated dominantly through diet. Fluctuating Zn concentrations are also attributed to diet. The Sr concentrations detected within the otolith, which were consistently high in the majority of the fish, are attributed to a constant input from the local geology.

Acknowledgements

The author would like to acknowledge Dr. N. M. Halden of the University of Manitoba for all his enthusiasm and guidance during all aspects of this project. The author would further like to extend her enormous appreciation to John Babaluk of the Department of Fisheries and Oceans and Sergio Mejia of the University of Manitoba for all of their instruction during sample collection and preparation and sample analysis, respectively.

A special thank-you also goes to my husband Rob, my family and friends, and the staff at Tetr*ES* Consultants Inc. (particularly Mike McKernan, Don Harron and Mike Sweet) for all their patience, input, support, and encouragement.

Finally, the author thanks all the sport fishermen who took an interest in the project and contributed the heads of their catch to the sample set.

Table of Contents

List of Tables

List of Figures

List of Appendices

Chapter 1: Introduction

Otoliths are hard, stone-like, non-bony structures that are located in the inner ear and form part of the organs which sense position and motion in teleost or bony fish (Seyama et al., 1991). They are composed of alternating layers of calcium carbonate, in the aragonite crystal form, and protein, similar in composition to keratin (Degens et al., 1969). There are three pairs of otoliths present in the fish: the sagittae, the asteriscus, and the lapillus, of which the sagittae, or sagittal otoliths, are the largest and therefore the ones most often used for analysis (Figure 1.1).

The mechanism of crystal growth in otoliths, particularly the sagittae, is very unusual amongst biomineralized tissues in that most of the otolith does not grow in direct contact with any cellular tissue (Dale, 1976). Otoliths are joined by a protein matrix, the otic membrane, to the cells of the macula, a nervous-end organ, along the sulcul groove of the otolith (Dunkelberger et al., 1980). The cells of the macula are the only apparent source of the proteins that constitute the otolith (Gauldie and Nelson, 1990a; 1990b). The calcium deposited in the otolith comes predominantly from the surrounding water, via the gills, to the endolymphatic sac (Simkiss, 1974), with only a small proportion attributed to dietary sources (Ichii and Mugiya, 1983). Consequently, the otolith is crystallized out of the fluids of the endolymphatic sac in response to changing calcium, protein, and pH-modulating ions generated in, or transmitted by, the macula. In spite of this unlikely arrangement, otolith growth is so well modulated as to retain species-specific shape (Gaemers, 1984).

Otoliths are only susceptible to dissolution and resorption under rare conditions of extreme stress (Mugiya and Uchimura, 1989) and, unlike other calcified structures (e.g. scales), this creates a mark on the otolith that is easily identified (Campana, 1983).

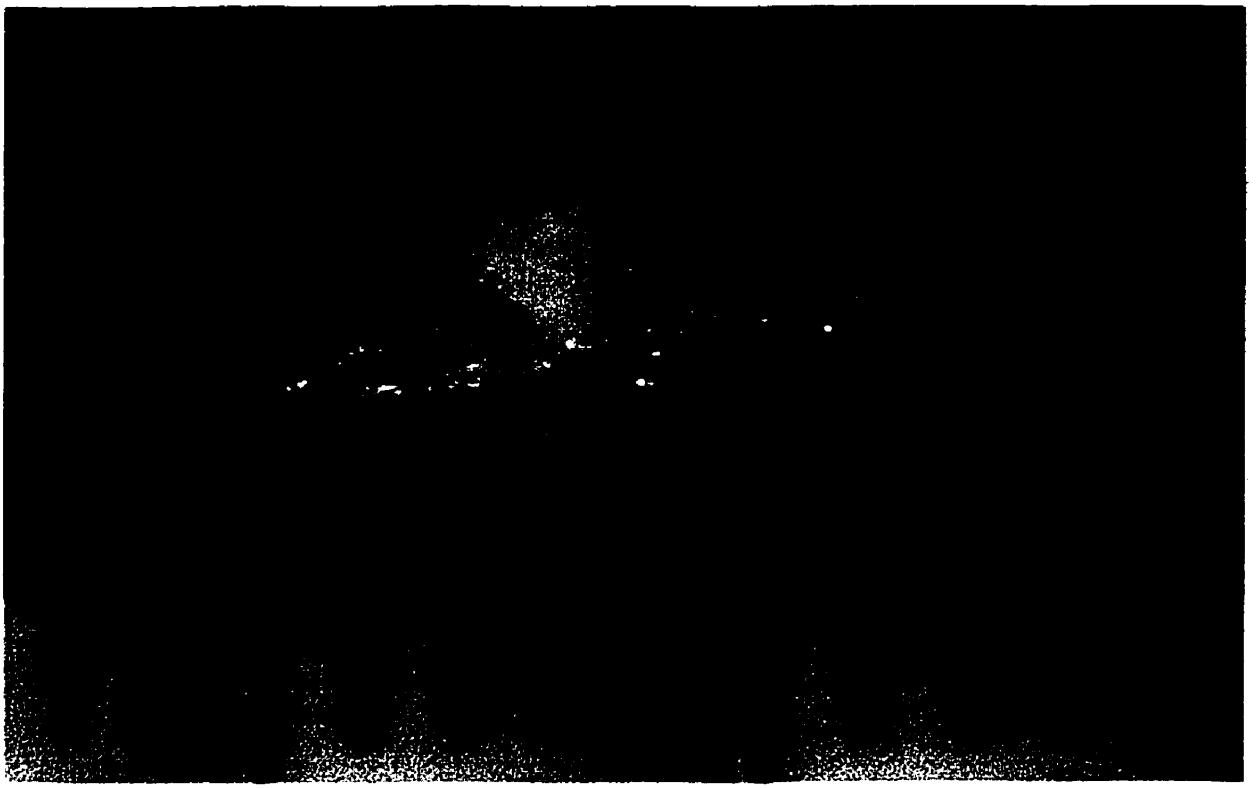

Figure 1.1. **Photograph of a sagittal otolith from a northern pike. Each of the black bars on the given scale represents one millimeter.**

Therefore, otoliths, more so than scales and other calcified structures, act as information storage structures from which important information about the life history of the fish can be accessed (Gauldie, West and Coote, 1993).

Previous studies have found that there are three types of information that can be obtained from the sagittal otoliths of teleost fish. First, the layers of aragonite and protein are thought to be deposited annually as the otoliths and fish grow and thereby may allow the age of the fish to be determined (Mugiya, 1964). Secondly, studies of the elemental composition of otoliths, like those of other calcareous tissues of biological origin, such as corals, may provide information about past environmental conditions (Radtke, 1989; Halden et al., 1995a). Thirdly, preliminary studies have suggested that the quantitative analysis of the microconstituents, or trace elements, can potentially provide information on population structure and movements (Mulligan et al., 1983; Halden et al., 1996; Babaluk et al., 1997).

1.1 Previous Studies

1.1.1 Fish Age

Fishes probably rank second only to humans in the amount of material published on their age (Gauldie, Coote, and West, 1993) mostly because new techniques are continually being developed to facilitate the estimation of age. Growth rings have been used to age fish for a long time (Jones, 1992). As long ago as 1759, annual rings in vertebrae were used to age eels (Hederstrom, 1959) while scales were first used to age fish in 1888 (Carlander, 1987). Otoliths have been used to age fish since Reibisch first observed annular ring formation in *Pleuronectes platessa* in 1899 (Ricker, 1975). The "annularity" of these rings has since been validated through studies of hatchery-reared fish. Counting annuli was not useful in estimating the age of young fish that have not formed their first annulus or for tropical or deep-sea adult fish whose growth is more

constant and annulus formation less certain (Jones, 1992). The daily increment technique, developed in the early 1970's, solved these problems by permitting the estimation of daily age. This technique has gained wide acceptance during the last twenty years, however, it should not replace the counting of annuli for older fish. Recently, it has also been suggested that fish can be aged through radiometric analysis (Fenton and Short, 1992).

The nucleus of an otolith is present at the beginning of larval life, and grows daily by the addition of layers to the outer surface (Seyama et al., 1991). In sections through an otolith there is usually visible evidence of periodicity in the formation of concentric layers on daily, annual, and sometimes intermediate time scales. Various hard parts of the fish that show periodic layering, including scales, bones, and fin-rays, have also been used in fish aging, however, according to Eggleston (1975) and Paul (1976) the scales of slow-growing fish do not contain full growth histories. Otoliths possess the advantage that they continue to thicken by the addition of layers to the medial surface even when the fish has ceased growing.

In some fish species the process of age-determination is straightforward, in others the layering is not clear and reading is somewhat subjective (Seyama et al., 1991). Pannella (1971) observed approximately 360 fine increments between the otolith annuli of temperate water adult fish (Figure 1.2). These increments were postulated to be daily changes in the microstructure of the otolith. Pannella (1974) observed what seemed to be daily increments in adult tropical fish and also observed that these patterns followed a larger, 14-day cycle that coincided with lunar behavior patterns. Within five years, Struhsaker and Uchiniyama (1976) validated the theory that the increments were being formed on a daily basis in a study on young Hawaiian nehu. By holding field-captured larvae and juveniles in the laboratory, the scientists developed growth curves and used this information to show growth rate differences between reef

Figure 1.2. Acetate replica of anterior growth patterns in *Merluccius bilinearis* (scale 100 um): (A) *S* - fast growth zone; *W* - slow growth zone; *t* - fortnightly patterns; *sy* - monthly patterns; and *Sp* - spawning zone (x125); (B) enlargement of part of (A), showing daily increments made of alternating densely-packed and sparsely-packed bands of organic fibres; *st* - 7 to 8 day patterns (x 400) (from Pannella, 1971).

areas. Conversely, Taubert and Coble (1977) applied the technique to freshwater fish and found that shortened day length and low temperatures resulted in the apparent cessation of daily increment formation in sunfishes. Further problems arose when researchers routinely started applying this technique to aging older adult fish because the allometric growth of otoliths results in a crowding of annuli on the edge (Beamish and McFarlane, 1987). Therefore, it has been concluded that, even though Pannella (1971;1974) began using the daily increment technique to define the age of adult fish, daily growth increments are of little use in aging older fish or in solving interpretation problems in adults and should be reserved only for establishing the age of young fish (Jones, 1992). Otoliths from older fish, which are much thicker than those from young fish, are best examined in cross section so that the thickened area containing the prominent pattern of growth zones is visible. Only the annular growth rings should be counted in adult fish to define an accurate age.

Trace amounts of radioactive radium and lead, ^{226}Ra and ^{210}Pb, have recently been used in estimating age from the ^{226}Ra: ^{210}Pb disequilibrium (Fenton et al., 1991). However, this method relies entirely on the assumption that the radioactive radon, ^{222}Rn, produced as the intermediate decay product between the radium and lead isotopes fails to diffuse out of the otolith. It has been argued by Gauldie and West (1992) that degassing of radon is unavoidable and that the ^{226}Ra: ^{210}Pb levels in the otolith are probably also driven by the well-known secular equilibrium of ^{226}Ra: ^{210}Pb levels in bottom sediments; thereby proving this method ineffective for fish aging.

1.1.2 Environmental Indicators

Trace elements, such as strontium (Sr), which are chemically similar to calcium

(Ca) are incorporated into the otoliths as they grow (Radtke and Targett, 1984). On average, seawater contains 8 ppm Sr while freshwater contains 0.1 ppm Sr (Rosenthal et al., 1970). Sr incorporation in biogenic carbonates, such as fish otoliths, in general, is related to the Sr content of the water in which they live (Odum, 1951). Therefore, variations in otolith Sr, and Sr/Ca ratios, are of special interest because of their potential usefulness as indicators of past environmental conditions. Sr/Ca ratios have been used to assess seasonal variations in water temperature (Kalish, 1989; Townsend et al., 1992). Sr variations have also been related to growth rate (Sadovy and Severin, 1994) and sample roughness (Arai and Sakamoto, 1993). However, before Sr/Ca or any other ratio in otoliths can be used definitively as an environmental indicator, the relationship of these ratios to water temperature, growth rate, etc. must be determined. There are currently many conflicting views.

Studies on juvenile Australian salmon by Kalish (1989) concluded that temperature plays a very minor role, if any, in the determination of Sr/Ca, Na/Ca and K/Ca ratios in fish otoliths. Townsend et al. (1992) concur with Kalish (1989) that at high temperatures (13 to 20^{0}C) measurable changes in Sr/Ca as a function of temperature become more difficult to detect. However, Townsend et al. (1992) also concluded from their study that at lower temperatures (mainly below 5 or 6^{0}C), where those physiological processes become slowed or impaired, strontium passes more readily into the endolymph and becomes incorporated into the otolith aragonite (Figure 1.3).

According to Sadovy and Severin (1994), the patterns of strontium abundance and Sr/Ca ratios across sectioned otoliths of wild red hind support the hypothesis that a simple inverse relationship exists between Sr/Ca ratios and the log of body growth rate (Figure 1.4). They also suggest that this Sr/Ca - growth rate relationship is a consistent alternative explanation for all published experimental results on Sr/Ca ratios in fish

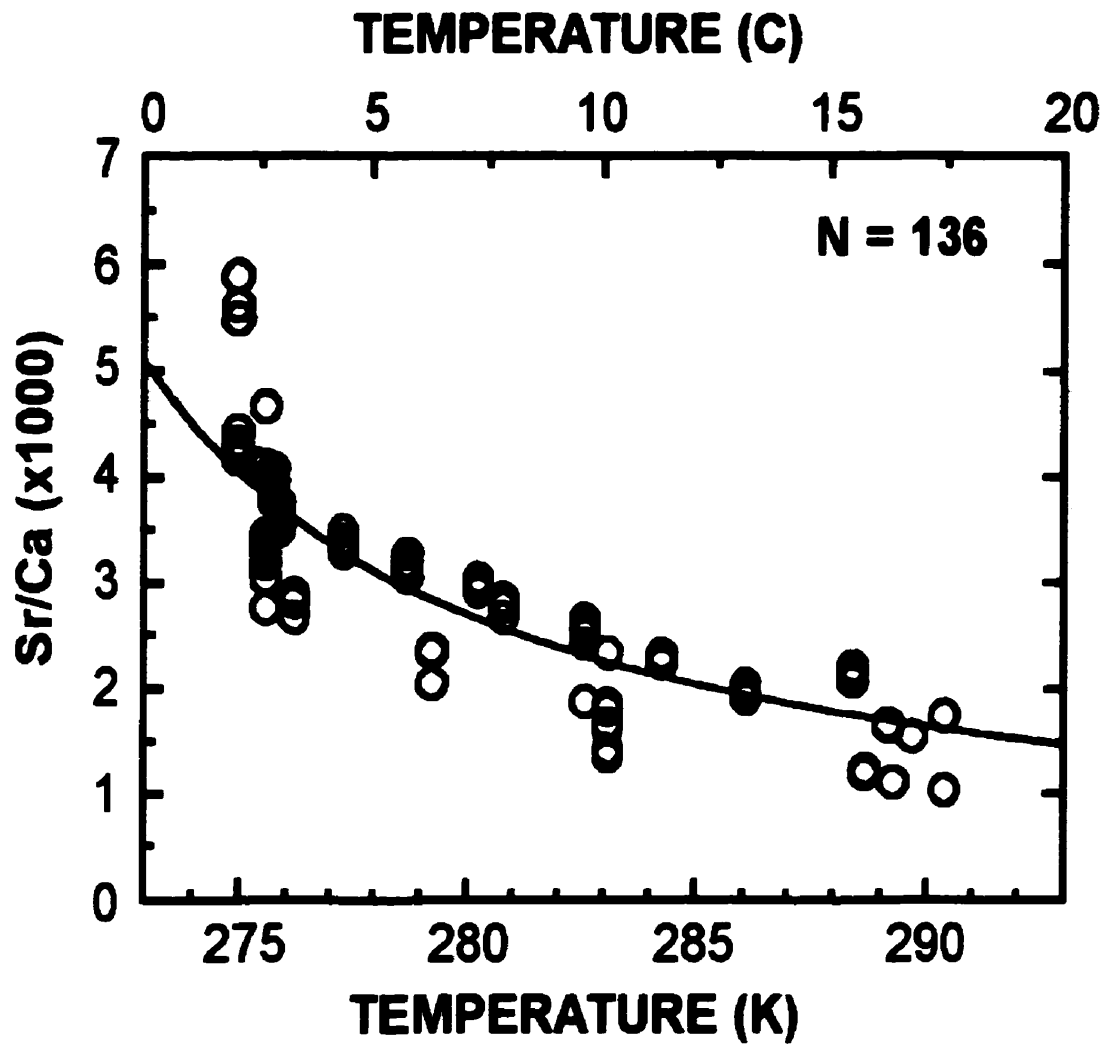

Figure 1.3. Plot of Sr/Ca ratios of samples of outermost edges of otoliths of 136 juvenile Atlantic herring from holding experiment as a function of the average temperature (in degrees Kelvin and degrees Celsius) of experimental tanks. At lower temperatures, Sr passes more readily into the endolymph and becomes incorporated into the otolith aragonite because the fish's physiological processes are slowed or impaired (from Townsend et al., 1992).

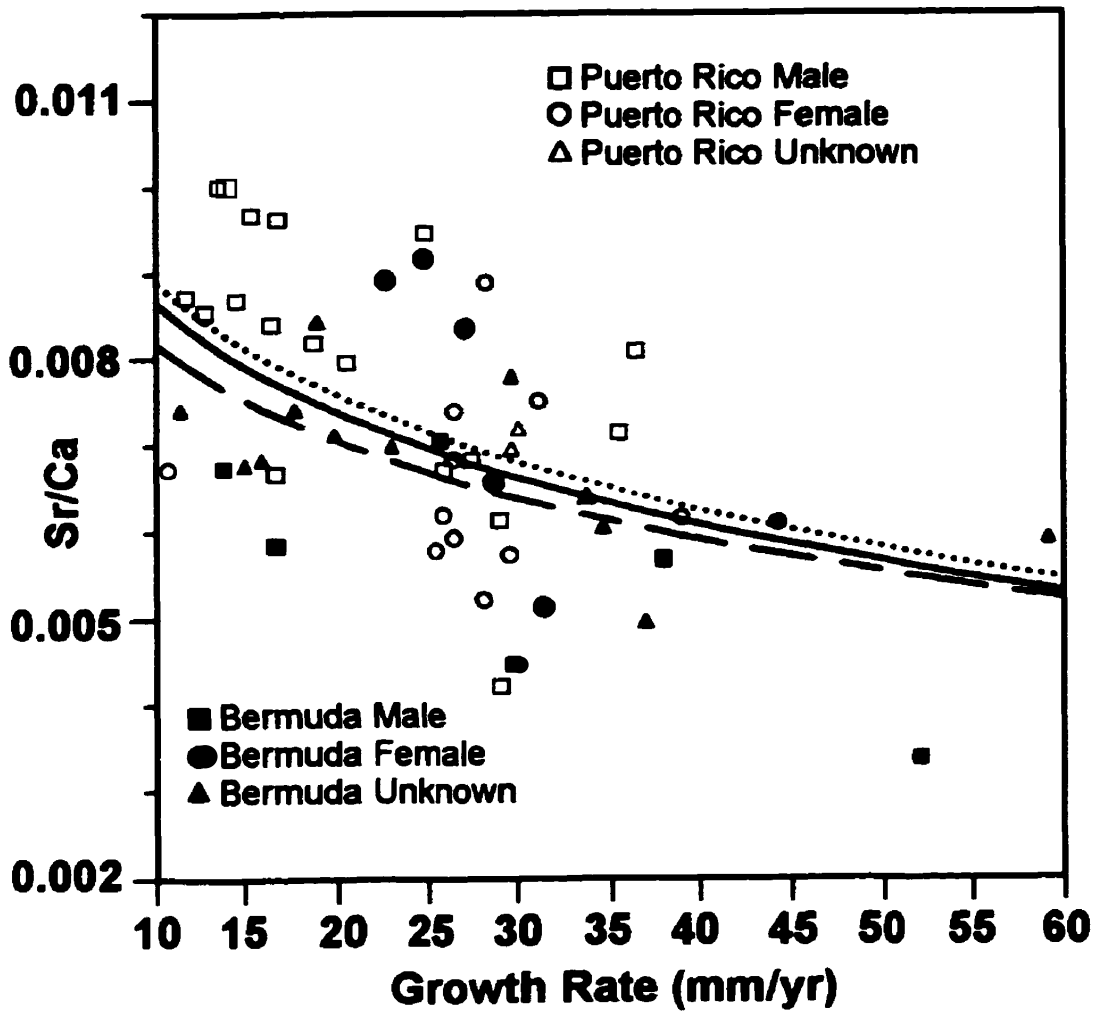

Figure 1.4. Growth rate versus Sr/Ca ratios. The solid line is the regression based on data from Puerto Rico and Bermuda fish combined, the dotted line is based on data from Puerto Rico fish only, and the broken line is based on data from Bermuda fish only. The figured regressions describe the data equally well and suggest a significant relationship between log growth rate and Sr/Ca ratios (from Sadovy and Severin, 1994).

otoliths for which a temperature relationship has been proposed (e.g. Kalish, 1989; Townsend et al., 1992).

Arai and Sakamoto (1993) applied proton-induced X-ray emission (PIXE) to uncut and unpolished red sea bream otoliths. They found that the Sr/Ca ratios determined by the X-rays' yields) in the older fish did not correlate consistently with the measured sea water temperature (Figure 1.5) due to sample roughness. The youngest otoliths, such as sample M5930629, are so small that the proton beam (100 μm x 16 μm) can irradiate the large portion of the otoliths surface and the effect of topographies may be negligible. However, the area of detection is comparably small in the older, larger otoliths and, therefore, rough topography of the surface is not negligible in these otoliths.

The scattering of diffracted X-rays will change depending on whether the irradiated beam area is rough or smooth, thereby affecting the Sr/Ca ratios. Arai and Sakamoto (1993) used a larger beam (3 mm x 5 mm) on the older, larger otoliths and found that this removed the Sr/Ca ratio errors produced by sample roughness. Furthermore, their new results indicate an inverse relationship between Sr/Ca ratio and temperature (Figure 1.6).

1.1.3 Population Structure

The ability to identify fish stocks and their movements is of critical importance because, in theory, each must be managed separately to optimize its yield and prevent any sharp decline in numbers (Mulligan et al., 1987). Traditional methods used to identify fish stocks and their movements included tagging experiments, meristic and morphometric indices, and electrophoretic techniques. However, it is now known that genetic differences between populations or differences in the environments to which

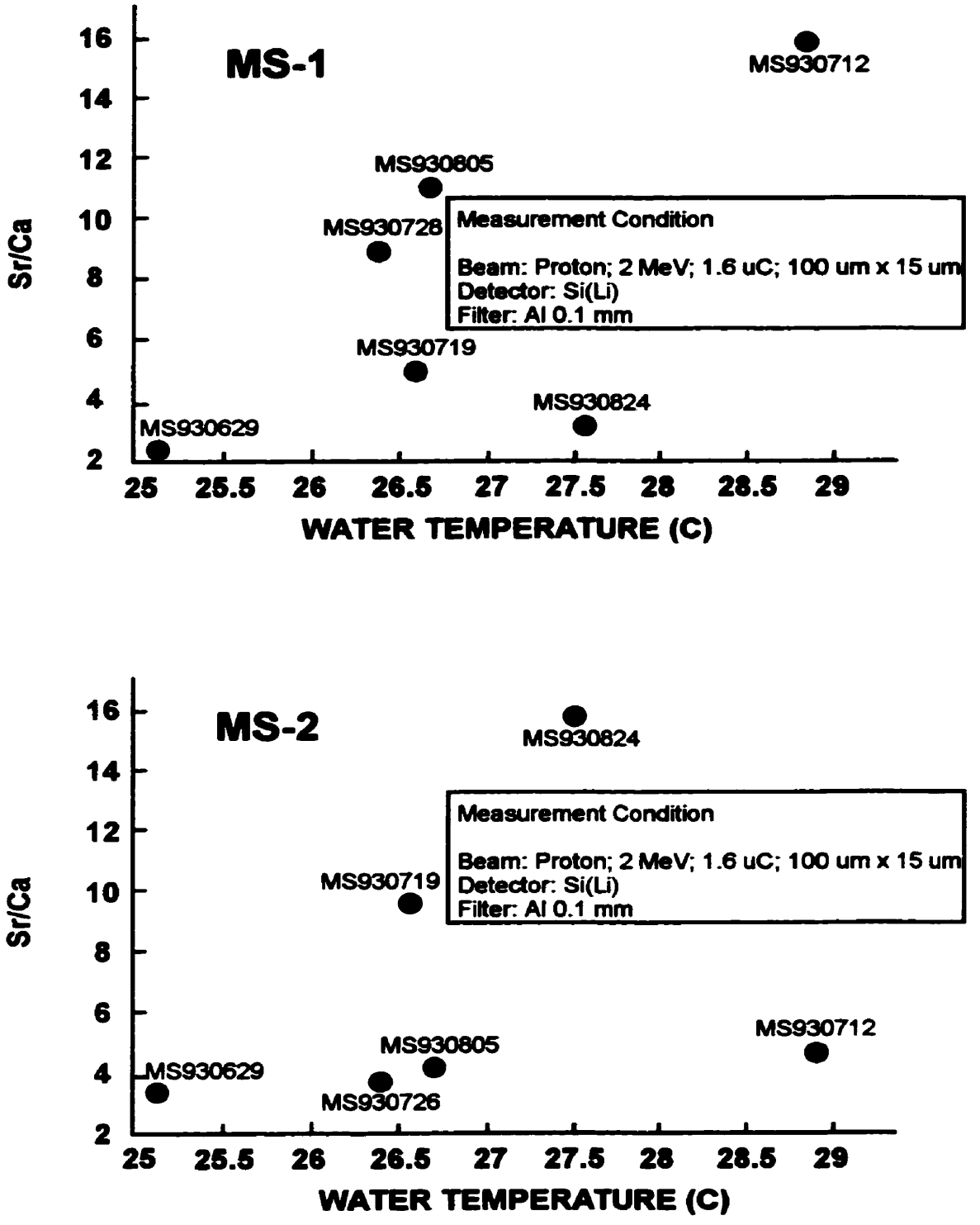

Figure 1.5. Sr/Ca ratios versus water temperature (in degrees Celsius) with micro beam (100 um x 16 um) PIXE (from Arai and Sakamoto, 1993).

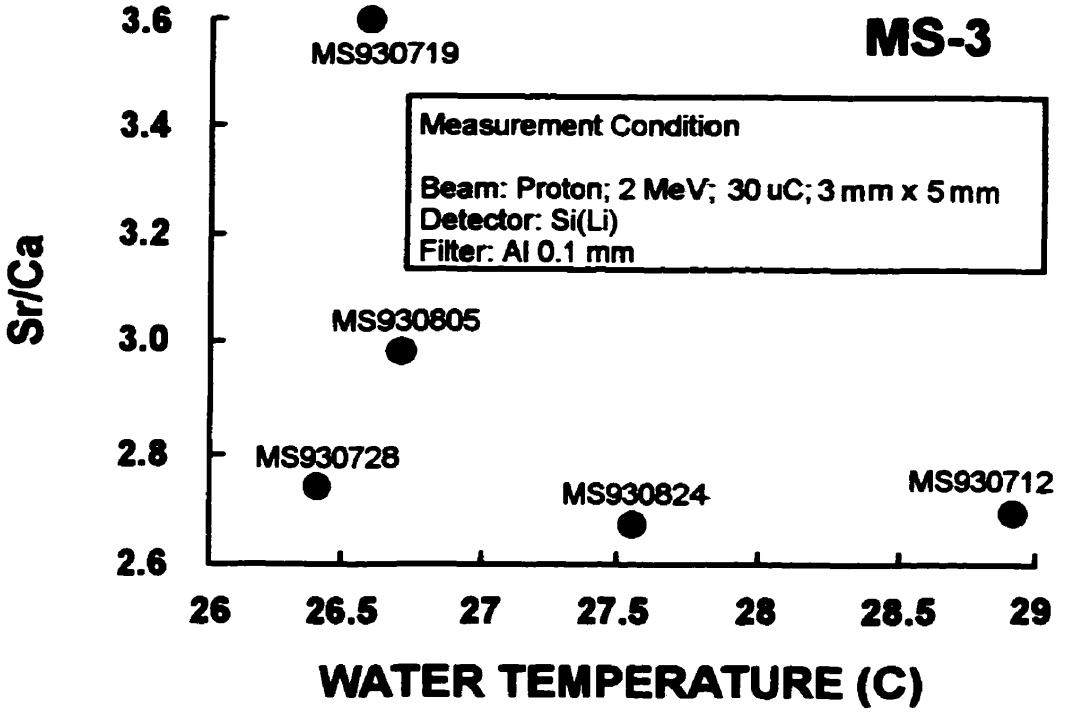

Figure 1.6. Sr/Ca ratios versus water temperature (in degrees Celsius) with 3 mm x 5 mm proton beam PIXE (from Arai and Sakamoto, 1993).

each fish population is exposed affect the incorporation of trace elements in calcified tissues, which results in chemical compositions specific to each (Gunn et al., 1992). The first calcified tissues to be examined were scales (Lapi and Mulligan, 1981) and vertebrae (Mulligan et al., 1983), but due to the previously mentioned problems of resorption and dissolution, otoliths proved to provide a more complete chemical record.

Mulligan et al. (1987) analyzed striped bass populations from four tributaries of Chesapeake Bay, U. S. A, and found that >70% of all individual fish could be correctly assigned to stocks based on the composition of their otoliths and much improved discrimination (>90%) resulted from broader geographical groupings. Since this study, numerous other studies, including Radtke and Morales-Nin (1989); Edmonds et al. (1989); Kalish (1990); Edmonds et al. (1992); Rieman et al. (1994); Radtke (1995); and Radtke et al. (1996), have been conducted on the other species (bluefin tuna, pink snapper, various freshwater salmonoids, yellow-eye mullet, sockeye salmon, and Arctic char, respectively). Electron probe micro-analysis (EPMA) was the principal technique used to determine the chemical composition of otoliths in all of these studies and the main determinant for distinguishing anadromous from non-anadromous, was Sr/Ca ratios.

More recently, due to technological advances, micro-proton induced X-ray emission (micro-PIXE) studies have shown both that anadromous and non-anadromous fish can be easily distinguished solely on the basis of the pattern of Sr distribution in their otoliths (Halden et al., 1995a; 1996; Babaluk et al., 1997). Further, the absolute levels of Sr in the primordium and first few annuli can indicate the fish's lake of origin (Halden et al., 1996). Furthermore, the age the fish first migrated and the age of maturation and first spawning can be determined by overlaying the Sr data on the image of the otolith.

Recent Studies by Halden et al. (1995; 1996) and Babaluk et al. (1997),

determined the distribution of Sr in otoliths from Arctic char of known anadromous (Halovik River), known non-anadromous (Craig Lake), and unknown life histories (Lake Hazen) (Figure 1.7). Part of the interest in Lake Hazen arose because its population contained two morphotypes, large and small char, and the question arose as to whether the large group were anadromous (Reist et al., 1995). This view was reinforced by the observation that Craig Lake, with no sea outlet, contained only the small morphotype. The line-scan from an anadromous Halovik River char, shown in Figure 1.7a, consists of a flat Sr profile corresponding to the primordium and first six annuli and then a marked increase in Sr in the seventh annuli, corresponding to the first migration to sea (Halden et al., 1996; Babaluk et al., 1997). The elevated Sr content in the oscillatory peaks is easily distinguishable from the background levels typical of the early part of the life history. All of the Halovik River fish showed such patterns. In contrast, the line-scan from a non-anadromous Craig Lake char, shown in Figure 1.7b, shows a relatively uniform Sr content with no oscillatory zoning. Figures 1.7c and 1.7d are line-scans from large and small Lake Hazen char, respectively, and they show a relatively constant Sr content from the nucleus to the outer edge of the otolith. These profiles are the same as the Craig Lake profile and therefore, it was concluded that neither the small or large morphotype in Lake Hazen migrates to sea.

Figure 1.7 also illustrates that the geographic origin of the populations can be distinguished on the basis of the Sr content (Halden et al., 1996). The primordium and first few annuli of the Halovik River char have a concentration of about 70 ppm of Sr, while the concentrations are about 670 ppm in Craig Lake char and 490 ppm in the Lake Hazen char.

Figure 1.8 shows Sr and Zn profiles from a Halovik Lake anadromous Arctic char overlaid on the image of an otolith from that fish (Halden et al., 1999). The Zn and Sr

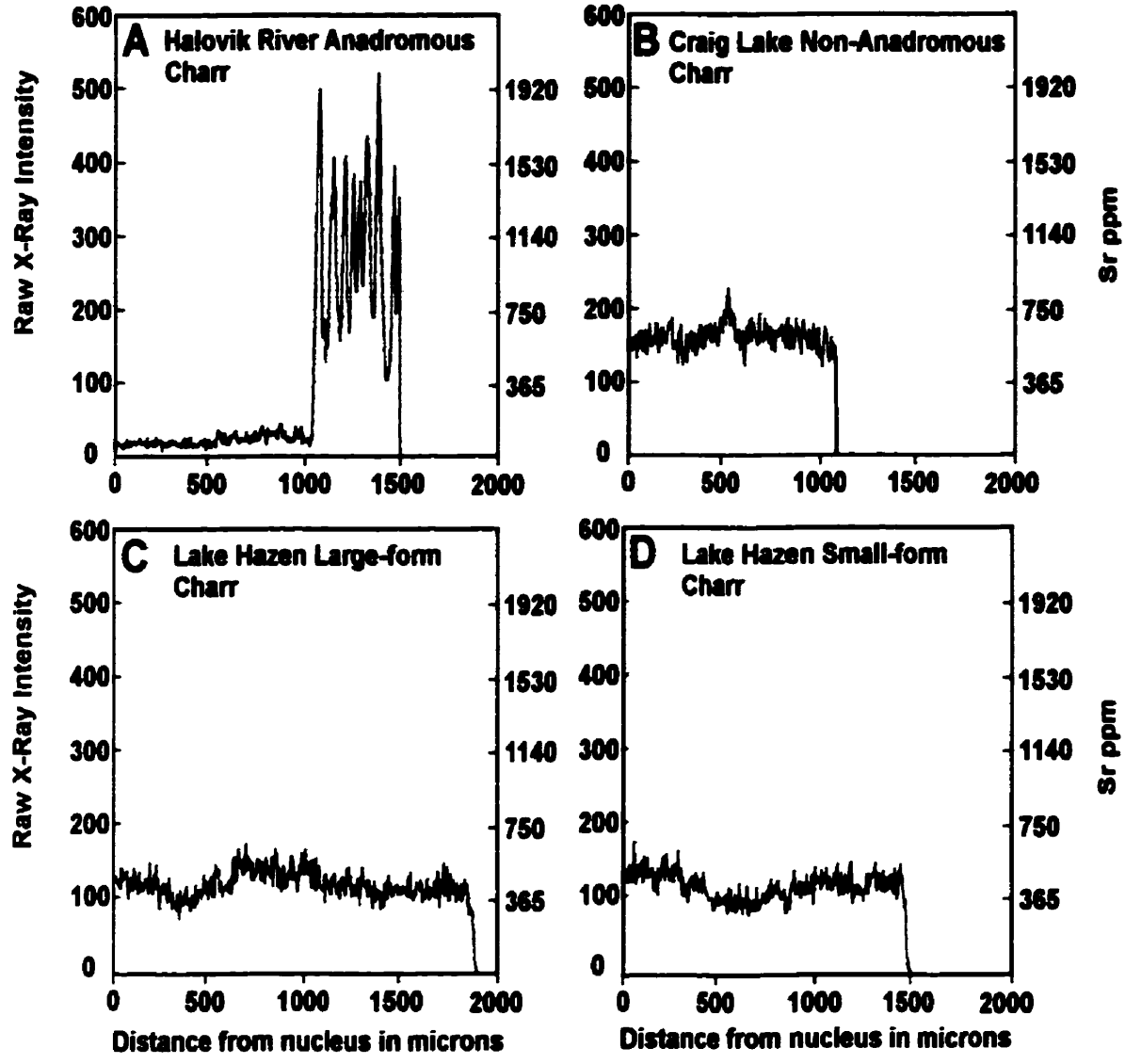

Figure 1.7. Typical strontium PIXE line-scans from arctic charr otoliths from (A) the Halovik River; (B) Craig Lake; and (C) and (D) Lake Hazen (from Halden et al., 1996; Babaluk et al., 1997).

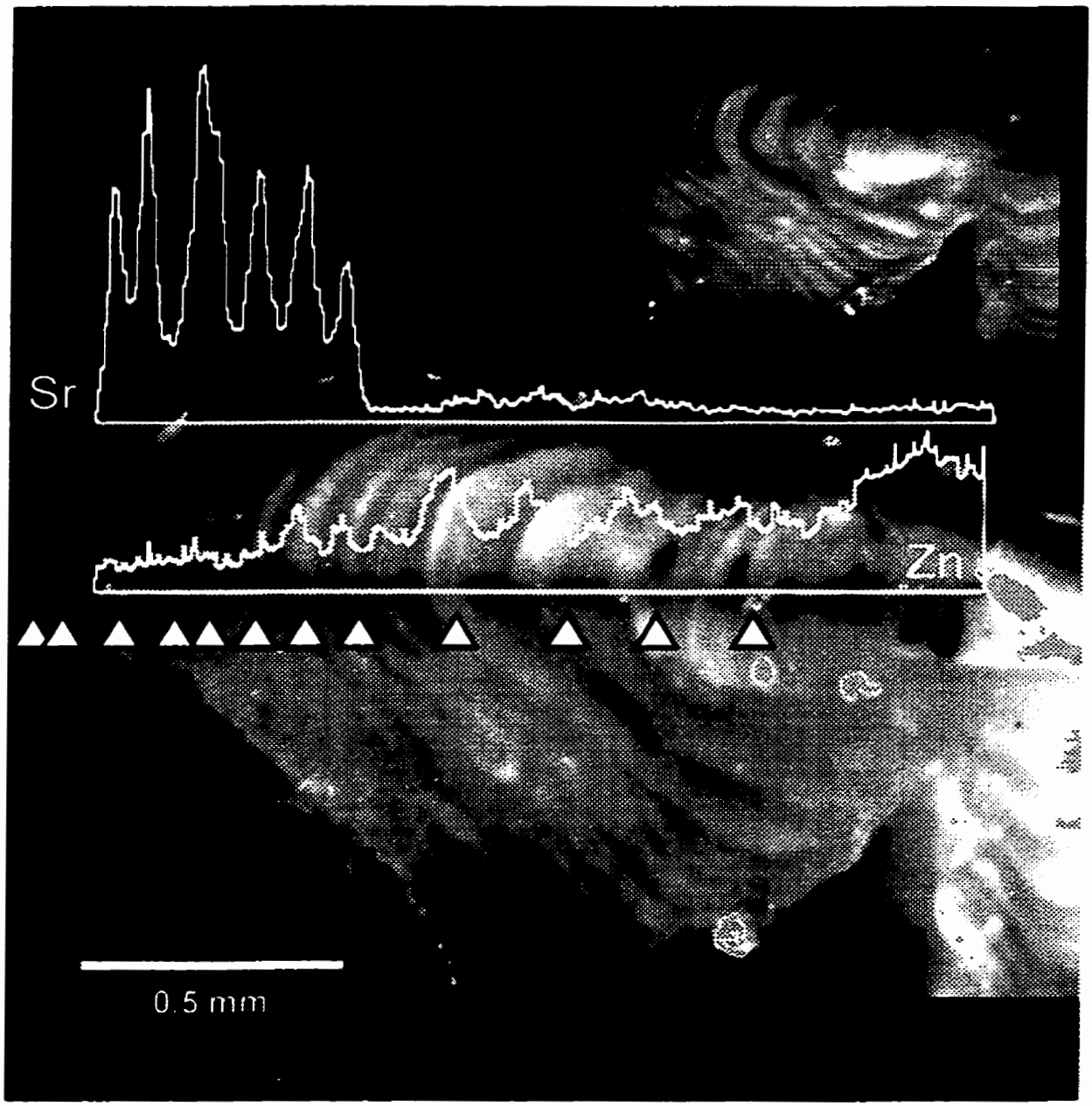

Figure 1.8. **Strontium and zinc PIXE profiles overlaid on the image of an otolith from an anadromous charr (after Halden et al., 1999). The triangles mark the otolith annuli.**

distributions shown in Figure 1.8 are both oscillatory. The Zn peaks are similar in width to the annuli with the peaks coinciding with the light part (summer) of each annulus. The overall concentration of Zn is highest in the primordium and first several annuli. Annuli 1 to 8 have elevated oscillatory Zn concentrations; annuli 7 and 8 also show elevated Sr concentrations indicating that this fish migrated out to sea when it was seven to eight years old. The Zn concentrations decrease after annuli 8 and the Sr concentrations remain elevated. This suggests there is some overlap of the Zn signature with the onset of anadromy. According to Halden et al. (1999), an idealized interpretation of these patterns might be that:

(1) at approximately 0 to 7 years, the fish underwent a freshwater phase where Sr was low and Zn was available for cyclical uptake dependant possibly on food source, temperature and alkalinity;

(2) the gradual increase in the Sr content (and decrease in Zn) in years 7 through 9 is a result of the fish remaining in the channel leading to the sea, before the first full migration; and

(3) at approximately 9 to 10 years, the fish entered a migratory adult phase, where the bulk of the feeding was being done in a high- Sr, low- Zn environment followed by a number of returns to freshwater. In the freshwater environment, however, with no significant feeding, there is little uptake of Zn and Sr is characteristically low.

If this idealized interpretation is valid, then it is likely that the productivity of an environment may influence when fish migrate. Furthermore, if the productivity is linked to local weather, the annular record of the otolith may also be linked in a general way to climate.

1.2 Experimental Approach

Chemical analyses of otoliths represents a new approach to the evaluation of

critical periods during the life histories of fish; an approach capable of documenting past environmental conditions encountered by an individual (Radtke and Shafer, 1992). This approach is possible because of the dramatic advances in analytical techniques over the years. The following is a brief look at the techniques that have been used in the chemical analysis of otoliths; their benefits and limitations.

1.2.1 Atomic Absorption Spectrometry

Atomic absorption spectrometry (AAS) was one of the first techniques used in the bulk chemical analysis of otoliths (Gauldie and Nathan, 1977; Gauldie et al., 1980). However, there are two main problems to using AAS in the bulk chemical analysis of otoliths. First, the otolith must be dissolved in solution in order to be analyzed and, therefore, all spatial information concerning element distribution is destroyed (Halden et al., 1995a; 1996). This also prevents the sample from undergoing further analysis by other methods. Secondly, in comparison to more modern instruments, AAS can not generally compete in speed with multi-element techniques as only one element can be determined at once (Potts, 1987).

1.2.2 Electron Probe Micro-Analysis

Electron probe micro-analysis (EPMA) has been used extensively to analyze the distribution of elements in different fish species (Radtke et al., 1990; Radtke and Shafer, 1992; Gunn et al., 1992; Thresher et al., 1994). Microprobe techniques differ from most other techniques, such as AAS, in that they are for the most part non-destructive, involving the excitation and chemical analysis of selected areas of diameter as small as a few microns on the surface of samples. An electron beam, normally in the range of 15 to 30 kV, is focused on the surface of the sample and interactions between this primary electron beam and the sample cause the generation of X-rays characteristic of the

atoms of the excited sample (Potts, 1987). The intensity of these X-rays is measured using a wavelength-dispersive (WD) or energy-dispersive (ED) spectrometer and after correction for matrix effects, count data are compared with data from minerals of standard composition in order to quantify the analysis (Gunn et al., 1992).

With respect to otolith life-history, the conventional ED electron probe is severely limited in its ability to detect elements present in concentrations less than 1000 ppm because of difficulties in resolving line overlaps, the presence of spectral artifacts, and the generally low peak-to-background ratios, and low peak count rates (Gunn et al., 1992). WD-based EPMA is, therefore, generally recommended in the analysis of otoliths, particularly for life-history scans.

There are, however, drawbacks (though much more minor) to using WD-based EPMA in the analysis of otoliths. First, while having the necessary spatial resolution, ~1 μm, to address the analysis of small zones, EPMA is incapable of routine trace element analysis at the few ppm level; the level of most trace elements, such as Fe, Mg, Zn, REE, etc. (Halden et al., 1995a; 1996). Secondly, sample ablation produces chemical changes, pitting, and a disruption of the surface coating which can result in the charging of the target (Gunn et al., 1992). This type of damage results in erroneous estimates and, and perhaps more importantly, the extent of this error is difficult to quantify.

1.2.3 Laser Ablation Microprobe - Inductively Coupled Plasma - Mass Spectrometry

Laser ablation microprobe - inductively coupled plasma - mass spectrometry (LAM-ICP-MS) is a new technique that can be used for the multi-element analysis of otoliths at specific loci (Fowler et al., 1995). With the activation of the high-powered pulsed laser beam, focused onto a selected position on the otolith, photon energy is converted to thermal (kinetic) energy and some of the otolith is vaporized and swept by a

flow of argon gas into the plasma where it is atomized and ionized. The analyte ions are then extracted and analyzed by a mass spectrometer. This technique combines the benefits of point sampling with the sensitivity of ICP-MS, and avoids the sample preparation by acid dissolution used in AAS.

There are two major advantages to using LAM-ICP-MS in the analysis of otoliths in comparison specifically to EPMA. First, there is little or no sample preparation, resulting in high sample throughput. Secondly, while spatial resolution is about the same, the sensitivity of LAM-ICP-MS is much higher.

There are also, however, two drawbacks. First, the laser beam diameter is approximately 30 μm and it, therefore, operates at a relatively large lateral spatial scale, providing an "elemental fingerprint" that integrates over many days (Fowler et al., 1995). Secondly, the laser beam is quite destructive, restricting its use to only two pulses per sample locus, separated by distances of 500 μm across the otolith surface. For many small otoliths, these ablation pits are larger than the width of an individual annulus, and sometimes large sections of the otoliths are blasted from the surrounding resin.

1.2.4 Proton Microprobe Analysis

The proton microprobe is the proton analogue to the electron microprobe (Campbell et al., 1995) and is a very useful technique for the multi-element analysis of geological samples (Potts, 1987; Campbell et al., 1995; Halden et al., 1995b). It delivers a focused beam of protons to a sample, which emits X-rays characteristic of its elemental constituents and their concentrations. The X-ray spectrum is recorded in energy-dispersion mode by a Si(Li) detector. Proton-induced X-ray emission (PIXE) with such a microbeam (micro-PIXE) provides spatial resolution similar to that of the electron microprobe (ca. 5 to 10 μm) but offers significantly lower limits of detection, commonly in

the 1 to 20 ppm range for most trace elements of interest.

In the analysis of otoliths, Coote et al. (1991) were the first to use micro-PIXE to image elemental distributions. However, they concluded that it was difficult to relate the determined elemental composition to physical features in the otoliths. The combination of micro-PIXE with a scanning proton microprobe (SPM), has enabled the use of micro-PIXE in both point analysis and imaging modes to study trace element variation in otoliths. The SPM has the necessary spatial resolution and micro-PIXE has the necessary detection limits for such analyses. Together they provide both a non-destructive analysis of the trace element content of otoliths as well as one- (line scan) and two-dimensional maps of the distribution of trace elements for comparison with optical images (Halden et al., 1995b). Correlation between the chemical record observed using SPM and the optical record of annuli further allows the establishment of the age at which the fish either entered a chemically distinct environment or their environment was altered by input from an external source.

1.3 Objectives

Rare earth elements (REE) and other trace elements, such as Mn, Sr, Zn, Fe, Th, U, and F, can substitute in carbonate minerals (Henderson, 1984). A recent geological study on the pegmatites of the Eden Lake Complex, which neighbors the lake, by Arden (1995) found that two of these pegmatites contain abundant REE-bearing minerals, as well as minerals with high concentrations of Sr, Zn, Mn, Fe, U, Th, and F. Biogeochemical and radiometric studies of the vegetation surrounding Eden Lake found light rare earths and other trace element concentrations, particularly in alder twigs (Fedikow et al., 1993; 1994), indicating that some REE and other trace elements are mobile in the Eden Lake environment.

Many studies have focused on the concentration of various trace elements in

otoliths. However, most of these studies have focused specifically on whether or not these bioaccumulations are a health risk due to anthropogenic activities and/or related to species; gender; temperature; or age. This, however, is the first detailed investigation or baseline study into the incorporation of trace elements into otoliths from fish in their natural setting at Eden Lake where the only source of these trace elements is the local geology.

The objectives of this research are to:

(1) determine the bioavailability and concentration of rare earths and/or other trace elements in the otoliths of the fish species of Eden Lake;

(2) determine the distribution of these trace elements within the annuli; and

(3) relate their distribution to seasonal variations of element input (i.e. environmental conditions) or to fish behavior and life history.

Chapter 2: Eden Lake Geology and Physiography

Eden Lake (56°38' latitude and 100°15' longitude) is located ~1000 kilometres north of Winnipeg, Manitoba, approximately half way between the towns of Leaf Rapids and Lynn Lake in northern Manitoba (Figure 2.1) (Arden, 1995). It is the site of the Eden Lake Complex, which is interpreted as being a post-orogenic intrusive complex with alkaline characteristics. Eden Lake is accessible from Provincial Highway 391 and the main outcrops of the Complex are accessible from the lake, approximately 6.5 km by boat south from the highway.

2.1 Geology of the Eden Lake Complex

The Eden Lake Complex, at its present level of erosion, covers approximately 15 km^2; intruding the granitic rocks between the Lynn Lake and Leaf Rapids greenstone belts within the juvenile Reindeer Zone of the Trans Hudson orogenic terrane (Figure 2.1; cf. Arden, 1995). Geological mapping of the Eden Lake area was undertaken by Cameron (1988) and McRitchie (1988). The complex is made up of a number of intrusive units the most prominent of which is an aegirine-bearing monzonite (Halden and Fryer, 1999). The principle units were informally termed as syenite based on field data, however, modal analysis indicates that they are actually monzonite to quartz monzonite. The Eden Lake Complex is one of a group of alkaline intrusions found within the Churchill province that includes other similar complexes at McVeigh, Brezden, and Burntwood Lakes (McRitchie, 1988). These complexes are interpreted as post-orogenic because they intrude foliated country rocks and are characteristically, themselves largely unfoliated (Halden and Fryer, 1999).

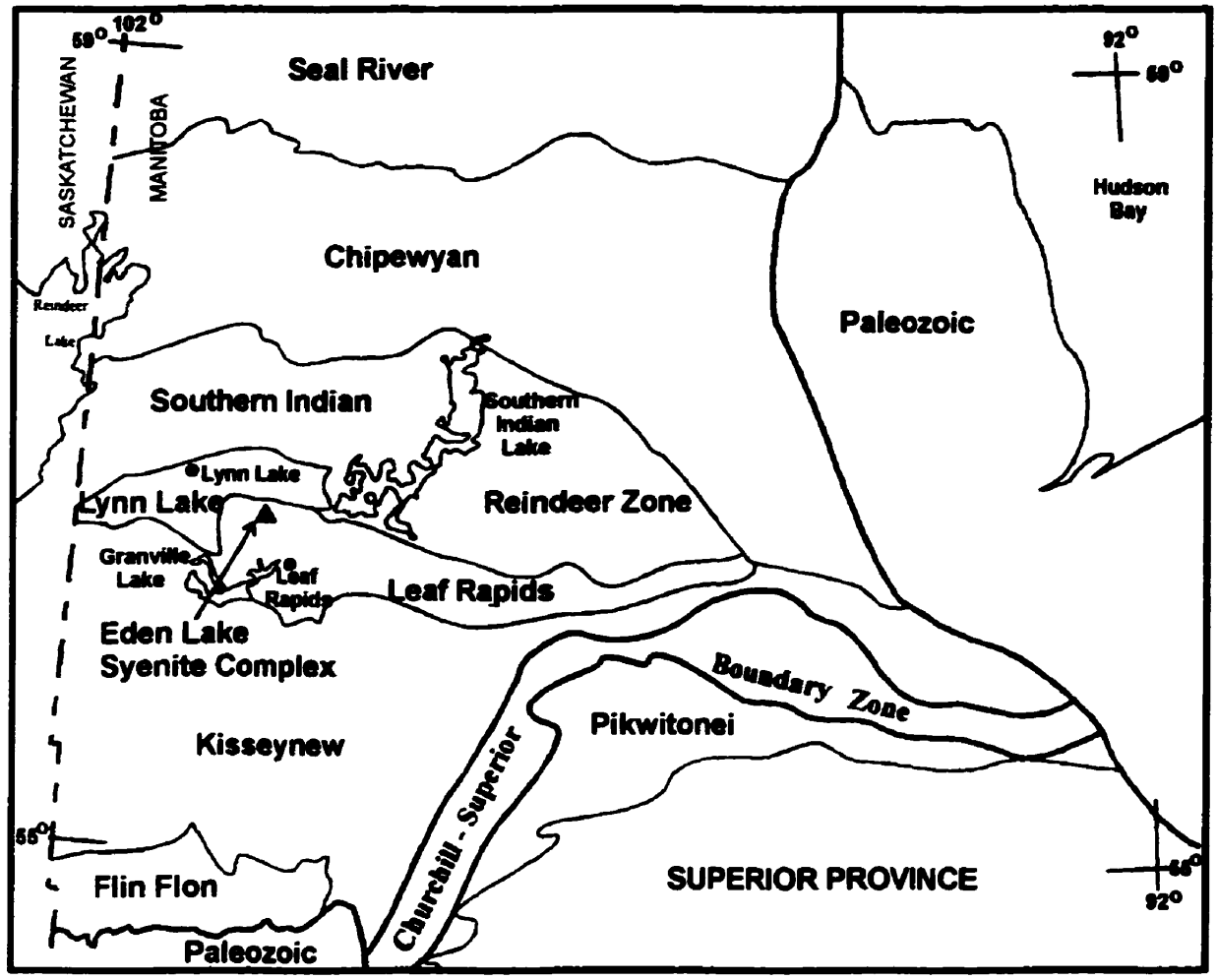

Figure 2.1. Map of the southeastern portion of the Reindeer Zone of the Trans Hudson Orogenic terrane and the adjacent Superior Province in northern Manitoba, showing the principle geological domains and the location of the Eden Lake Complex, marked with a black triangle (from Arden, 1995).

The Eden Lake Complex is currently exposed in three topographically high, north-south, linear ridges on a peninsula on the eastern side of the lake (Figure 2.2) (Arden, 1995). At its highest point, the Complex is >380 metres (1150 feet) above sea level. It is composed of 2 main intrusive phases, an earlier weakly-foliated mafic monzonite and a late non-foliated felsic monzonite (cf. Arden, 1995). The mineralogy of these two phases is given in Table 2.1. In addition, there are four young pegmatite phases that intrude both of the monzonite phases. These pegmatite phases are of particular interest to this research because of their exotic mineralogy and the influence of this mineralogy on the overall geochemical character of the complex.

2.2.1 Pegmatite Mineralogy

The first pegmatite unit, the mafic pegmatites, contain coarse-grained aegirine-augite with hornblende and magnetite, as well as K-feldspar and quartz (Arden, 1995). These pegmatites occur as discontinuous stringers approximately 2 metres long and 20 cm wide.

The second pegmatite unit, which is younger than the mafic pegmatite unit, contains blocky quartz and K-feldspar graphically intergrown, along with some plagioclase (Arden, 1995). These granitic pegmatites occur as patches and veins, 10 to 30 metres long, and 3 to 50 centimetres wide.

The third and most abundant pegmatite unit is also a granitic pegmatite, however, in addition to quartz, K-feldspar, and plagioclase, this unit contains, in decreasing abundance, aegirine-augite, andradite, titanite, fluorite, apatite, zircon, allanite, thorite, burbankite, and strontianite (Figure 2.3 and 2.4; Table 2.2) (Arden, 1995). This unit is associated predominantly with the felsic monzonite occurring as

Table 2.1. **Mineralogy of the mafic and felsic monzonite units of the complex; mineral abundance was determined at the outcrop scale (after Arden, 1995).**

MINERALS	ABUNDANCES	
	MAFIC MONZONITE	FELSIC MONZONITE
Aegirine-augite	15 – 40%	5 – 51%
Hornblende		
Magnetite		
K-feldspar	15 – 30%	40 – 50%
Plagioclase (albite to andesine	10 – 25%	20 – 35%
Quartz	<1 – 5%	5%
Titanite	<1%	<1%
Apatite	<1%	<1%
Zircon	0%	<1%

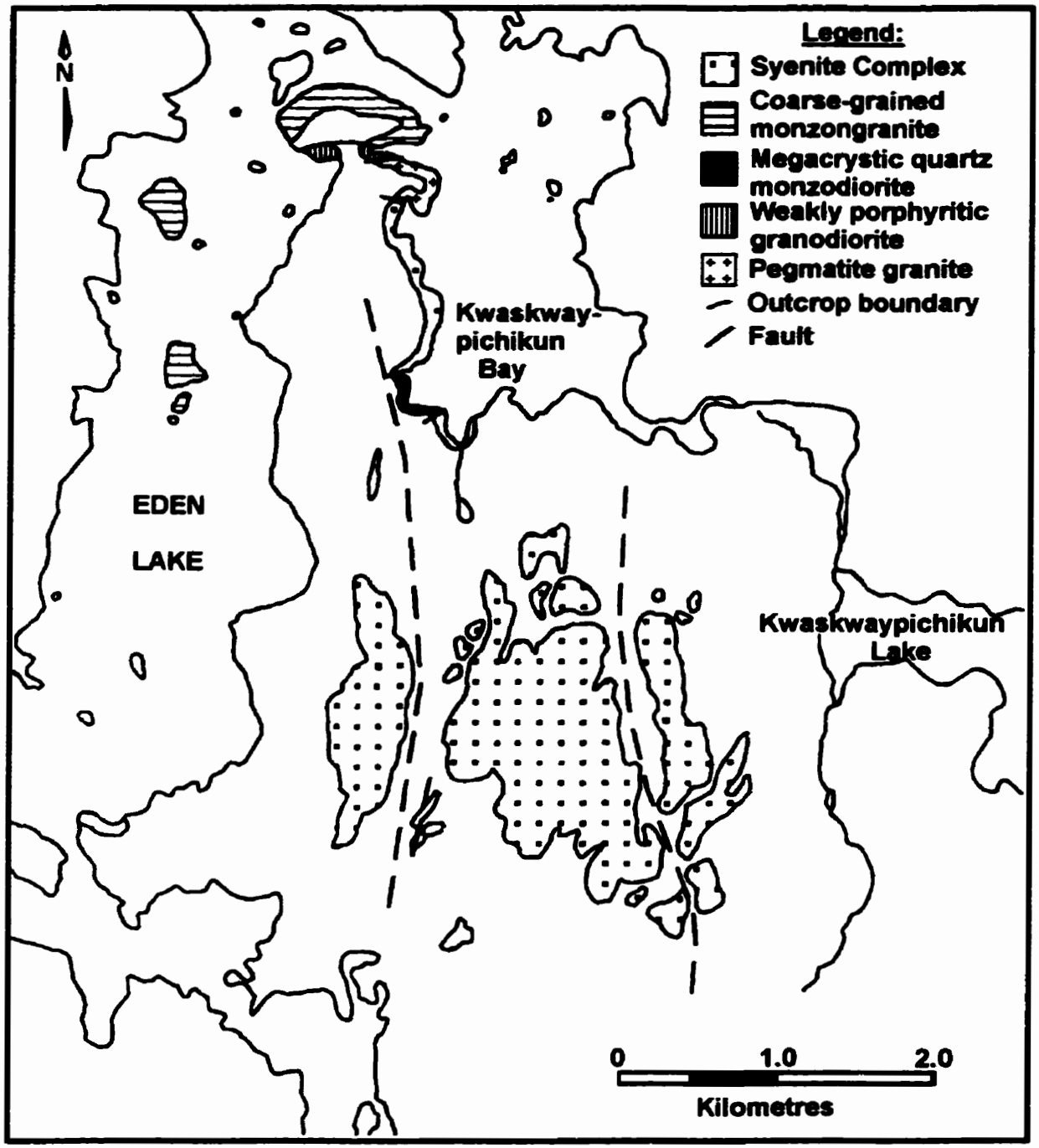

Figure 2.2. Detailed geological map of the Eden Lake Complex and the surrounding country rocks (after McRitchie, 1988; Arden, 1995).

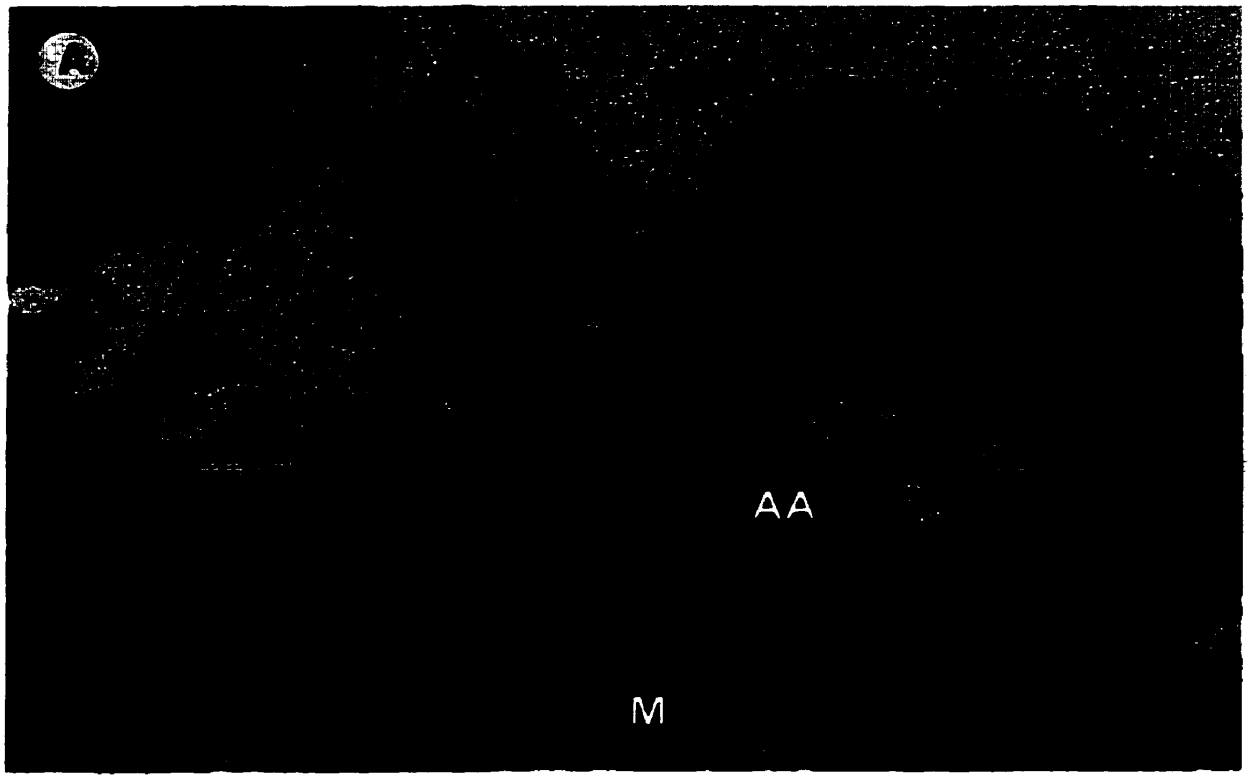

Figure 2.3. **Photomicrographs of some of the minerals found in the Type 3 pegmatites (from Arden, 1995). (A) The field of view is 2.8 mm across. Mineral abbreviations are as follows: AA - aegirine-augite; KF - K-feldspar; M - magnetite; Q - quartz, and TI - titanite. (B) The field of view is 2.8 mm across. Mineral abbreviations are as follows: PG - plagioclase and TI - titanite.**

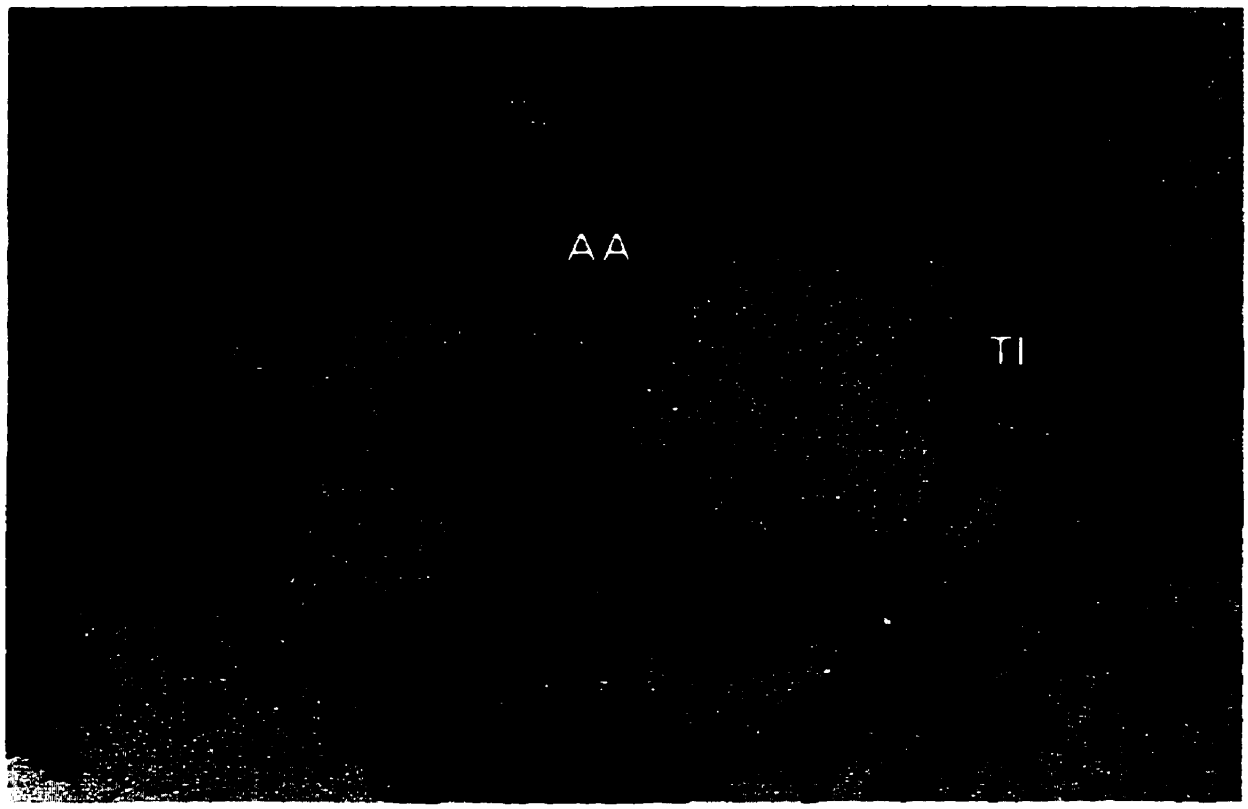

Figure 2.4. Photomicrograph of some of the minerals found in the Type 3 pegmatites. The field of view is 0.7 mm across. Mineral abbreviations are as follows: AA - aegirine-augite; F - fluorite; PG - plagioclase; Q - quartz; and TI - titanite (from Arden, 1995).

Table 2.2. Abundance of minerals within the Type 3 granitic pegmatites; abundance determined at the outcrop and thin section scales (after Arden, 1995).

MINERAL PHASE	MINERAL ABUNDANCE
Aegirine-augite	5 – 25%
K-feldspar Microcline Orthoclase	5 – 55%
Plagioclase (albite to andesine)	0 – 30%
Quartz	0 – 20%
Fluorite	0 – 5%
Andradite	0 – 10%
Apatite	0 – 5%
Zircon	0 – 2%
Titanite	0 – 10%
Allanite	0 – trace
Thorite	0 – trace
Burbankite	0 – trace
Strontianite	0 – trace

irregular patches that range in size from a few cm^2 to 10 m^2.

The final pegmatite unit is the least abundant; it is typically found as discontinuous, 30 to 40 centimeter wide veins associated with shear zones in the easternmost outcrop (Arden, 1995). This pegmatite unit contains, in decreasing abundance, titanite, aegirine-augite, K-feldspar, plagioclase, quartz, apatite, fluorite, zircon, britholite, allanite, and weloganite (Figure 2.5 and 2.6). The britholite and allanite in this pegmatite are thoroughly metamict and the surrounding minerals are heavily fractured. For this reason, it is called "radioactive pegmatite" (Table 2.3).

Rare-earth elements, Sr, Zn, Mn, Fe, Th, U and/or F, which are known to substitute in carbonate minerals (i.e. aragonite otoliths), are found in the apatite, titanite, zircon, allanite, andradite, fluorite, aegirine-augite, feldspar (K-feldspar and plagioclase), and britholite in one or both of the type 3 and 4 pegmatites. Representative chemical compositions, including the abundance of REE; Mn; Th; U and F, of these minerals are provided in Arden, 1995. The britholite is the principal mineral hosting a considerable abundance of REE (ca. 55 weight %), followed by, in decreasing overall concentrations, allanite (ca. 25 wt. %), apatite (ca. 8 wt. %), titanite (ca. 2 wt. %), zircon (ca. 1 wt. %), aegirine-augite (ca. 0.3 wt. %), K-feldspar (ca. 1800 ppm), andradite (ca. 1000 ppm), plagioclase (ca. 425 ppm), and fluorite (none) (Arden, 1995). Strontium, zinc, manganese, iron, thorium and uranium content varies within the grains of one mineral. From the chemical composition data, listed in Arden (1995), Sr content is highest in the britholite (0.46 wt. %) followed by, in decreasing overall concentrations, plagioclase (0123 to 0.217 wt. %), K-feldspar (0.97 to 0.185 wt. %), apatite (6387 to 7220 ppm), zircon (22 to 5798 ppm), allanite (2356 to 2650 ppm), and titanite (74 to 2463 ppm). Sr data is not provided for aegirine-augite and andradite. Zn content is highest in the allanite (606 to 697 ppm) followed by andradite (206 to 345 ppm), zircon (0 to 116 ppm),

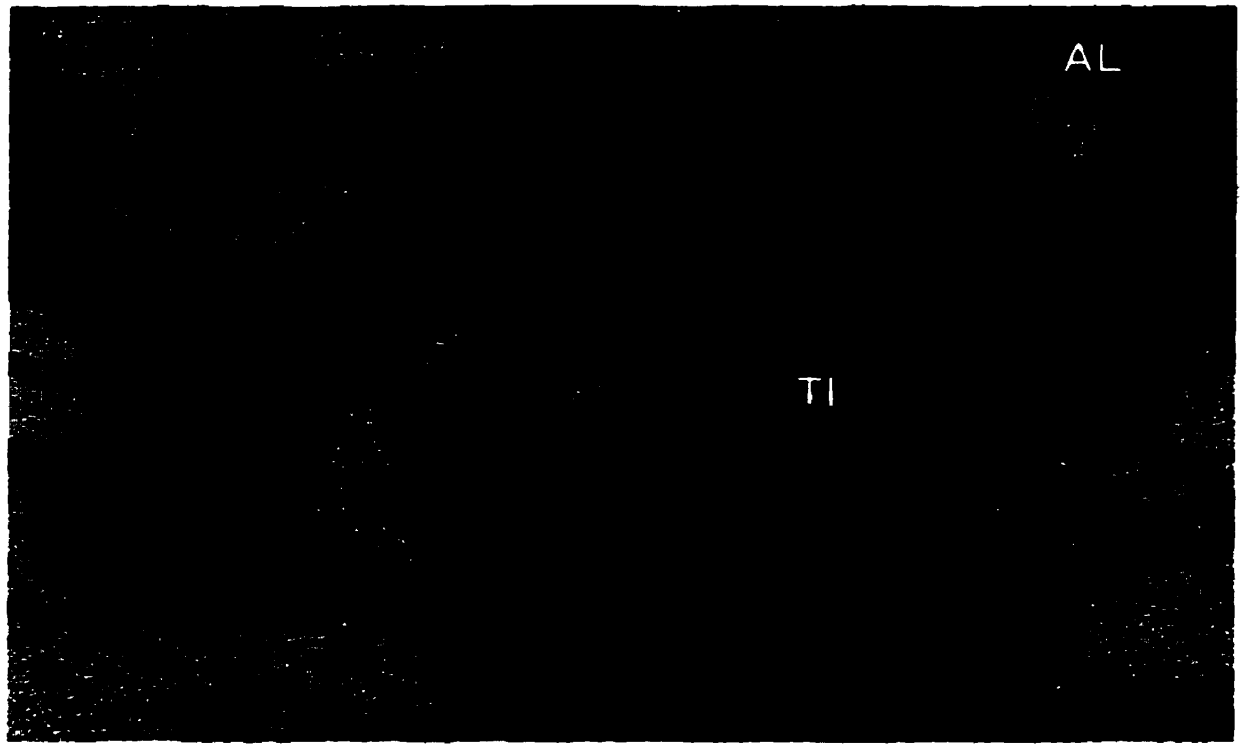

Figure 2.5. **Photomicrograph of some of the minerals found in the Type 4 pegmatites. The field of view is 2.8 mm in the long dimension. Mineral abbreviations are as follows: AA - aegirine-augite; AL - allanite; AP - apatite; B - britholite; TI - titanite; and Q - quartz (from Arden, 1995).**

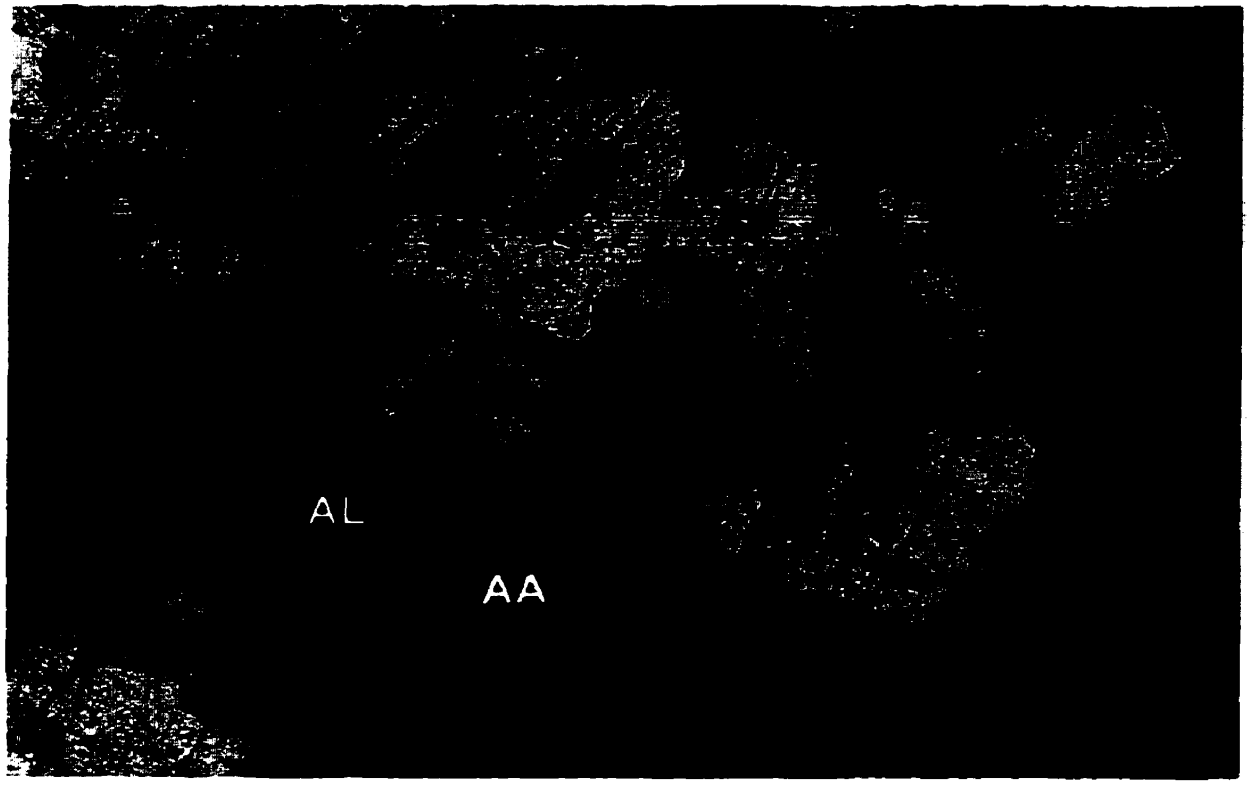

Figure 2.6. **Photomicrograph of some of the minerals found in the Type 4 pegmatites. The field of view is 0.7 mm across. Mineral abbreviations are as follows: AA - aegirine-augite; AL - allanite; AP - apatite; B - britholite; and F - fluorite (from Arden, 1995).**

Table 2.3. **Mineral abundance in the Type 4 radioactive pegmatites; abundance determined at both the outcrop and thin section scale (after Arden, 1995).**

MINERAL PHASE	MINERAL ABUNDANCE
Aegirine-augite	5 – 30%
K-feldspar Microcline Orthoclase	0 – 30%
Quartz	1 – 10%
Plagioclase (albite to oligoclase)	0 – 25%
Fluorite	0 – 5%
Apatite	0 – 35%
Zircon	0 – trace
Titanite	0 – 5%
Britholite	0 – 70%
Allanite	0 – 20%
Weloganite	0 - trace

apatite (0 to 53 ppm) and titanite (2 to 42 ppm). Zn data is not provided for britholite, aegirine-augite and feldspar (K-feldspar and plagioclase). Mn content is highest in the fluorite (1.002 to 1.365 wt. %) followed by aegirine-augite (0.819 to 1.138 wt. %), andradite (0.10 to 1.29 wt. %), apatite (0.003 to 0.048 wt. %), zircon (0 to 3483 ppm), and titanite (8 to 2345 ppm). Mn data is not provided for britholite and feldspar (K-feldspar and plagioclase). Fe content is highest in the andradite (28.296 to 30.081 wt. %) followed by aegirine-augite (14.155 to 20.737 wt. %), allanite (7.93 to 20.563 wt. %), titanite (1.946 to 3.942 wt. %), plagioclase (0.189 to 0.251 wt. %), K-feldspar (0.146 to 0.150 wt. %), apatite (0 to 0.024 wt. %) and britholite (0 to 0.005 wt. %). Th content is highest in zircon (0 to 7935 ppm) followed by apatite (0 to 1016 ppm), titanite (0 to 56 ppm), britholite (0 to 0.143 ppm), and allanite (0 to 0.005 ppm). Th data are not provided for andradite, aegirine-augite, K-feldspar, or plagioclase. U content is highest in britholite (0.79 to 0.81 wt. %) followed by zircon (0.071 to 2.895 wt. %), allanite (0 to 1065 ppm), titanite (935 ppm), apatite (86 to 866) and andradite (77 to 180 ppm). U data is not provided for aegirine-augite, K-feldspar, or plagioclase. Fluorite, is the principal mineral hosting considerable F, followed by, in decreasing overall concentrations, apatite (ca. 4 wt. %), britholite (1.33 to 3.80 wt. %), titanite (ca. 1 wt. %), and allanite (0.196 to 0.5 wt. %). F data is not provided in Arden 1995 for zircon, andradite, aegirine-augite, and feldspar (K-feldspar and plagioclase).

Examination of back-scattered electron (BSE) images of britholite, the mineral with the most REE and Sr, reveals that it has an annealed polygonal texture and that the polygons are altered (Figure 2.7) (Arden, 1995). The alteration has a vermicular to colloform appearance and is concentrated along the margins of the polygons (Figure 2.7A). The alteration advances from these grain boundaries to the center and polygons range from partially to completely altered and in the most altered samples, the polygonal boundaries are completely obliterated (Figure 2.7B). This alteration is due to water

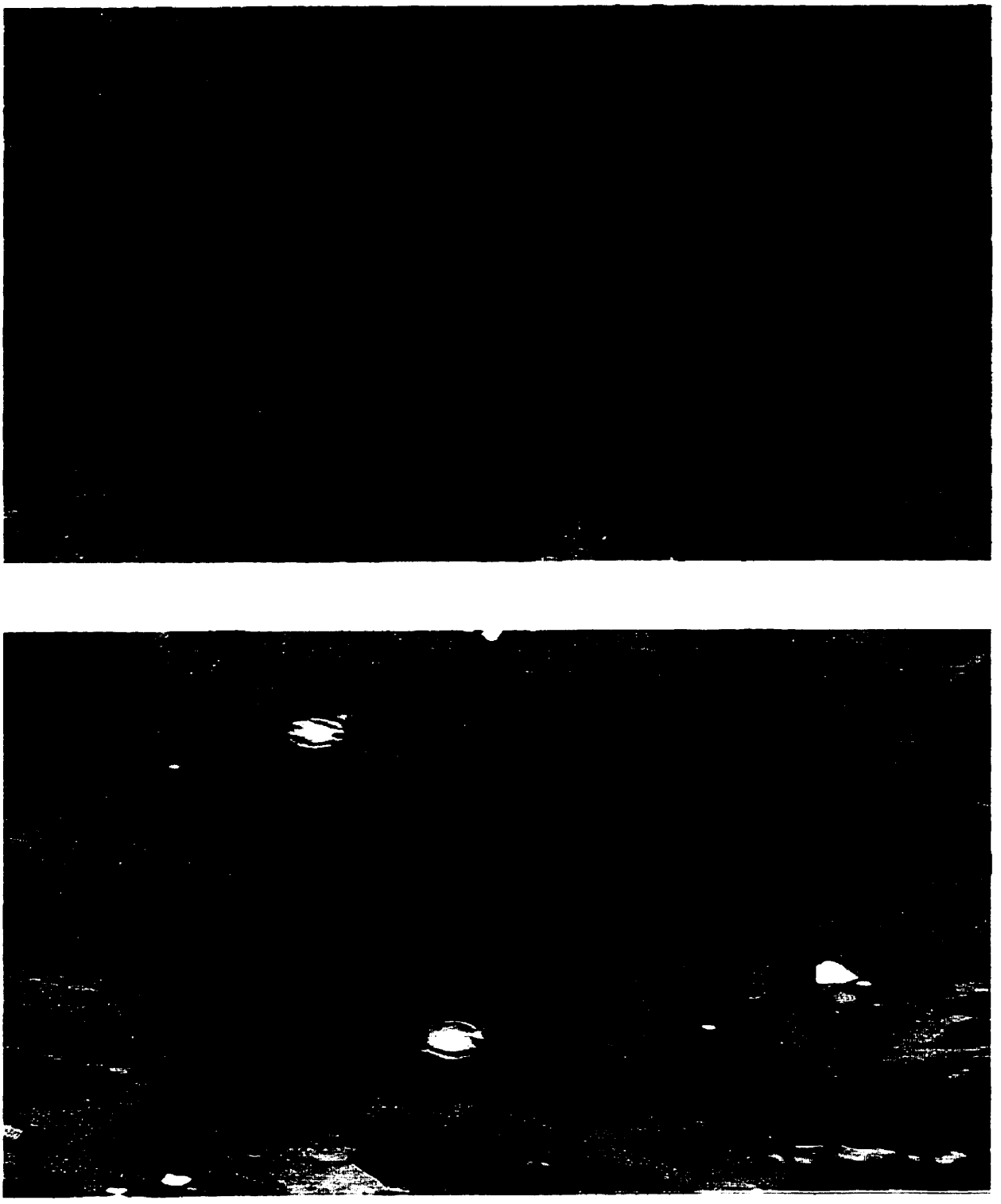

Figure 2.7. **Photographs of BSE images showing altered britholite from the Type 4 pegmatites. (A) Very slightly altered britholite - note the control of the polygonal boundaries on the alteration. The field of view is 400 microns across. (B) Complete alteration of the britholite polygons; boundaries have been completely destroyed. The field of view is 200 microns across (from Arden, 1995).**

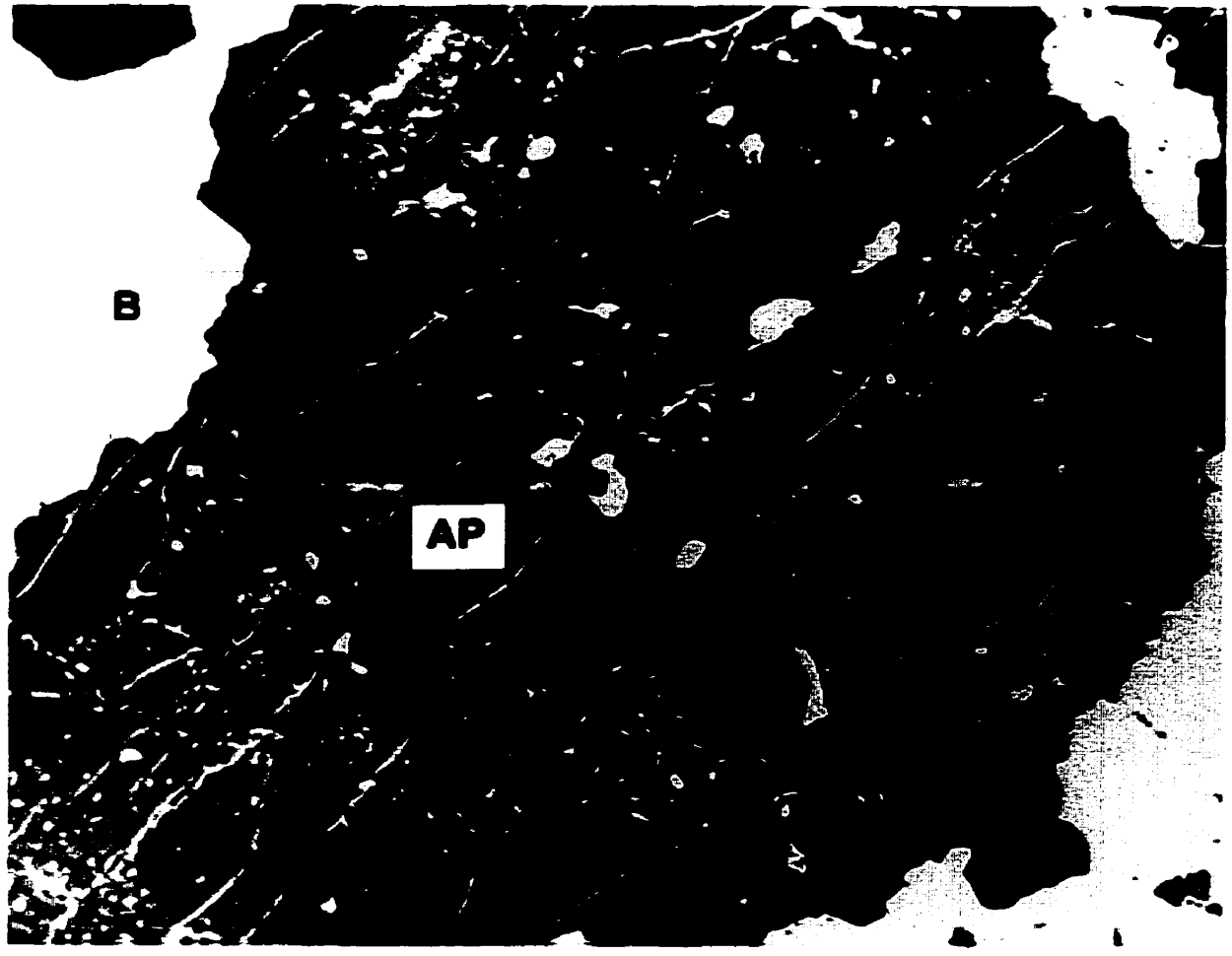

Figure 2.8. Photograph of a BSE image of an apatite grain from the Type 4 pegmatites. The patchy coloring is due to alteration; the bright fractures are filled with REE-enriched apatite. The field of view is 300 microns across. Mineral abbreviations are as follows: AP - apatite and B - britholite (from Arden, 1995).

percolating through between the grain boundaries, leaching out elements as the edges of the grains break down. This indicates that REE, Sr, Fe, Th, U, and F, as well as other trace elements (possibly Mn and Zn as no data was available for this element in britholite), are being liberated from the mineral and released into the environment at Eden Lake. Other REE-, Sr-, Zn-, Mn-, Fe-, Th-, U-, and F-bearing minerals show similar alteration (e.g. Figure 2.8), further liberating even more elements (Arden, 1995).

2.2.2 Geochemical Character of the Complex

The Eden Lake Complex has many characteristics that support the view that it is an A-type granitoid due to the mineralogy of the pegmatite units, particularly units 3 and 4 (Arden, 1995; Halden and Fryer, 1999). These include high $Na_2O + K_2O$ values (11 to 13 weight %), a significant abundance of F (200 to 4000 ppm), relatively constant Y/Nb and Yb/Ta ratios, and a characteristic mineral assemblage consisting of magnetite, fluorite, titanite, aegirine-augite, apatite, and zircon.

The SiO_2 content of the complex ranges from 57 to 77 weight % with a continuous fractionation trend from low to high silica phases (Halden and Fryer, 1999). The rocks of the complex can be divided into three groups based on trace element characteristics and silica content: (1) the low silica group (LSG) with SiO_2 contents ranging from 57 to 62 weight % SiO_2 that has elevated U, P, and total REE contents (ca. 1000 ppm); (2) the main phase monzonite (MPM) with 64 to 71 weight % SiO_2; and (3) the high silica group (HSG) with 71 to 77 weight % SiO_2 that has similar trace element patterns to the LSG, but lower trace element and REE abundance (ca. 20 ppm).

Chondrite-normalized REE plots for the complex as a whole are shown in Figure 2.9; the plots are light REE-enriched and lack europium anomalies (Arden, 1995). Preliminary whole-rock analysis of the type 4 pegmatite unit containing britholite show

that it is considerably light-REE enriched, in some cases up to 50,000 x chondrites (McRitchie, 1989; Arden, 1995). The LREE are concentrated in britholite and allanite in the order (Young and McRitchie, 1990):

britholite: Ce>Nd>La>Pr>Sm

allanite: Ce>La>Nd>Pr>Sm

Total REE content decreases with increasing SiO_2 content which is somewhat unexpected as the main mineral phases dominating major element fractionation (aegirine-augite and K-feldspar) have a bulk distribution coefficient less than one, which would result in incompatibility of the REE (Halden and Fryer, 1999). There is a distinct compositional gap between the main phase monzonites and the silica-rich rocks where the latter are significantly depleted in REE; this is inconsistent with a smooth uninterrupted liquid line of decent dominated by crystal fractionation. The spatial association of the pegmatites with the complex, and their compositional similarities to the complex, suggest that there is a genetic association. The compositional gap in terms of REE content, between the main phase and the more evolved silica-rich rocks, might be explained by the physical separation of a REE-enriched vapor phase. Such a REE-enriched phase will also have been enriched in F and P, therefore, the REE would have been scavenged as ionic complexes.

2.2 Radiometric Surveys

A 1977 airborne gamma-ray survey identified uranium, thorium, and potassium anomalies in the Eden Lake area (Geological Survey of Canada, 1977). These anomalies were concentrated over the complex and in monzonites to the east of Eden Lake. Follow-up geochemical studies detected anomalous levels of uranium and fluoride in lake waters and uranium in lake sediments (Schmitt et al., 1989). Continued interest in the REE potential of the Eden Lake Complex prompted the need to complete

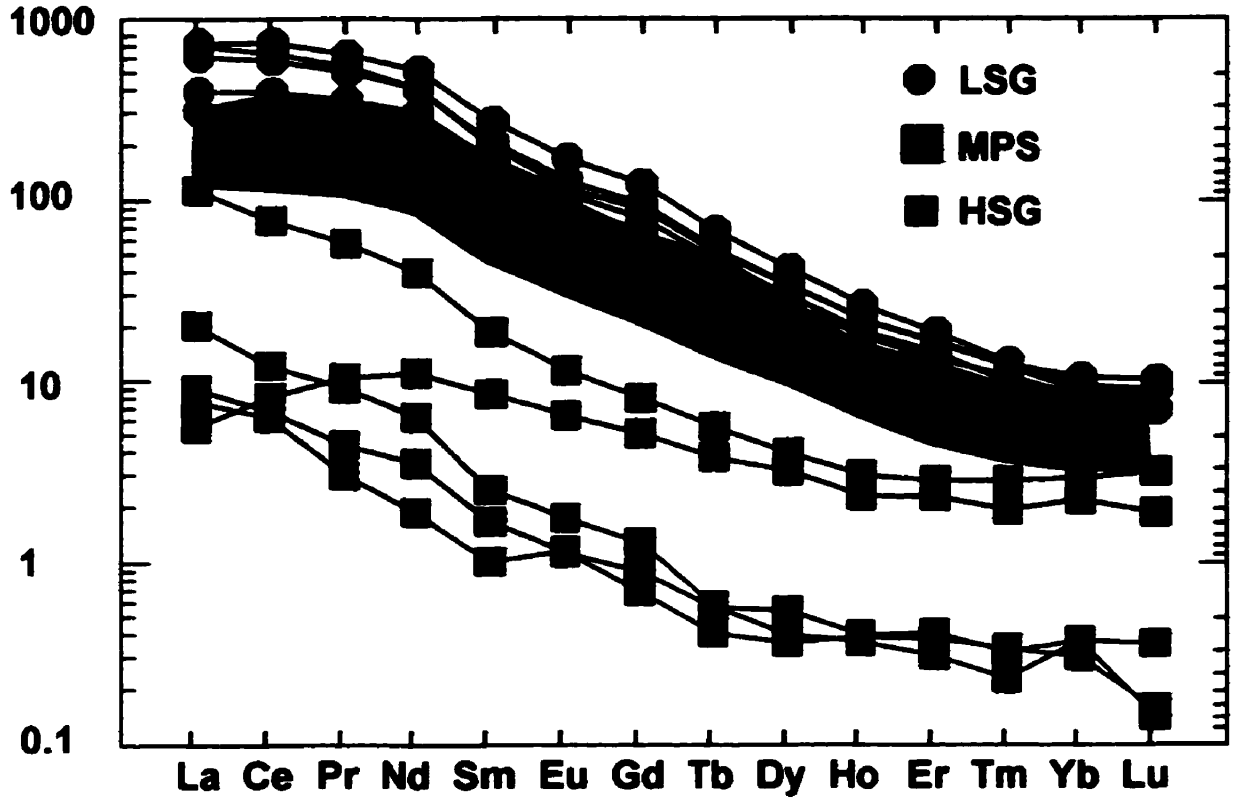

Figure 2.9. Chrondrite-normalized REE plot of the rocks from the Eden Lake Complex (from Halden and Fryer, submitted).

reconnaissance ground scintillometer surveys over the intrusion to provide a ground-based radiometric signature for the intrusion, find any other anomalously high areas previously unidentified, and delineate the occurrence and nature of these radioactive zones (McRitchie, 1989; Young and McRitchie, 1990; Gunter et al., 1995). Three surveys were conducted: one in 1989 by McRitchie, one in 1990 by Young and McRitchie, and another in 1993 by Fedikow, Dunn, and Kowalyk.

Figure 2.10 shows the results of the 1989 ground scintillometer reconnaissance, conducted using a Scintrex Broadband gamma-ray scintillometer model BSG-1SL (with a 1.5" x 1.5" thallium activated sodium iodide crystal; McRitchie, 1989). The radiometric readings are recorded as counts per second (cps), with total cps recording potassium, equivalent uranium, and equivalent thorium. Daily background readings ranged from 25 to 30 cps and noticeable drop-off in counts per second occurred over all overburden areas, especially in wet open swamps where source rocks are presumably covered by thick overburden. Waist-level and on-the-ground measurements differed markedly over hot-spots (which tended to be clustered locally in all three outcrops) and along zones of strong radioactivity, however, little or no contrast was noted for background readings taken in areas of open outcrop. A thin veneer of soil or clay (10 to 20 cm) was found to cause a moderate reduction in readings taken at waist level. The monzonite outcrops in all three ridges consistently gave readings of 150 to 300 cps. The greater proportion of the readings were near the upper level of this range which is consistently higher than the 150 to 250 cps readings obtained from the outlying granitic phases.

Most occurrences with elevated readings exhibit a prominent rusty weathering, that is associated with oxidized pyrite mineralization (McRitchie, 1989). Forty of the features were hot-spots of limited lateral extent (Figure 2.10). The extremely localized (1200 to 6000 cps) hot-spots (10 to 20 cm) corresponded to individual or clustered radioactive minerals while the local hot-spots (1000 to 4000 cps) corresponded with 30

cm to 1.5 m fractures exhibiting splayed terminations. Four hot-spots constituted pyroxene and allanite-enriched zones ranging in length from 1.5 to 40 m with 2500 to 7000 cps, and there were 3 m, 5 x 150 m and 11 x 25 m zones of moderately elevated readings ranging from 400 to 500, 400 to 800, and 400 to 1500 cps, respectively.

The 1990 ground scintillometer reconnaissance survey traversed an area west of "Spur" Lake, crossing the regional trend of the zones of REE enrichment defined by McRitchie (1989) south of Kwaskwaypichikun Bay (Figure 2.11 and 2.12). Both the background radiation and elevated responses detected in this area were generally lower than those detected by McRitchie (1989), but were attributed to the same features (Young and McRitchie, 1990).

The 1993 ground scintillometer survey was carried out in conjunction with a vegetation geochemical study (Fedikow et al., 1993). The study area is shown in Figure 2.13. A Scintrex Broadband gamma-ray scintillometer (model BSG-1SL with a 1.5" x 1.5" thallium activated sodium iodide crystal) was used again; this time taking measurements at ground level from each of the vegetation sampling stations on the grid (Figure 2.14). Radiometric readings are plotted on Figure 2.15 with the addition of a 500 cps contour. This contour effectively delineates the allanite- and britholite-bearing fractures, as well as the smaller rusty-weathered pyrite-bearing fractures in the study area. Background measurements ranged from 100-220 cps. The highest responses in this survey (1150 to 3900 cps) correlate with pegmatite-hosted occurrences of pods, lenses, veinlets, and disseminated grains of britholite and allanite. These veinlets, pods, and lenses are spatially associated with faults in the monzonite which have a strike of 014°. The faults have been traced intermittently for up to 80 m and are generally rusty weathered and show a marked increase in radioactive response relative to the surrounding country rocks (Figure 2.15).

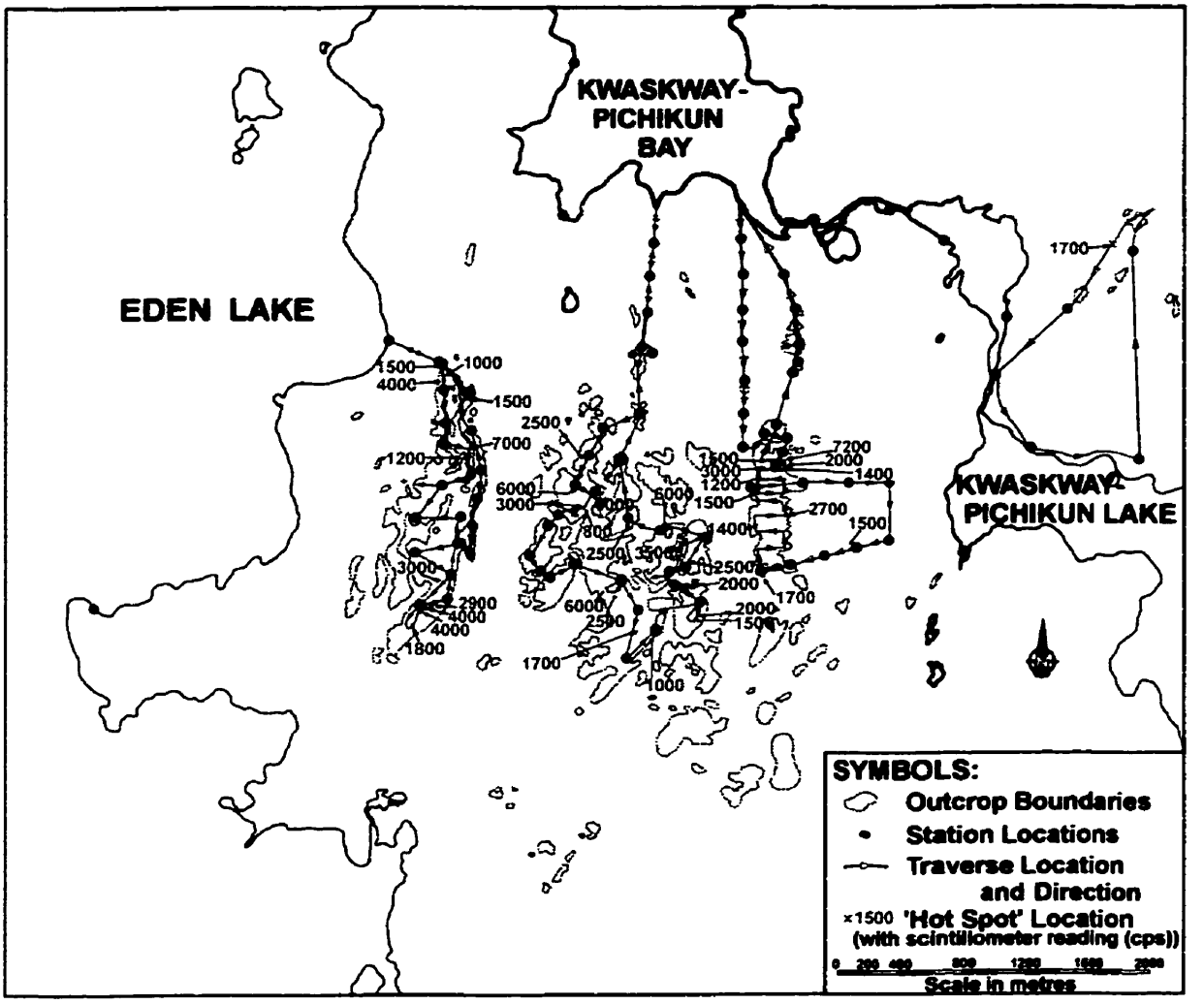

Figure 2.10. **Results of the 1989 ground scintillometer reconnaisance of the Eden Lake monzonite. All radiometric measurements were taken at waist level and on the ground (after McRitchie, 1989). Station location numbers and scintillometer readings at each station are provided in McRitchie (1989).**

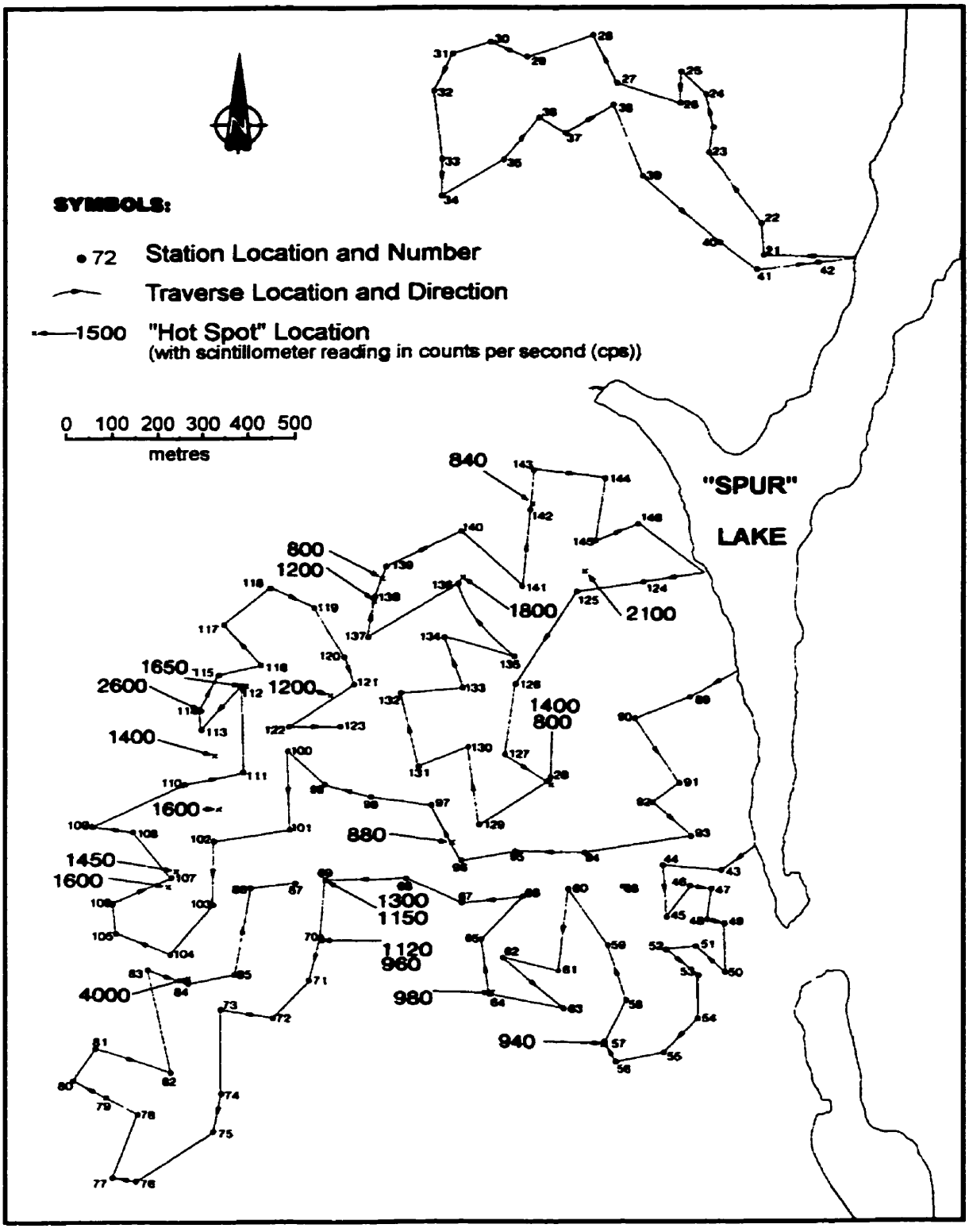

Figure 2.11. Results of the 1990 ground scintillometer reconnaissance of the Eden Lake biotite monzogranite. All radiometric measurements were taken at waist level and on the ground (after Young and McRitchie, 1990).

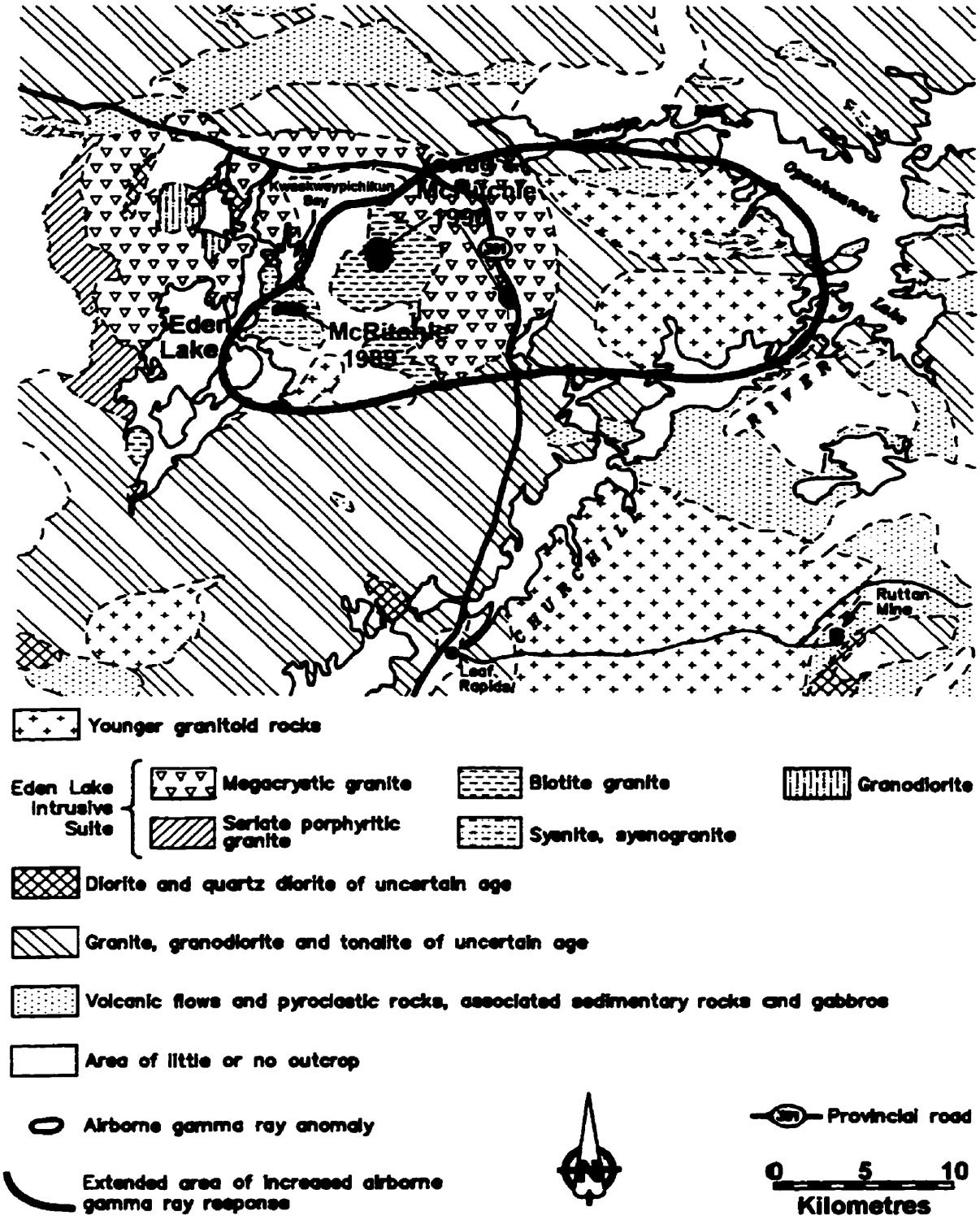

Figure 2.12. Simplified geological map showing the location of anomalous areas of radioactivity in the Eden Lake area and the locations of the 1989 and 1990 ground scintillometer surveys (after Young and McRitchie, 1990).

2.3 Biogeochemistry

Vegetation geochemical surveys were carried out at Eden Lake by Fedikow et al. (1993;1994). These studies were aimed at determining if vegetation geochemistry could assist in delineating the REE-enriched mineralization since Eden Lake is considered to be free of anthropogenic contamination. The study area (Figure 2.13) contained mature boreal forest growing on isolated outcrop and outcrop ridges and in low-lying areas of swamp and muskeg developed on glacial clay and sand till. The vegetation in the survey area was dominantly black spruce and lesser stands of jack pine, with white spruce, birch, poplar, and willow occurring sporadically. Alder and Labrador tea were predominant among the shrubs and the outcrop areas were covered by a mixture of lichen and blueberry.

In the first orientation survey, in 1993, vegetation tissues were collected from within a 5 m^2 sampling box centered on the vein-type allanite and britholite mineralization (Fedikow et al., 1994). Approximately 350 g of eight year old black spruce twigs were collected from the north, south, each, and west sides of the tree (about chest height) at each sampling station (Figure 2.14), and one sample was taken representing the crown (or upper 40 cm) of a black spruce (Fedikow et al., 1993). For jack pine, alder, and birch the most recent 45 cm of growth was sampled. The leaves or needles of all collected samples were separated from the twigs and both of these were separated from both bark and cones. The samples were then ashed (470 °C) for analysis by neutron activation. The needles and twigs collected at chest height from the black spruce were kept separate from the needles and twigs collected from the crown of the tree to allow comparison.

A summary of the available geochemical data for the vegetation species and tissues sampled in 1993 is provided in Appendix A (Table 1; Fedikow et al., 1994). The

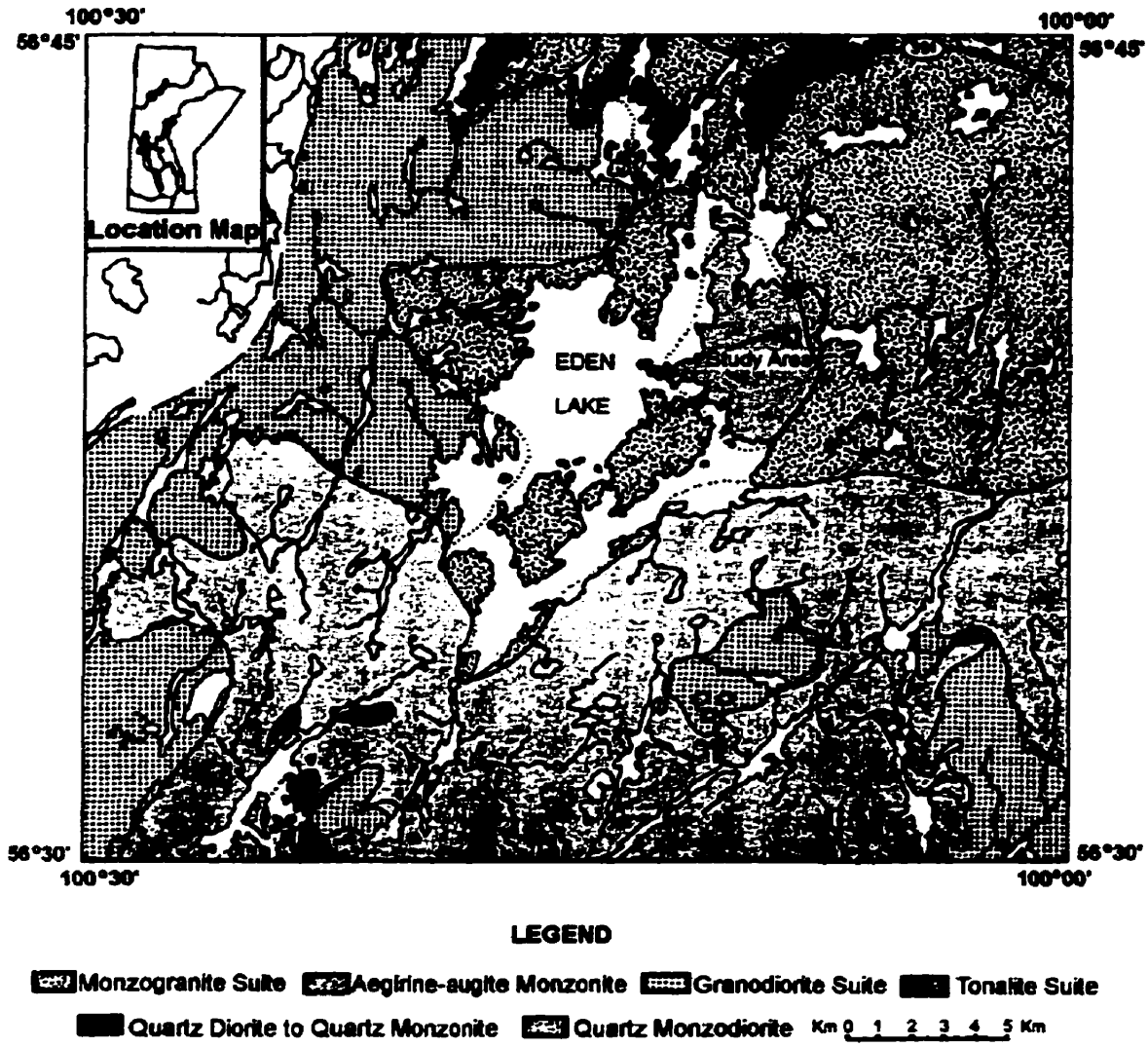

Figure 2.13. Location map and regional geological setting for the Eden Lake vegetation geochemical and radiometric survey area (from Fedikow et al., 1993).

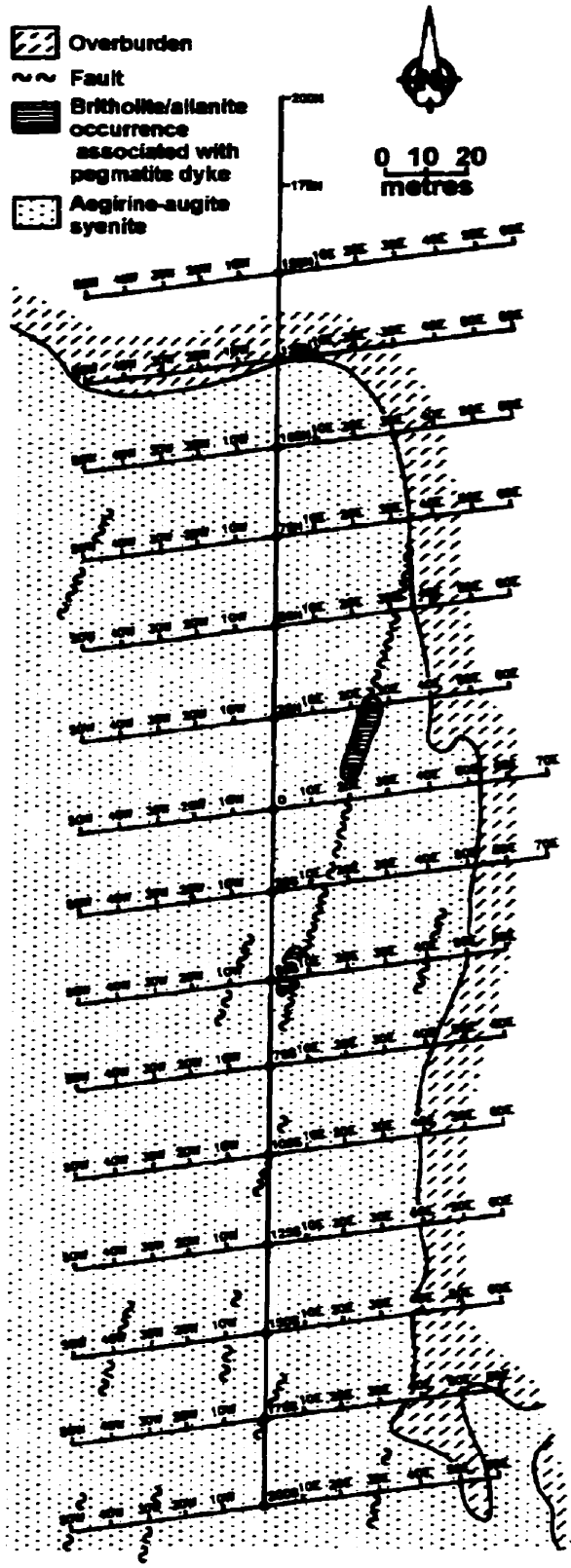

Figure 2.14. Geological and vegetation sampling and radiometric survey grid map (stations were set at 10 m intervals from lines 25 m apart) (from Fedikow et al., 1993).

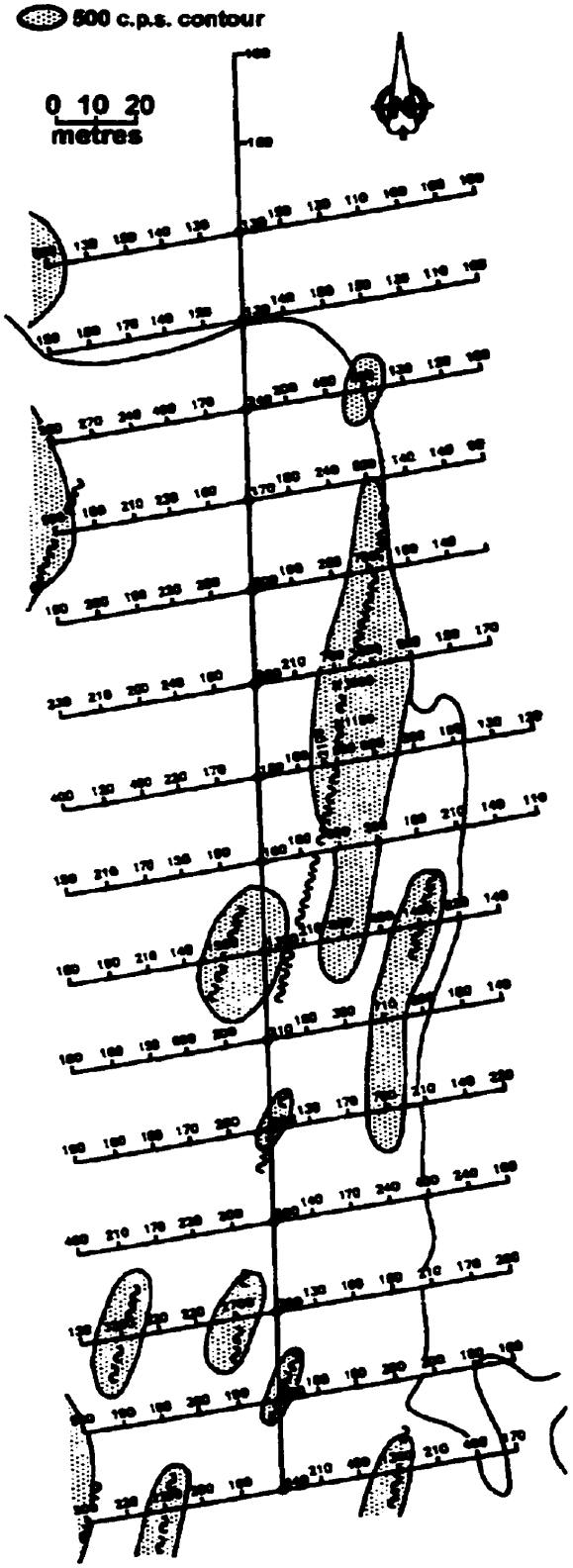

Figure 2.15. **Results of the 1993 ground scintillometer survey. All radiometric measurements were taken at ground level (from Fedikow et al., 1993).**

enrichment of the LREE La, Ce, and Nd indicated in the analyses of the allanite and britholite (Young and McRitchie, 1990) are reflected in the analyses of some of the vegetation tissues sampled for the orientation survey. The highest concentration of La, Ce, Nd, and, to a lesser degree, Sm are present in the alder twigs. The total REE content of the alder twigs is 757.5 ppm that exceeds that of lichen at 415.3, the second most efficient vegetative tissue for concentrating these elements at the site. Alder leaves also contain highly elevated LREE concentrations: Ce = 120 ppm; La = 93 ppm; Nd = 66 ppm.

The LREE contents of the black spruce needles collected at chest height are comparable to those from the crown whereas chest height twigs contain higher LREE and total REE (57.2 ppm) than the crown twigs (14.6 ppm) (Fedikow et al., 1994). Crown cones have comparable LREE and total REE to both crown needles and twigs. Overall, the chest high twigs from the black spruce contain approximately twice the total REE and higher LREE (57.2 ppm) than any other collected tissues on the tree (Table 1; Appendix A).

The jack pine samples contain significant concentrations of REE (Table 1; Appendix A; Fedikow et al., 1994). The highest REE contents of the six tissue types collected occur in the outer bark (total REE = 165.0 ppm). Jack pine twigs, needles, cones, trunk wood, and inner bark have a lower range of total REE of 9.8 to 25.6 ppm. Base and precious metal contents of all vegetation tissues are low, with the exception of a single analysis of 2% Zn in birch twigs (Fedikow et al., 1994). However, exceptional contents of Ba and Sr are found in tissues from black spruce, alder, and birch (Table 1; Appendix A). Chest high black spruce tissues contain 2050 to 4300 ppm Ba and 5100 to 6400 ppm Sr. Alder twigs contain both the highest Ba (6900 ppm) and Sr (1.2%) of all the vegetative tissues collected in the 1993 orientation survey. The proposed source for this Ba and Sr is twofold: (1) from the rocks (aegirine-augite monzonite) of the complex

which contain between 1300 and 3300 ppm Ba and 1400 and 2200 ppm Sr (McRitchie, 1989; Halden and Fryer, 1999) and the soil horizon developed above this bedrock (Fedikow et al., 1994); and (2) from the allanite-britholite mineralization (cf. Arden, 1995).

The U and Th contents for the Eden Lake monzonite are in the range of 690 to 1400 ppm and 775 to 3500 ppm respectively (McRitchie, 1989; Young and McRitchie, 1990). However, despite this high background level, all tissues collected in the orientation study in 1993, with the exception of lichen and jack pine outer bark, are below 1 ppm for both U and Th (Table 1; Appendix A). Lichen contains 8.1 and 4.5 ppm Th and U, respectively, whereas jack pine outer bark contains 4.5 ppm Th and 2.4 ppm U. Alder twigs do not contain measurable Th and U (<0.1 ppm Th and <0.2 ppm U) despite their high concentrations of LREE. No data was available for Mn concentrations in the vegetation.

The 1993 orientation study concluded that LREE concentrations in alder twigs could be used to delineate the occurrences of some of the REE-enriched pegmatites associated with the complex (Fedikow et al., 1994). In 1994, guided by this conclusion, sampling was concentrated to an area approximately 200 m downslope from the allanite-britholite mineralized zone in relatively well drained areas of no outcrop (Figure 2.16) (Fedikow et al., 1994). Alder twigs were collected from 57 sites and ashed (470 $^{\circ}$C) for analysis by neutron activation. The results of this vegetation survey are not yet available.

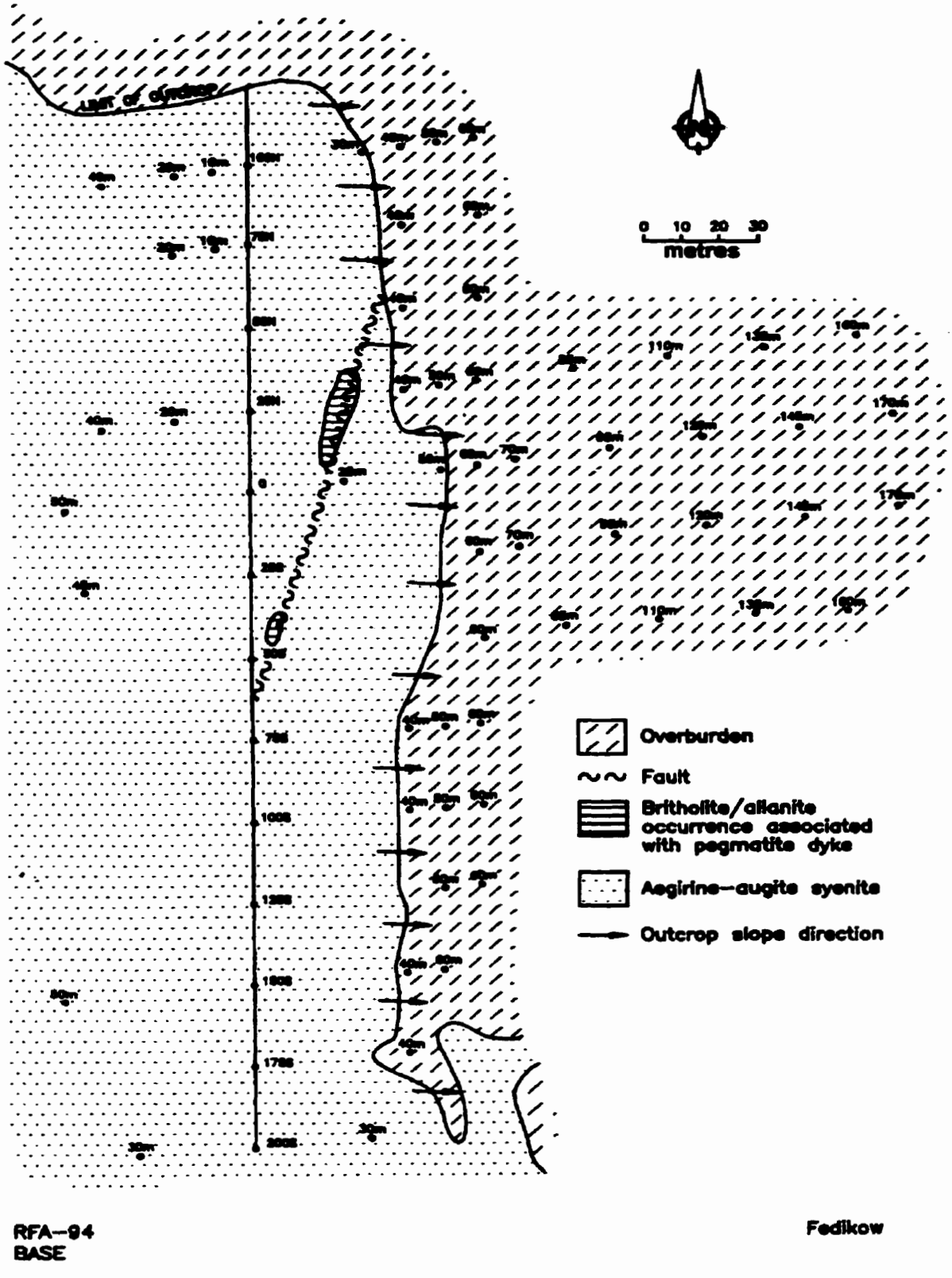

Figure 2.16. Location of alder twig samples collected at the allanite-britholite occurrence, Eden Lake area, 1994 (from Fedikow et. al, 1994).

2.4 Eden Lake Physiography

Eden Lake is an irregularly-shaped lake (Figure 2.17) that is approximately 18 kilometres long, 12 kilometres wide and covers an estimated 150 km^2. The Eden Lake shoreline sits at 300 metres (900 feet) above sea level and is rocky and highly vegetated (Figure 2.18). The northern outflow point of the lake (by the campsite and Hwy. 391 (marked "camp")) up to the central part of the lake, by the Eden Lake Complex (marked "ELC") is less than 7 metres (20 feet) deep (Figure 2.17). The water depth gently shallows to <1 m towards shore all around the lake and around the islands. The islands are also rocky and highly vegetated (Figure 2.19) to sparsely vegetated (Figure 2.20). The lake's average depth is ~7 to 10 m, but it reaches >27 metres (80 feet) in the central part of the lake and in the south near the Numakoos River (Figure 2.17). The lake bottom varies from rock, gravel, or coarse sand near shore (<2 metres deep) to fine mud as the water depth increases to >2 metres. Many shallow shoals and large rocks are present around the lake and some of these are shown by an "x" in Figure 2.21. These shoals are often reedy.

Eden Lake flows under Hwy. 391 into the Hughes River and on into Adam Lake at the northern end (Figure 2.21). This outflow is through a rock-filled culvert next to the campsite area. Northern pike are the only large fish known to inhabit the lake, suggesting that not many fish, if any, leave Eden by this route. Eden Lake also flows out at the south into the Numakoos River and into Kakinokumak Lake (Figure 2.21).

Inflow sites to Eden Lake are from Kwaskwaypichikun Bay, which is fed by Kwaskwaypichikun Lake, to the east; from Muskose Bay, which is fed by Kaministokos Lake, to the west; and from the Hughes River, which is fed by Pilote Lake, in the northwest (Figure 2.21). These inflow points are shallow sites of rapidly moving water over a very rocky substrate.

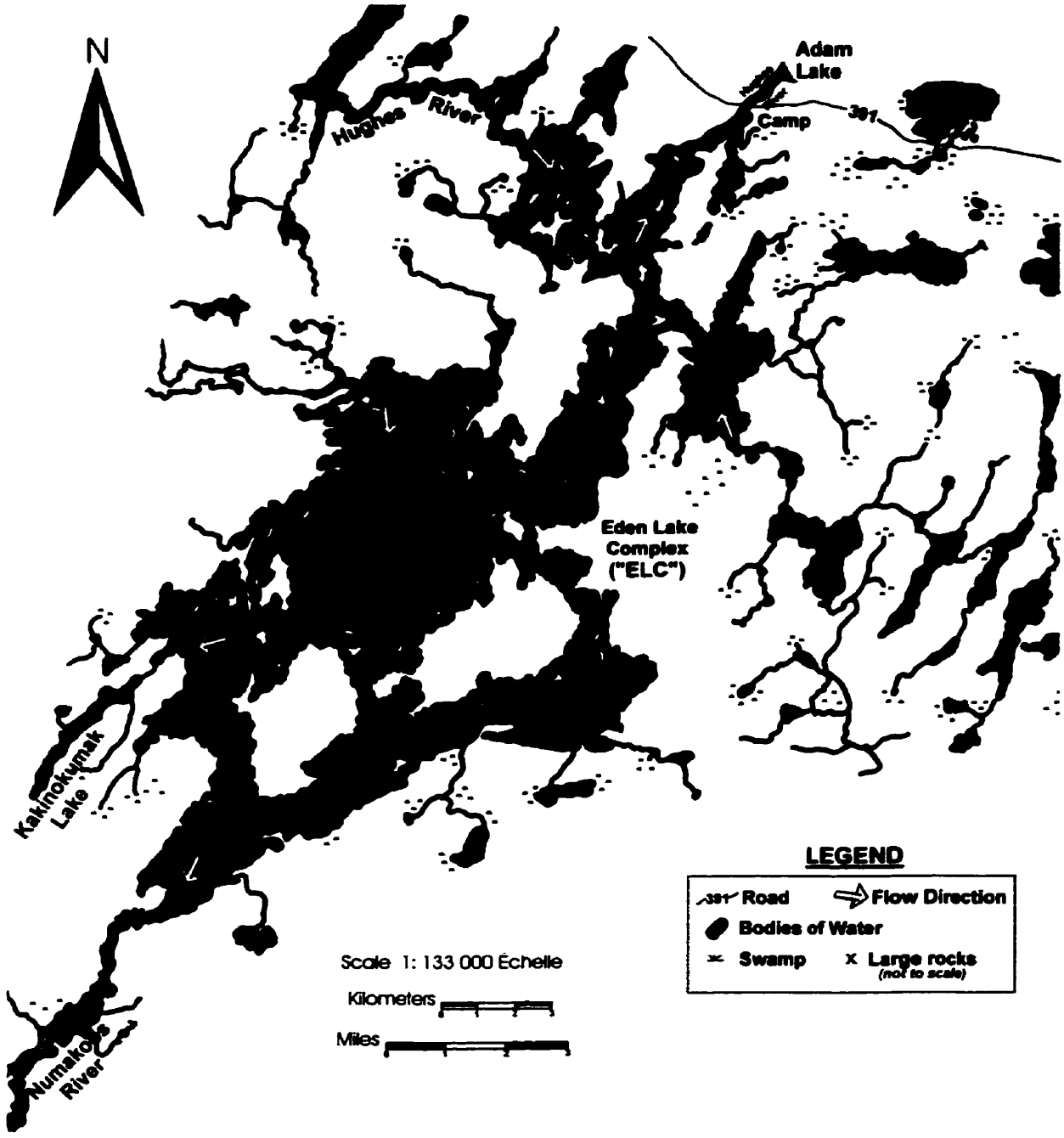

Figure 2.17. Map of Eden Lake. Eden Lake is approximately 18 kilometres in length, 12 kilometres wide and covers about 150 square kilometres. Also shown are the locations of large rocks ("x") and lake flow direction (yellow arrows).

Figure 2.18. **Photograph of the highly vegetated Eden Lake shoreline.**

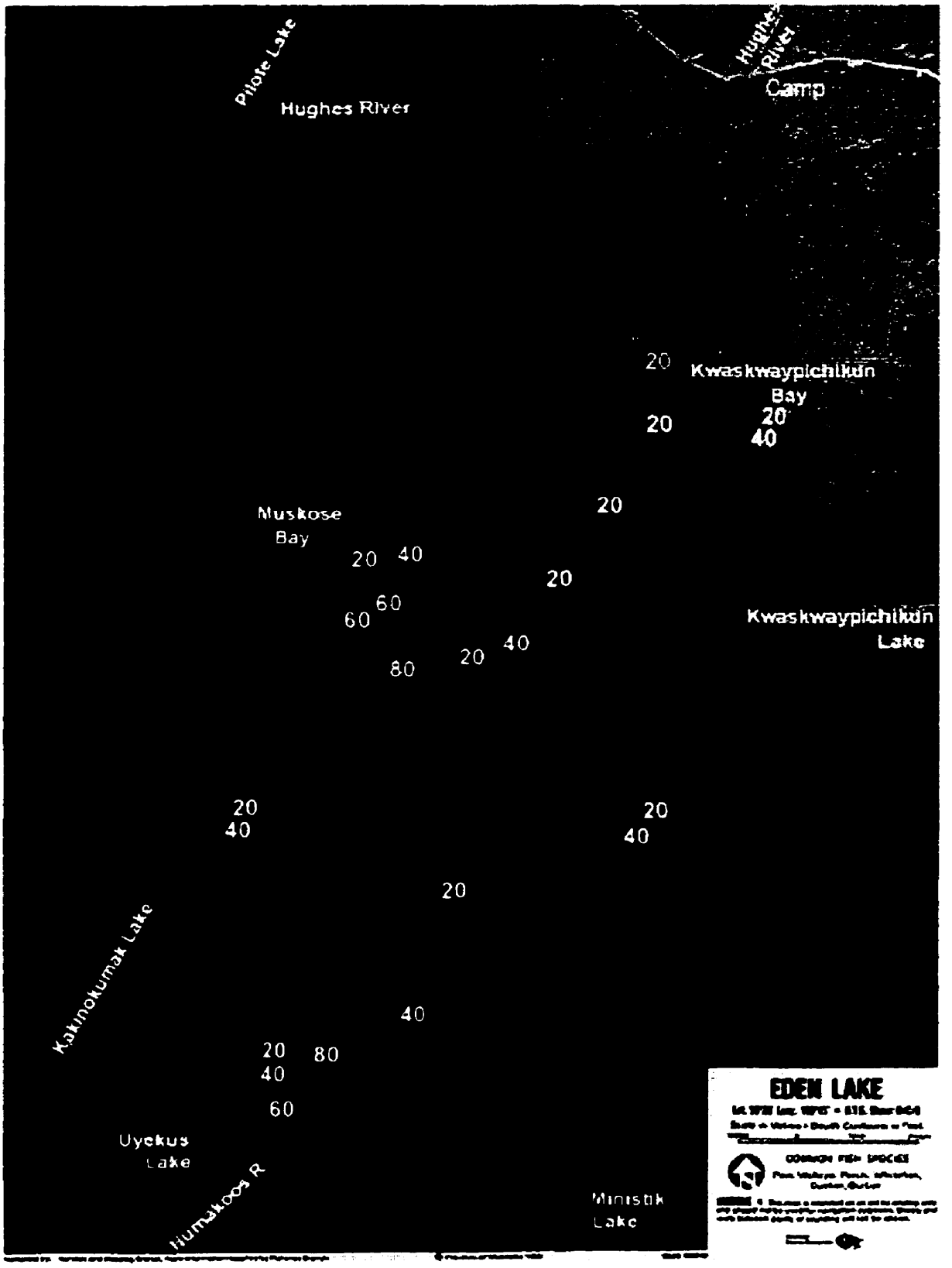

Figure 2.19. **Aerial photograph of Eden Lake showing water depths in feet.**

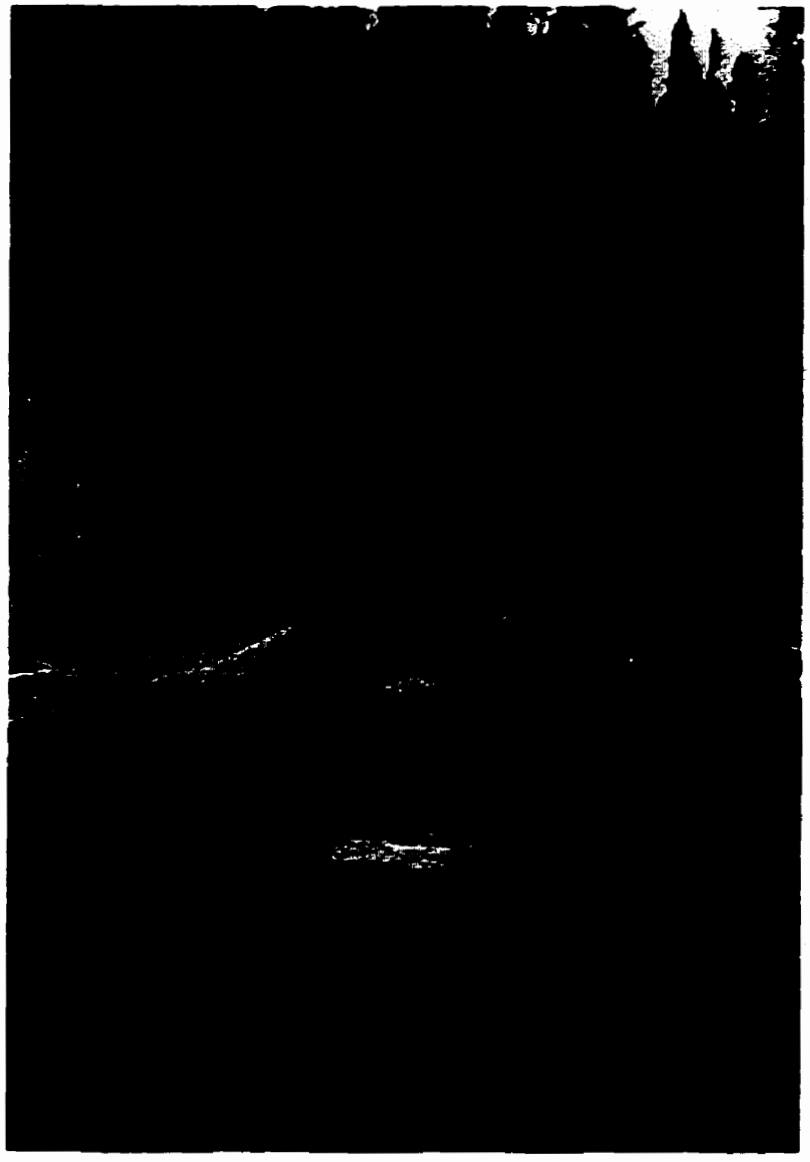

Figure 2.20. **Photograph of the rocky and highly vegetated islands in Eden Lake.**

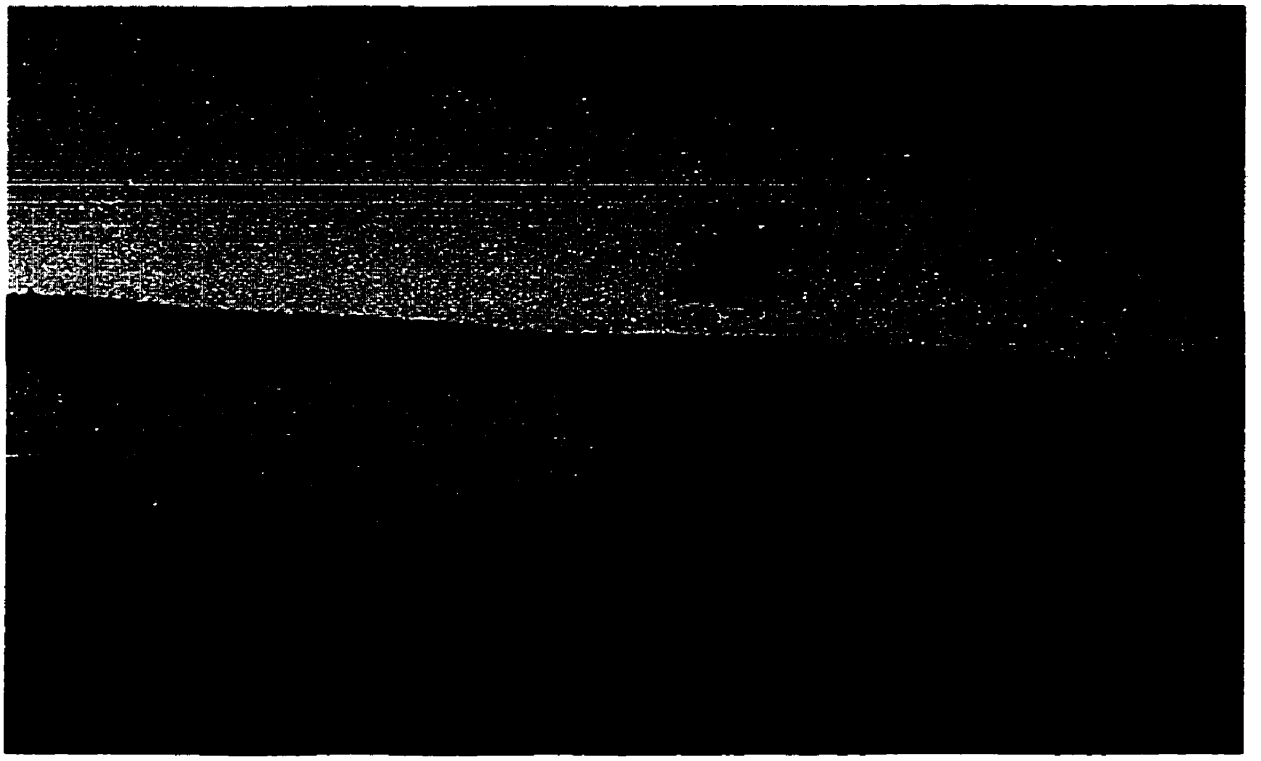

Figure 2.21. **Photograph of the rocky and sparsely vegetated islands in Eden Lake.**

There is no information available regarding the hydrology and limnology of Eden Lake (Natural Resources, August 1999, *pers. comm.*). The water is presumably derived primarily from river inflow and direct precipitation and diffuse runoff, though groundwater inflow also likely contributes. There is no data on the chemical signatures of these sources, nor any information on the hydrologic budget for the lake. Additionally, there is no systematic information on the degree of thermal stratification in the lake, though the potential for it exists. Warm surface waters (~0.7 to 1 m deep) were observed during the summer months, however, this developing thermal stratification is continually disturbed by the prevailing wind.

The closest anthropogenic influence to Eden Lake is the mine in Lynn Lake, located 50 km west of Eden Lake. This mine has been periodically operational over the past 50 years. No measurements have been done regarding any aerosol input to the Eden Lake region from Lynn Lake, however, it is likely that the northwesterly winds preclude any significant distribution to the area.

Climate, flood and fire data is the only environmental information available for the Eden Lake area. There is an Environment Canada Climate Station located in Lynn Lake that records daily temperature and precipitation. This data indicates that the climatic environment of Eden Lake has remained relatively constant over the last 21 years. The mean spring (i.e., March, April and May), summer (i.e., June, July and August), fall (i.e., September, October and November) and winter (i.e., December, January and February) temperatures are -3°C, 14°C, -5°C and -22°C, respectively.

Flooding is a relatively common occurrence in the Eden Lake area, however, many of the floods are small, only marginally increasing the water levels (Natural Resources, February 1999, *pers. comm.*). There have been four "good-size" floods in the Eden Lake area, in 1974, 1975, 1976 and 1977.

Forest fires are also very common in the Eden Lake area. The area is a spruce boreal forest and at least one fire occurs somewhere between Leaf Rapids and Lynn Lake every year, with 90% of these fires occurring between the 1st of July and the beginning of August.

Chapter 3: Experimental Methods

3.1 Sample Collection

Four netting locations, KAP, KAP1, ED1, and ED2 were chosen in the immediate vicinity of the Eden Lake Complex (Figure 3.1). Samples taken from these localities would comprise the bulk of the catch (Table 3.1). To limit the number of fish caught in each net, each net was set out at night and collected early the following morning (Table 3.2).

Two additional netting locations, BAK1 and BAK2, were chosen at inflow sites far from the complex (Figure 3.1). These were intended to provide background samples for comparison to the fish caught at the other four locations proximal to the intrusion (Table 3.1). To further limit by-catch, these nets were set even later at night and collected earlier in the morning than the other four as only about two fish of each species were desired from each location (Table 3.2). The period of time each net was set could not be shortened in order to ensure that a sufficient number of species were caught. A selection of fish, representative of each species, from each net were taken, the same day they were caught, to the Energy and Mines freezer in Lynn Lake and frozen until they could be transported back to Winnipeg (Table 3.3).

Additional fish and fish heads were angled and acquired from sport fishermen staying at the Eden Lake campsite, respectively (Table 3.4). The sport fishermen, aware of our project, kept track of where they were fishing and gave us the heads when they were filleting at the end of each day. This provided a good overall sample set of Eden Lake as most of the fishermen were fishing in areas that were not netted and were not accessible by the zodiac. In total, 172 fish, including walleye; northern pike; lake whitefish; white and long-nose suckers; cisco; yellow perch; and burbot, were brought back for analysis.

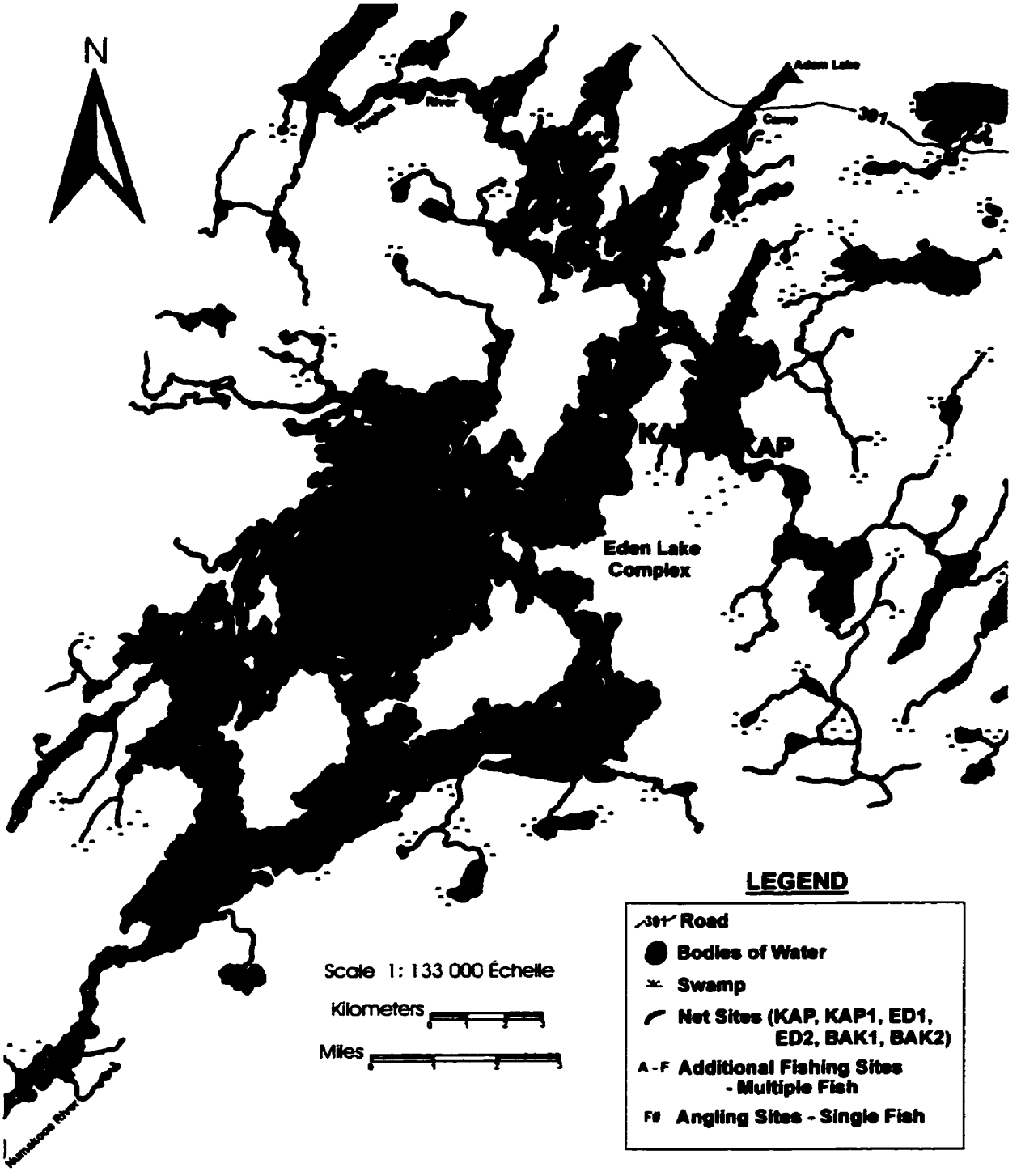

Figure 3.1. Map showing the locations of the six nets set up on Eden Lake: KAP, KAP1, ED1, ED2, BAK1 and BAK2, and the additional fishing and angling sites.

Table 3.1. **Total catch from the six nets.**

KAP YIELD	KAP1 YIELD	ED1 YIELD	ED2 YIELD	BAK1 YIELD	BAK2 YIELD
1 lake whitefish	3 lake whitefish	1 lake whitefish		4 lake whitefish	6 lake whitefish
1 long-nose sucker					
16 white suckers	25 white suckers	35 white suckers	17 white suckers	17 white suckers	41 white suckers
21 northern pike	7 northern pike	17 northern pike	11 northern pike	21 northern pike	6 northern pike
11 walleye	4 walleye	3 walleye	5 walleye	16 walleye	15 walleye
2 cisco	17 cisco			1 cisco	
13 yellow perch	2 yellow perch	1 yellow perch	4 yellow perch	5 yellow perch	4 yellow perch
		1 burbot		1 burbot	
8 trout perch	1 trout perch	7 trout perch	1 trout perch	19 trout perch	
		1 mottled sculpin		2 mottled sculpins	
13 spottail shiners	16 spottail shiners	7 spottail shiners	2 spottail shiners	26 spottail shiners	47 spottail shiners
				2 log perch	
1 emerald shiner					13 emerald shiners
		1 clam	1 clam	1 clam	3 clams
	11 unknown small fish		4 unknown small fish	1 unknown small fish	2 unknown small fish
= 87 fish	= 86 fish	= 73 fish	= 44 fish	= 115 fish	= 134 fish

Total netted catch = 539 fish

Table 3.2. **Setting and collecting times for the six nets.**

NET LOCATION	SET TIME		COLLECTION TIME	
	TIME	DATE	TIME	DATE
KAP	3:00 p.m.	June 8, 1997	10:00 a.m.	June 9, 1997
KAP1	9:30 p.m.	June 8, 1997	10:30 a.m.	June 9, 1997
ED1	5:00 p.m.	June 9, 1997	12:10 a.m.	June 10, 1997
ED2	5:15 p.m.	June 9, 1997	12:20 a.m.	June 10, 1997
BAK1	9:45 p.m.	June 10, 1997	9:20 a.m.	June 11, 1997
BAK2	10:30 p.m.	June 10, 1997	10:00 a.m.	June 11, 1997

Table 3.3. **Number of fish (of each species) from each net selected for sample set.**

KAP	KAP1	ED1	ED2	BAK1	BAK2
5 walleye	3 walleye	3 walleye	5 walleye	3 walleye	2 walleye
6 white suckers	6 white suckers	6 white suckers	5 white suckers	2 white suckers	2 white suckers
1 long-nose sucker					
6 northern pike	7 northern pike	5 northern pike	5 northern pike	2 northern pike	2 northern pike
6 yellow perch (one from NP stomach)			4 yellow perch (one from NP stomach)	2 yellow perch	2 yellow perch
		1 burbot		1 burbot	
1 whitefish	3 whitefish			3 whitefish	2 whitefish
	8 cisco				
25 fish	27 fish	15 fish	19 fish	13 fish	10 fish
Total for Sample Set (from nets) = 109 fish					

Table 3.4. **Additional fish and fish heads brought back to be part of sample set.**

Species	Source	Part of Fish Collected	Location
2 Northern Pike	Sport fishermen	Head only	See map
1 Northern Pike	Angled	Whole fish	See Map
2 Walleye	Angled	Whole fish	See Map
8 Walleye	Sport fishermen	Head only	Narrows
6 Walleye	Angled	Whole fish	Narrows
6 Northern Pike	Angled	Whole fish	Narrows
1 White sucker	Angled	Whole fish	Narrows
2 Northern Pike	Angled	Whole fish	Pt. A
5 Walleye	Sport fishermen	Head only	Pt. B
11 Walleye	Sport fishermen	Head only	Pt. C
1 Walleye	Angled	Whole fish	Pt. D
6 Walleye	Sport fishermen	Head only	Pt. E
1 Walleye	Angled	Whole fish	Pt. E
1 Northern Pike	Angled	Whole fish	Pt. F
4 Walleye	Sport fishermen	Head only	KAP
1 Northern Pike	Angled	Whole fish	Campsite
2 Northern Pike	Angled	Whole fish	Adam Lake
3 Northern Pike	Angled	Whole fish	Jackson Lake
Total for Sample Set = 63 fish			

Clams were also collected from a few different locations in Eden Lake and from the neighboring Adam Lake (Table 3.5). These organisms were of interest because they are sessile (in comparison to the fish), tending to stay on rocks or plants or in the sediment, and therefore could potentially provide valuable supporting information as to the trace element concentrations in different areas of the lake as determined by the fish. In total, 8 live clams of two different species were collected from 5 different locations.

3.2 Sample Preparation

3.2.1 Fish

The weight, sex, maturity, and fork length (FL) of each fish in the select sample set was recorded before the otoliths were extracted (Tables 2 and 3; Appendix A). The otoliths in all species of fish are encased in an aqueous sac called the endolymphatic sac and located at the top of the head, approximately 1 inch in front of the join between the head and body (Figure 3.2). The original procedure for removing the otoliths is to go in from the underside of the fish (Figure 3.3). However, most of the fish brought back were very large and their spines were too thick to be cut using the bone cutters. Therefore, an easier way to access the otoliths was to use a hacksaw and cut into the head approximately 1.5 inches from the join between head and body and then remove the otoliths with a pair of forceps. Once removed from the fish, the endolymphatic sac was removed and the otolith dried off and placed in a labeled sample envelope until the samples could be sectioned.

Before sectioning, the otoliths were embedded in epoxy as they were very small (from millimetres to a centimeter wide and millimetres to more than a centimeter long) and very brittle. This procedure involved lining ice cube trays with parafilm, to ease removal after curing, and filling the trays with enough epoxy to cover the otolith (Figure 3.4). The epoxy, which was cold curing, was left to cure for 2 full days.

Table 3.5. **Clam (CL) samples collected from Eden and Adam Lakes.**

CLAM (CL) NUMBER	LOCATION COLLECTED
CL1	ED1
CL2	Adam Lake
CL3	Adam Lake
CL4	BAK1
CL5	ED2
CL6	BAK2
CL7	BAK2
CL8	BAK2

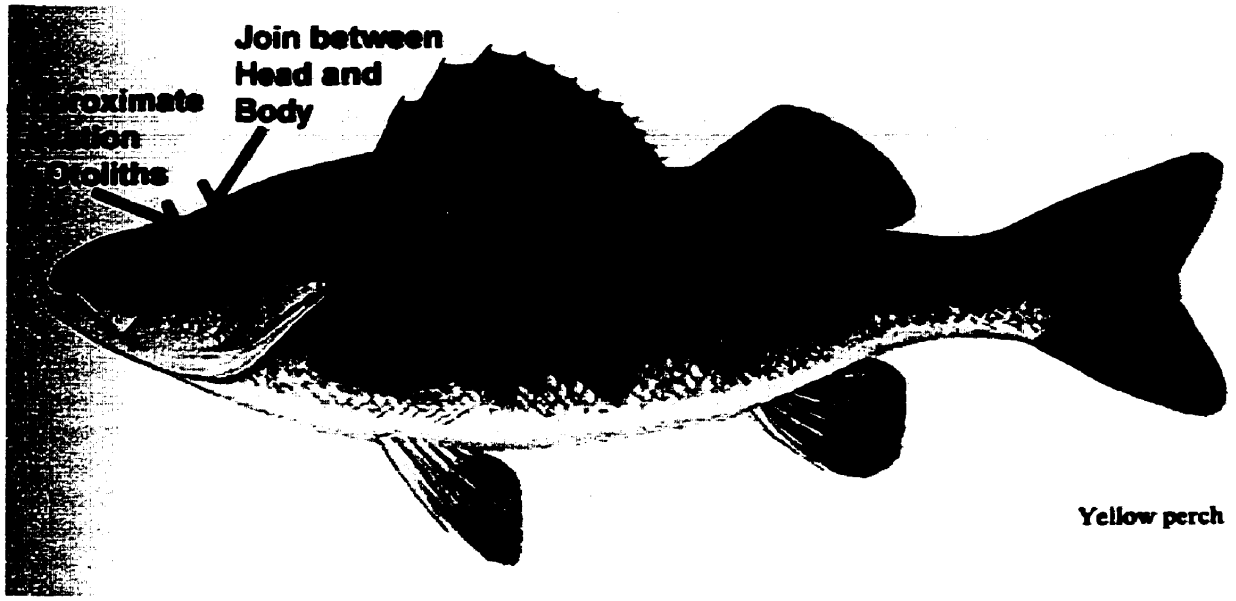

Figure 3.2. **Illustration showing the approximate location of the otoliths in a fish.**

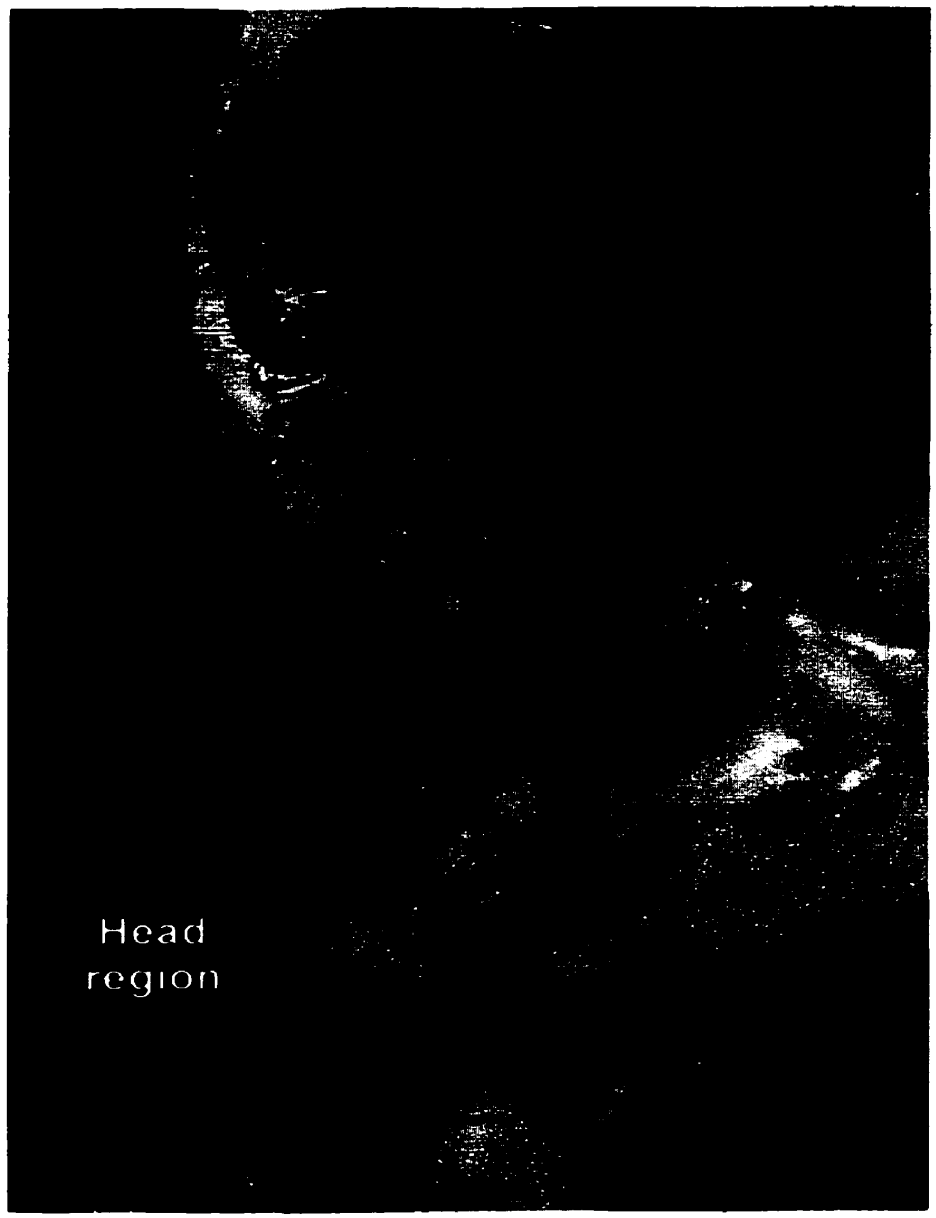

Figure 3.3. **Photograph of the traditional procedure for removing otoliths by going in from the underside of the fish.**

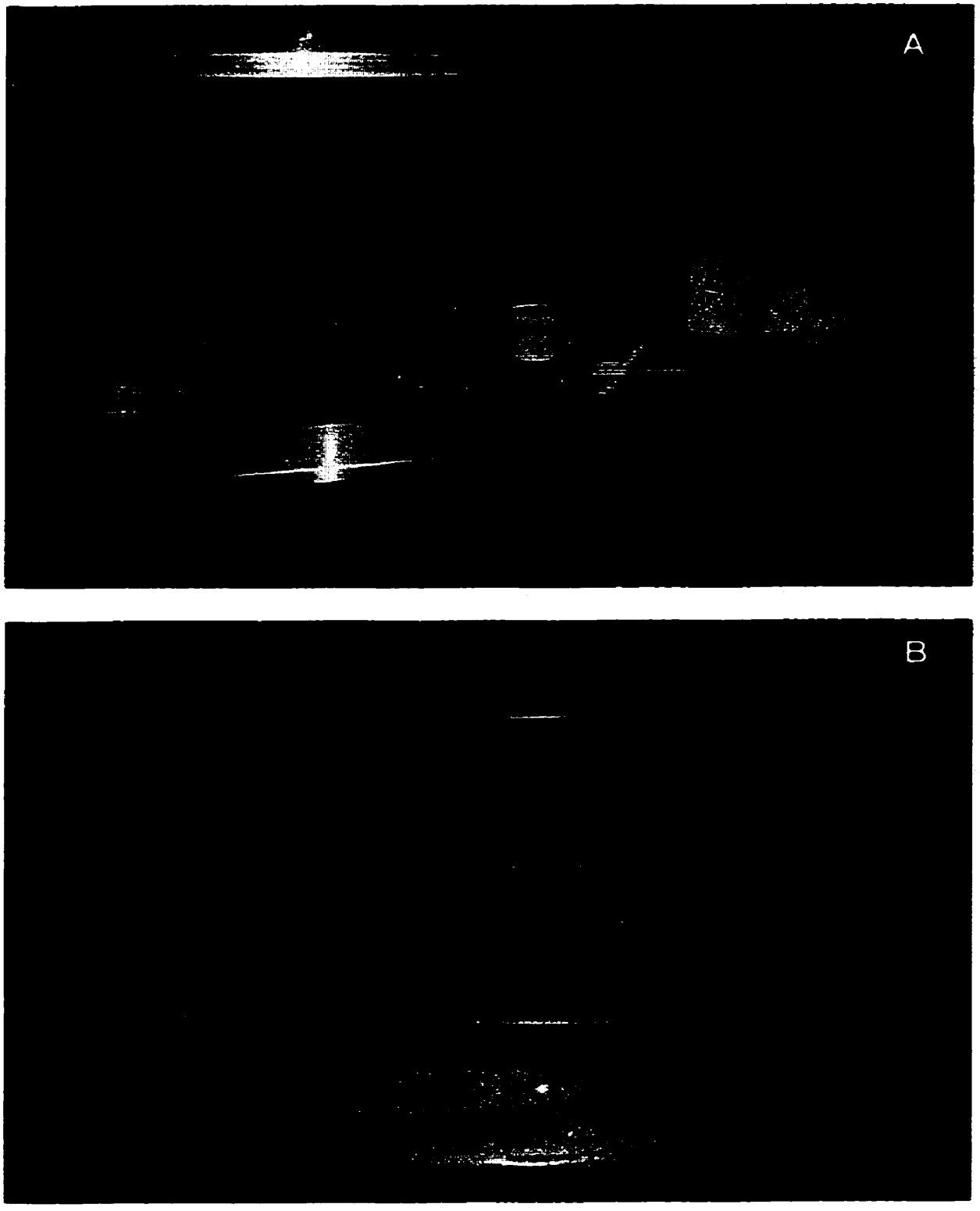

Figure 3.4. Photographs of the embedding process. (A) Under a fume hood, the ice cube trays are lined with parafilm and filled with a few millimeters of epoxy. (B) A close-up of one of the ice cube trays full of embedded otoliths.

The epoxy-embedded otoliths were then sectioned using a thin-section saw with a 4 x 0.004 x 0.5 diamond wafering blade (Figure 3.5). They were cut in half along a longitudinal section through the primordium and then further trimmed to fit into holes that have been made in a 1" thick perspex disk. A longitudinal section is preferred because the annuli are vertical and of uniform thickness from one side of the otolith to the other while in a sagital section, the annuli dip at a shallow angle towards the center of the otolith.

The original method for mounting the otoliths is to first secure the perspex disks containing the holes into a holder lined with tin foil. The tin foil prevents any epoxy from leaking out of the disk and prevents the disk from sticking to the holder. The otoliths are segregated according to species and location and then placed into the holes (anywhere from 4 to 7 per disk) (Table 4; Appendix A), such that the sides of the otoliths that are of interest are face down and all aligned (Figure 3.6). This part of the procedure is very time consuming, as it is necessary to fit the epoxy-embedded otolith perfectly in the hole to insure that it stays flush with the surface of the disk. This involves custom-fitting each hole to each otolith. This would not be a problem if the otoliths were all approximately the same size, however, the Eden Lake otoliths, because they were from fish of all ages, varied considerably in size at each location. More epoxy resin is added to fill the holes and then the disk is put in a preheated oven (approximately 120 °C) for 45 - 60 minutes so the epoxy can cure. This part of the procedure is also difficult, as it is necessary to insure that no air bubbles are caught in the epoxy.

After the disks of otoliths had cooled, they are polished to remove any surficial epoxy and expose the annuli of each otolith. Polishing generally starts with coarse sandpaper and works down to about a 0.3-micron polish. The desired composition of the polish is either Al or Si carbide or even a fine diamond polish. The reason for this is to avoid the introduction of any elements of interest, such as Zn or other trace metals,

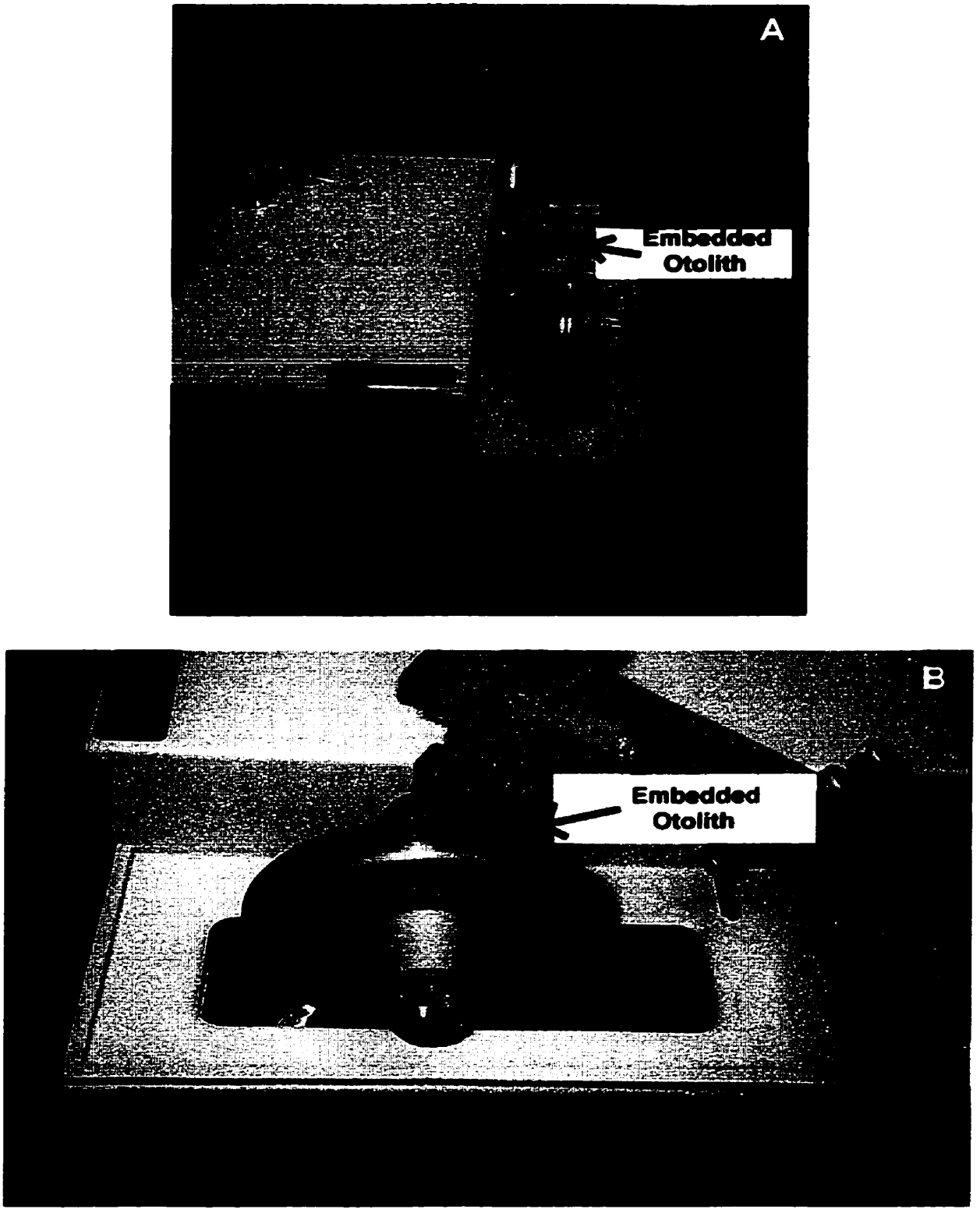

Figure 3.5. **(A) Photograph of the embedded otolith being longitudinally sectioned using a 4 x 0.004 x 0.5 diamond wafering blade. (B) Close-up of the embedded otolith being sectioned.**

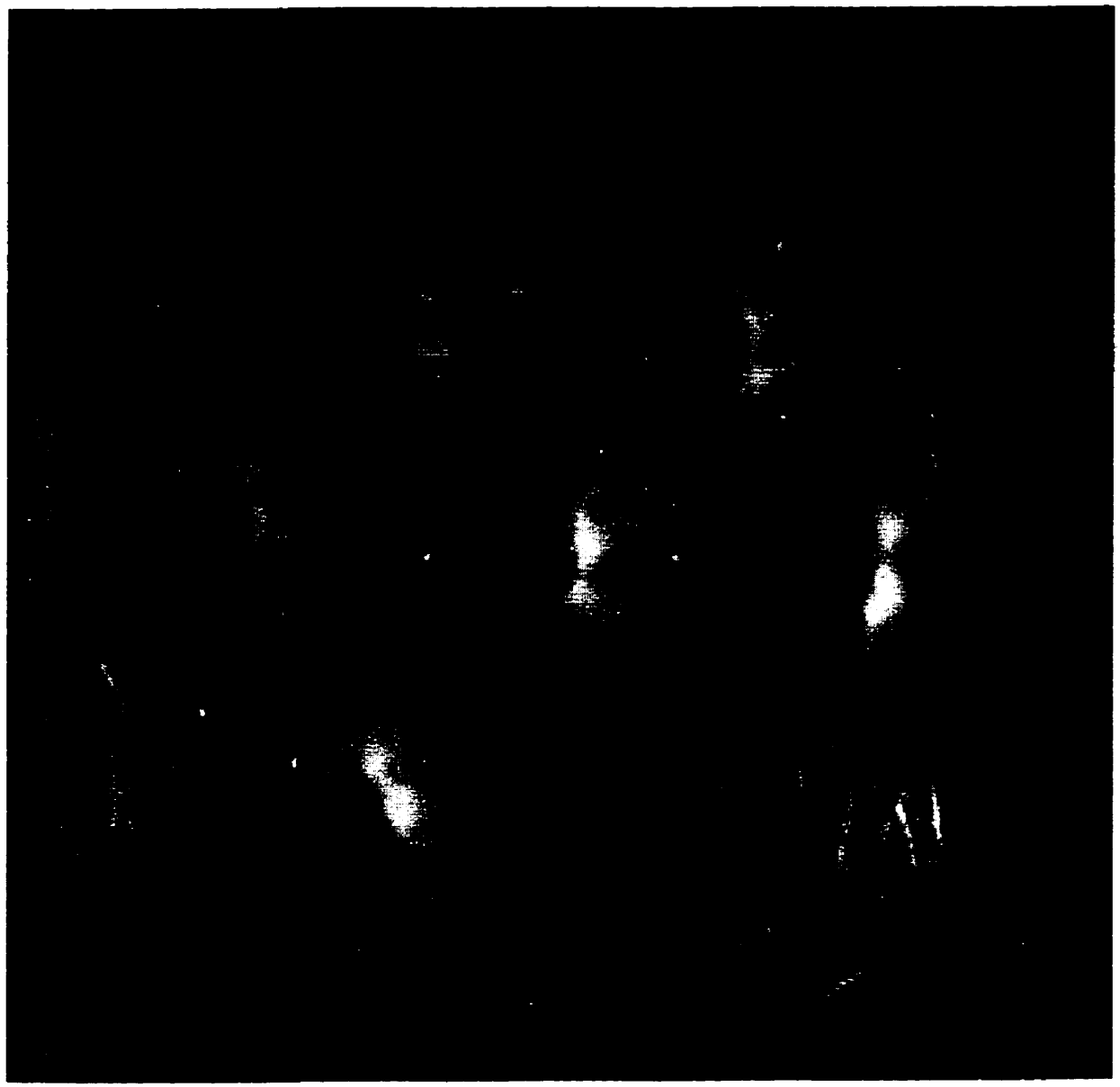

Figure 3.6. **Photograph showing an example of seven aligned and mounted Eden Lake otoliths (mounted in a perspex disk rather than a perspex ring).**

that might already be in the annuli. The progression from coarse to finer polish is to remove large scratches made by the coarser polish. The cleaner, less scratched, the otoliths are, the easier it is to see the details of the annuli.

There are two reasons for mounting the samples in this fashion. Firstly, to achieve a good polished surface to provide optimum optical resolution to (a) define the annuli and (b) to locate the microbeam for chemical analysis. Secondly, sufficient depth of aragonite is needed to assure that during PIXE analysis the x-rays are coming solely from the aragonite and the beam does not penetrate to the mounting medium. If the proton beam penetrates the mounting medium, the X-rays from this medium will contaminate the x-ray spectrum from the aragonite.

A problem arose when the first otoliths, from KAP and BAK2, were mounted in the disks using the aforementioned "original" procedure. When heated, the epoxy that the otoliths were embedded in melted and bubbled. This meant that the otolith was no longer secured in place and it floated up in the hole. This resulted in a lot of polishing to expose it. The rest of the disks were subsequently prepared with cold-curing epoxy.

The problem, however, with preparing all the otoliths with cold-curing epoxy is that each disk takes at least 2 days to cure, with only four disks fitting in the holder at one time. This, along with the hours of time it takes to fit the otoliths in the holes, makes the whole process time consuming and labor-intensive. Therefore, a different method was devised.

The new method involves using perspex rings of the same dimensions as the disks. The rings are secured in the holder with the piece of aluminum foil underneath and then a millimeter of epoxy is placed into the ring (Figure 3.7). The otoliths are placed, side of interest down, into the epoxy in an arrangement similar to that shown in Figure 3.6. The thin layer of epoxy holds the otoliths perfectly in place, thus, eliminating the time-consuming and difficult task of fitting individual otoliths to individual holes. This

thin a layer of epoxy dries overnight and then more epoxy can be poured in to fill the ring without any risk of the otoliths moving around. This second batch of epoxy takes about two days to fully cure, however, the rings can be removed from the holder after a day so that more rings of otoliths can be made. After all the epoxy has fully cured, the rings can be polished in the same fashion as the disks. This method has proven to be far more practical than the original disk method and a good polished surface and sufficient penetration depth are still achieved.

3.2.2 Clams

The procedure for preparing the clam shells for analysis is similar in some ways to that of the otoliths. First, the clam shells were washed and dried in the lab and then identified (Table 3.6). Unfortunately, some of the clam shells were either already broken or deemed too fragile to be properly prepared for analysis. The few clam shells that were still intact were dominantly *Lampsilis radiata*. This is possibly because *Lampsilis radiata* live a lot longer than *Pyganodon grandis* (the other species identified) and, therefore, have a longer time to make their shells thicker and stronger.

Even the *Lampsilis radiata* shells, however, needed protection (like the otoliths) prior to sectioning. These shells were placed, concave side up, in small aluminum pie plates and covered in Fiberglass Autobody Resin (first batch) or cold-curing epoxy (second batch). The resin- or epoxy-embedded clams were then left overnight to cure. Both the resin and epoxy worked equally well for embedding the clams.

The shells were sectioned in a similar way to the otoliths, through the center of the umbo, along the longest axis of the shell, perpendicular to the growth lines (Figure 3.8). A second parallel section was then made so that the thickness of each shell was approximately 3 mm thick. Each shell was then mounted using Crystal Bond on a slide and polished in the same fashion as the otoliths.

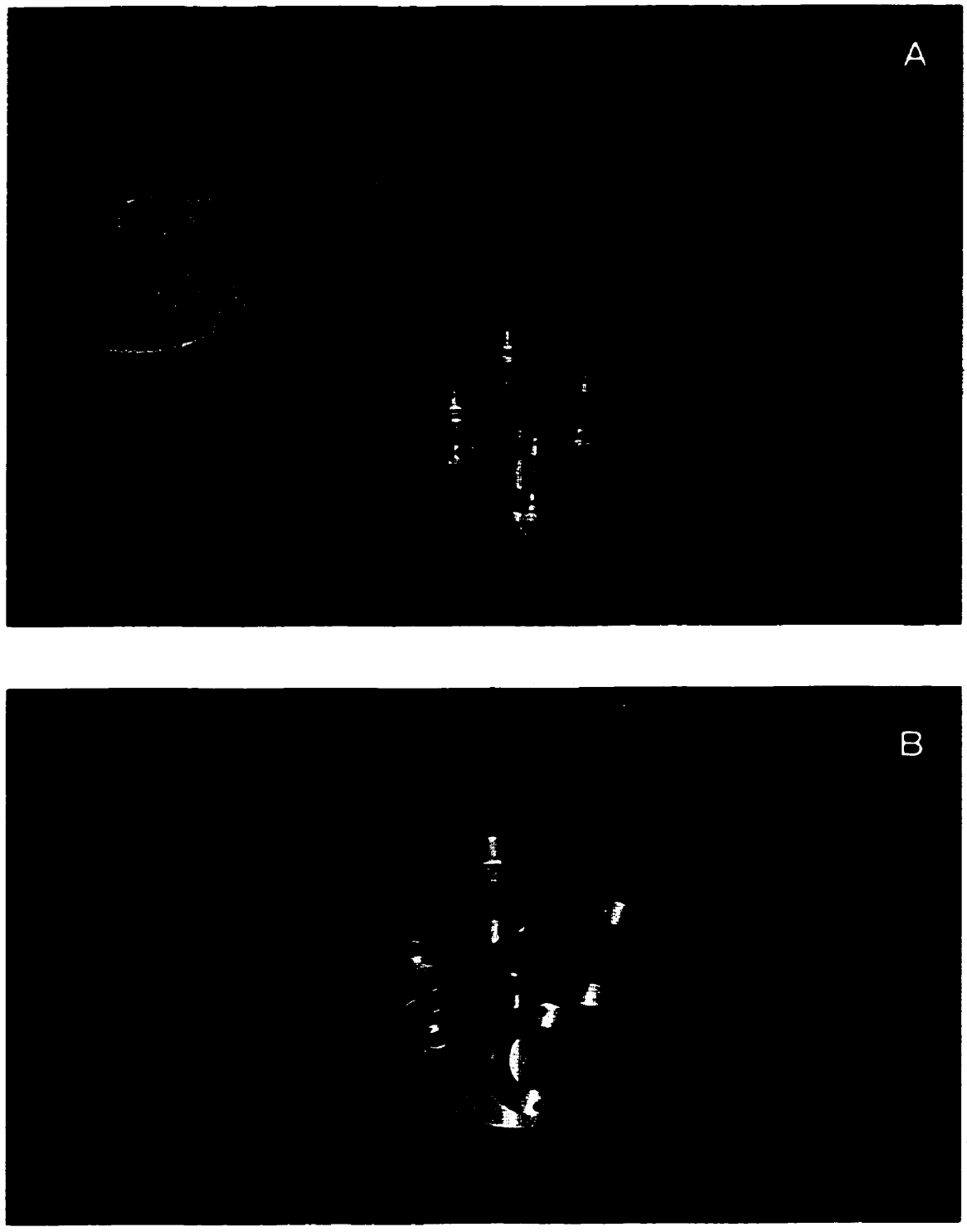

Figure 3.7. (A) Photograph of some of the tools used in the procedure of mounting otoliths in perspex rings rather than disks. (B) Close-up of the holder lined with tin foil holding two rings of otoliths.

Table 3.6. **Identified (species and genus) snail (SN) and clam (CL) specimens in sample set.**

CLAM (CL) NUMBER	LOCATION COLLECTED	SPECIES AND GENUS	COMMON NAME
CL1	ED1	*Pyganodon grandis simpsoniana*	Northern floater
CL2	Adam Lake	*Lampsilis radiata siliquoidea* (female)	Fat mucket
CL3	Adam Lake	*Lampsilis radiata siliquoidea* (male)	Fat mucket
CL4	BAK1	*Pyganodon grandis simpsoniana*	Northern floater
CL5	ED2	*Pyganodon grandis simpsoniana*	Northern floater
CL6	BAK2	*Pyganodon grandis simpsoniana*	Northern floater
CL7	BAK2	*Pyganodon grandis simpsoniana*	Northern floater
CL8	BAK2	*Lampsilis radiata siliquoidea* (male)	Fat mucket

3.3 Cathodoluminescence Microscopy

Cathodoluminescence (CL) is a non-destructive petrographic microscope technique used for the examination of thin sections and other types of geological samples (Marshall, 1988), such as otoliths. In CL, the sample is bombarded by an energetic electron beam and often responds by emitting light of various wavelengths in the ultra-violet, visible, and near infrared range. Emissions are the result of electronic transitions between the conducting band and the valence band and when light is emitted, the wavelength and intensity of this light characterizes the mineral and the distribution of impurities in it. These distinctive patterns often provide textural information that would not be obtained by other microscopic techniques.

The cathodoluminescence set-up in the Image Analysis Lab at the University of Manitoba is schematically shown in Figure 3.9. The CL instrumentation consists of a Nikon microscope equipped with a Technosyn cold-cathodoluminescence stage. The stage itself consists of a sample holder in a vacuum system, a cathode gun, and a power unit to control the voltage and current (cf. Marshall, 1988). The cathode gun is the source of the electron beam that bombards the sample. It is necessary for the vacuum to be at the right pressure (approximately 0.1 torr) and for there to be sufficient voltage and current to develop the luminescence but not so high that the sample is damaged.

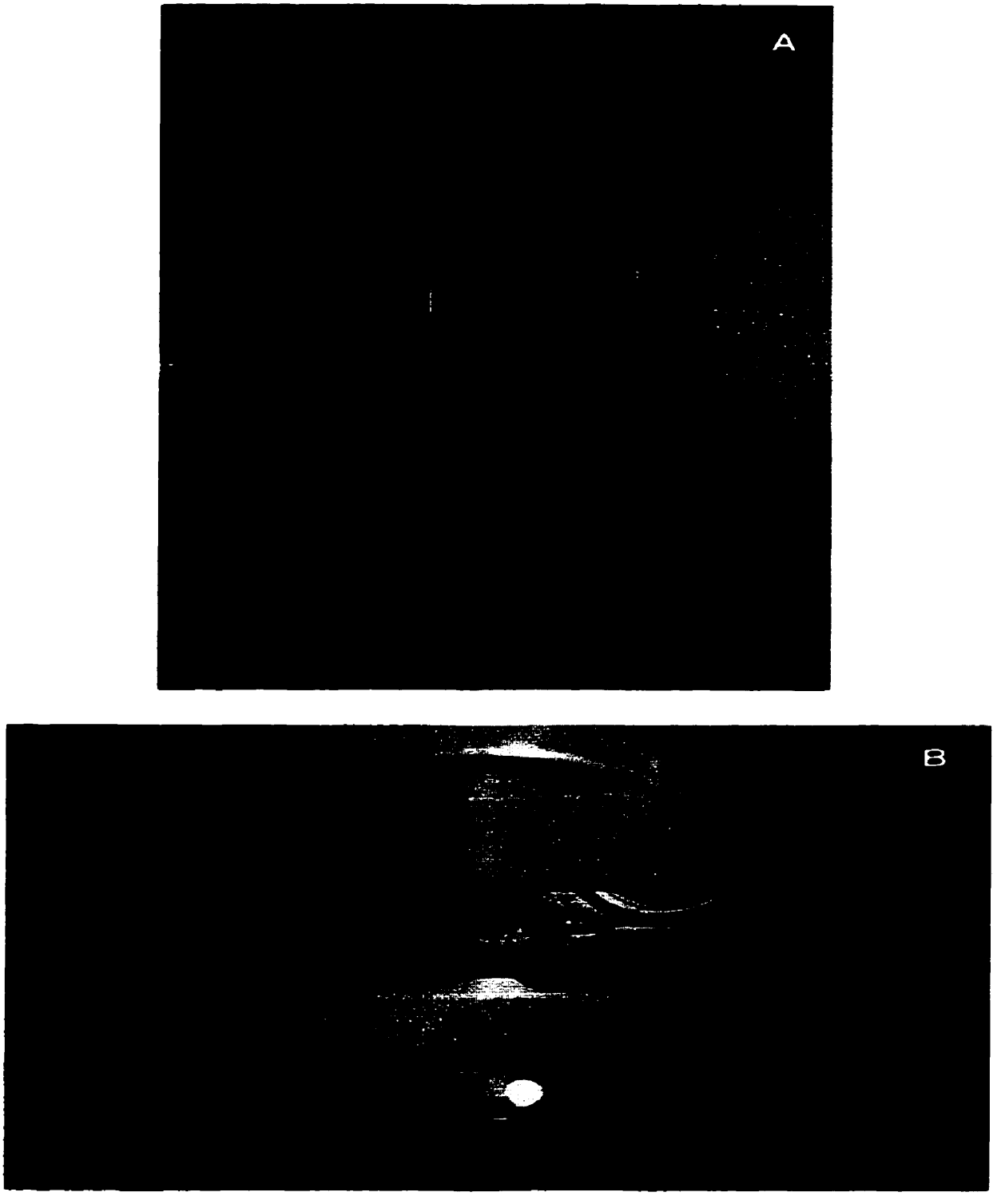

Figure 3.8. (A) Photograph of the Department of Fisheries and Oceans' saw used to section the Eden Lake clam shells. (B) Close-up photograph of a clam shell being sectioned through the center of the umbo, along the longest axis of the shell; perpendicular to the growth lines.

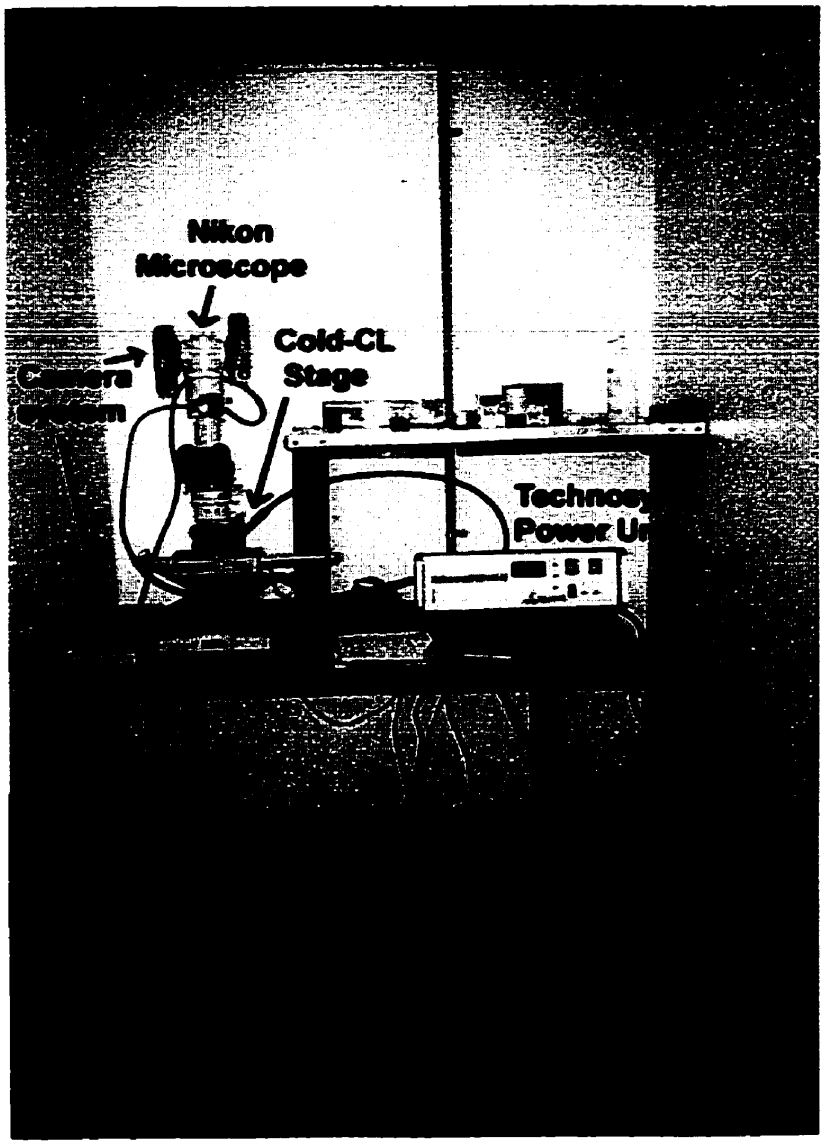

Figure 3.9. Photograph of the cathodoluminescence (CL) instrumentation set-up at the University of Manitoba.

3.4 Reflection Microscopy

Reflection microscopy is a microscopic technique using reflected light, rather than the usual transmitted light, to look at a sample. A secondary light source (fiber optic) is set up next to the microscope and set at a glancing angle (ca. 10-20°) to the otolith disk (Figure 3.10). This technique works especially well for otolith analysis because when the angle of incidence is just right, all of the annuli are clearly visible. This technique was used for two reasons: (1) to be able to understand the luminescence distribution, found from CL, by comparing it with light optical images which are typically used in aging the fish and (2) to be able to get some additional photographs of the otoliths and their internal structure.

In preparation for probe work, a Kontron image analysis system connected to a reflection microscope using glancing reflected light from a fiber optic was used to collect a high-resolution monochrome image of each otolith (e.g., Figure 3.11). This image provides for clear optical contrast and differentiation of the annuli that can be used for comparison and interpretative purposes following microprobe analysis. This imaging is always done before carbon coating as carbon coating tends to degrade the optical images.

These reflection microscopy images are further used to specifically mark the desired starting and end points for the PIXE line scan (i.e., the central nucleus or primordium and the otolith edge, respectively) to facilitate programming of the PIXE system. It has been found through studies done on arctic char that there is no difference between the right and left otoliths in terms of element concentration (Norman Halden, July 1999, *pers. comm.*). There is further no notable difference in element concentration along different transects across the annuli in one otolith; it does not matter where the scan is done on the otolith so long as all of the annuli are analyzed. The orientation of the line scan to the annuli, however, is important. The line selected should be located

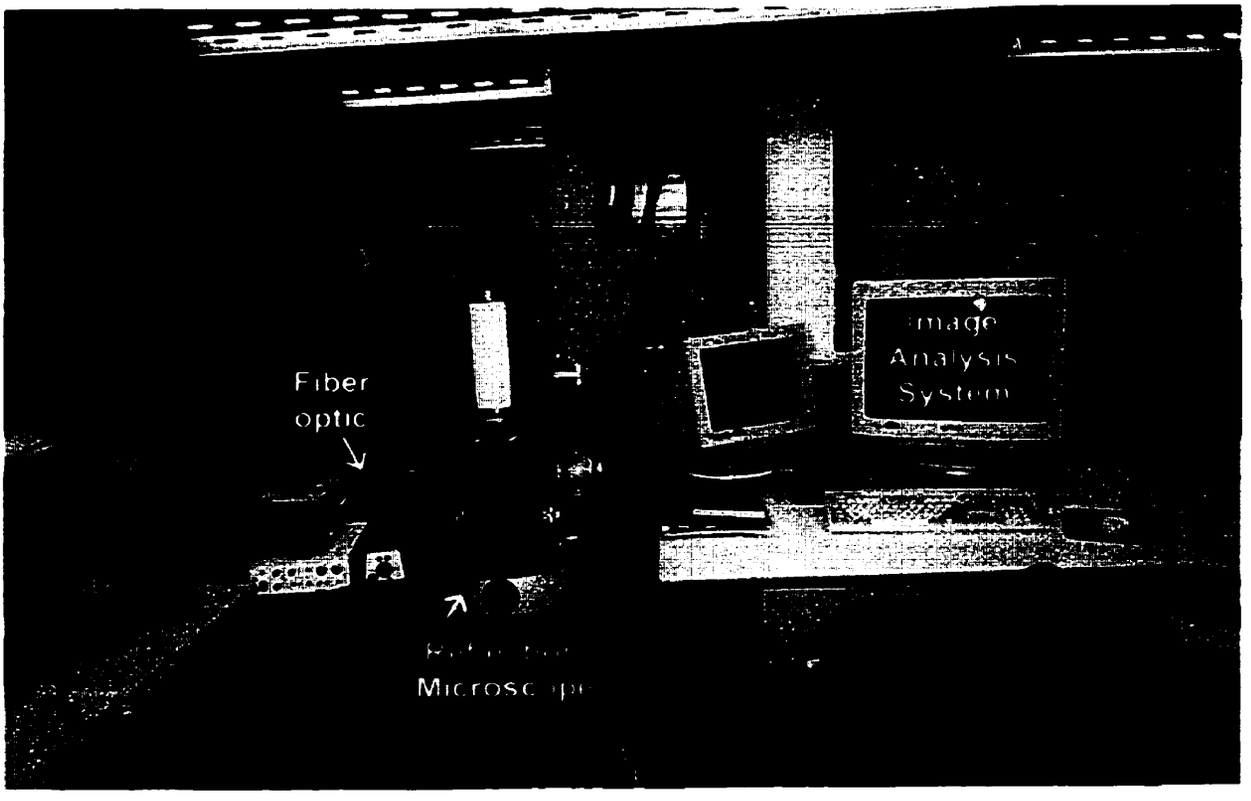

Figure 3.10. **Photograph of the reflection microscopy set-up.**

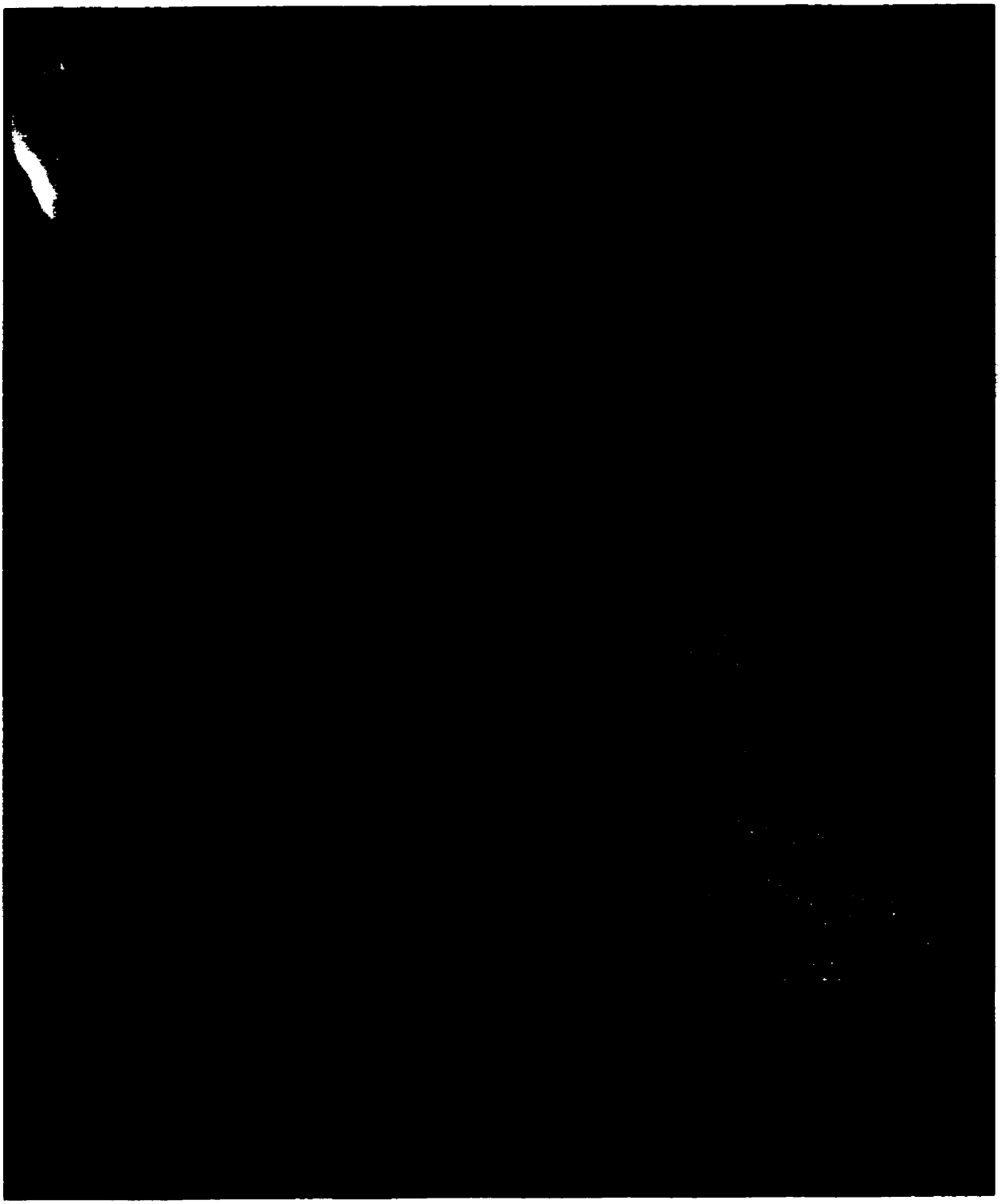

Figure 3.11. A high-resolution monochrome image of a walleye otolith collected using a Kontron image analysis system connected to a reflection microscope using glancing reflected light from a fiber-optic. The field of view is approximately 2 mm across.

Figure 3.12. A high-resolution monochrome image of a northern pike otolith collected using a Kontron image analysis system connected to a reflection microscope using glancing reflected light from a fiber-optic. The field of view is approximately 4 mm across. Marked on the image are the starting and end points for the PIXE line scan (i.e., central nucleus or primordium and the otolith edge, respectively). The line selected is located perpendicular (or almost perpendicular) to the annuli.

such that the line scan is perpendicular (or as close to perpendicular as possible) to the annuli (e.g., Figure 3.12). This is to ensure that the beam is analyzing one annulus at a time and the line-scan is an accurate reflection of the elements within the annuli.

3.5 SPM Measurements

One-dimensional line scans are elemental maps obtained by appropriately rastering the proton beam (5 x 5 μm at 3 MeV); X-ray intensities and corresponding X-Y coordinates are recorded to computer disc in list mode. The data was originally collected as X-ray intensity and coordinates, however, new software presents the line scans in terms of trace element concentration versus position. The sum spectrum of all recorded X-ray events is assembled, and energy windows for the trace elements of interest are defined. The sum spectrum is fitted by the GUPIX software thereby providing the continuum background intensity in each window per μ:C of proton charge (Campbell et al. 1998).

On completion of the line scan, the otolith is re-imaged to verify the location of the proton beam relative to the annuli which can be seen as a discoloration of the carbon coat and as a line in the epoxy where the beam crosses the edge of the otolith (e.g., Figure 3.13). The PIXE line scan file for the element(s) of interest is imported into the image analyzer. The start of the file is identified with the selected scan origin in the primordium, and the end is identified in the line scan by the disappearance of the Ca signal as the beam moves from the otolith rim to epoxy. The optical image and the concentration scan(s) are then scaled to have the same lateral extent in a compound image (cf. Figure 1.8).

For point analyses, a 5 x 5 μm 3 MeV proton beam is used with average beam-currents of 6-7 nA and the time integrated charge for each analysis is 2.5 μC with X-ray spectra recorded using a Si(Li) detector. The X-rays of the trace elements of

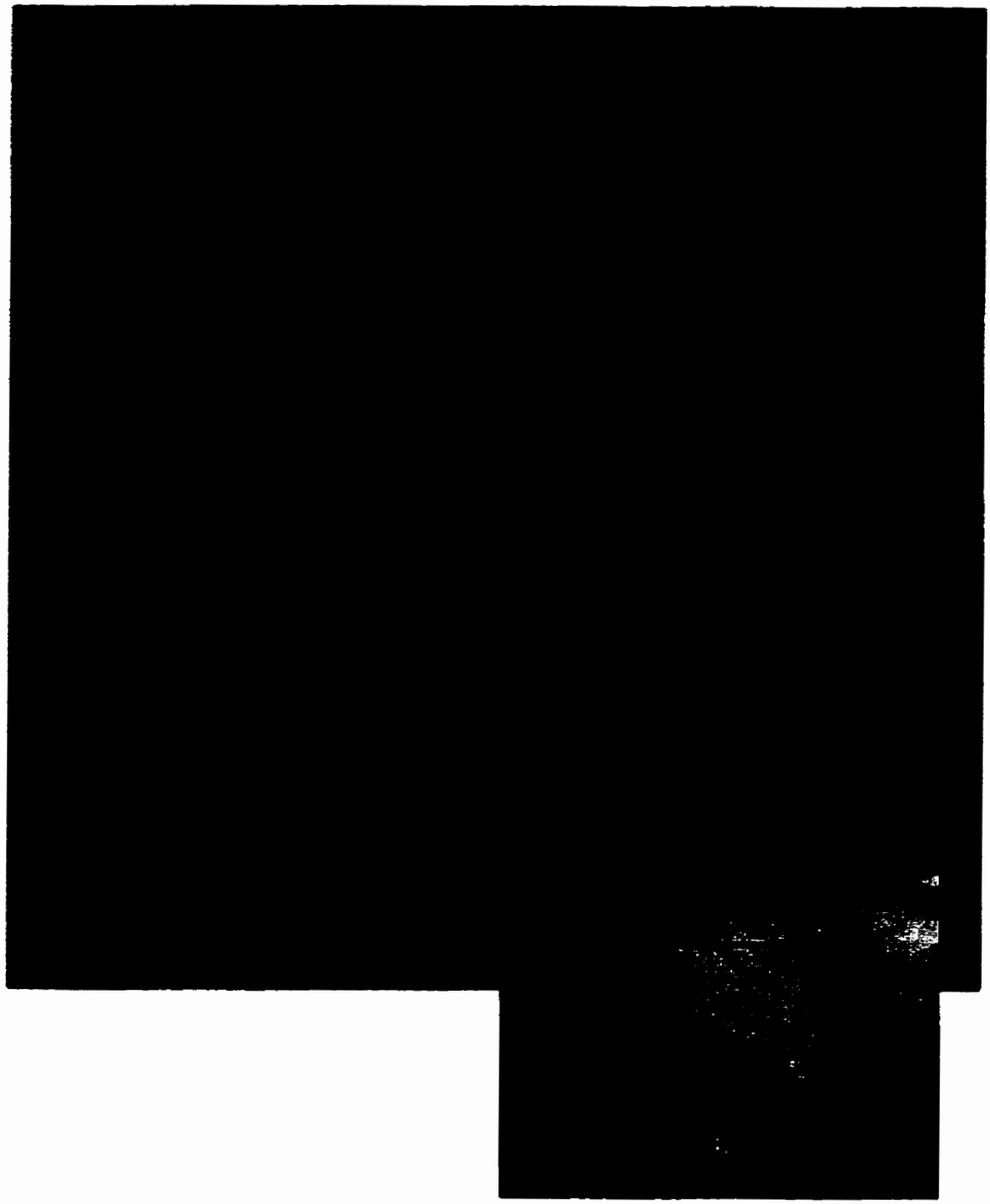

Figure 3.13. A cathodoluminescence photograph of a northern pike otolith that has been re-imaged to verify the location of the proton beam relative to the annuli. Notice the slight difference in position between this photograph (showing the actual position of the PIXE line-scan) versus the inset reflection microscopy image showing the chosen position for the PIXE line-scan. The field of ciew in both images is approximately 2 mm across.

interest occur in the energy region 6 - 14 keV, so a combination of 0.125 μm mylar and 106 μm Al filters are used to suppress the intensity of the lower-energy region of the spectra. This reduces the Ca X-rays reaching the detector and gives better counting statistics for the trace elements. Spectra are then processed using the GUPIX software package (Maxwell et al. 1989). GUPIX extracts peak areas from a spectrum using a nonlinear least-squares-fitting procedure. A synthetic spectrum is derived using estimated concentrations of elements of interest and a database that includes relative X-ray intensities. The background is removed via a top-hat filter method. The calculations for the element concentrations are then iterated until the best fit between the synthetic and observed spectrum is attained. Further details on spectrum fitting and calibration procedures are given by Campbell et al. (1995, 1998) and Campana et al. (1997).

3.6 LAM-ICP-MS

The recent coupling of a laser ablation microprobe (LAM) with inductively coupled plasma - mass spectrometer (ICP-MS) has yielded a relatively simple and inexpensive instrument capable of direct analysis of elemental and isotope ratios in solid samples, such as otoliths, with extremely low limits of detection (Jackson et al., 1992).

The University of Windsor microbeam analytical system, shown in Figure 3.18, consists of a Surelite I-20 Q-switched Nd:YAG laser at the fundamental wavelength of 1064 nm with a repetition rate 20 Hz (Fryer et al., 1995). An ultraviolet wavelength of 266 nm is produced by frequency quadrupling using second and fourth harmonic generators and a wavelength separation package (WSP). The 266 nm laser pulses are attenuated to the working energy by using a combination of a rotatable half-wave plate and a glan laser calcite polarizer. The UV laser beam is then split by a beamsplitter (40% to the sample cell and 60% to a power meter), allowing an operator to simultaneously monitor the laser beam energy during the ablation. After splitting, the

40% of the laser beam (headed to the sample cell) is steered to a petrographic microscope by means of UV dielectric mirrors, then focused through a silica window onto the sample in the sample cell. An energy of 0.4 mJ/pulse is used to perform sample analysis. The typical pit sizes range from 20 to 30 microns in diameter.

The ablated material is transported via the argon carrier gas into the ICP torch of the ICP-MS (Fryer et al., 1995). The analyzer is a VG PQ3(S) with especially high performance characteristics. Typical solution mode sensitivities are between 100 and 500 million cps/ppm. Argon gas flow rates, torch position, and lens setting are adjusted daily to optimize the sensitivity and oxide level. Optimizations of these parameters for LAM is performed on selected elements (e.g. Ca, La, Th, U, and ThO) in spiked synthetic glass (NIST 612). Typical sensitivities for spot size of 20 to 30 microns in NIST 612 are: 3.19×10^3 cps/ppm for Y; 8.4×10^3 cps/ppm for La; 5.9×10^3 cps/ppm for Th; and 7.8×10^3 cps/ppm for U and the ThO/Th ratio is around 0.3%. Typical detection limits are 140 ppb for Mn; 200 ppb for Zn; 16 ppb for Sr; 4 ppb for Y; 5 ppb for Sn; 26 ppb for Ba; 2 ppb for La; 1 ppb for Ce; 5 ppb for Nd; 7 ppb for Sm; 2 ppb for Eu; 8 ppb for Gd; 3 ppb for Dy; 1 ppb for Tm; 6 ppb for Yb; 3 ppb for Pb; 1 ppb for Th; and 1 ppb for U.

Data is acquired by rapid peak jumping (dwell time of 10 ms) (Fryer et al., 1995). A typical run of LAM analyses consists of 4 NIST 612 standards (first and last two) and 16 samples in between. Instrument background levels are established by acquiring data for approximately 60 s prior to commencing ablation for each analysis. The laser is fired for 15 to 60 s depending on the sample thickness. The total time for data acquisition per analysis is about two minutes.

The raw data (counts per second) is then transmitted to a remote PC by network communication, and processed off-line using a spreadsheet macro program (Fryer et al., 1995). The first three data points are rejected to minimize surface contamination. The

sample intensity for each element is then calculated as the mean count-rate during the ablation. The intensities after background correction are converted to concentration by calibration to NIST 612 synthetic silicate glass reference material. Matrix effect and ablation efficiency is corrected using Ca as the internal standard. Drift is corrected by frequent recalibration, in addition to internal standardization.

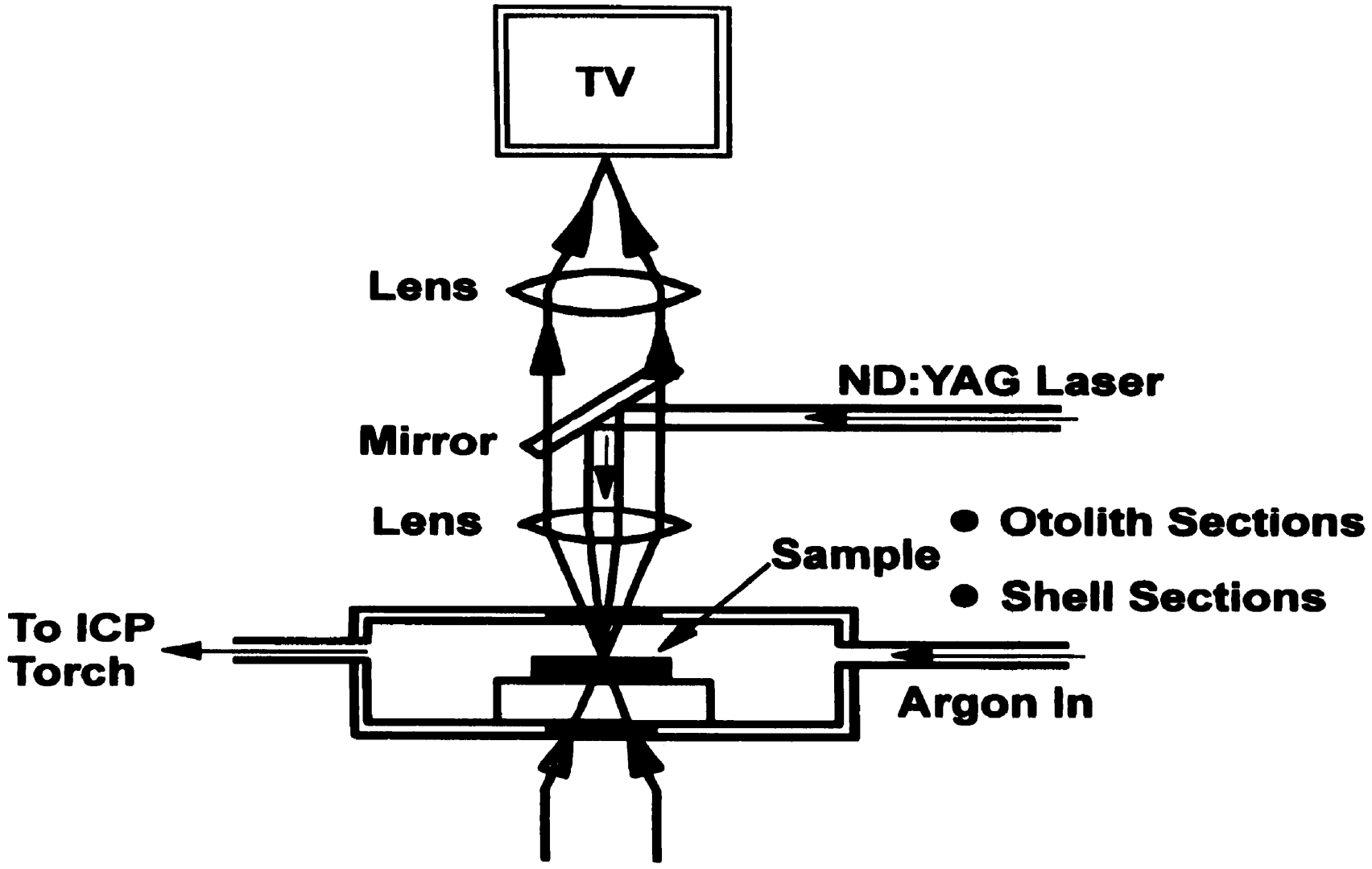

Figure 3.14. Illustration of the Windsor Laser Ablation Microprobe (LAM) system (Fryer et al., 1995).

Chapter 4: The Eden Lake Fauna

To put the trace element information in context, the ecology of each fish and clam species must be understood. Eight species of fish and two species of clams were sampled: walleye, northern pike, white sucker, longnose sucker, whitefish, burbot, yellow perch, cisco, *Pyganodon grandis* and *Lampsilis radiata siliquoidea*, respectively. Physical descriptions and illustrations of each species are provided in Appendix B. A discussion of each fish and clam's typical diet and movements around the lake, including spawning habits, is provided below.

4.1 Walleye

Stizostedion vitreum or, more commonly, walleye are limited to freshwater in North America and are probably the most economically valuable species in Canada's inland waters (Scott and Crossman, 1973).

Adult and juvenile walleye are largely piscivorous (Colby et al., 1979). The food of the walleye shifts very quickly, with increase in size, from invertebrates to fish; in part a reflection of their change in habitat from surface to bottom as their phototacticity increases (Scott and Crossman, 1973). During the first six weeks of life, food consists mostly of copepods, Cladocera, and forage fish, such as yellow perch. Adult walleye feed to the greatest extent from the early evening to early morning, however, storm events and strong winds, which decrease light intensity, can stimulate daytime feeding (Colby et al., 1979). Walleye are highly cannibalistic if small forage fish are not readily available (Scott and Crossman, 1973). The relative amounts of various species of fish eaten by walleye depend greatly on availability. Other species of fish, besides yellow perch and other walleye, that have both been documented as a source of food for older walleye and are found in Eden Lake (according to our nets) are: ciscoes, sticklebacks,

white and longnose suckers, lake whitefish, spottail shiners, trout perch, emerald shiners, and burbot. It would, therefore, seem safe to say that they utilize any species of fish that are available to them, except northern pike. Other species, such as snails, frogs, and small mammals are also eaten by walleye but only rarely, and usually when fish and insects are scarce, which was certainly not the case at Eden Lake.

Spawning occurs in the spring to early summer depending on latitude and water temperature (Scott and Crossman, 1973). Normally spawning begins shortly after ice breaks up in the lake, at optimum water temperatures of 6.7 to 8.9 °C, however, pre-spawning behaviour may commence much earlier, when water temperature is 1.1 °C. Northern populations do not spawn in some years when temperature is not favorable. Spawning grounds are commonly rocky or coarse-gravel areas in tributary rivers or shallow shoals. In Eden Lake, there are many possible spawning grounds, including the "Kap" Bay area, the Hughes River, "the Narrows", and around the small islands scattered around the lake (Figure 4.1). The males move to the spawning grounds first and spawning takes place at night, in groups of one larger female and one or two smaller males or two large females and up to six smaller males. The males are not territorial and no nest is built. Eggs are deposited and fall into crevices in the substrate and hatch within 12 to 18 days. Newly hatched fry are 6.0 to 8.6 millimetres in length. Growth in Eden Lake is slow as shown by Figure 4.2 depicting a new fry, a one-year old, and a two-year old walleye.

Movements, other than the spring spawning run, include daily vertical movements in response to light intensity and daily or seasonal movements in response to temperature or food availability (Scott and Crossman, 1973). Their summer wanderings are usually limited to 5 to 8 kilometres and there is evidence of homing to spawning grounds year after year in certain populations. Most walleye seem to remain in loose but discrete schools with separate spawning grounds and summer territories.

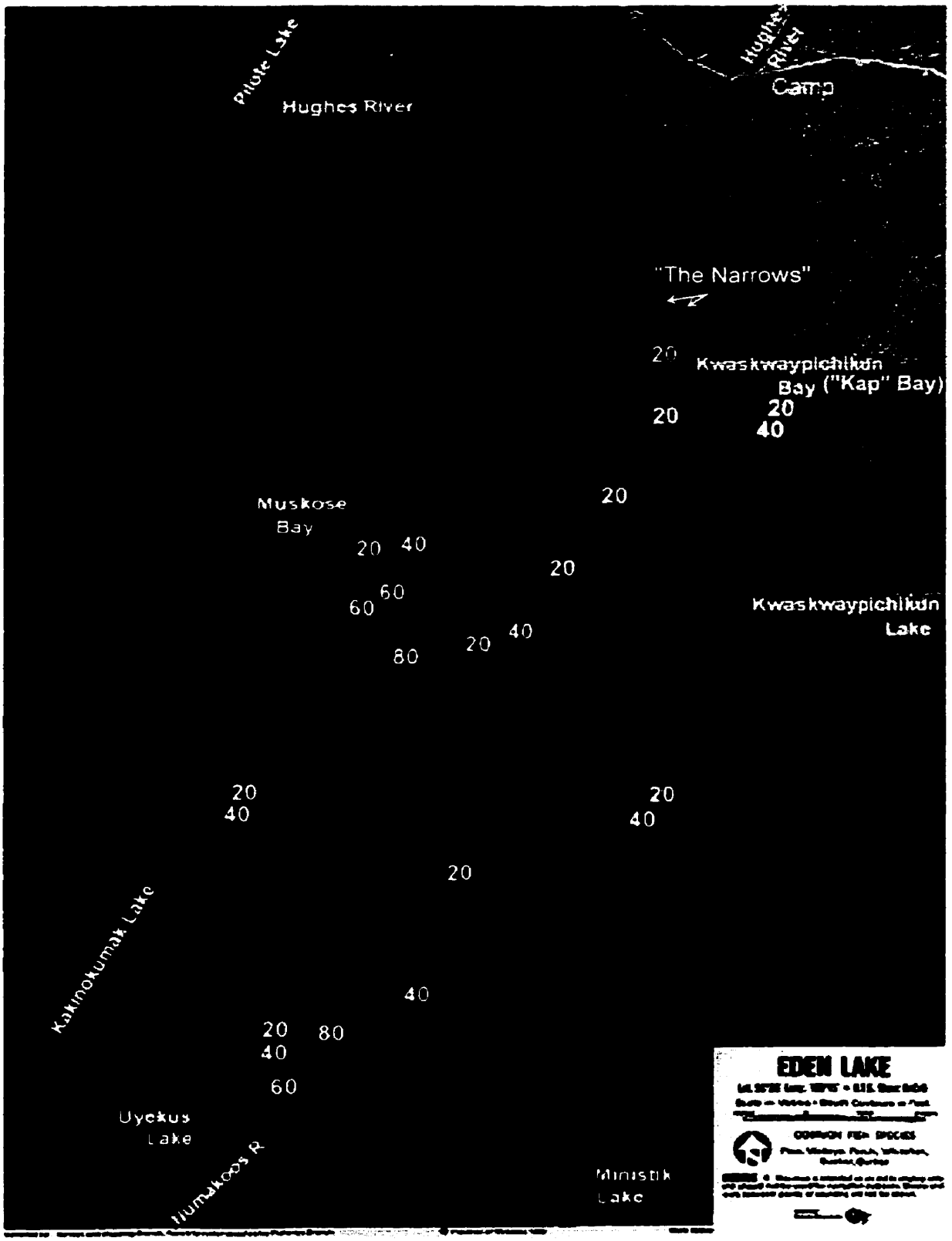

Figure 4.1. **Aerial photograph of Eden Lake showing the possible spawning locations, including "Kap" Bay, "The Narrows", Muskose Bay, the Hughes River, etc. Water depths are shown in feet.**

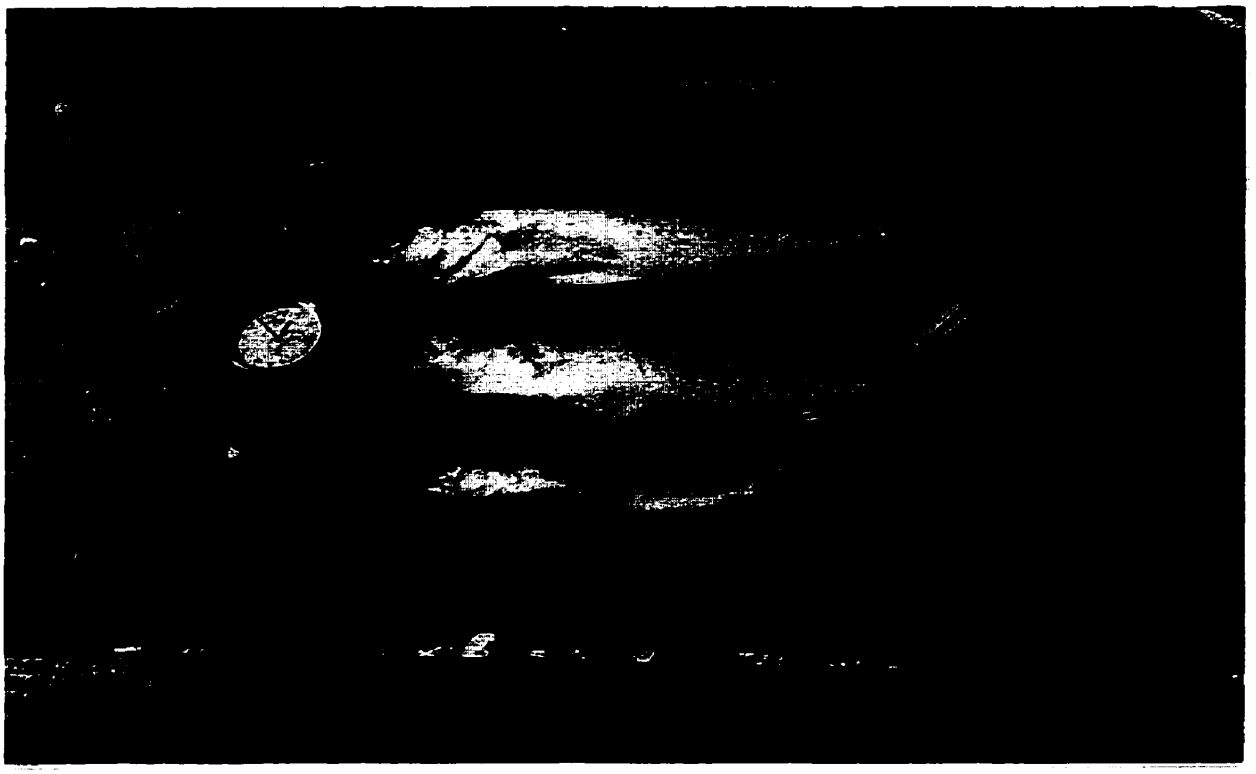

Figure 4.2. Photograph showing a new fry (bottom), a one-year old walleye (middle), and a two-year old walleye (top) from Eden Lake. The face of the watch is 30 millimeters in diameter.

Adult walleye are extremely light sensitive (phototactic) due to the presence of *Tapitum lucidum* in the retina of the eye and, therefore, frequent depths between 1 and 17 metres depending on turbidity and, of course, the depth of the lake (Colby et al., 1979). They can tolerate a wide range of temperatures, from 0 to 30 ^{0}C, however, they prefer water temperatures between 20 to 23 ^{0}C. Total population mortality has been found to occur at temperatures above 34 ^{0}C. The optimum pH range for walleye is between 6 and 9.

Northern pike are probably the most important predator of walleye (Scott and Crossman, 1973). They are also an important competitor because they are the only other major, shallow-water predator in the north.

4.2 Northern Pike

Esox lucinius or, more commonly, northern pike have a circumpolar distribution in the northern hemisphere, with a distribution across Canada, except in the Maritime provinces (Scott and Crossman, 1973).

The northern pike is a spring spawner and spawning takes place immediately after the ice melts in April to early May, when water temperatures reach 4.4 to 11.1 ^{0}C (Scott and Crossman, 1973). In general, this species spawns during daylight hours over a vegetated substrate. In Eden Lake, possible northern pike spawning grounds are in "Kap" Bay and in the more highly vegetated shoreline areas and bays (Figure 4.1). One or two smaller males usually attend the larger female and they swim and roll together over the vegetation in water often no deeper than 178 millimetres. The spawning act is repeated many times a day for 2 to 5 days. The eggs settle, scatter, and attach to the vegetation. Eggs usually hatch in 12 to 14 days at prevailing water temperatures but can hatch in 4 to 5 days at 17.8 to 20 ^{0}C.

Upon hatching the fry are usually 6 to 8 millimetres in length. They remain inactive, often attached to vegetation by means of adhesive glands on the head, for 6 to 10 days, and feed on the stored yolk. Growth is very rapid in comparison to walleye and some other fish, however, it is still a great deal slower at higher latitudes. With the decreased growth northward, however, there is an increase in longevity.

Northern pike generally occupy shallower water in spring and fall and move to deeper cooler water at the height of summer (Scott and Crossman, 1973). In general, northern pike are fairly sedentary, establishing a vague territory where food and cover are adequate. They are plentiful in Eden Lake and were observed everywhere from shallow areas near the campsite dock to deep in the central area of the lake.

After the yolk is absorbed, young northern pike feed heavily on zooplankton and some immature aquatic insects for 7 to 10 days (Scott and Crossman, 1973). At this point, small fish enter their diet and by the time the young reach 50 millimetres, fish assume predominance. Adult pike are classified as omnivorous carnivores in that they eat virtually any living vertebrate available to them within the size range they can engulf. The optimum food size has been calculated to be between one-third and one-half the size of the pike. Adult northern pike, even though their food over a whole season is 90% fish, do at times feed heavily on frogs and crayfish, where readily available. Other vertebrates, such as mice, muskrats, and ducklings often enter the diet.

The eggs of northern pike are prey to a wide variety of other fishes, including minnows, perch, and other northern pike; large larval aquatic insects; waterfowl and other diving birds; and aquatic mammals (Scott and Crossman, 1973). The mortality rate on the spawning grounds of eggs and young by predation, or by stranding due to lowering water levels, has been estimated as high as 99%. In general, adult pike are large enough and secretive enough that man is probably their only important predator. During spawning, however, when the northern pike are in very shallow water and are

unwary, the smaller ones often fall prey to bears, dogs, and eagles.

4.3 Suckers

There are two types of suckers found in Eden Lake, white suckers and longnose suckers. The latter is much less abundant, with only one being caught at the KAP netting site.

4.3.1 White Suckers

Catostomus commersoni or, more commonly, the white sucker is restricted to North America and has a wide distribution in Canada (Scott and Crossman, 1973).

White suckers spawn in spring, usually from early May to early June (Scott and Crossman, 1973). Adults usually migrate from lakes into streams when stream temperatures first reach 10 °C, but they are also known to spawn on lake-margins, or quiet areas in the mouths of blocked streams. Spawning sites are usually in shallow water with a gravel bottom but they may also spawn in rapids. In Eden Lake, the possible white sucker spawning areas are the Hughes River, "the Narrows", the Muskose Bay area, the "Kap" Bay area, outflow point into the Numakoos River and in any of the bays or inlets along the shoreline of the lake (Figure 4.1). Adults return to certain spawning sites year after year. Spawning generally takes place at dusk and dawn; however, some spawning may take place during daylight hours, but to a very limited extent. Two or four males may crowd around a female during spawning activities and these irregularly spaced acts last 3 to 4 seconds, occurring 6 to 40 times in an hour. White suckers do not build nests. Their eggs are scattered and adhere to gravel or drift downstream and adhere to the substrate in quieter areas. Adults begin leaving the spawning grounds 10 to 14 days later. The eggs hatch about 2 weeks after being deposited and the young fry remain in the gravel for 1 to 2 weeks before they start to

migrate into the lake. There may be as little as 3% survival from egg to migrant fry. The growth of white suckers is extremely variable from lake to lake.

In addition to spawning migrations, movements, other than the tendency to move offshore with increasing age, are random; probably in response to temperature (Scott and Crossman, 1973). White suckers are moderately active during the daytime but active feeding is usually restricted to near sunrise and sunset when they move into shallower water.

The fry, at about 12 millimetres long, begin feeding near the surface on plankton and other small invertebrates as the mouth is terminal rather than ventral (Scott and Crossman, 1973). At about 16 to 18 millimetres, the mouth shifts ventrally and there is a shift to bottom feeding (other invertebrates and fish eggs). Large white suckers also consume small fish, such as logperch, sometimes in great abundance.

White suckers, when less than 305 millimetres, constitute a major food item of a wide variety of predatory fish, such as northern pike, walleye, and burbot. Predaceous birds or other stream spawners often eat smaller white suckers.

4.3.2 Longnose Suckers

Catostomus catostomus or, more commonly, the longnose sucker occurs all over Canada, especially in the northwest and is generally more common than lake trout and northern pike (Scott and Crossman, 1973). Only one longnose sucker was caught at Eden Lake.

Longnose suckers spawn in the spring, in streams where available, otherwise in shallow areas of the lake (Scott and Crossman, 1973). In Eden Lake, the possible spawning locations are the same as those for the white suckers. Longnose suckers enter these areas as soon as the temperature exceeds 5 °C, usually mid-April to mid-May. The spawning run of this sucker begins and reaches a peak several days before

the run of white suckers in the same area. Spawning often takes place between 6 a.m. and 9 p.m. in water 152 to 279 millimetres deep, with a current from 30 to 45 cm/s and a bottom of gravel 50 to 100 millimetres in diameter. Spawning activities usually involve two to four males and one female and, similarly to white suckers, last 3 to 5 seconds occurring 6 to 40 times in an hour. The spawning period in general is of short duration and immediately after the eggs are deposited the sexes separate and leave the spawning area. Longnose suckers do not build nests. The eggs are laid in small numbers and adhere to the gravel and substrate. The eggs hatch about 2 weeks later but the young remain in the gravel for 1 to 2 weeks before they fully emerge. Longnose fry, unlike baby white suckers, have a ventrally located mouth and, therefore, start as bottom feeders right away.

The food of this sucker is variable from place to place, season to season, and by size (Scott and Crossman, 1973). It is, however, all invertebrates (taken from the bottom), no vertebrates have ever been reported. A typical food list in order of frequency of occurrence is as follows: Amphipods, Trichoptera, chironomid larvae and pupae, Ephemeroptera, ostracods, gastropods, Coleoptera, pelecypods, copepods, cladocerans, and plants.

As bottom feeders, longnose suckers are competitors for food with all other bottom feeders, except those that prefer much deeper water. The young of this species fall prey to a wide variety of predaceous fish and fish-eating birds. Even larger longnose suckers are preyed on by northern pike. Spawning longnose suckers often fall prey to bears, other mammals, osprey, and eagles.

4.4 Lake Whitefish

Coregonus clupeaformis or, more commonly, lake whitefish are widely distributed in North American fresh waters, all across Canada (Scott and Crossman, 1973).

Spawning occurs in fall, usually November to December, but earlier farther north (Scott and Crossman, 1973). Spawning usually occurs in shallow water at depths of less than 8 metres, at temperatures around 0 °C, but spawning in deeper and colder water has been reported in some localities. Possible spawning locations for lake whitefish in Eden Lake are the Hughes River, "the Narrows", "Kap" Bay and in and around the small islands and bays of the lake (Figure 4.1). Lake whitefish may also spawn in the open waters of Eden lake. Spawning lake whitefish are very active and may thrash and leap completely out of the water, especially at night. The preferred substrate is a hard or stony bottom and the eggs are deposited more or less randomly over the area. The eggs remain on the spawning ground until they hatch in April or May and the young whitefish generally leave the spawning grounds and move to deeper water in early summer. The rate of growth of lake whitefish varies but is generally relatively rapid.

Movements, aside from spawning migrations to shallow water, vary as a reflection of temperature (Scott and Crossman, 1973). The lake whitefish is a cool water species and therefore, does not move around as much in northern lakes, in comparison to southern lakes, because thermal stratification of these lakes is not as developed.

Adult lake whitefish are bottom feeders over most of their distribution range, consuming a wide variety of bottom-dwelling invertebrates and small fish (Scott and Crossman, 1973). If these are in short supply, however, lake whitefish have also been found to feed on planktonic creatures and terrestrial insects. There is notably a relationship between the number and length of gill rakers and the types of food consumed such that lake whitefish with short gill rakers and high gill raker counts ate a higher proportion of benthic food (Kliewer, 1970). Where available, copepods appear to be most important in the diet of lake whitefish initially, while cladocerans become

significant later in spring. By early July, bottom organisms begin to enter the diet, however, cladocerans remain dominant. On entering deeper water, as the young lake whitefish grow, the diet changes to resemble that of the adults and more aquatic insect larvae, gastropods, fingernail clams, amphipods, isopods, and ostracods are eaten; but planktonic crustaceans continue as dietary items.

Small whitefish fall prey to a number of predatory fish (Scott and Crossman, 1973). The major predators of lake whitefish found in Eden Lake are: northern pike, burbot, walleye, and even whitefish themselves at times when they consume their own eggs. Yellow perch and cisco are also a threat to larval lake whitefish.

4.5 Burbot

Lota lota or, more commonly, burbot are generally distributed, in all suitable habitats, all across Canada (Scott and Crossman, 1973).

The burbot is one of the few Canadian freshwater fish that spawns in midwinter (January to March), under the ice (Scott and Crossman, 1973). They usually spawn in the lake but sometimes move into rivers in order to find a spawning site in 2 to 3 metres of water over a gravel shoal. Possible spawning sites for the burbot in Eden Lake include the gravel shoals in "Kap" Bay, around some of the islands in the lake and the Hughes River (Figure 4.1). Male burbot arrive at the spawning site first, followed in 3 or 4 days by the females. Spawning takes place only at night and involves 10 to 12 individuals. Surface temperatures in the water during the spawning period are usually between 0.6 to 1.7 °C. Burbot eggs are semipelagic and hatch in 30 days. Growth in the first 4 years of the burbot's life is relatively rapid but after that time there is a gradual decrease in length increment and an increase in weight.

Burbot are usually residents of deep water but move into shallower water during summer nights. Other movement includes post-spawning movement into tributary rivers

during late winter and early spring.

The burbot is a voracious predator and night feeder (Scott and Crossman, 1973). Small burbot, 51 to 305 millimetres long, feed on *Gammarus*, mayfly nymphs, and crayfish, where available. Older burbot, over 500 millimetres long, feed exclusively on fish, such as (in Eden Lake) ciscoes, walleye, yellow perch, sculpins, trout perch, sticklebacks, and logperch, depending which species are available.

The burbot shares the hypolimnion with lake whitefish and eats the same food. It is, thereby, an important direct competitor to this species. Yellow perch and walleye are two of the most important predators of very young burbot in Eden Lake.

4.6 Yellow Perch

Perca flavescens or, more commonly, yellow perch occur, in Canada, from Nova Scotia west through to Alberta and in the Pend Oreille, Kootenay, and Okanagan watersheds in British Columbia, as a result of introductions from Washington State (Scott and Crossman, 1973).

The yellow perch spawns in the spring, usually April 15 to early May, but spawning may extend into July in some areas (Scott and Crossman, 1973). Water temperatures of 6.7 to 12.2 °C are preferred. The adults migrate shoreward into the shallows of the lake, and often into tributary rivers. In Eden Lake, the yellow perch can likely effectively spawn all around the lake due to the large number of bays, islands and inlets (Figure 4.1). The smaller males move into the spawning grounds first, followed shortly thereafter by the females. The males remain longer overall at the spawning grounds than the females. Spawning takes place during the night and early morning, usually near rooted vegetation, submerged brush, or fallen trees, but at times over sand or gravel. Spawning activities usually involve one larger female and many males that swim in a long, compact queue. No nest is built by yellow perch. The transparent eggs

are extruded in a unique, gelatinous string which may be as long as 2.1 metres, as wide as 51 to 102 millimetres, and weigh up to 2 pounds. These egg masses are semi-buoyant and usually adhere to submerged vegetation or the substrate. Hatching usually takes approximately 8 to 10 days. The young, after hatching, are inactive for about 5 days, during the absorption of the yolk. Growth is extremely variable, depending on the population size, habitat size, and productivity, and stunting often occurs in crowded populations. Northern populations grow more slowly than southern populations, but live considerably longer.

Yellow perch are usually considered shallow water fish and are usually not taken below 10 metres. Adults and young are gregarious, often moving about in loose aggregation of 50 to 200 individuals, segregated by size. The young, in shallower water and nearer shore than the adults, are often found in mixed schools with other small minnows, such as spottail shiners. Yellow perch are inactive at night and rest on the bottom. There are migratory movements in the spring, movements inshore and out, up and down over the day, and seasonal movements out of and into deeper water in response to temperature and food distribution. Seasonal vertical movements of adult yellow perch suggest they move to follow the 20 °C isotherm. Yellow perch are active all winter under the ice in shallow water or in deeper water.

The food of the yellow perch changes with size and season but is largely immature insects, larger invertebrates, and fish taken in open water or off the bottom (Scott and Crossman, 1973). Active feeding takes place in the morning and evening (7 a.m. to 6 p.m.) with little to none at night.

Yellow perch are preyed on by almost all other warm to cool water predatory fish (Scott and Crossman, 1973). In Eden Lake, their main predators are northern pike, walleye, burbot, and other yellow perch. Other predators, such as water birds, are also a big threat. Yellow perch may compete for food with, in Eden Lake, lake whitefish,

ciscoes, and possibly suckers.

4.7 Cisco

Coregonus artedii or, more commonly, cisco/lake herring have the most extensive North American distribution of any cisco since it is found in the north-central and eastern United States and throughout most of Canada.

Like most coregonids, spawning takes place during times of declining temperatures in the fall of the year; the exact date depending on water temperature (Scott and Crossman, 1973). Large schools or aggregations are formed during spawning at sites where the water is shallow, 1 to 3 metres, over a gravel or stony substrate. Eden Lake ciscoes spawning locations likely include the bays and inlets around the lake, "Kap" Bay, "the Narrows", where the Hughes River enters Eden Lake, and where Eden Lake outflows into Kakinokumak Lake and the Numakoos River (Figure 4.1). Males always move onto the spawning grounds a few days before the females. After spawning activities, the eggs are deposited on the bottom and abandoned by the parents. Development of the eggs proceed slowly at the low winter temperatures and hatching does not usually occur until spring. The newly hatched fry remain at the spawning site until all of the yolk is absorbed and then they move into deeper water.

Ciscoes are a pelagic species that usually form large schools in midwater, however, this midwater depth varies with the seasons and the temperature (Scott and Crossman, 1973). In general, apart from spawning migrations, ciscoes tend to move in spring and early summer from shallow to deep water. They remain in the cooler, deep water until late summer (when upper waters start to cool) and they move back to the shallow areas.

Ciscoes, in keeping with their pelagic habit, are dominantly plankton feeders but can consume a wide variety of foods (Scott and Crossman, 1973). Larval ciscoes

require light to feed and eat dead zooplankton at first. At about 10 days old, their diet consists of algae, copepods, and Cladocera. Food items of adult ciscoes vary with season and location, however, immature aquatic insects such as *Daphnia* and mayfly nymphs are a staple of most ciscoes. Ciscoes have also been found to eat their own eggs and the eggs of other species. Some larger ciscoes may also eat smaller fish, such as minnows.

Ciscoes are prey to many predatory fish (Scott and Crossman, 1973). At Eden Lake, the main predators of the cisco are northern pike, burbot, yellow perch, and walleye.

4.8 Clams

Clams belong to the Kingdom Animalia, Phylum Mollusca, and Class Pelecypoda or Bivalvia; (Clarke, 1981; Clarkson, 1986). All Canadian freshwater clams belong to the order Eulamellibranchia; a group characterized by:

- a hinge containing a few teeth of diverse shapes and sizes;
- two large adductor muscles of about the same size, one anterior and one posterior;
- a partly closed mantle with well-developed siphons; and
- leaf-like gills within the mantle cavity.

Two superfamilies of this order are represented in Canada, Unionacea and Sphaeriacea. Both of these superfamilies are present at Eden Lake and in the surrounding waters, though no clams were collected that belonged to the latter (Table 4.1). The Eden Lake clams collected were identified as belonging to the family Unidonidae (Pearly Mussels). Clams of the Family Unidonidae are principally found in rivers and lakes, partly buried in the bottom, where the water is about one-third of a metre to two metres deep. Within the

Family Unidonidae, two subfamilies were found at Eden Lake, Anodontinae and Lampsilinae.

4.8.1 Subfamily Anodontinae

Clams belonging to the Subfamily Anodontinae, which has recently been renamed Pyganodoninae, are characterized as having absent or incomplete hinge teeth, whole outer demibrachs only used as marsupial (for enclosing the young), hooked glochidia, and short-breeding seasons (Clarke, 1981). Only one species belonging to this subfamily was collected from Eden Lake and the surrounding waters, *Pyganodon grandis* (Table 4.1).

Pyganodon grandis, or northern floater, have a distribution limited to the Canadian Interior Basin in the boreal forest region from northern Quebec west to central Alberta, and northwest to the mouth of the Mackenzie River (Clarke, 1981). They have been found in permanent ponds, in lakes, and in rivers more than about 9 metres wide.

Pyganodon grandis does not have a preferred substrate. Gravid or pregnant specimens with glochidia (larvae) have been collected from various locations in Canada between July 22 and August 24, but the duration of this species' gravid period is not known. Glochidia are triangular-ovate, with hooks, and measure about 0.36 millimetres long and 0.35 millimetres high. The host fish is unknown.

4.8.2 Subfamily Lampsilinae

Clams belonging to the Subfamily Lampsilinae are characterized as having well-developed hinge teeth, posterior part of the outer demibranchs only used as marsupial (for enclosing the young), hookless glochidia, and long-breeding seasons (Clarke, 1981). Only one species belonging to this subfamily was collected from Eden Lake and the surrounding waters, *Lampsilis radiata siliquoidea* (Table 4.1).

Table 4.1. **Taxonomic information on the snail (SN) and clam (CL) samples collected from Eden Lake and the surrounding waters.**

CLAM (CL) NUMBER	LOCATION COLLECTED	SUPERFAMILY, FAMILY, AND SUBFAMILY	SPECIES AND GENUS	COMMON NAME
CL1	ED1	Unionacea Unionidae Anodontinae	*Pyganodon grandis*	Northern floater
CL2	Adam Lake	Unionacea Unionidae Lampsilinae	*Lampsilis radiata siliquoidea* (female)	Fat mucket
CL3	Adam Lake	Unionacea Unionidae Lampsilinae	*Lampsilis radiata siliquoidea* (male)	Fat mucket
CL4	BAK1	Unionacea Unionidae Anodontinae	*Pyganodon grandis*	Northern floater
CL5	ED2	Unionacea Unionidae Anodontinae	*Pyganodon grandis*	Northern floater
CL6	BAK2	Unionacea Unionidae Anodontinae	*Pyganodon grandis*	Northern floater
CL7	BAK2	Unionacea Unionidae Anodontinae	*Pyganodon grandis*	Northern floater
CL8	BAK2	Unionacea Unionidae Lampsilinae	*Lampsilis radiata siliquoidea* (male)	Fat mucket

Lampsilis radiata siliquoidea, or fat mucket, have a distribution limited to the Canadian Interior Basin from Quebec to Alberta; Mackenzie River system north to the vicinity of Great Slave Lake; Great Lakes drainage from the Lake Superior to Lake Erie watersheds; and upper Ohio-Mississippi drainage from New York to Minnesota and Arkansas (Clarke, 1981).

Lampsilis radiata siliquoidea are very abundant, occurring in rivers and lakes of all sizes (Clarke, 1981). They also do not appear to have a preferred substrate as they have been found on all types of bottoms (clay, mud, sand, or gravel). This species often lives near shore in water as shallow as 5 to 8 centimetres. They are long-term breeders, with gravid periods extending from the first part of August to the middle of the following July. Glochidia are purse-shaped, without hooks, and measure from 0.24 to 0.26 millimetres in length and 0.26 to 0.30 millimetres in height. The only host fish of this species that is found in Eden Lake is the yellow perch.

Chapter 5: Experimental Results

5.1 Age Determination

Otoliths are commonly, but not universally, used in aging fish (Don Harron, June 1998, *pers. comm.*); it depends on the species. Some species are easily aged using otoliths while others are more easily aged using different body parts (e.g. fin rays or cleithrum).

Since only otoliths were collected from each Eden Lake fish, three different methods had to be employed to determine age. The application of each method depended dominantly on species but also, to some extent, on age (as gauged by the size of the otolith). For walleye, lake whitefish, cisco, yellow perch, burbot, and some young white suckers age determinations were done using reflection microscopy (cf. Section 3.4) because the annuli were easily distinguished from core to rim.

Other older white suckers and young northern pike were aged using a modified Power's (1978) "break and burn" or "break, polish and burn" method. This method, or some modification of it, is the second most commonly used method (next to reflection microscopy) in age determination using otoliths and is a relatively straightforward procedure (John Babaluk, September 1998, *pers. comm.*). An unembedded otolith is manually broken longitudinally and/or ground down using a small tabletop grinder equipped with fine sandpaper to expose the primordium. The otolith is then held in a flame for a short period of time until it starts to brown. The optically dark and light alternating bands making up the annuli burn to a differing extent (due to the differences in the organic content), such that they become more distinguishable from one another (Figure 5.1). Once browned, the otolith is placed in a small dish of ethanol, which acts to cool the otolith without damaging it. Reflection microscopy techniques are then used to age the otolith whose annuli are now prominent.

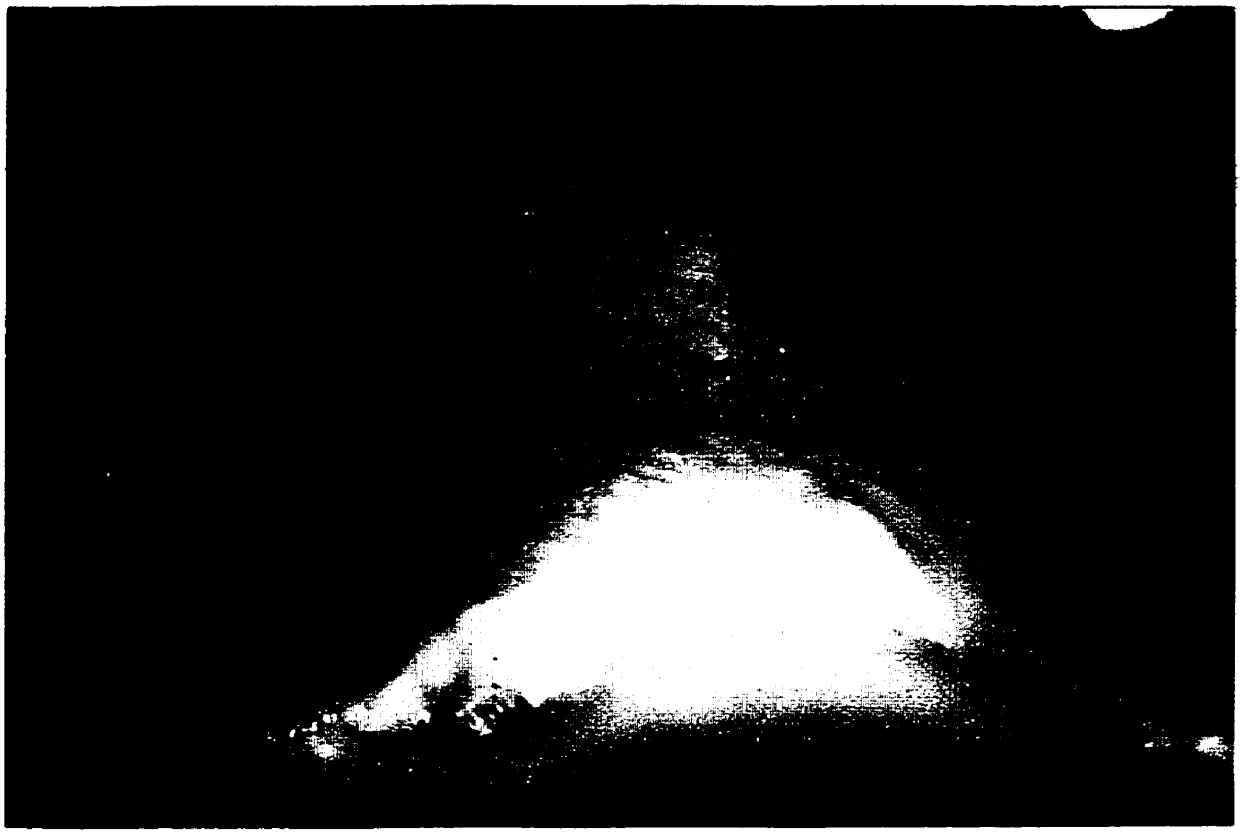

Figure 5.1. **Black and white photograph of a burned white sucker otolith. The field of view is approximately 2 mm across. Each pair of black dot marks one annuli, making the fish 18 years old. Notice how the annuli get thinner as the fish ages.**

Cathodoluminescence (CL) microscopy (cf. Section 3.3) was the third technique used in aging the Eden Lake fish. CL microscopy has not been previously described as an aging method, however, it was the only viable method with some potential for older northern pike due to the complexity of their annuli.

The ages determined for the Eden Lake fish are provided in Appendix A (Table 5). Walleye ranged in age between 3 and 23, with 72% falling between the ages of 9 and 15. Northern pike ranged in age from age 4 to 22, with 73% falling between the ages of 8 and 13. The white suckers exhibited a narrower age range, between 10 and 25 years, however, no one age class was prominent within this range. The 13 yellow perch ranged in age between 5 and 10, with 85% falling between the ages of 5 to 8. The few lake whitefish that were caught were well spread between the ages of 11 and 29, with the 29-year-old fish being the oldest-aged fish in the entire sample set. The 8 cisco ranged in age between 4 and 22, with no prominent age class observed among the catch (probably due to the small number of this species caught). The two burbot were aged at 9 and 10 years. The one longnose sucker was likely >15 years old, but, this is only approximate because the one otolith extracted from the fish was damaged during sample preparation.

A recommended age validation technique for otoliths is to compare the fish's age against its recorded length. Length is preferred to other morphometric measurements, such as weight because if the fish ate just prior to being caught, it will weigh more than a fish of the same age that did not. However, at least 30 fish are required for the age-length comparisons to be considered reliable (Don Harron, June 1998, *pers. comm.*). Therefore, age versus length comparisons could only be made for the walleye and northern pike species within the Eden Lake sample set. These are shown in Figures 5.2 and 5.3.

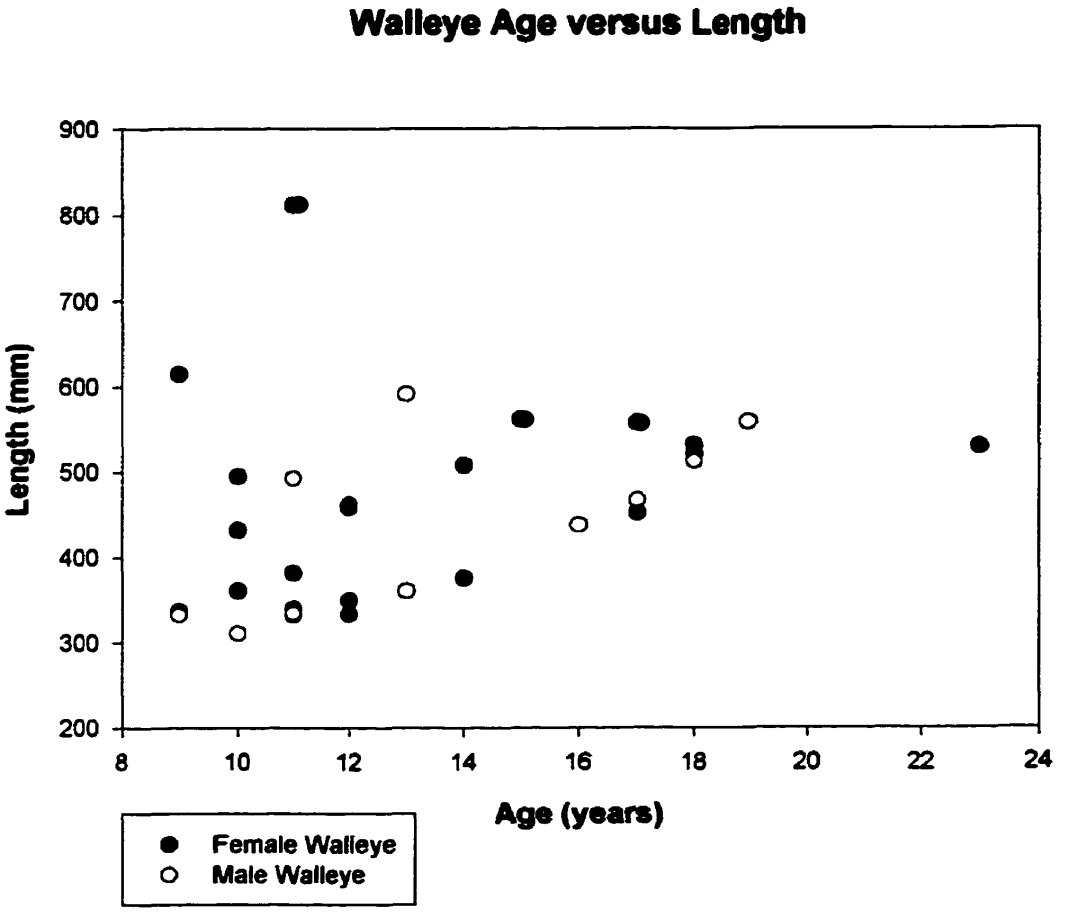

Figure 5.2. Age versus length comparisons for female and male Eden Lake walleye. The graph shows a moderately good correlation for the male walleye but a poor correlation for the female walleye.

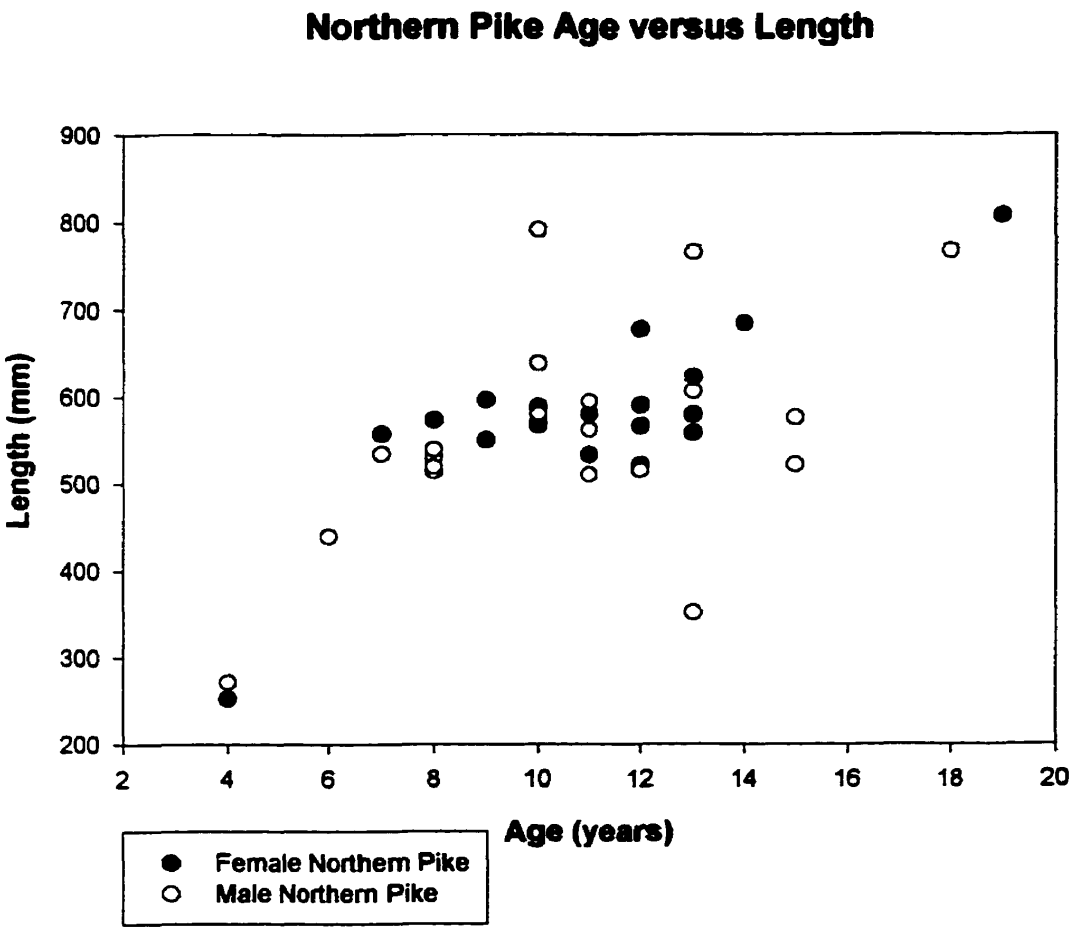

Figure 5.3. Age versus length comparisons for female and male northern pike from Eden Lake and the surrounding water bodies. The graph shows a moderately good correlation for the female northern pike but a poor correlation for the male northern pike.

For the walleye (Figure 5.2), exactly 30 of the fish could be compared because only the heads were collected from the other 34 walleye in the sample set (i.e., the ones caught by sport fishermen) and, therefore, no length data was available for comparison. The age versus length graph depicts only a moderate to poor correlation overall for both male (unfilled circle) and female (solid black circle) walleye. Statistical analysis on the two genders would likely yield an acceptable correlation coefficient for the males but, a poor correlation coefficient for the females, due to the three outliers. The majority of both the female and male walleye within the sample set fall into a narrow length grouping of between 300 and 600 mm, however, this is likely a function of the largest caught in each net being desirable for inclusion in the sample set for otolith analyses. While there appears to be no age grouping among the male walleye, there is an obvious concentration of females between the ages of 9 and 14 in the sample set. The female walleye lengths corresponding with the ages of 10, 11 and 12 are highly variable; ranging from ~350 to ~500 mm, ~325 to ~825 mm, and ~325 to ~450 mm, respectively.

For the northern pike (Figure 5.3), only 2 of the 45 fish in the sample set could not be compared because their heads were collected from sport fishermen. The age versus length graph for the pike shows an overall moderate correlation for the female pike but a poor correlation for the male pike. Between the ages of 7 and 15 years there is an obvious clustering at the 600-mm length for both males and females. This may be due to natural variation in this northern lake and/or that cathodoluminescence microscopy, without cleithrum for validation, is not a reliable technique to age northern pike due to the complexity of their annuli as they get older. Using the luminescence to identify annuli may not have been consistently accurate, especially if one or more of the annuli were lacking the activator elements.

5.2 Cathodoluminescence Microscopy

Cathodoluminescence microscopy (CL) was the first qualitative analytical technique used to assess the Eden Lake otoliths. It provided new information on:

- the distribution of trace elements (because of its sensitivity to low concentrations of activator elements); and
- the fine-scale annular features.

As previously mentioned in Section 3.3, under CL the otoliths are bombarded by an electron beam. The wavelength and intensity of the emission is a function of the activator concentration and the site it occupies within the mineral (Marshall, 1988). Under CL, pristine calcium carbonate will only faintly luminesce and the luminescence will be very uniform.

Photographs were taken under CL of all the otoliths showing moderately strong to very strong luminescence; exposure times were usually less than 400 seconds using 400 ASA film. Photographs had to be taken rapidly as the electron beam tended to ablate the epoxy surrounding the otolith, spreading it over the otolith, and this greatly reduced the intensity of the luminescence. After each ring of otoliths was photographed, it was repolished to remove this epoxy build-up. Only the fine polishes (e.g., 5.0 μm, 1.0 μm and 0.3 μm) were used so as not to wear down the otolith and remove any of the center annuli. Repolishing in this manner proved satisfactory in maintaining the original intensity of the luminescence, allowing otoliths to be re-examined as many times as necessary.

5.2.1 Fish

Similarities, and some distinct differences, were observed in both the intensity and luminescence distribution in the otoliths suggesting differences in the amount of trace elements and timing of their incorporation in the otoliths. Some anomalies were also observed.

Typical Luminescence

The majority of the Eden Lake walleye and white suckers (e.g., Figures 5.4 and 5.5) exhibited weak to no luminescence regardless of where they were caught. The weak luminescence observed was confined to the primordium, a few annuli and/or the most recent annulus. In all cases where the luminescence was restricted to a few annuli and/or them most recent annulus, the luminescence occurred as faint, single, thin to moderately thick yellow-green lines in the walleye and white suckers, respectively. The longnose sucker caught at the KAP site also did not exhibit any luminescence.

Northern pike, conversely, exhibited moderate to strong luminescence at all capture locations. Figure 5.6 is a CL photograph of part of a northern pike otolith caught in Adam Lake. Eden Lake flows into Adam Lake in the north (through a large culvert under Hwy. 391; cf. Figure 3.1). All of the northern pike caught in Eden Lake displayed this type of yellow-green luminescence, but to varying intensities. The luminescence observed in all of the pike was confined to discrete "packets" of luminescent lines (usually 4 to 12 lines per packet) and the luminescence was always observed, in differing intensities, from the primordium through all the distorted annuli to the most recent annulus. Further, within the distorted annuli, the luminescence was always brightest in the optically light bands, versus the alternating optically dark bands.

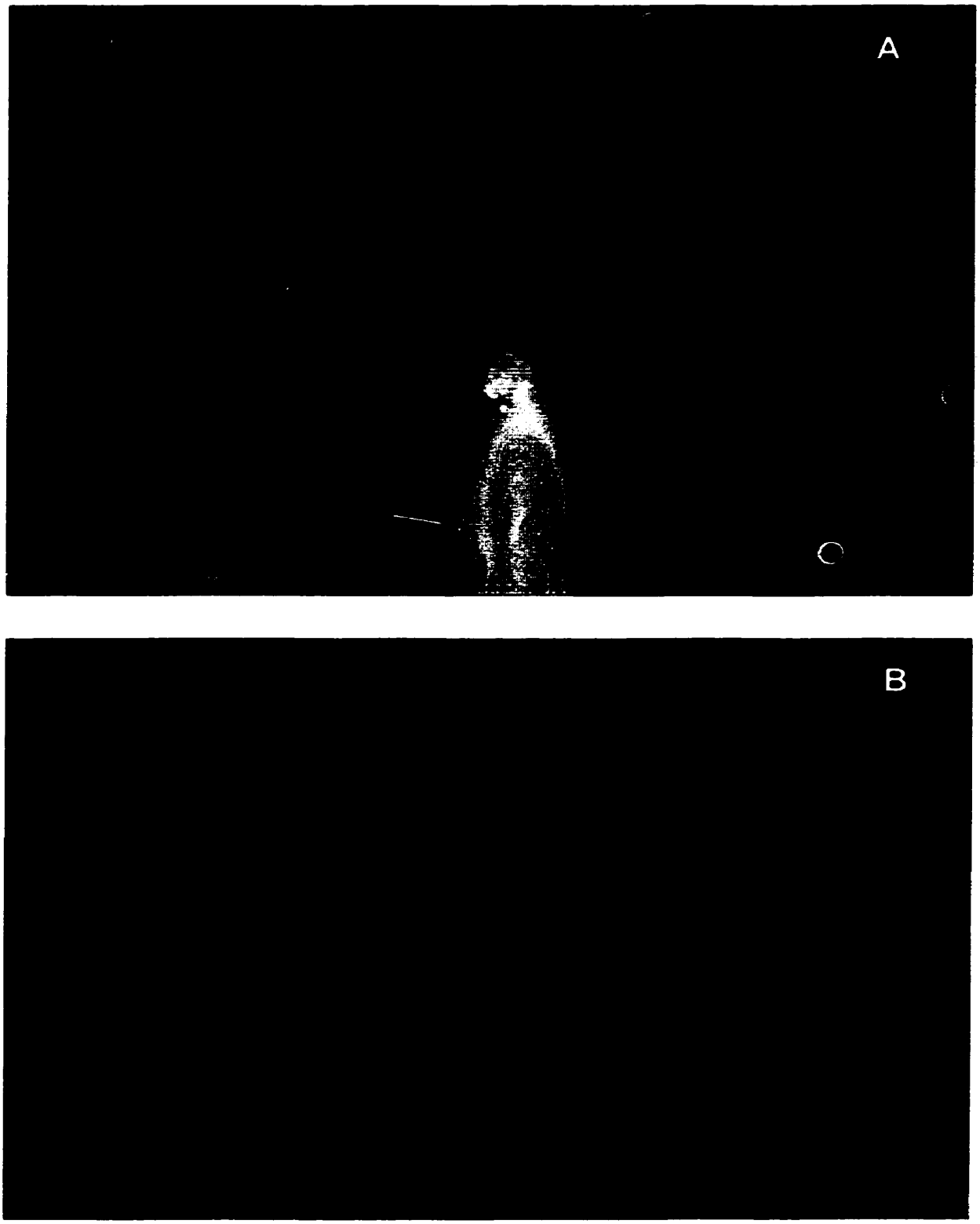

Figure 5.4. **Cathodoluminescence photographs of two Eden Lake walleye otoliths exhibiting the typical weak luminescence. (A) Photograph of a walleye otolith with only one luminescent annulus. The field of view is approximately 2 mm across. (B) Photograph of a walleye otolith with luminescence only in the most recent annulus. The field of view is approximately 1 mm across.**

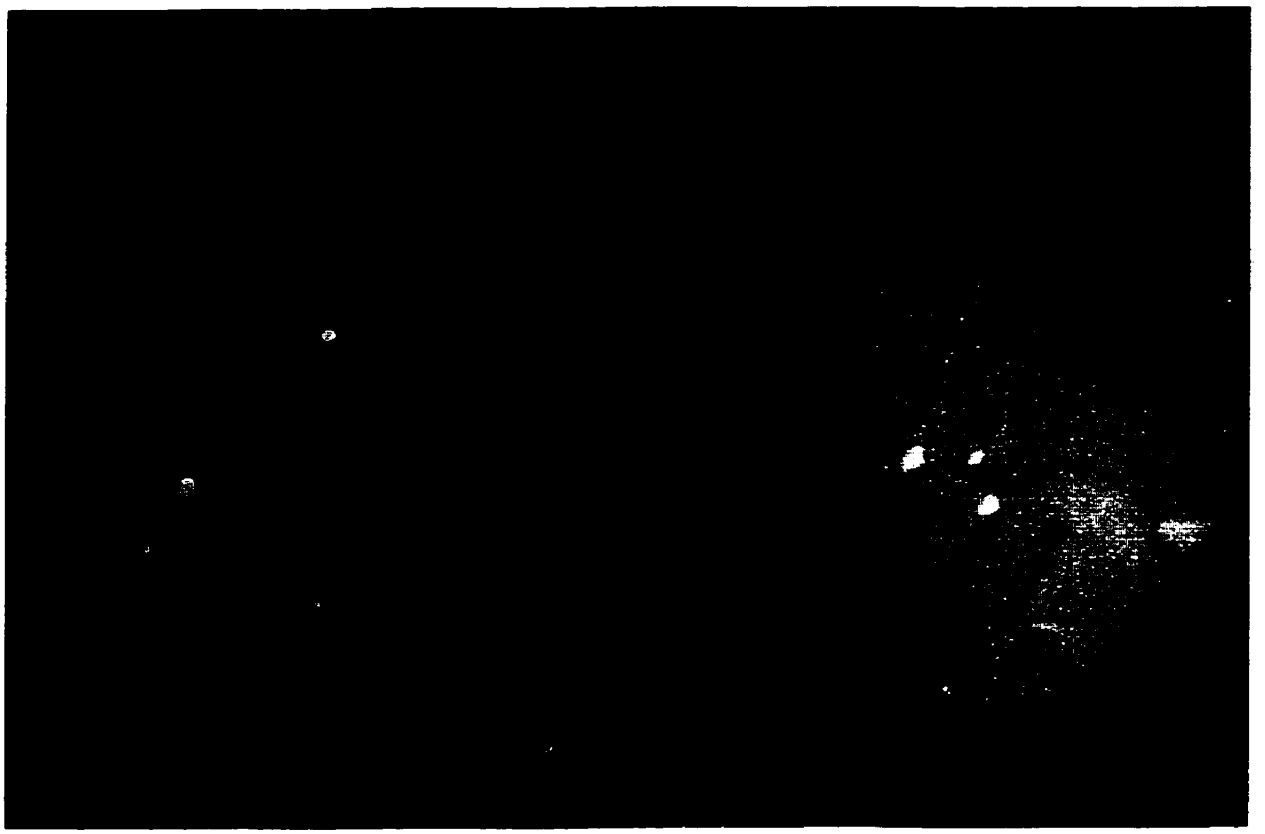

Figure 5.5. A cathodoluminescence photograph of a white sucker otolith exhibiting very weak luminescence. The field of view is approximately 2 mm across.

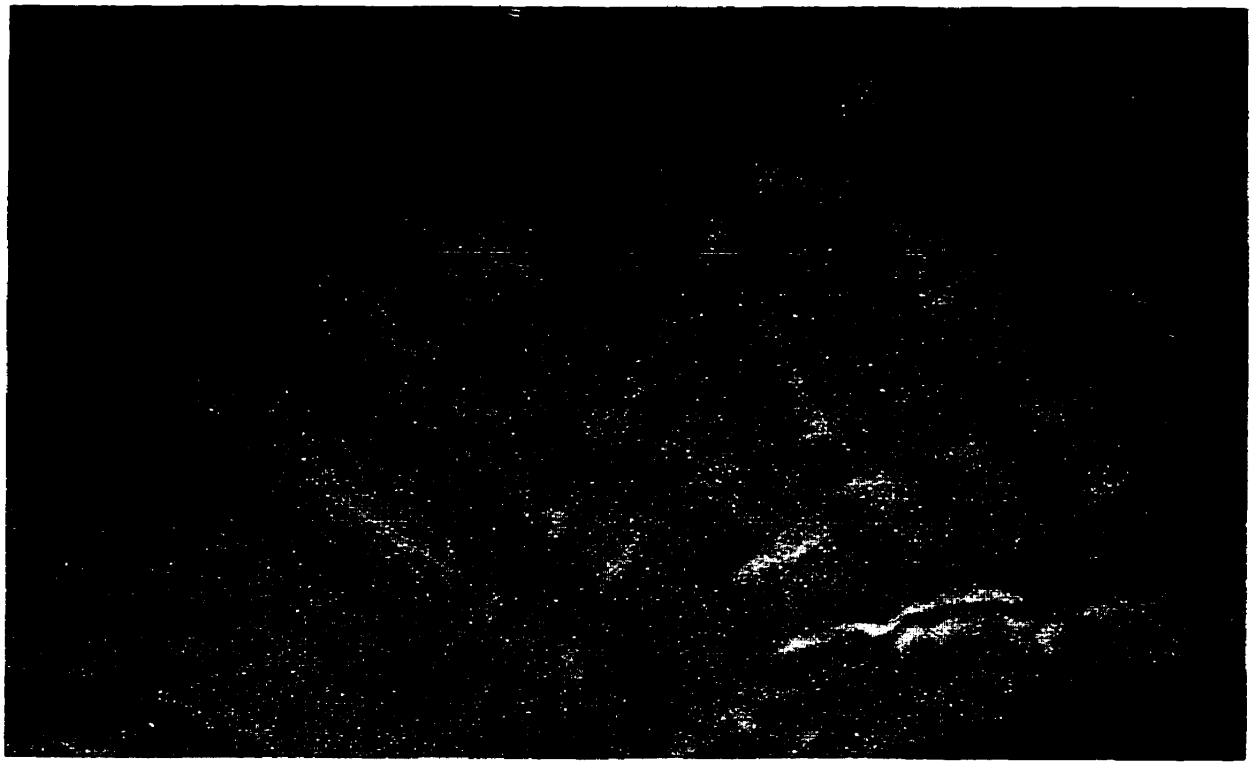

Figure 5.6. A cathodoluminescence photograph of a northern pike otolith exhibiting the discrete "packets" of bright yellow-green luminescence typically observed in the Eden Lake northern pike otoliths. The field of view is approximately 1.5 mm across. This fish was angled from Adam Lake at the inflow point between Eden Lake and Adam Lake.

The cisco, lake whitefish, and yellow perch all exhibited strong luminescence, however, the luminescence differed from that of the northern pike in its intensity and distribution throughout the annuli. In the northern pike, all of the annuli (from core to rim) exhibited luminescence (to varying intensities; e.g., Figure 5.7). The cisco, lake whitefish, and yellow perch otoliths (e.g., Figure 5.8, 5.9 and 5.10, respectively), all exhibited strong to moderately strong luminescence, however, the luminescence was not always continuous from the core to rim. All three of these species frequently exhibited years wherein annuli appeared to have absorbed higher concentrations of activator elements and years wherein they appeared to have absorbed little or none at all. A few of the cisco and lake whitefish also exhibited strong luminescence only in the most recent annulus (e.g., Figure 5.11). The luminescence within these three species ranged from single thin to moderately thick luminescent lines (like the walleye and white suckers) to discrete "packets" of a few luminescent lines within one annulus (like the northern pike). The luminescence was also, as was observed in the northern pike, brightest in the optically light bands of each annulus in all three species.

The burbot from the BAK1 net site exhibited a few yellow-green luminescent annuli similar to the yellow perch, lake whitefish, and cisco, however, the luminescence was markedly weaker.

Atypical Luminescence

There were three otoliths, from different species, that exhibited very different luminescence from that described in the previous section. Since these were the only otoliths out of the entire sample set that displayed these marked differences it was assumed that these fish were atypical.

Figure 5.7. A cathodoluminescence photograph of a northern pike otolith exhibiting a brightly luminescent primordium and slightly weaker luminescent annuli. The field of view if approximately 4 mm across.

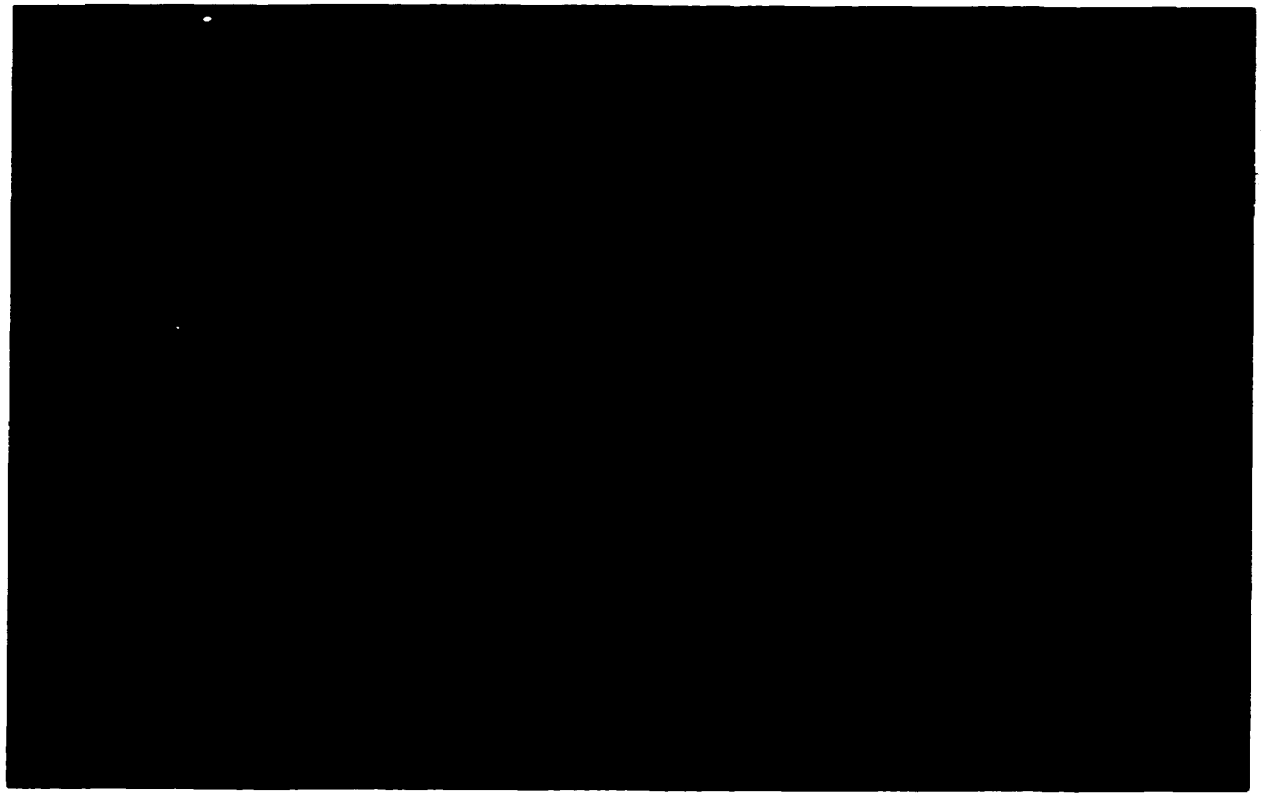

Figure 5.8. A cathodoluminescence photograph of a typical cisco otolith exhibiting strong luminescence. The distribution of the luminescence is continuous from the primordium to the most recent annuli, though it varies in intensity. The field of view is approximately 4 mm across.

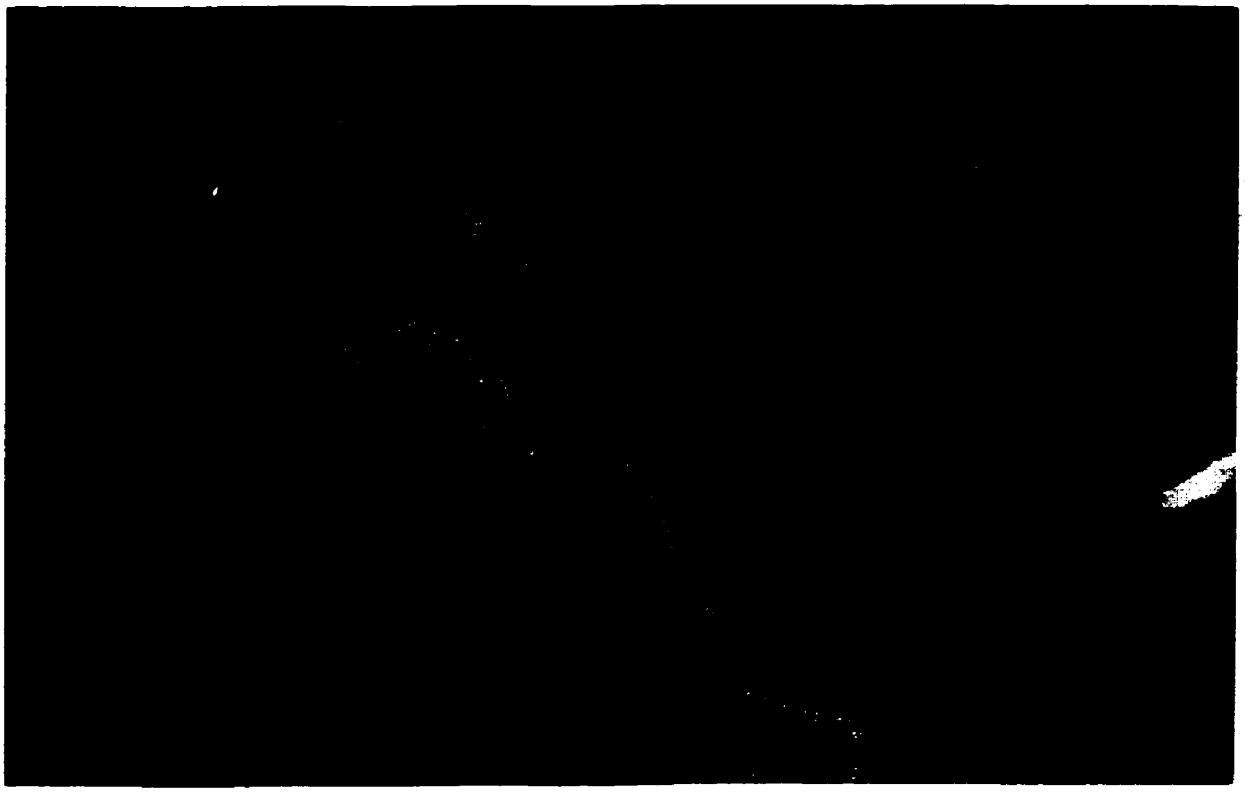

Figure 5.9. A cathodoluminescence photograph of a lake whitefish otolith exhibiting only a few brightly luminescent annuli, typical of the Eden Lake lake whitefish examined. The field of view is approximately 1 mm across.

Figure 5.10. A cathodoluminescence photograph of a yellow perch exhibiting strong luminescence typical of all of the Eden Lake yellow perch. The distribution of the luminescence is such that there appear to be years wherein higher activator element concentrations were absorbed and years wherein little or no activator elements were absorbed. The field of view is approximately 3 mm across.

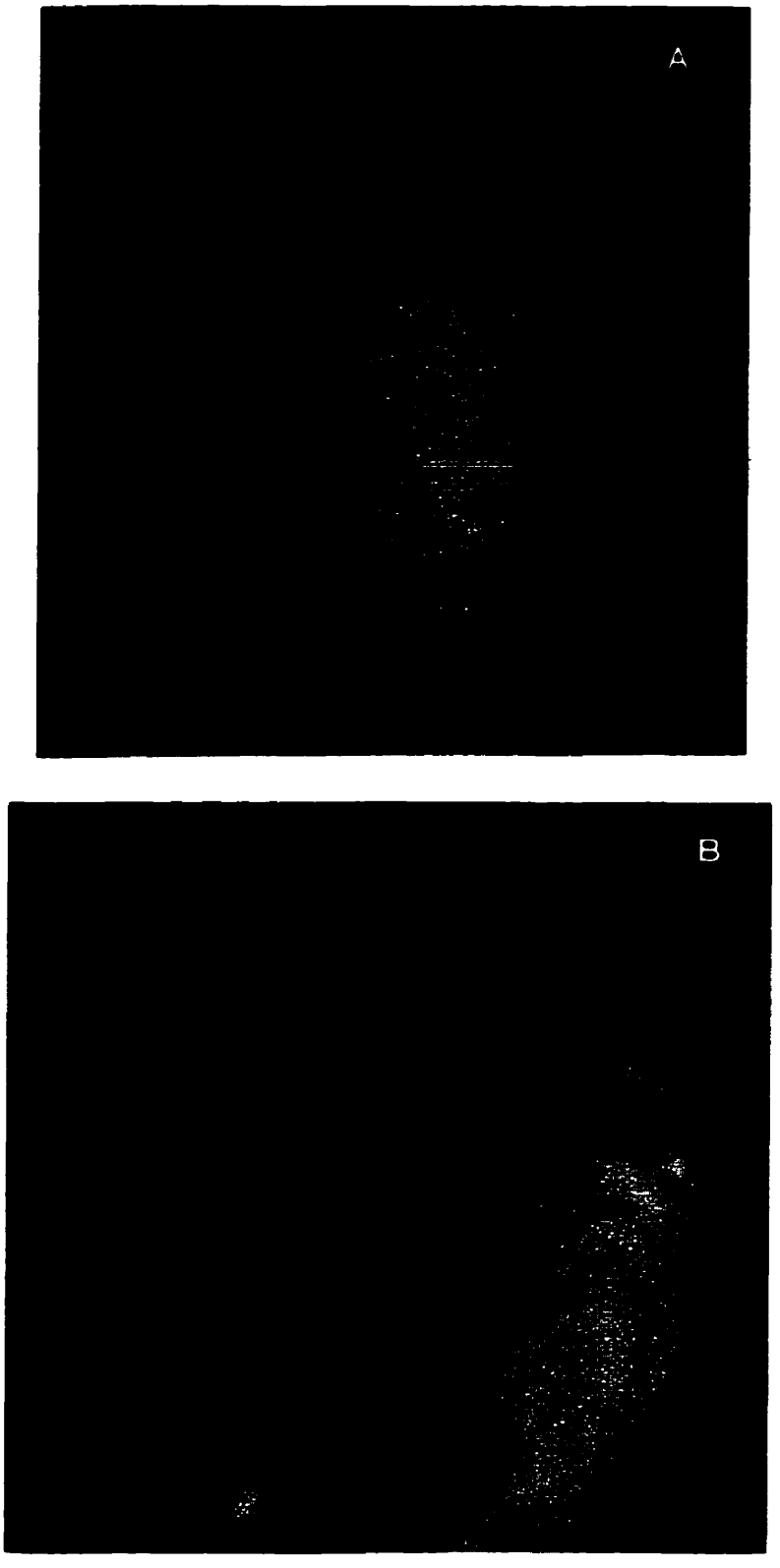

Figure 5.11. **Cathodoluminescence photographs showing fish otoliths that displayed only one strongly luminescent annulus (the most recent). (A) Photograph of a cisco otolith. The field of view is approximately 2 mm across. (B) Photograph of a lake whitefish otolith. The field of view is approximately 2.5 mm across.**

Atypical luminescence was observed in a white sucker caught near the Eden Lake Complex at the ED1 net site (Figure 5.12). The typical white sucker otoliths exhibited weak to no luminescence. This white sucker exhibited a very strong red luminescence that was brightest in the primordium but continued through to the rim. Further, the luminescence within each annulus appeared to be brightest in the optically light bands as was observed for all the other fish that exhibited the yellow-green luminescence.

The second otolith atypical luminescence was from a cisco caught at the KAP1 net site. The luminescence exhibited by this fish was a bi-colored luminescence (Figure 5.13). The luminescence in the core was purplish-red while a few of the more recent annuli were yellow-green.

The last atypical otolith was from a walleye caught at Point E, one of the sport fisherman sites located at the northeast end of "KAP" Bay. This walleye otolith displayed no luminescence in the primordium (typical for Eden Lake walleye) but then bright red luminescent lines within the later annuli (Figure 5.14), similar to the luminescence observed in the atypical white sucker (cf. Figure 5.12). The luminescence in this otolith was distinctly cyclical with a bright luminescent line defining the start of the annulus and less luminescent lines between each bright one.

Luminescence Trends

In order to be able to determine which species at which location(s) exhibited the greatest luminescence, and therefore likely contained the most trace elements; a qualitative rating system was devised. The intensity of the luminescence was rated on a scale of 0 to 10 whereby "0" indicated that no luminescence was observed and "10" indicated that a very strong luminescence was observed. These ratings are provided in

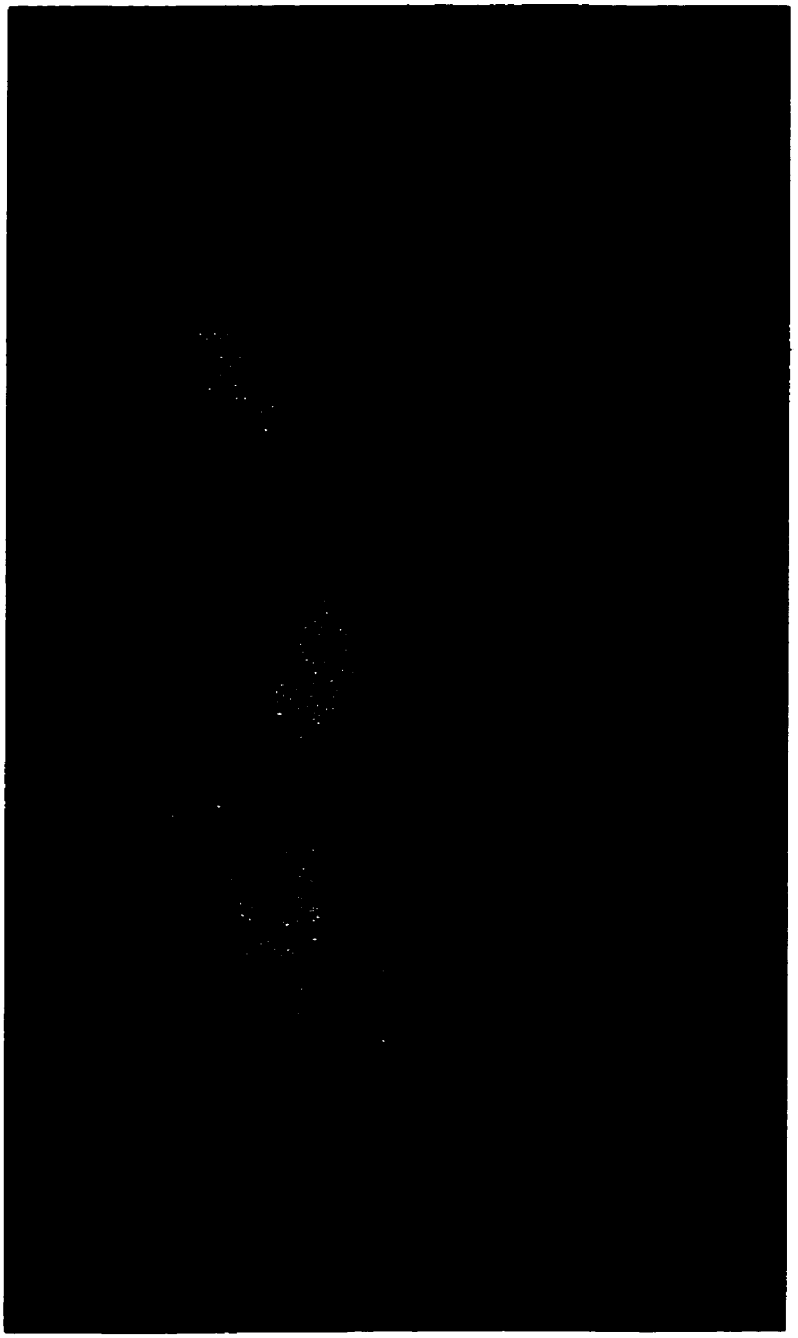

Figure 5.12. **A cathodoluminescence photograph of a white sucker otolith exhibiting atypical and very strong red-orange luminescence. The field of view is approximately 2 mm across.**

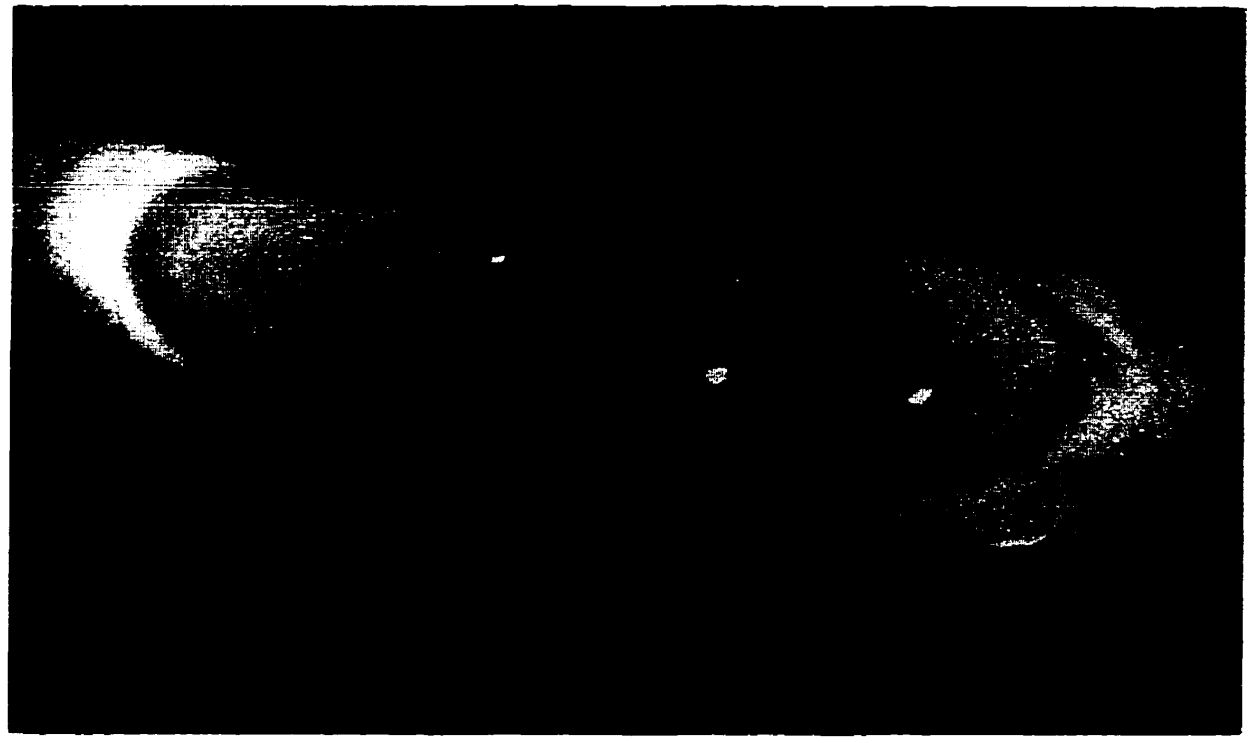

Figure 5.13. A cathodoluminescence photograph of a cisco otolith exhibiting atypical bi-color luminescence. The primordium appears purplish-red while the annuli were the more typical yellow-green color found in the other cisco otoliths from Eden Lake. The field of view is approximately 4 mm across.

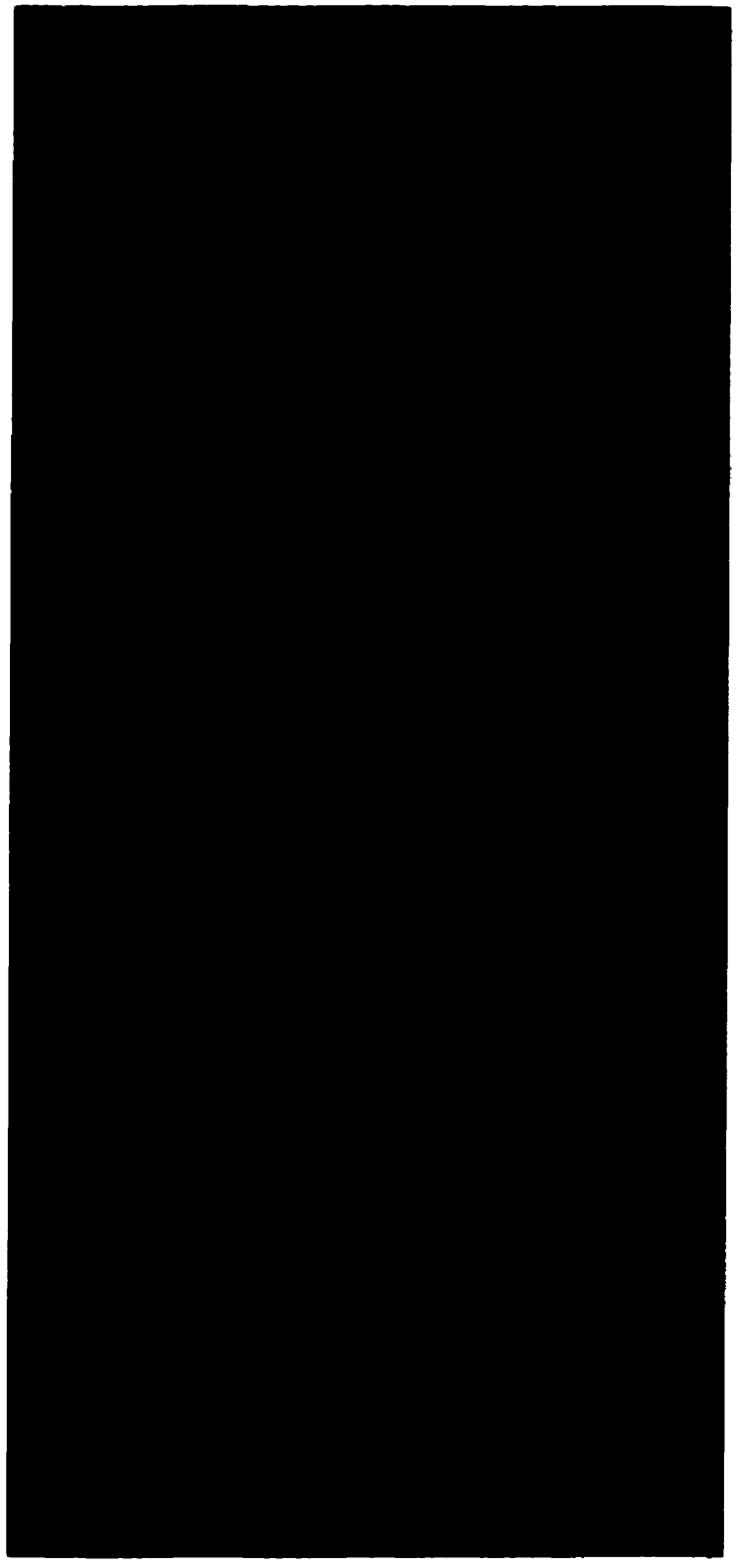

Figure 5.14. **A cathodoluminescence photograph of an Eden Lake walleye otolith exhibiting atypical red luminescence, similar to that observed in the atypical white sucker (Figure 5.12). The field of view is approximately 1 mm across.**

Appendix A (Table 6).

It was assumed that the fish caught at each site were representative of the fish frequenting that location of the lake at any given time. Working with this assumption, an attempt was made to determine the location(s) on Eden Lake exhibiting the strongest luminescence for each species by averaging the CL ratings of each fish of each species caught at that location (Figures 5.15 to 5.20). For example, if the all 5 walleye caught at KAP1 were each given a CL rating of 0, the average CL rating at KAP1 for walleye would be 0.

The white sucker and walleye otoliths did not show any distinct trends in their luminescence distribution and no systematic variations in the intensity of the luminescence at each site were observed. Both species exhibited weak luminescence (CL ratings of 0-2) at all locations of capture and, therefore, averaging of the ratings at the separate locations indicates that no singular location contains walleye or white suckers with a greater concentration of trace elements (Figure 5.15 and 5.16).

Similarly, there were no systematic variations observed, at each capture site, in the distribution and intensity of the luminescence in the lake whitefish, cisco, yellow perch and burbot otoliths. At all locations around the lake, these four species' otoliths displayed moderate to strong continuous luminescence or years of strong luminescence coupled with years of very weak or no luminescence (CL ratings from 5 to 10 at every location of capture). Further, the years of strong, weak and no luminescence within the otoliths of both the same and different species, caught at the same or different locations, could not be correlated. Averaging of the ratings assigned to the coregonids (i.e., cisco and lake whitefish) together and the burbot and yellow perch together (as only 2 burbot were caught) supports that no one site was contributing more trace elements to the otoliths than any other (Figures 5.17 and 5.18).

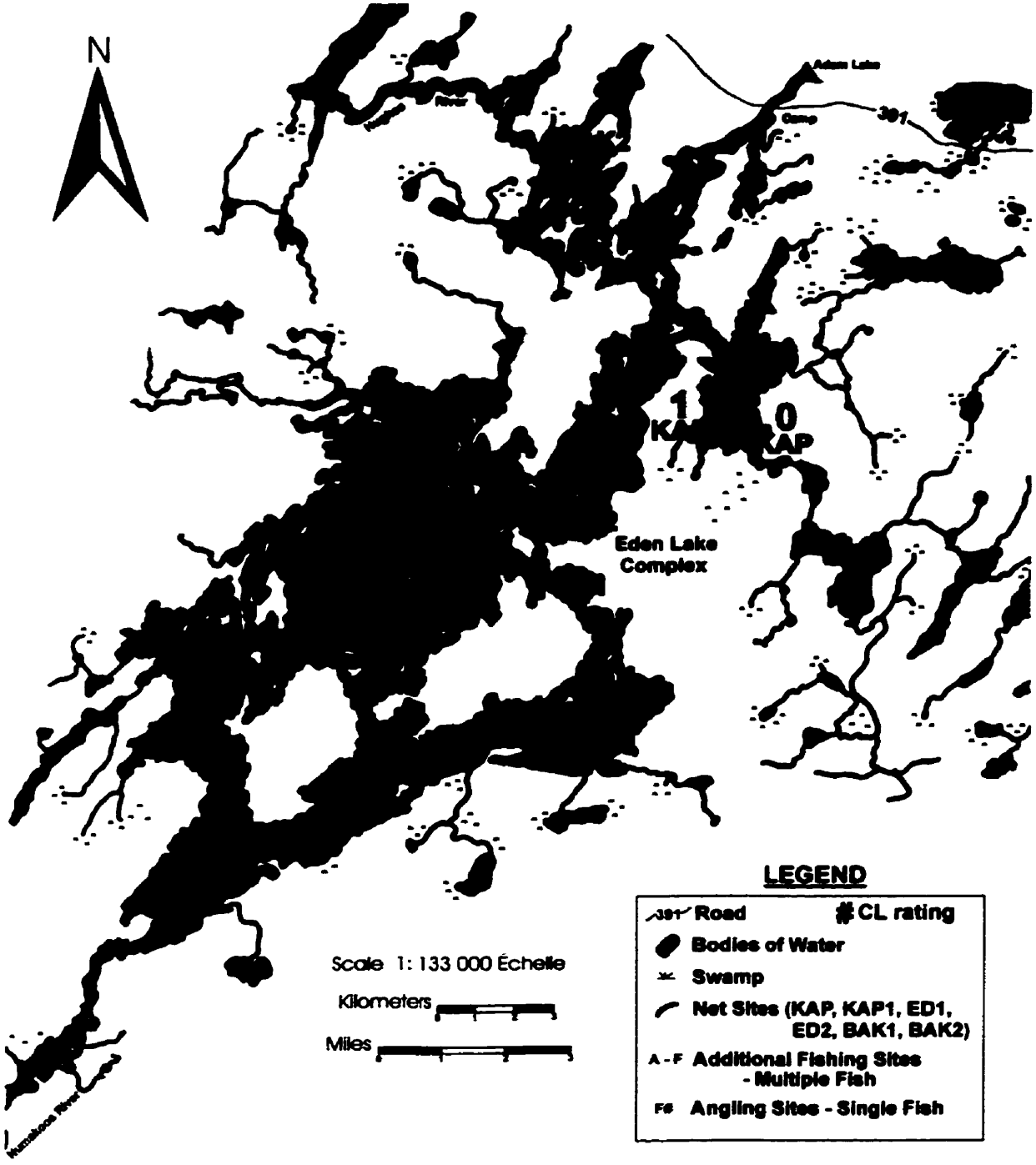

Figure 5.15. **Map showing the averaged CL ratings (on a scale of 1 to 10) for the white suckers at each capture location.**

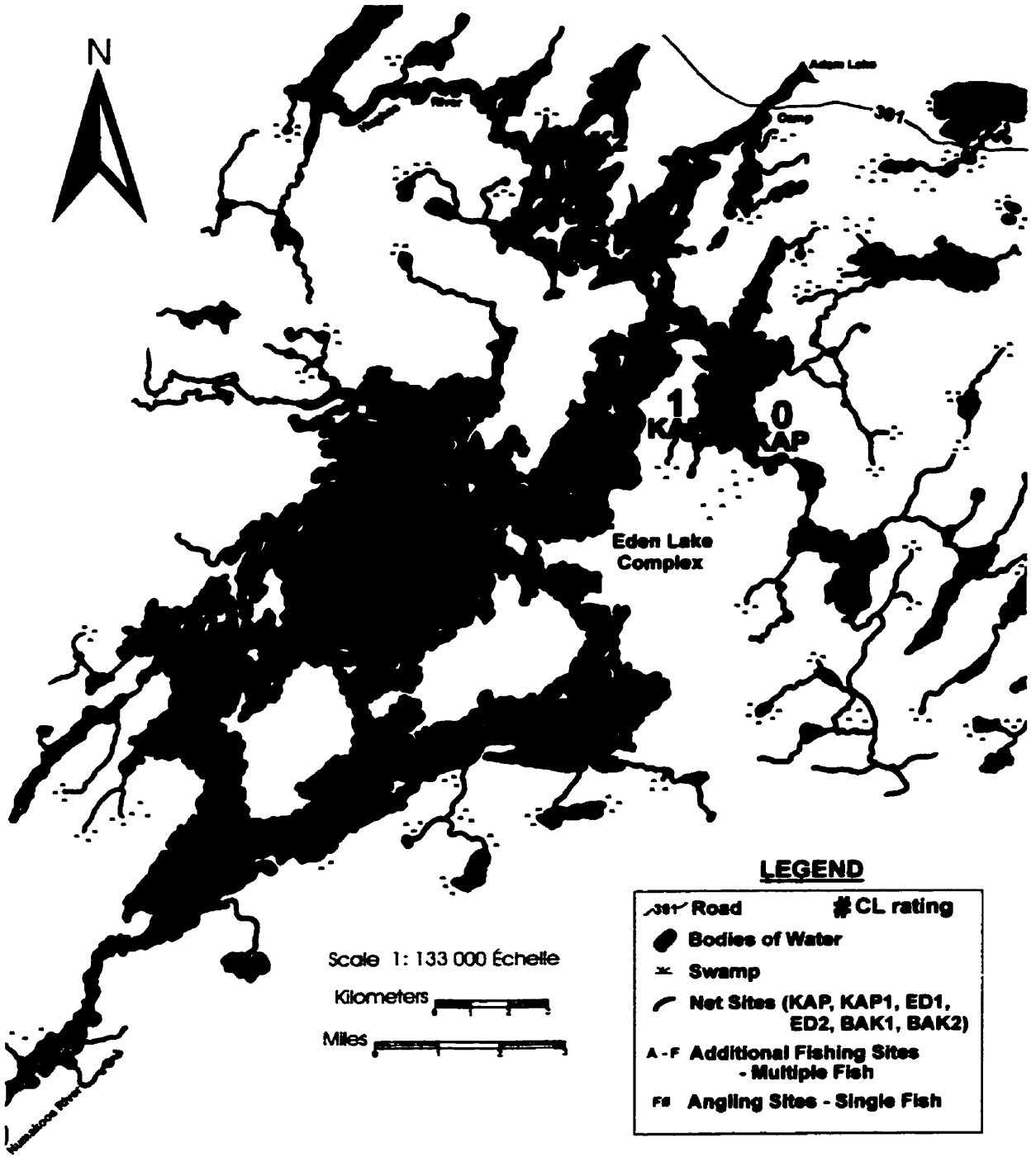

Figure 5.16. Map showing the averaged CL ratings (on a scale of 1 to 10) for the walleye at each capture location.

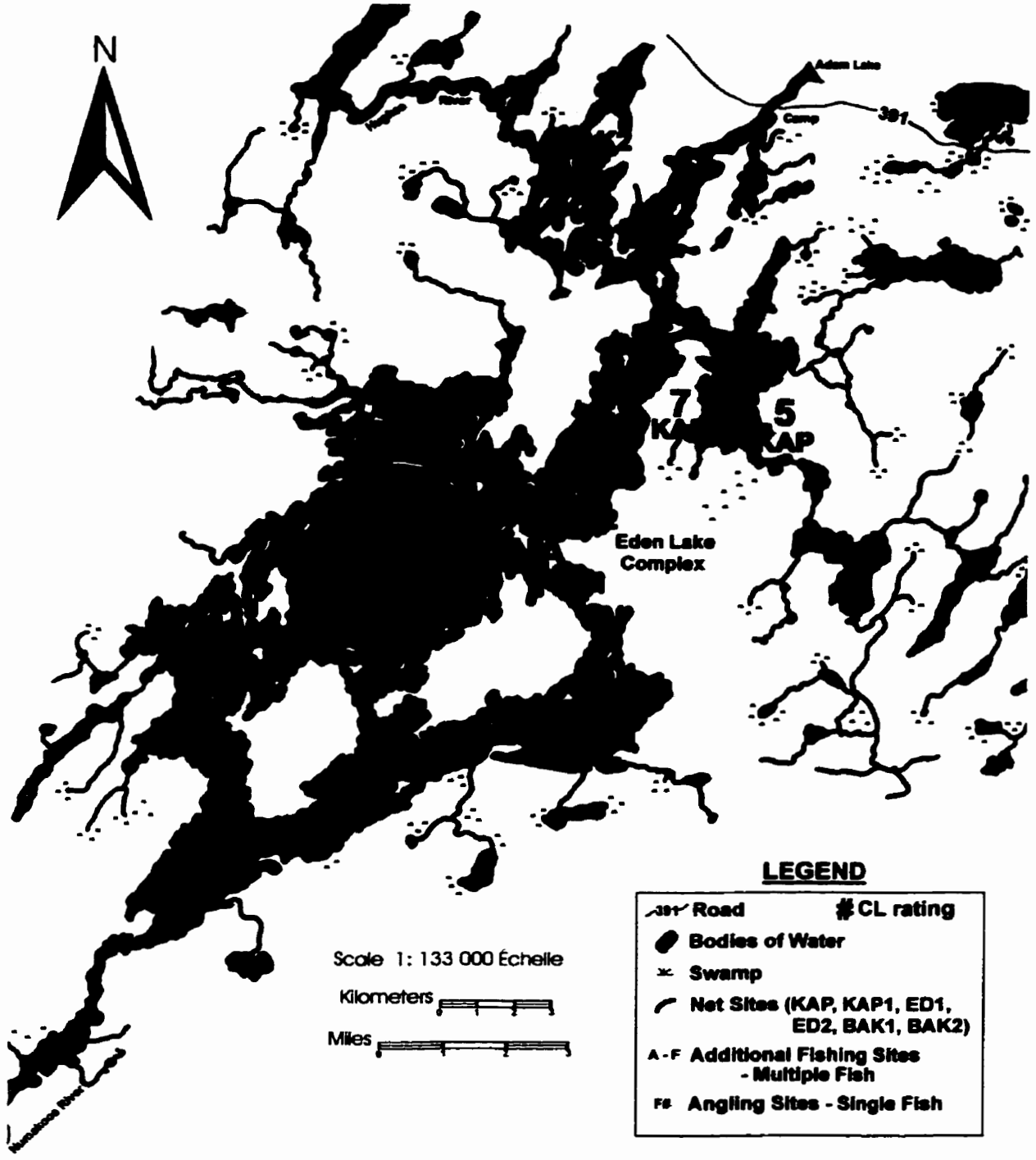

Figure 5.17. Map showing the averaged CL ratings (on a scale of 1 to 10) for the lake whitefish and cisco at each capture location.

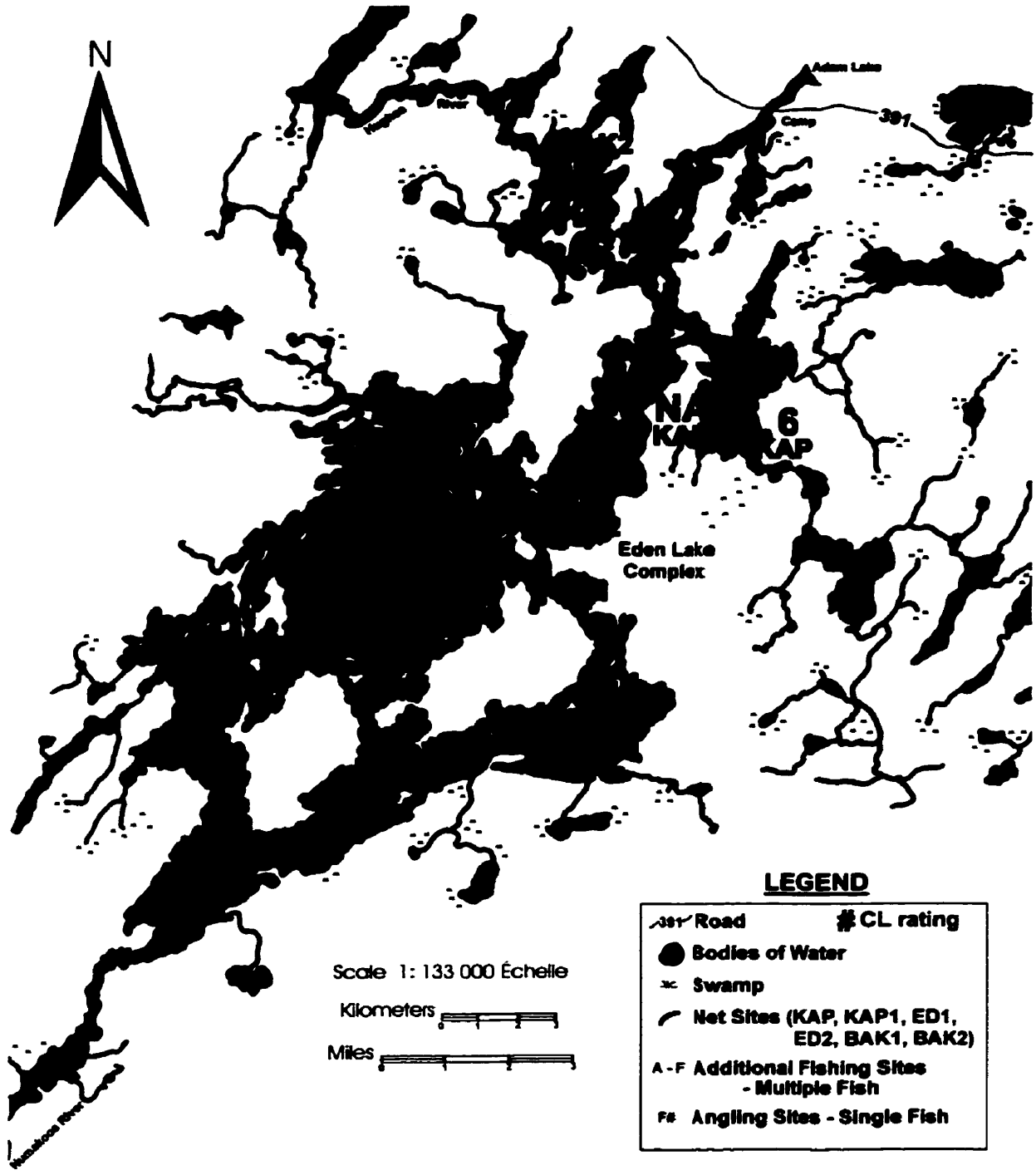

Figure 5.18. Map showing the averaged CL ratings (on a scale of 1 to 10) for the yellow perch and burbot at each capture location.

In contrast to all of the other species, there were definite trends in the distribution and intensity of the luminescence observed in the northern pike otoliths from the different capture locations. The pike caught for background comparisons (i.e., BAK1 and BAK2) all contained otoliths which exhibited a weaker luminescence than the pike caught in the ED1 and ED2 nets, angled in Eden Lake close to the Complex (e.g., Point A), or off the dock at the Campsite (*cf.* Figure 3.1). These "background" pike otoliths, however, showed a greater degree of luminescence than then otoliths from pike caught in the KAP and KAP1 nets. The pike caught close to the Complex, at the Campsite and at the ED1 and ED2 sites exhibited both a brightly luminescent primordium and brightly luminescent annuli similar to that shown in Figure 5.6 (CL rating between 8 and 10). In contrast, the majority of the BAK1 and BAK2 pike displayed a strongly luminescent primordium but weaker annuli (CL rating between 6 and 8). The KAP and KAP1 pike displayed moderate luminescence from primordium to outer edge (CL rating of 5). The few pike angled in the first set of Narrows in Eden Lake (cf. Figure 4.6) displayed variable luminescence ranging from a brightly luminescent primordium and weaker luminescent annuli (similar to BAK1 and BAK2 pike) to brightly luminescent primordium and brightly luminescent annuli (similar to the ED1 and ED2 pike).

Averaging of the CL ratings of the pike, at each different location of capture, however, found that the trends were not as definite as they appeared. According to Figure 5.19, there is likely no one site contributing greater concentrations of trace elements to the pike otoliths than another site. Neighboring capture sites, less than a couple kilometres from one another, also show different averaged CL ratings and it is highly unlikely that the fish, particularly young pike, remained within a kilometre of the net or angling site.

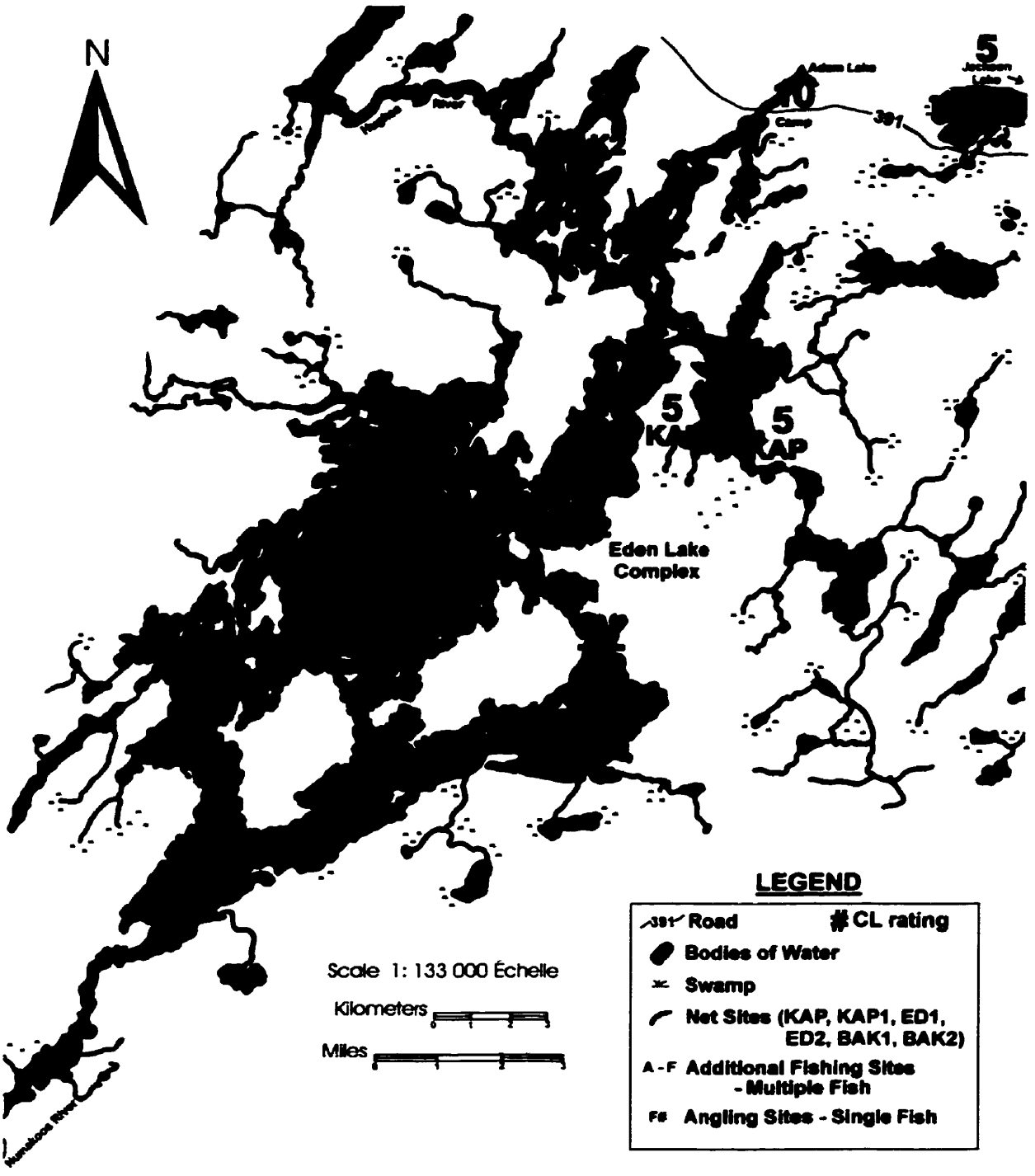

Figure 5.19. Map showing the averaged CL ratings (on a scale of 1 to 10) for the northern pike at each capture location.

As a final confirmation, to determine that no area(s) of Eden Lake contained the fish with the strongest luminescence and/or, conversely, the weakest, the CL ratings that were determined for each species at each location were averaged. For example, if the walleye at KAP1 had a total rating of 0 and the northern pike had a total rating of 8, and the yellow perch had a total rating of 7, the averaged CL rating for KAP1 would be 5. The result of assessing the luminescence at the different capture locations for all the species combined (Figure 5.20) was that there is no systematic variation or trend to the luminescence in the lake. The overall CL ratings range between 3 and 5, with the "background" sites (i.e., BAK1 and BAK2) rating identically to or higher than the "Complex" sites (i.e., ED1, ED2, KAP and KAP1).

5.2.2 Clams

The eight clam shells that were collected from the five locations in Eden and Adam Lake were also looked at using CL microscopy. The clams are less mobile but still have a calcium carbonate shell. All of the clam shells that were examined showed an even stronger luminescence than was observed in the different fish species and the luminescence varied with varying growth regions. The intensity of the luminescence was strongest in the pearly nacreous or lamellar layer (inside of shell) in comparison to the prismatic layer (where the crystals of calcium carbonate are oriented perpendicular to the outside of the shell). The distribution of the luminescence in all the clams examined, though varying in intensity, was continuous throughout the shell. The color of the luminescence observed in the clam shells was also much more green than that observed in the otoliths. This is possibly due to crystal structure differences between the calcium carbonate in the shell in comparison to the otolith or the incorporation of different trace element concentrations.

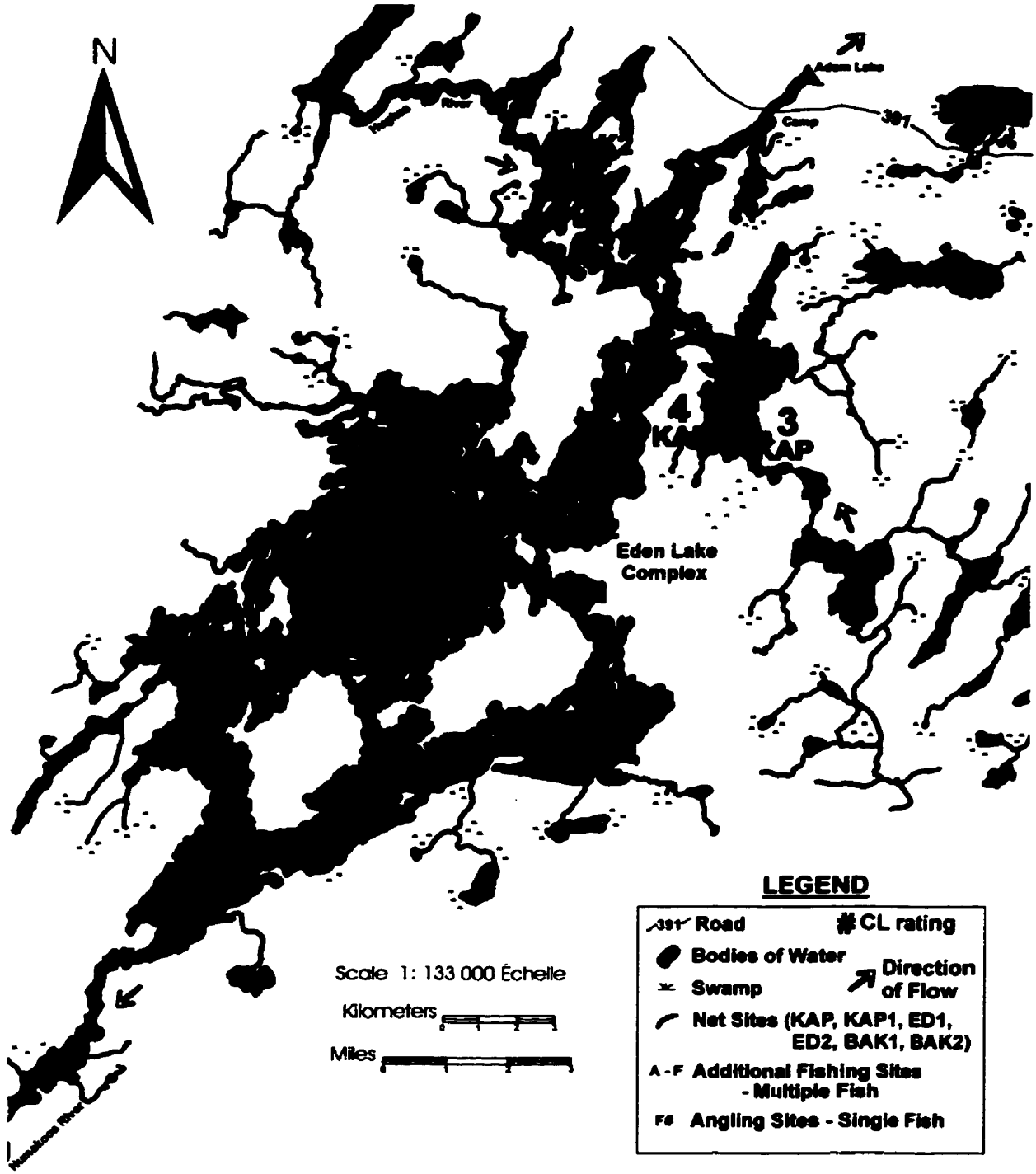

Figure 5.20. Map showing the averaged CL ratings (on a scale of 1 to 10) for all of the species of fish combined, at each Eden Lake capture location. The direction of water flow (i.e., inflow and outflow points) is also shown.

The clams collected at the ED1 and ED2 sites (e.g., Figure 5.21) exhibited the strongest luminescence while the weakest luminescence (comparatively) was observed in the clam shells collected from the BAK1 and BAK2 sites (e.g., Figure 5.22). Adam Lake clam shells fell in between the ED1 and BAK2 clams in terms of the intensity of their luminescence (e.g., Figure 5.23).

5.3 Reflection Microscopy

As mentioned in Section 3.4, reflection microscopy was used for two reasons. First, the light optical images can be compared to the CL photographs to be able to understand the luminescence distribution (e.g., Figure 5.24). Second, reflection microscope images help in the analysis of the otoliths' internal structure (e.g., annuli widths and the widths of the optically light and dark bands within each annulus).

A Kontron image analysis system connected to a reflection microscope using glancing reflected light from a fiber optic (cf. Figure 3.10) was used to collect the high-resolution monochrome images (cf. Figure 3.11) of each otolith showing strong luminescence, unusual luminescence or no luminescence (Table 5.1). These reflection microscopy images were then used to specifically mark the starting and end points for the LAM-ICP-MS and PIXE line scans (i.e. the central nucleus or primordium and the otolith edge, respectively) to facilitate scanning using the two systems. The line selected was located such that the line scan was perpendicular or as close to perpendicular as possible to the annuli (cf. Figure 3.12).

5.4 LAM-ICP-MS

The cathodoluminescence photographs clearly showed that there was a finely resolved "chemo-stratigraphic" signal preserved in the Eden Lake otoliths that must in

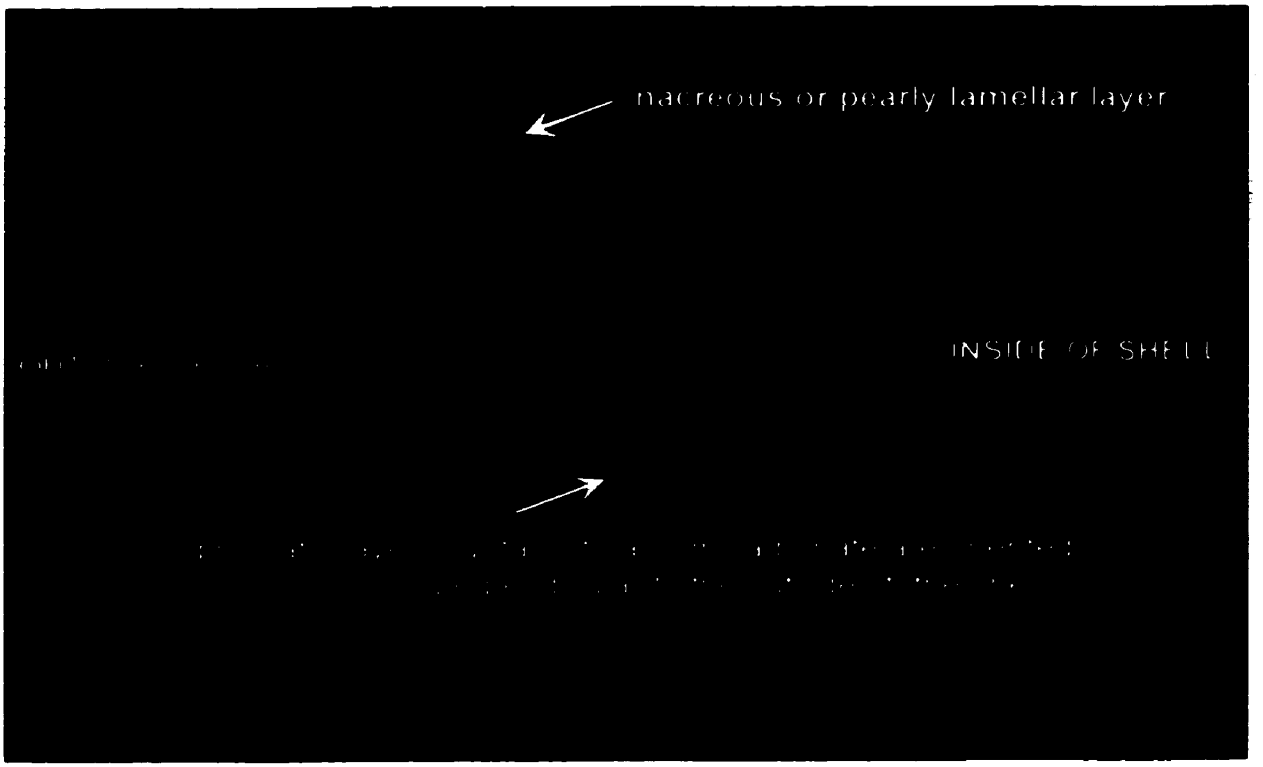

Figure 5.21. **Cathodoluminescence photograph of a strongly luminescent section of clam shell from the ED1 site. The field of view is approximately 3 mm across.**

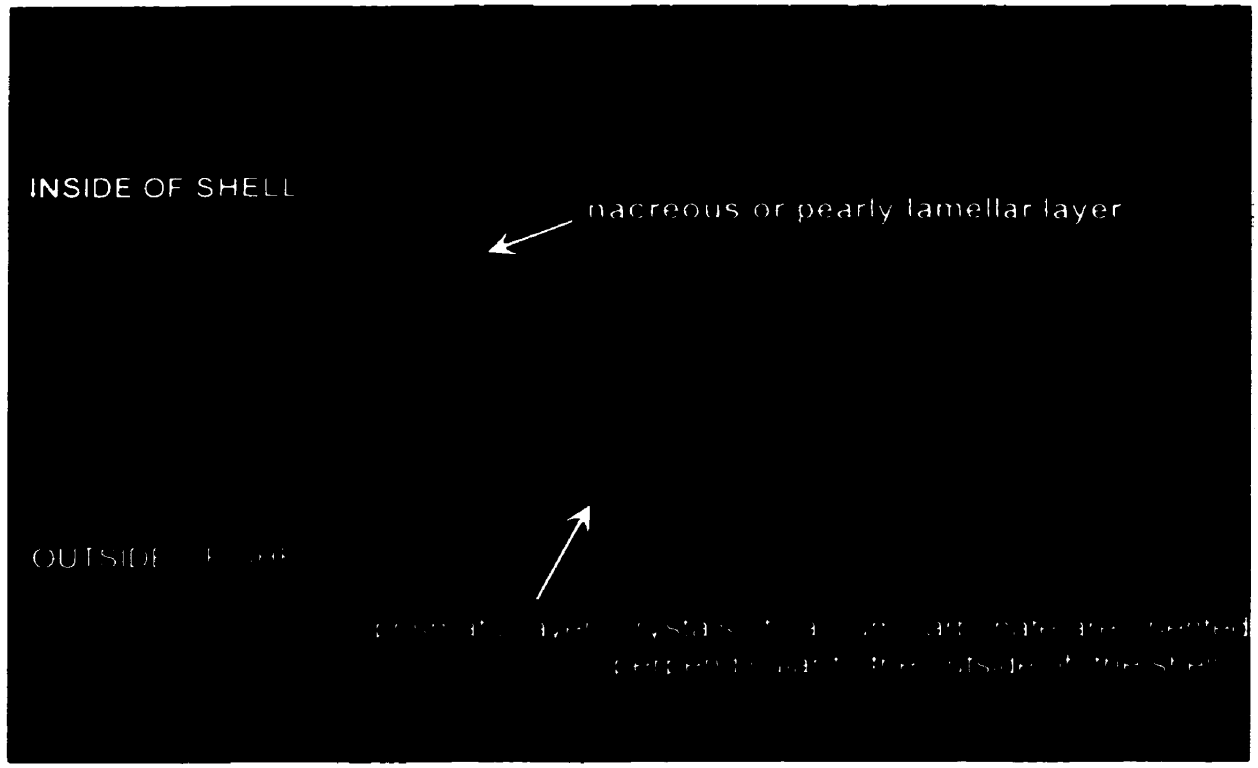

Figure 5.22. **Cathodoluminescence photograph of a weakly luminescent section of clam shell (in comparison to Figure 5.21) from the BAK2 site. The field of view is approximately 3 mm across.**

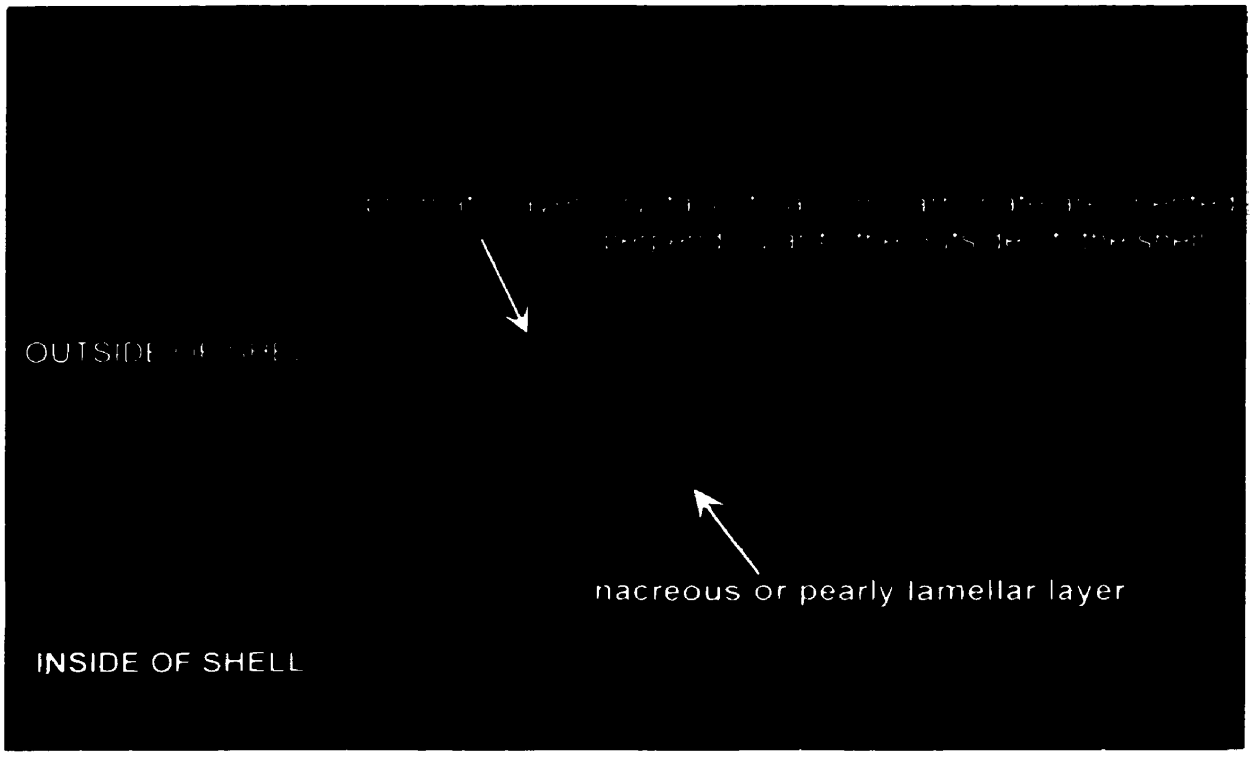

Figure 5.23. **Cathodoluminescence photograph of a moderately luminescent section of clam shell (in comparison to Figures 5.21 and 5.22) from Adam Lake. The field of view is approximately 3 mm across.**

Figure 5.24. **Comparison of a light optical image of an otolith with its respective CL image in order to better understand the luminescence distribution and its relationship to the annular structure. The field of view for both images is approximately 3 mm across.**

Table 5.1. Otoliths (a few of each fish species) from a variety of sites selected from the sample set for LAM-ICP-MS or PIXE because of their strong luminescence (i.e., high CL rating), unusual luminescence or lack of luminescence.

DISK NAME (AND LOCATION)	DISK #	SAMPLE #	SPECIES	CL RATING	CHOSEN ANALYTICAL METHOD
KAP-B	3	F27	White sucker	1	PIXE
	6	F30	White sucker	0	PIXE
KAP-E	3	F149	Yellow perch	10	PIXE
KAP1-A	1	F166	Whitefish	10	PIXE
	2	F167	Whitefish	7	PIXE
	3	F168	Whitefish	10	PIXE
KAP1-D	1	F142	Cisco	8	PIXE
	2	F155	Cisco	7	PIXE
	3	F156	Cisco	7	PIXE
KAP1-E	2	F157	Cisco	6	LAM-ICP-MS
ED1-A	4	F21	Burbot	7	PIXE
ED1-B	2	F6	White sucker	10	LAM-ICP-MS
ED2-C	1	F134	N. pike	10	LAM-ICP-MS
ED2-D	1	F143	Yellow perch	7	PIXE
	3	F145	Yellow perch	8	PIXE
BAK1-A	7	F128	N. pike	8	PIXE
BAK1-B	3	F120	Burbot	8	PIXE
BAK1-C	1	F153	Yellow perch	8	PIXE
BAK2-A	3	F123	N. pike	8	PIXE
BAK2-B	1	F164	Whitefish	8	PIXE
	4	F165	Whitefish	5	PIXE
N-B	1	F3	Walleye	2	PIXE
C+A+J (Jackson L.)	1	F74	N. pike	4	PIXE

Table 5.1 continued.

DISK NAME (AND LOCATION)	DISK #	SAMPLE #	SPECIES	CL RATING	CHOSEN ANALYTICAL METHOD
C+A+J (Jackson L.)	3	F72	N. pike	5	PIXE
(Campsite)	4	F42	N. pike	9	PIXE
(Adam L.)	5	F55	N. pike	10	PIXE
(Adam L.)	6	F56	N. pike	10	PIXE
C	4	F88	Walleye	2	PIXE
E	6	F80	Walleye	0	PIXE
	7	F81	Walleye	8	PIXE

some way relate the fish (and clam) to their surrounding environment including the rocks. The recent coupling of a laser ablation microprobe (LAM) with inductively coupled plasma – mass spectroscopy (ICP-MS) provides an analytical technique, with sensitivity in the ppb, able to assess the trace elements that may be contributing to the luminescence.

The University of Windsor's LAM-ICP-MS system (cf. Section 3.6) proved to be very successful in analyzing the Eden Lake otoliths and clam samples for most trace elements. Point analyses did not detect any REE but did detect many other elements (Table 5.2). Sr concentrations in the otoliths ranged from 15.65 ppm in the white sucker to 4.84 ppm in the cisco. The Sr concentration in the clam, however, was 14 times higher than that of the white sucker. Mn and Ba concentrations were similar in the white sucker, cisco and clam (6.17 to 8.85 ppm and 2.69 to 4.14 ppm, respectively), whereas the northern pike contained Mn concentrations that were higher (14.41 ppm) and no detectable Ba. Co was not detected in the white sucker otolith but was present in very low concentrations in the clam. The cisco in particular, as well as the northern pike, contained much higher Co, 61.58 and 23.24 ppm, respectively. The levels of Cu present in the otoliths and clam were very high, ranging between 63.33 ppm and 886.33 ppm. Zn concentrations were very low in the white sucker (0.66 ppm), moderate in the northern pike (5.80 ppm) and high (13.89 ppm) to very high (30.32 ppm) in the cisco and clam, respectively. Of all of these elements, only Mn causes any luminescence in calcium carbonate.

A traverse across the atypical white sucker otolith with the red luminescence revealed a variation in the Mn content from the core to the most recent annulus (Table 5.3). This variation may correspond to the lateral distribution of Mn with successive annuli, however, this was not possible to ascertain to any degree of certainty because

Table 5.2. Representative LAM-ICP-MS data in ppm from point analyses of a northern pike, cisco and white sucker otolith and a clam from Eden Lake. ND = below detection limits which are on the order of 100 to 10 ppb depending on the element.

SAMPLE	Sr (ppm)	Mn (ppm)	Ba (ppm)	Co (ppm)	Cu (ppm)	Zn (ppm)
White sucker	15.65	6.17	3.07	ND	63.33	0.66
Cisco	4.84	8.85	4.14	61.58	886.33	13.89
Northern Pike	10.33	14.41	ND	23.24	362.71	5.80
Clam	228.28	6.95	2.69	0.75	215.51	30.32

Table 5.3. Mn analyses across a white sucker otolith showing variation that may correspond to the lateral distribution of Mn with successive annuli.

POSITION REFERENCE	READING NUMBER	Mn CONCENTRATION (ppm)
8D15A03 1	03	18.92
8D15A04 1	04	18.09
8D15A05 1	05	20.87
8D15A06 1	06	24.35
8D15A07 1	07	32.50
8D15A08 1	08	25.67
8D15A09 1	09	21.88
8D15A10 1	10	13.13
8D15A11 1	11	6.84
8D15A12 1	12	6.63
8D15A13 1	13	9.03
8D15A14 1	14	14.05
8D15A15 1	15	12.42
8D15A16 1	16	7.90
8D15A17 1	17	9.29
8D15A18 1	18	8.73

the region sampled by the laser is much broader than the luminescent zone.

5.5 SPM Scans

Scanning proton microprobe (SPM) analysis and imaging was used to produce one-dimensional line-scans or "elemental maps" of 28 otoliths selected from the Eden Lake sample set (cf. Table 5.1). This technique, in contrast to LAM-ICP-MS, is non-destructive, delivering a smaller focused beam of protons (5 x 5 μm that penetrates to a depth of ~30μm) to the sample (cf. Section 1.2.4) and the concentration scans for all the elements of interest could be overlain on the optical images of the respective otoliths (e.g., Figure 1.8).

The three elements of interest that were fitted to the optical images for each Eden Lake otolith analyzed were Sr, Zn and Mn. Sr and Zn were chosen because both elements have recently been correlated to the annular structure of otoliths (cf. Figure 1.8; e.g., Halden et al., 1999) and their peaks were observed to be well above background in the PIXE X-ray spectra for all 28 otoliths analyzed (e.g., Figure 5.25). Mn was chosen because it was identified by LAM-ICP-MS as the likely activator element responsible for the luminescence in the Eden Lake fauna. An additional reason to choose Sr, given that Mn was suspected of causing the luminescence, was because Sr is it a known sensitizer for Mn luminescence in carbonates.

All three elements were detected in the majority of the Eden Lake otoliths and the line-scan data showing the elemental variation (in ppm) for all 28 otoliths analyzed is provided in Appendix C.

Peaks corresponding to Fe were also observed in the otoliths' X-ray spectra (e.g., Figure 5.25). The PIXE detection limit for Fe is 5 ppm. Average Fe concentrations, in all of the species, ranged between 30 and 60 ppm and showed an

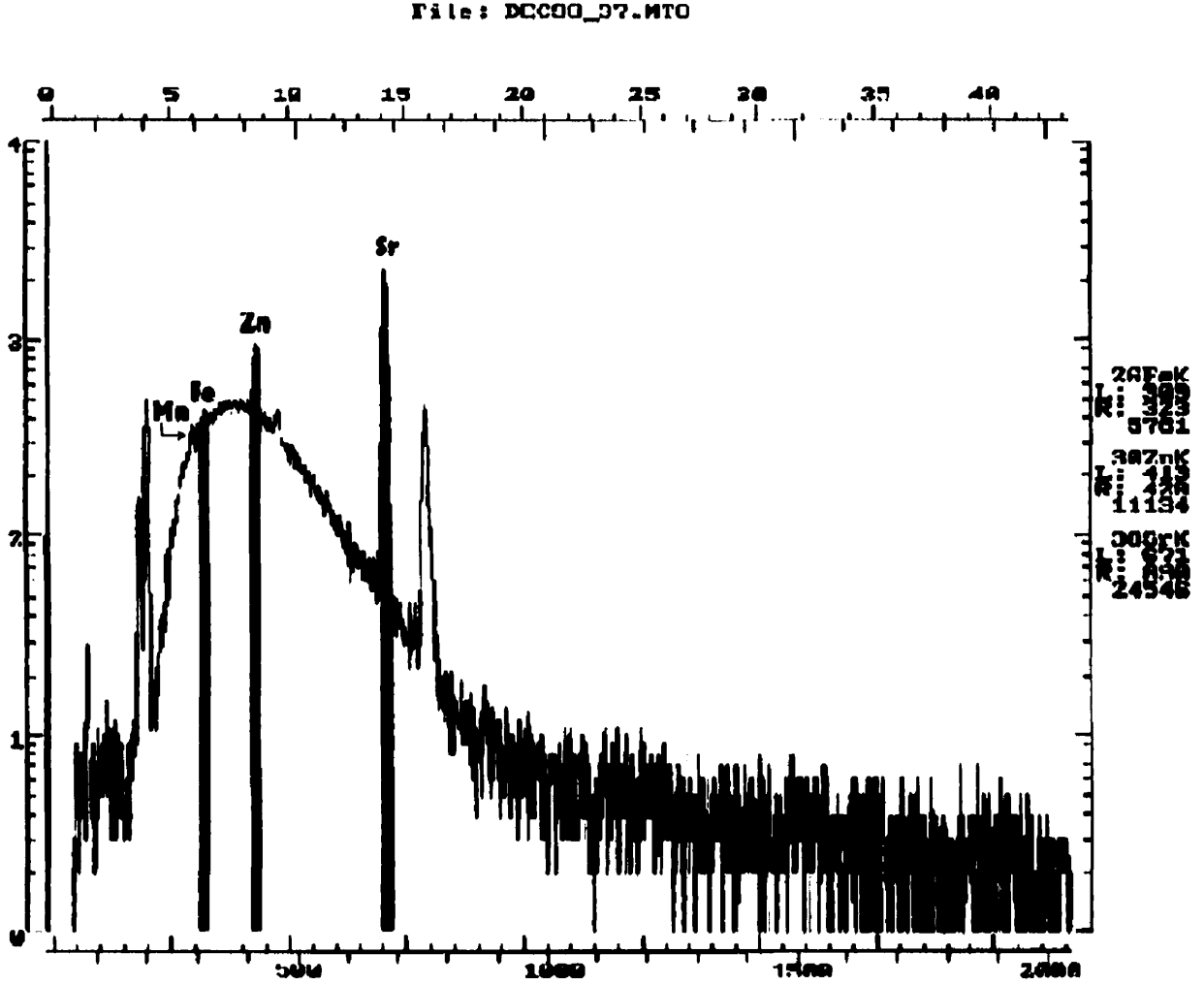

Figure 5.25. An X-ray spectrum of a northern pike collected during PIXE analysis.

overall oscillatory pattern. In terms of their peak Fe concentrations (up to 100 to 125 ppm), the 28 Eden Lake otoliths, when compared by species, ranked as follows:

> Northern Pike > Lake whitefish > Yellow perch + Cisco + Walleye + White suckers + Burbot.

5.5.1 Manganese

The Mn distribution was extremely variable across the majority of the otoliths; ranging from >2 (PIXE Mn detection limit) to 205 ppm and showing an overall oscillatory pattern. The maximum Mn concentrations detected in the 28 Eden Lake otoliths corresponded to the brightly luminescent annuli observations (i.e., CL microscopy; cf. Section 5.2). Each species ranked as follows:

N. Pike > Yellow perch > Cisco > Lake whitefish and Burbot > Walleye > White suckers

Some exceptions to the above ranking were found. These were also the atypical luminescent otoliths identified during cathodoluminescence microscopy (cf. Section 5.2.1). For example, the atypical walleye which displayed strong red luminescence had Mn concentrations ~160 ppm while all other walleye analyzed had concentrations between ~115 and 130 ppm.

5.5.2 Strontium

High levels of Sr were detected in all 28 otoliths, varying concentrations depended on species (Appendix C). These concentrations were considerably higher than the levels detected by LAM-ICP-MS. Cisco and lake whitefish exhibited the highest Sr content, ranging from 800 to 1500 and 700 to 1400, respectively. Burbot were the

next highest with Sr concentrations ranging from 550 to 900 ppm. All of the other species Sr concentrations ranged from 100 to 650 ppm. The PIXE detection limit for Sr is 1 ppm.

As mentioned in Section 1.1.2, freshwater contains, on average, about 0.1 ppm Sr and seawater contains, on average, about 8 ppm Sr (Rosenthal et al., 1970). The Sr concentrations detected in the Eden Lake otoliths are considerably higher than is commonly detected in otoliths from a freshwater environment and are more similar to that observed in fish living in a marine environment.

The distribution patterns were observed to be very similar between all species; relatively constant Sr content from the primordium to the most recent annulus, very rarely increasing or decreasing by more than 100 to 200 ppm and never falling below 200 to 800 ppm, depending on the species. Two of the fish analyzed, however, were found to be exceptional. Both the walleye E #7 and the northern pike CAJ #4 exhibited Sr distribution patterns with significant variation. Both of these fish had considerably higher Sr in the primordium range that sharply decreased by 350 to 500 ppm in the first few annuli. The E#7 walleye Sr concentration decreased more than the CAJ#4 pike, however, down to less than ~80 ppm. This might suggest these fish "migrated" from near a high Sr source to a region with low Sr. Note, however, that they were also caught in Eden Lake, which appears to have a significant source of Sr, all the other fish caught in Eden Lake exhibit very high Sr concentrations in their otoliths.

5.5.3 Zinc

Zn was detected in all 28 otoliths in varying concentrations. Also observed was that the distribution patterns were variable between and, in some cases, within the different species (Appendix C).

All of the walleye and burbot analyzed exhibited an oscillatory Zn pattern with

concentrations ranging from >2 (PIXE Zn detection limit) to 35 ppm and >2 to 30 ppm, respectively. For the walleye, there was no consistency to the location of the highest Zn peaks (i.e., located in the annuli corresponding to the core, middle years, or recent years) while the burbot's highest Zn peak was always found in the annuli corresponding to the core.

The majority of northern pike analyzed, in contrast to the walleye and burbot, exhibited an asymmetrical Zn pattern where the highest concentrations (up to 290 ppm) were always located in the annuli corresponding to the primordium and first few years. This distribution pattern is similar to that consistently observed in char (Halden et al., 1999) and is attributed to nutrient availability (cf. Section 1.1.3). One exception, however, to the Zn distribution patterns observed in the Eden Lake northern pike was found. CAJ #3, which also contained both the lowest concentrations of Zn and no Mn, exhibited a Zn distribution pattern that resembled the walleye and burbot's oscillatory distribution patterns.

The two white suckers analyzed exhibited different patterns to both the walleye and burbot and the northern pike. Their distribution patterns, though oscillatory, contained the highest Zn peaks (45 to 65 ppm) in the most recent annuli.

The majority of yellow perch analyzed were similar to the walleye, exhibiting Zn concentrations that ranged from >2 to 35 ppm with oscillatory distribution patterns and no consistency to the location of the highest Zn peaks. One exception among those yellow perch analyzed was ED2-D #3 (Appendix C). The Zn concentrations in ED2-D #3 were higher, up to 50 ppm, and the distribution pattern was asymmetrical, similar to the majority of northern pike, with the highest Zn peaks located in the range corresponding to the primordium and first few annuli.

The cisco and lake whitefish both exhibited very high Zn concentrations in all otoliths analyzed, up to 240 and 220 ppm, respectively. Zn distribution patterns were

more similar in appearance to the Sr distribution patterns than the Mn distribution patterns in that the Zn concentrations tended to increase or decrease on average only ~30 ppm rather than jumping, for example, from >2 to 120 ppm to >2 ppm, etc. In addition, it was also observed that the highest Zn concentrations were consistently found in the annuli corresponding to the primordium and first few years, with the exception of one of the line-scans done on a cisco (Scan A of KAP1-D #1, Appendix C).

5.5.4 Superimposition of Data on Optical Images

Superimposition of the Mn, Sr and Zn line-scan data on the CL images of the otoliths permitted the correlation of elemental uptake with the otolith's annular structure. Mn distribution could also be correlated with the observed luminescence.

Mn, Sr and Zn PIXE line-scans from two northern pike, one caught in Adam Lake (CAJ #5) and one caught at the BAK1 net site (BAK1-A #7), are shown superimposed on their respective CL images in Figures 5.26 and 5.27. The CAJ #5 northern pike (Figure 5.26) exhibited very strong luminescence within the optically light bands of the annuli; the highest Mn concentrations correlate with this luminescence and the lowest (>2 to 10 ppm) concentrations fall onto the areas of lower luminescence (i.e., in the optically dark bands). Further within the light bands, where the luminescence was observed to vary within the discrete "packets" of lines, proportional variations in Mn distribution was also observed. It should be noted that if the line-scan is not perpendicular to the annuli, there is a possibility that the beam is crossing (and analyzing) more than one annuli at a time and, therefore, the peaks may not correspond exactly to the annuli. Overall, there is a good correlation between Mn and the luminescence observed in CAJ #5.

The BAK1-A #7 northern pike (Figure 5.27), in contrast to the CAJ #5 pike, exhibited bright luminescence in the primordium and first annulus but weaker luminescence from the first annulus to the most recent one. Again, a clear relationship

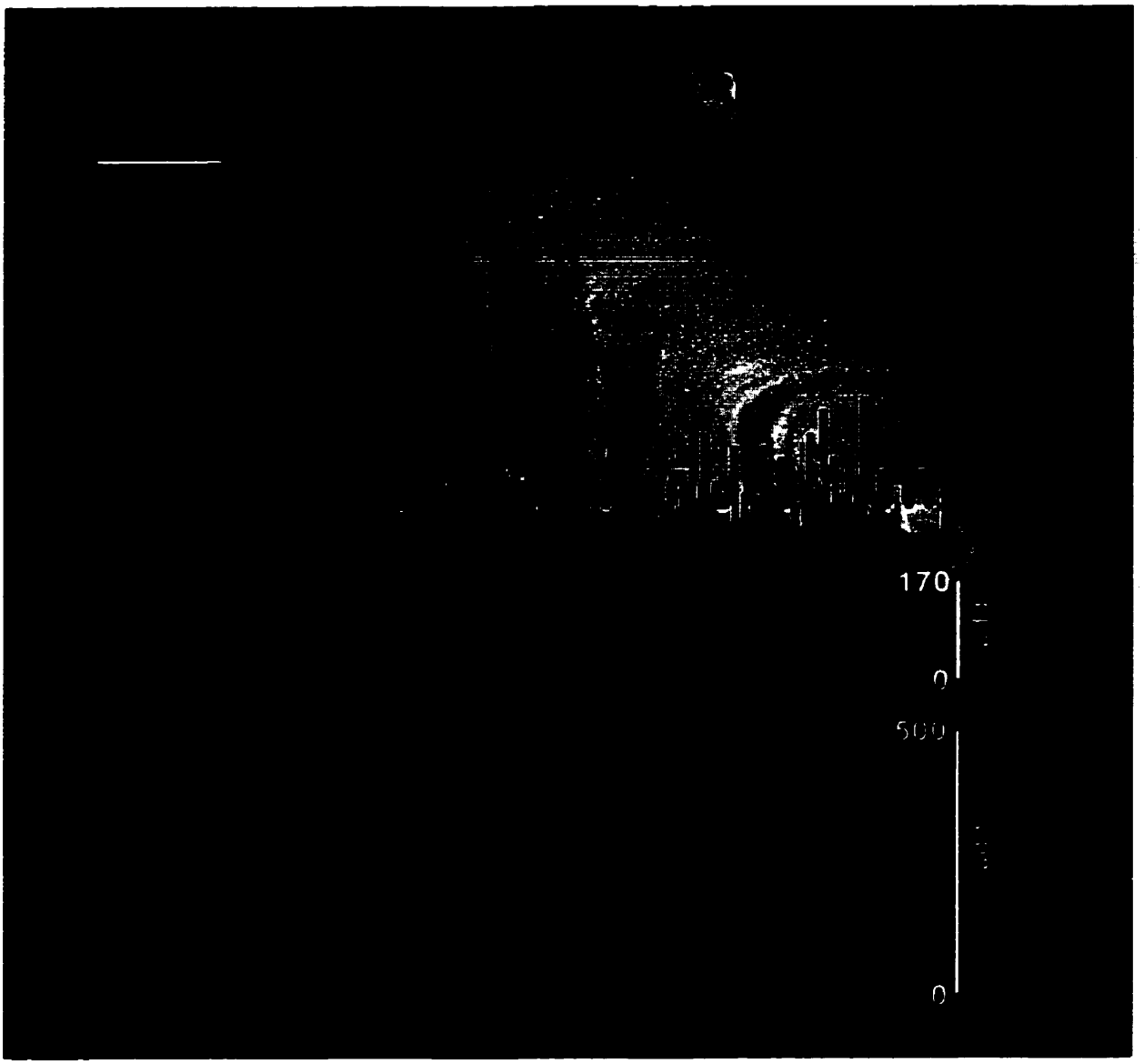

Figure 5.26. **Mn, Sr and Zn PIXE line-scans from a northern pike (CAJ #5) caught in Adam Lake shown superimposed on the CAJ #5 CL image of the otolith. The Mn line-scan is positioned on top of the actual PIXE line-scan. The Zn and Sr line-scans are offset. The highest Mn concentrations directly correlate to the bright luminescence within each annulus while the lowest Mn concentrations fall onto areas of decreased luminescence.**

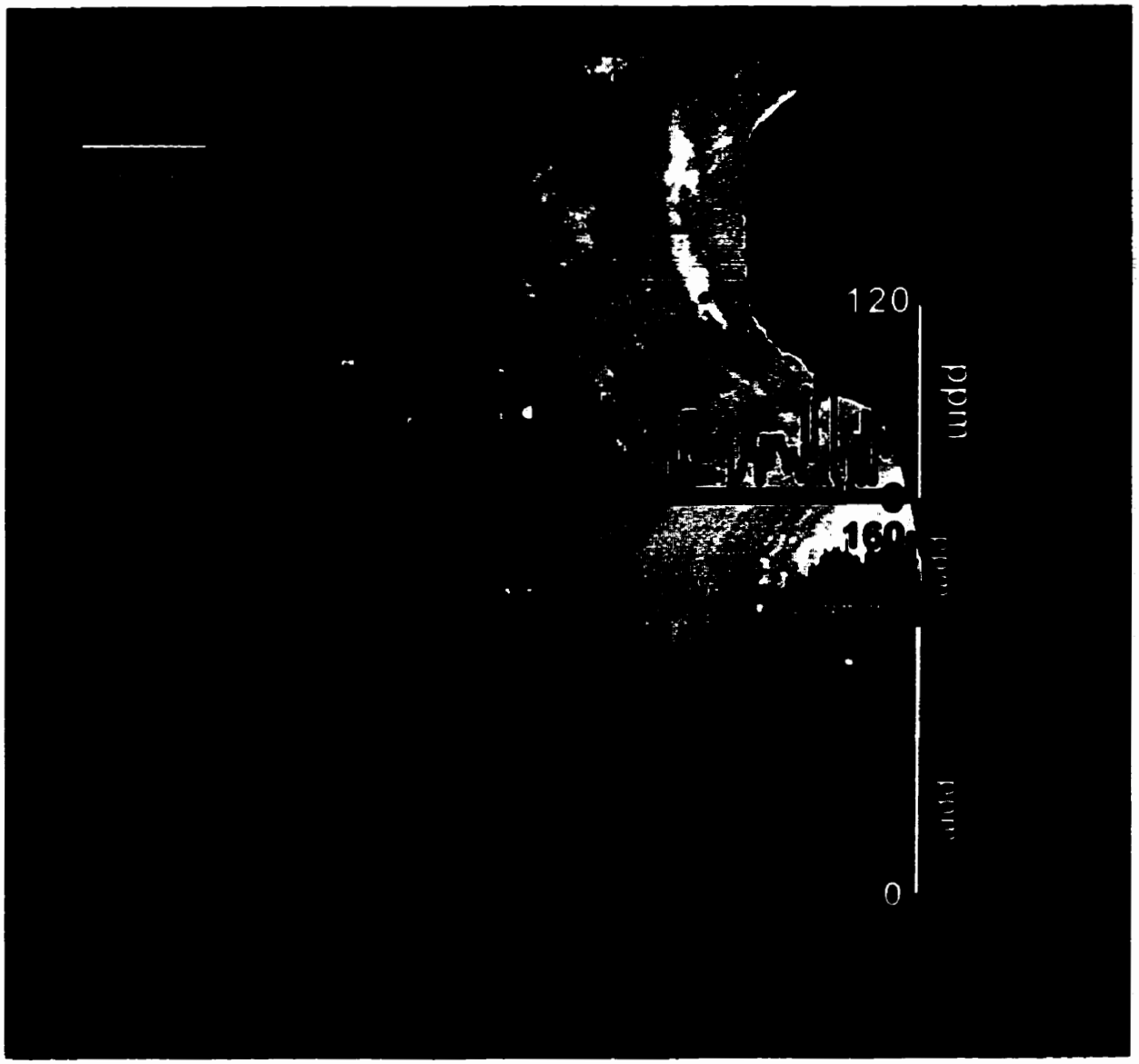

Figure 5.27. **Mn, Sr and Zn PIXE line-scans from a northern pike (BAK1-A #7) caught at the BAK1 net site shown superimposed on the BAK1-A #7 CL image. The Mn line-scan is positioned on top of the actual PIXE line-scan. The Zn and Sr line-scans are offset. The highest Mn concentrations directly correlate to the bright luminescence within each annulus while the lowest Mn concentrations fall onto areas of decreased luminescence.**

between Mn distribution and luminescence was observed. The highest Mn concentrations detected in BAK1-A #7 are found overlying the primordium and first annuli, within the light bands. After the first annuli, the Mn concentrations oscillate with the luminescence. The Mn concentrations are observed to be proportional to the varying intensities of luminescence. Further, as was observed for CAJ #5, the luminescence varies within the optically light bands of the annuli (i.e., within the discrete "packets" of lines) and this is reflected in the Mn distribution.

The Zn distribution in both northern pike is highest in the primordium and decreases in the first annuli. In CAJ #5, the Zn concentration remains constant after this decrease, oscillating slightly, at a low concentration of >2 to ~40 ppm. In BAK1-A #7, the Zn concentration remains constant (>2 to ~50 ppm) after the decrease but only until the most recent annuli, when the Zn concentration sharply increases to over 100 ppm. The Zn concentrations in both northern pike can be correlated to the Mn concentrations as both elements visibly decrease in concentration during the optically dark band or "winter" portion of the annuli.

The Sr distribution pattern differs only slightly between the two northern pike; overall Sr concentrations are similar (~200 to 500 ppm). For both CAJ #5 and BAK1-A #7, a decreasing Sr concentration is observed in the primordium. For CAJ #5, the first annulus marks the point of a sharp increase in the Sr concentration, reaching a maximum of ~500 ppm. In the first annulus of BAK1-A #7, the increase in the Sr concentration is slightly more gradual, but, still reaches ~500 ppm. After the first annulus, the Sr concentration in CAJ #5 decreases again, remains relatively constant for 3 years and then increases and decreases twice during the next 6 to 7 years. The Sr concentration is observed to be increasing slightly where the most recent annulus ends (i.e., at the point of capture). For BAK1-A #7, after the first annulus, the Sr concentration remains relatively constant until the point of capture, between a minimum of 300 ppm

and a maximum of 500 ppm, with only one sharp decrease and increase during the eighth or ninth year.

Figure 5.28 is of a lake whitefish (KAP1-A #3). In Figure 5.28, a good correlation between the Mn distribution and the intensity of luminescence is clearly illustrated by the superimposition of the Mn line-scan data on the CL image of the lake whitefish, particularly in the peaks closest to the primordium.

The Zn and Sr concentrations vary across the lake whitefish otolith, KAP1-A #3, and no overall relationship between the two can be observed. The Zn concentration is highest (200 ppm) in the primordium but broadly oscillates between a minimum of 20 ppm and a maximum of 140 ppm over the annuli from the core to the most recent annuli. The Sr concentration is roughly constant across the otolith, producing a relatively flat distribution pattern. The highest Sr concentrations are located in the middle annuli, rather than the primordium.

The luminescence observed in all of the white suckers was very weak and this is reflected in the Mn distribution (e.g., Figure 5.29). The maximum Mn concentrations exhibited are between 110 and 130 ppm and these peaks correspond to the brightest luminescence within the optically light bands across the otolith. Further, a concentration of >2 to <20 ppm Mn corresponds to the optically dark bands or "winter" portions of the otolith.

Zn concentrations in the KAP-B #3 white sucker are very low, ranging from >2 to only ~45 ppm and exhibit an oscillatory pattern. The highest Zn peaks are located in more recent annuli (10+ years). Sr concentrations are moderate, ranging from 250 to almost 700 ppm. The highest Sr peaks are located in the middle annuli.

Mn, Sr and Zn PIXE line-scans across two yellow perch (KAP-E #3 and ED2-D #3) are shown in Figures 5.30 and 5.31 superimposed on the respective CL images of those fish. Both of these yellow perch exhibit annuli that are significantly brighter than

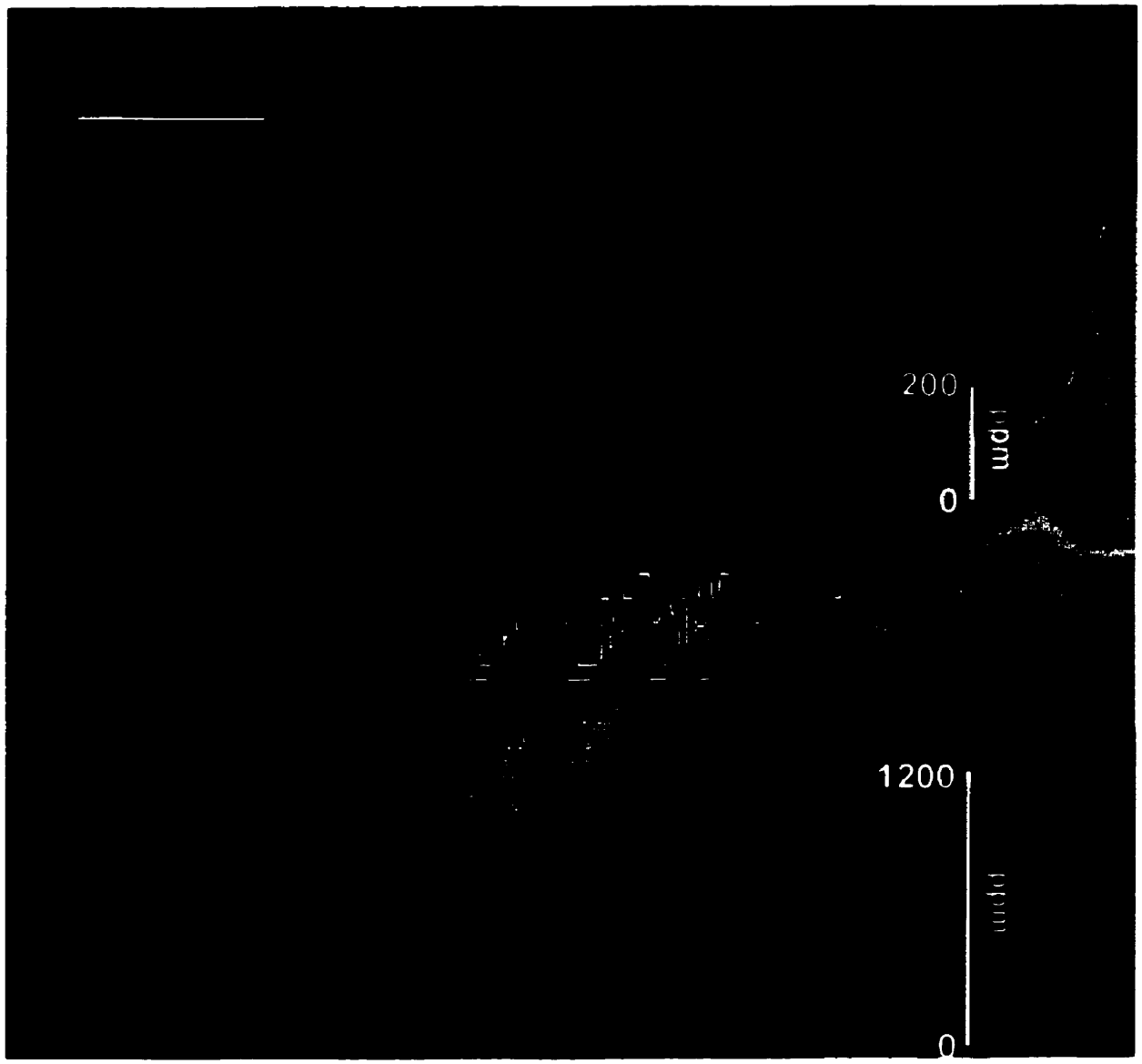

Figure 5.28. **Mn, Sr and Zn PIXE line-scans from a lake whitefish (KAP1-A #3) caught at the KAP1 net site shown superimposed on the KAP1-A #3 CL otolith image. The Mn line-scan is positioned on top of the actual PIXE line-scan. The Zn and Sr line-scans are offset. The highest Mn concentrations directly correlate to the bright luminescence within each annulus while the lowest concentrations fall onto areas of decreased luminescence.**

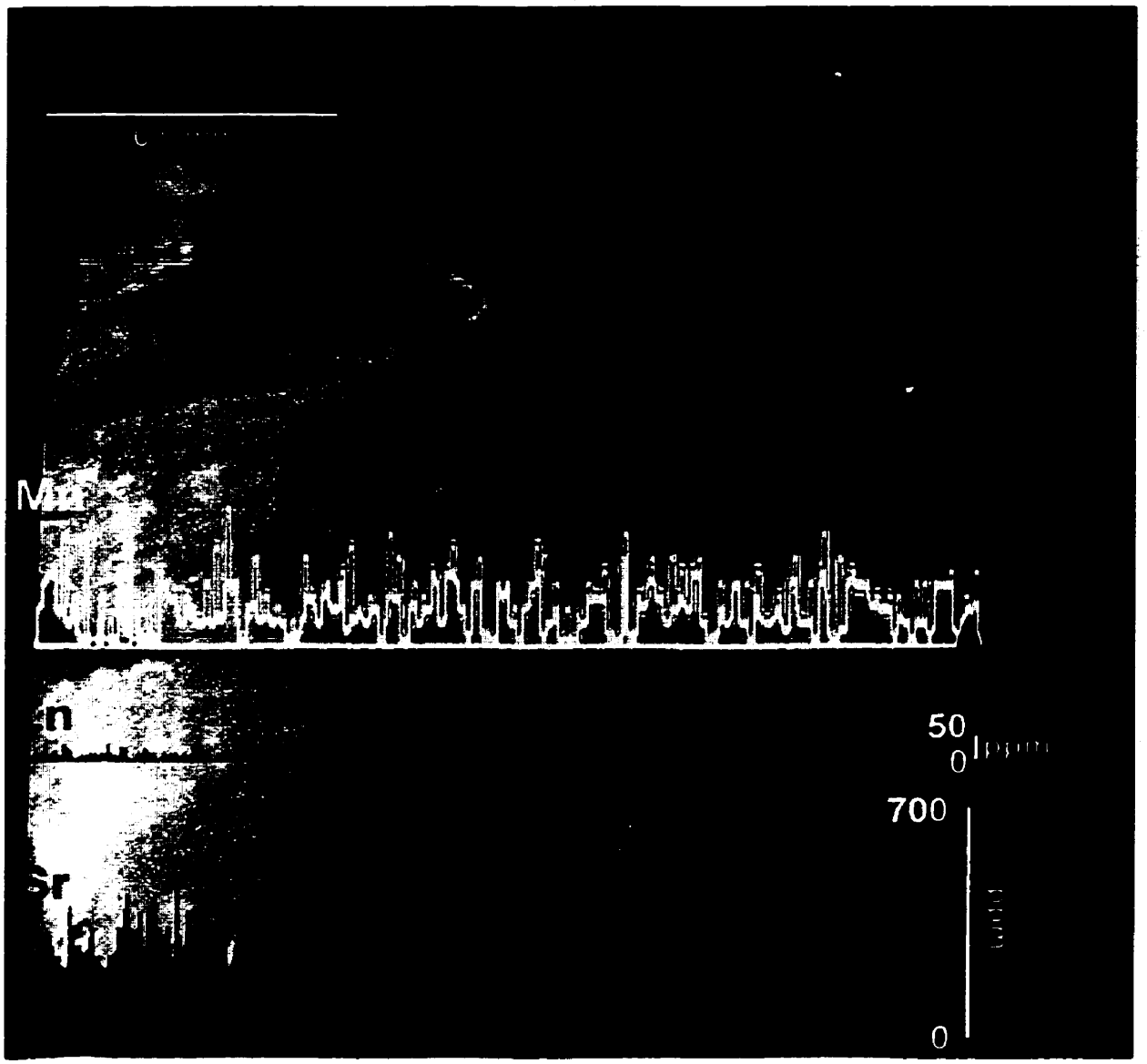

Figure 5.29. **Mn, Sr and Zn PIXE line-scans from a white sucker (KAP-B #3) caught at the KAP net site shown superimposed on the KAP-B #3 Cl otolith image. The Mn line-scan is positioned on top of the actual PIXE line-scan. The Zn and Sr line-scans are offset. As was observed in the northern pike and lake whitefish (Figures 5.26 to 5.28, respectively), Mn concentrations appear to directly correlate with the observed luminescence within each annulus.**

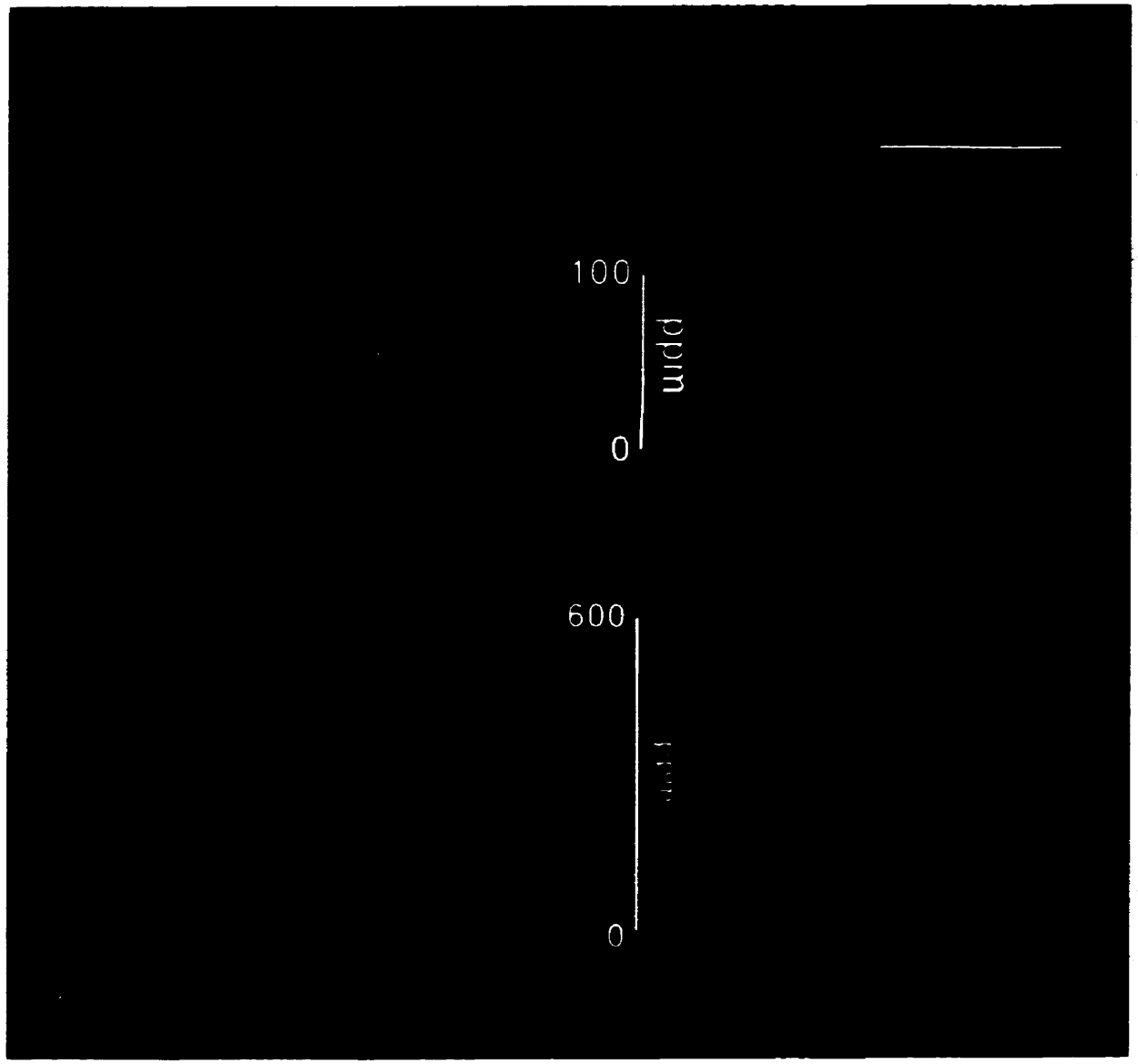

Figure 5.30. **Mn, Sr and Zn PIXE line-scans from a yellow perch (KAP-E #3) caught at the KAP net site shown superimposed on the KAP-E #3 CL image of the otolith. The Mn line-scan is positioned on top of the actual PIXE line-scan. The Zn and Sr line-scans are offset. This yellow perch exhibits some significantly bright annuli, particularly in years 3, 4 and 8. Though the luminescence pictured is slightly dull and out of focus in the vicinity of the line-scan, following the brightly luminescent annuli visible in other areas of the otolith shows that the highest Mn concentrations correspond to those years.**

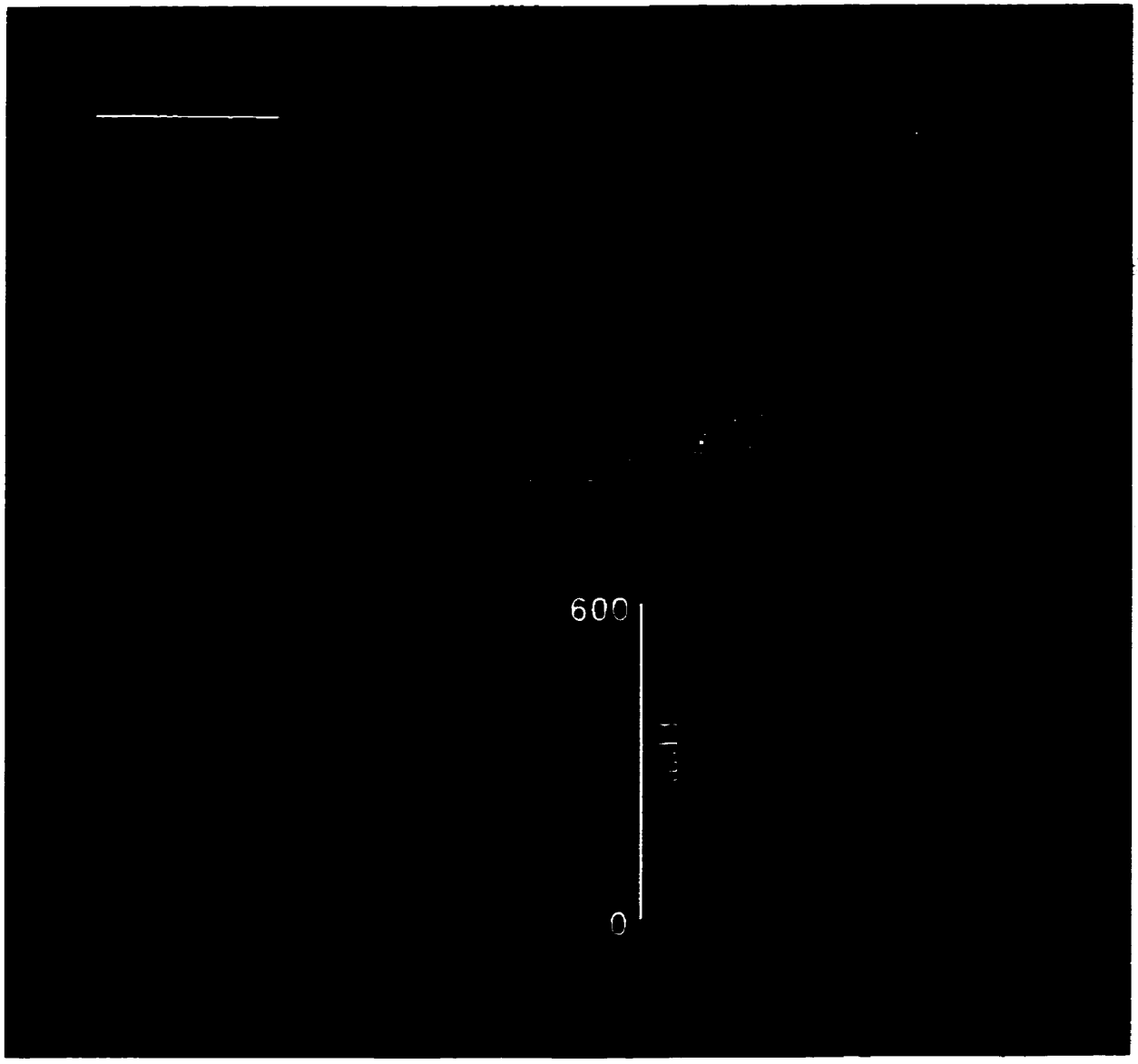

Figure 5.31. **Mn, Sr and Zn PIXE line-scans from a yellow perch (ED2-D #3) caught at the ED2 net site shown superimposed on the ED2-D #3 CL otolith imae. The Mn line-scan is positioned on top of the actual PIXE line-scan. The Zn and Sr line-scans are offset. This yellow perch exhibits one annulus that is significantly brighter than the other annuli, year 7. Though the luminescence pictured is slightly dull and out of focus in the vicinity of the line-scan, following this bright annulus visible in other areas of the otolith shows that the highest Mn concentration corresponds to that year.**

the rest, particularly years 3, 4 and 8 in KAP-E #3 and year 7 in ED2-D #3. Though the luminescence pictured is slightly dull and out of focus in the vicinity of the line-scan, following the brightly luminescent annuli visible in other portions of the otolith shows that the highest Mn concentrations correspond to those years.

The Zn and Sr concentrations within the two yellow perch are very similar. Both KAP-E #3 and ED2-D #3 contain a maximum of 40 to 50 ppm Zn and 600 ppm Sr. Their respective Zn and Sr distribution patterns, however, are distinctly different. The KAP-E #3 yellow perch has an oscillatory Zn pattern with the highest Zn located in about year 3 while the ED2-D #3 yellow perch has a Zn distribution pattern with the highest Zn located in the primordium. The highest Sr found in KAP-E #3 is located in the primordium and is followed by a slow decrease in the first annuli and a relatively constant profile to the most recent annulus. The Sr content in ED2-D #3 is high in the primordium, decreases during the first annulus and reaches a maximum within year 4. Following year 4, ED2-D #3's Sr decreases by 100 to 200 ppm and remains relatively constant until the most recent annulus.

Mn, Sr and Zn line-scans were also superimposed on the CL images from two walleye, one caught in the first set of Narrows (N-B #1) (cf. Figure 4.5) and one caught at Point E (E #7) (cf. Figure 3.1). The N-B #1 walleye otolith exhibited one very bright first annuli while the E #7 otolith was atypical and exhibited bright red luminescence throughout many annuli. The Mn line-scans superimposed on the CL images of these otoliths are shown in Figures 5.32 and 5.33, respectively. As was observed in the yellow perch images, some of the luminescence in Figures 5.32 and 5.33 are dull and slightly defocused in the vicinity of the line-scan. By following the luminescence in some of the annuli located in other portions of the otoliths, however, a direct correlation, similar to that observed for all of the Eden Lake species, between the Mn distribution and the intensity of the luminescence is observed.

An oscillatory Zn distribution pattern is visible in both walleye. The Zn concentration is very low, ranging from >2 to ~35 ppm across the otoliths. The Sr distribution in N-B #1 is relatively constant, between 250 and 500 ppm across the otolith. The Sr distribution pattern observed in the E #7 walleye, like it's luminescence, is atypical when compared to all of the other Eden Lake species and other walleye analyzed. The Sr pattern in the E #7 walleye is high in the primordium (between 350 and 550 ppm) but drops in the first annuli to less than 100 ppm.

An attempt was made to correlate the peaks and troughs of one element with the peaks and troughs of another (or both other) elements, in an effort to determine if any coupled substitution could be detected in the Eden Lake otoliths. A close look at some of the peaks and troughs observed in each of the element line-scans found that some of the peaks and troughs in the Mn, Zn and Sr profiles occur at the same location in either two or three of the three line-scans. An increase or decrease in one element, however, is not consistently proportional to an increase or decrease in the other(s). This suggests that there is no simple relationship between the elements incorporated in the Eden Lake fish.

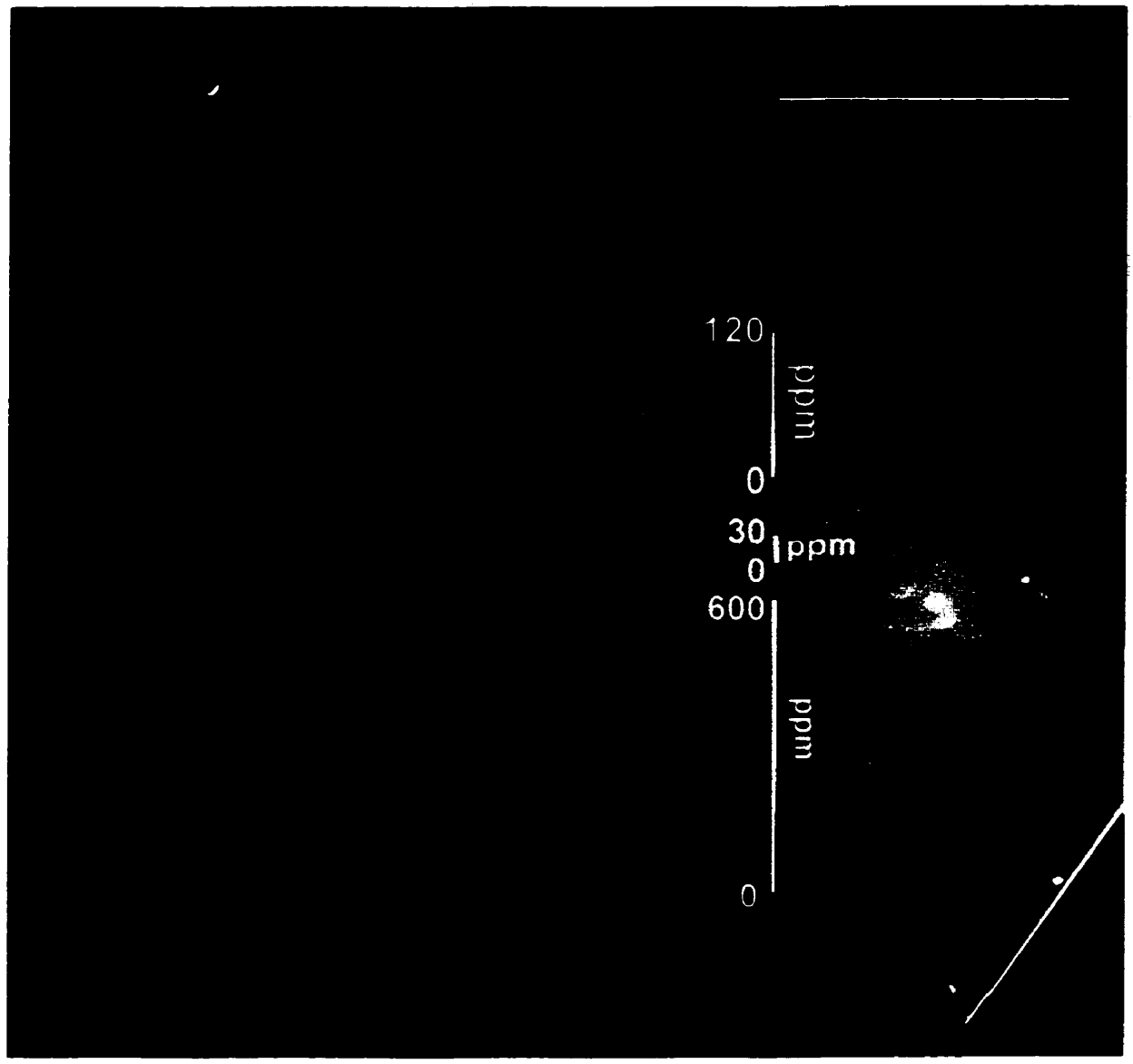

Figure 5.32. **Mn, Sr and Zn PIXE line-scans from a walleye (N-B #1) caught at the first set of Narrows shown superimposed on the N-B #1 CL image of that otolith. The Mn line-scan is positioned on top of the actual PIXE line-scan. The Zn and Sr line-scans are offset. This walleye exhibits a very bright primordium and first annulus and there is a direct correlation between the bright annuli and the Mn concentrations detected.**

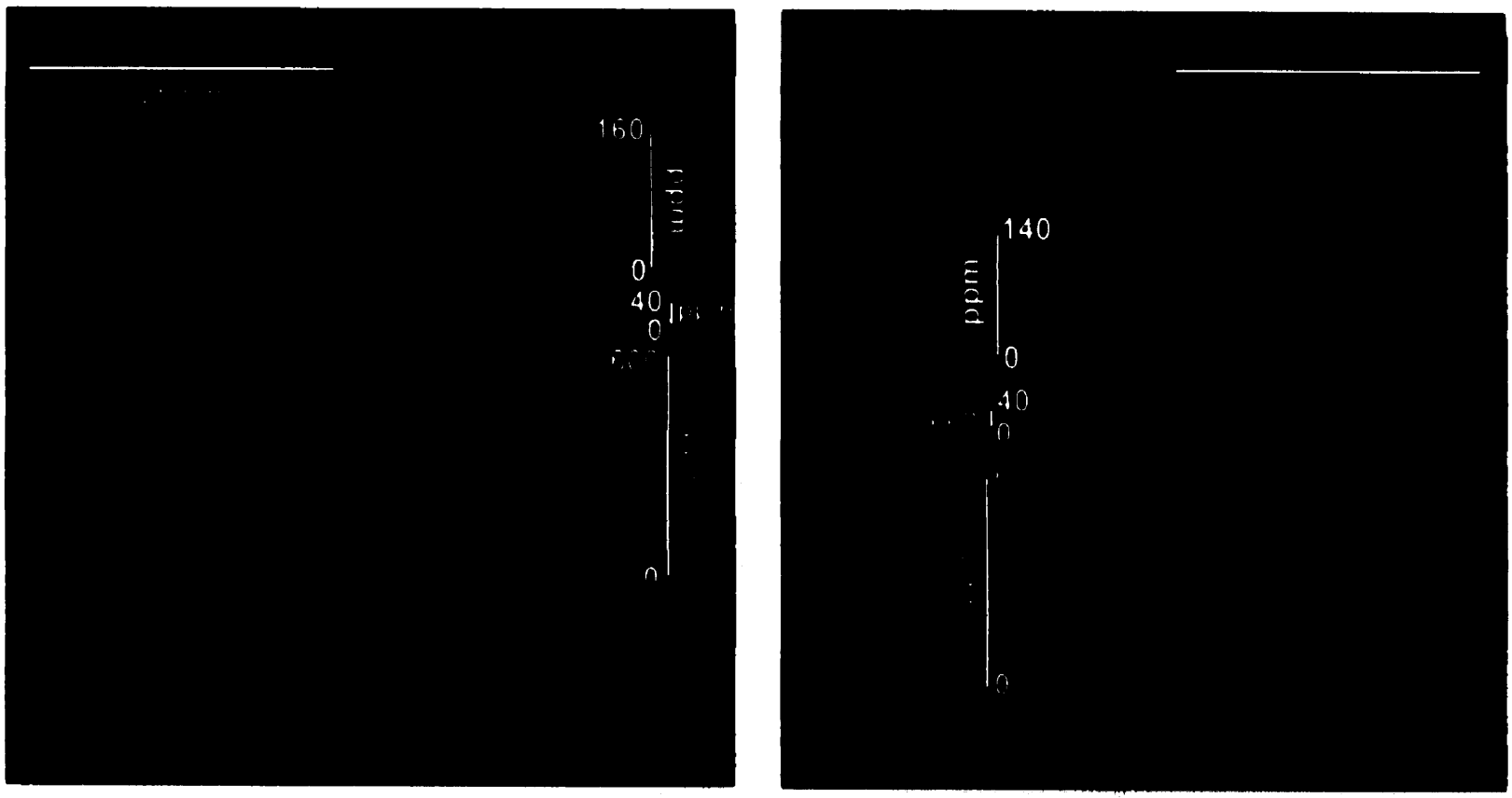

Figure 5.33. Mn, Sr and Zn PIXE line-scans from a walleye (E #7) caught at Point E shown superimposed on the E #7 CL image of that otolith. The Mn line-scan is positioned on top of the actual PIXE line-scan. The Zn and Sr line-scans are offset. This walleye is atypical and exhibits very bright red luminescence throughout many annuli. Some of the luminescence isdull and slightly out of focus in the vicinity of the line-scan, however, a direct correlation between the Mn distribution and the intensity of the luminescence can be observed by following the luminescence in other portions of the otolith. It should be noted also that the orientation of the line-scan to the annuli is better for the right-hand image than the left. The line-scan is not perpendicular to the annuli in the left-hand image.

Chapter 6: Discussion and Conclusion

6.1 Bioavailability and Concentration of Trace Elements

As with any mineral, substitution of other elements during mineral growth is possible depending on the environmental geochemistry present during crystallization. During otolith growth, substitutions occur because of the variability of the water chemistry in the fish's environment (i.e., Ca is not the only element available for incorporation into the otolith). The two most important factors determining ionic substitution, according to Klein and Hurlbut (1985), are the size of the ion and the crystallization temperature. The size of the ion is an important factor because analysis of mineral structures has shown that two elements can and will readily substitute for each other if their ionic radii are similar or differ by less than 15%. If the radii of two ions differs by 15 to 30%, substitution is limited or rare and if the radii differ by >30%, substitution is unlikely. In terms of temperature's role in substitution, the greater the thermal disorder the less stringent the space requirements within the structure. Therefore, crystals grown at higher temperatures may display extensive ionic substitution that would not have been possible at a lower crystallization temperature. Since the temperature of otolith crystallization is relatively uniform, regulated by the internal temperature of the fish and the temperature of the water flowing into the endolymphatic sac, the predominant factor controlling ionic substitution is ionic radii. Other factors influencing ionic substitution in biogenic carbonates (not mentioned by Klein and Hurlbut (1985) because they do not apply for all minerals) are element oxidation state, alkalinity, the organism's metabolism and diet and the abundance and availability of substitution elements (i.e., their concentration in the water).

6.1.1 Bioavailability of Trace Elements

Rare-earth elements, Sr, Zn, Mn, Fe, Th, U and/or F, which are known to substitute in carbonate minerals, are found in the apatite, titanite, zircon, allanite, andradite, fluorite, aegirine-augite, feldspar (K-feldspar and plagioclase), and britholite in one or both of the Type 3 and 4 pegmatites (cf. Arden, 1995). Signs of alteration visible in many of these minerals indicate that trace elements are being liberated from the minerals into the environment at Eden Lake. Evidence to support this assertion comes from radiometric surveys of the Eden Lake area (Geological Survey of Canada, 1977) and vegetation geochemical surveys (Fedikow et al., 1993 and 1994), both of which have detected many of these elements in the water and shoreline vegetation.

Sr has the closest or most similar ionic radius (2.45 for Sr versus 2.23 for Ca, a difference of 9%) and the same 2^+ oxidation state, of the elements that can substitute for Ca and are being released into the Eden Lake environment. The next closest radii is that of the REE (~16%) followed by Mn (20%), Fe (23%) and Zn (33%). REE, however, are 3^+ and 4^+ elements while Mn, ferric Fe and Zn are 2^+ like Ca. REE will not, therefore, substitute for Ca as readily as Mn, Fe (2^+) or Zn. In the Eden Lake otoliths, Sr substitution for Ca is expected followed in decreasing order by Mn, Fe and then Zn, provided these elements are present in the aqueous environment and/or available through diet.

6.1.2 Concentration of Trace Elements between the Species

Analysis using cathodoluminescence microscopy (CL) provided the first indication that trace elements were present in the Eden Lake fauna, however, it was the LAM-ICP-MS and PIXE analysis that determined the actual concentrations of the elements.

Fish

In the Eden Lake fish species, concentrations of Sr, Mn, Ba, Co, Cu and Zn were detected by LAM-ICP-MS and Sr, Zn, Fe and Mn were detected by PIXE. The LAM-ICP-MS analysis was done on just one white sucker, one cisco and one northern pike while PIXE analysis was done on a few fish of each species (except the longnose sucker).

The trace element concentrations detected by LAM-ICP-MS and PIXE were comparable for Mn and Zn, but not for Sr. The highest Mn concentrations were detected in the northern pike and the lowest were found in the white suckers. For Zn, the highest concentrations were detected in the cisco and the lowest in the white sucker, walleye, yellow perch and burbot. The concentrations of Sr detected during point analysis by LAM-ICP-MS were greatest in the white suckers, followed by the northern pike and cisco, respectively. Traverses across the otoliths using PIXE, however, found that Sr concentrations were highest is cisco and lake whitefish followed by burbot and then northern pike, yellow perch, walleye and white suckers all had the lowest Sr concentrations. Additionally, the Sr concentrations detected by LAM-ICP-MS (<15 ppm) were considerably lower than those detected by PIXE (>500 ppm).

Ba, Co and Cu, which were detected during point analyses by LAM-ICP-MS, were all highest in the cisco and Fe, which was detected during a traverse across the otolith by PIXE, was highest in the northern pike.

It is clear from the analyses that the fish are incorporating many trace elements from their aqueous environment. There are no anthropogenic sources for these elements in the area and therefore, the surrounding environment, particularly the local geology, is assumed to be responsible. The cisco, lake whitefish and northern pike appear to be incorporating the greatest amount while the walleye and white sucker

appear to be incorporating the least.

In terms of the relative maximum concentrations of trace elements detected by LAM-ICP-MS and PIXE in the Eden Lake fish as a whole, the order is as follows:

> Sr (up to 1500 ppm) > Cu (up to 890 ppm) > Zn (up to 290 ppm) > Mn (up to 205 ppm) > Fe (up to 125 ppm) > Co (up to 60 ppm) > Ba (up to 4 ppm)

In terms of ionic radii, the expected order (for the elemental substitution of Ca) would have been:

> Sr (9%) > Mn + Ba (20%) > Fe (23%) > Co (25%) > Cu (30%) > Zn (33%)

It is likely that the concentrations of trace elements in the water are variable (in both time and location) and that their incorporation into the otoliths is related to the changing aqueous conditions, water temperature, alkalinity and/or diet.

Cu was the second to Sr in terms of abundance in the Eden Lake otoliths. This was surprising because, even though it also has a +2 oxidation state, it was not generally considered to be an element that commonly substitutes for Ca in carbonates (it has a 30% smaller atomic radius than that of Ca). According to Arden (1995), Cu is present in many of the Type 3 and 4 pegmatite minerals. Zircon contains the highest Cu concentration (62 to 119 ppm) followed by titanite (5 to 56 ppm), apatite (12 to 44 ppm) and allanite (9 to 23 ppm). Copper concentrations are not provided for britholite, andradite, aegirine-augite, fluorite and feldspar (K-feldspar and plagioclase). The Cu concentrations in the minerals, however, seem to be low in comparison to the concentrations found in the fish, especially since the Cu-bearing minerals make up only ~17% to ~60% of the Type 3 and 4 pegmatites. Further, only some of these minerals are greatly altered.

According to a number of studies (e.g., Ahmad and Al-Ghais, 1997; Gauldie and Nathan, 1977), Cu is one of the common heavy metals found in otoliths, along with Zn, Fe, Mn, Ni, Cd and Pb. The study by Ahmad and Al-Ghais further found that at age two to three Cu concentrations were higher in female fish's otoliths. At age four, however, this difference becomes very small with males tending to be higher. No explanation, however, for the presence of Cu in the otoliths was given.

The concentration of Zn might be explained by diet. Recent studies aimed at understanding the concentration of trace elements in marine organisms show that food is probably a significant factor in the overall uptake of zinc (cf. Ichii and Mugiya, 1983; Halden et al., 1999). Other studies on the incorporation of trace elements in marine organisms (e.g., Bradley and Sprague, 1985) have found correlations between the organism's weight (and presumably size) and its trace element content. According to Bradley and Sprague (1985), as fish increase in size, their metabolic need for zinc declines and so does their tolerance. The geochemical surveys (Fedikow et al., 1993; 1994; cf. Section 2.3 and Appendix A, Table 1) further reveal that high Zn is present in the shoreline vegetation at Eden Lake. If there are contributions to the Zn content from food and the surrounding aqueous environment, this might explain why, even though its ionic radius is 33% smaller than that of Ca, the concentration of Zn is found to be higher than other elements whose radius is closer to Ca.

Mn and Fe are found in many of the minerals in the Type 3 and 4 pegmatites (cf. Section 2.2.1) and Fe was also found in abundance in the shoreline vegetation (Fedikow et al., 1993; 1994; cf. Section 2.3 and Appendix A, Table 1). Their ionic radii, which differ by 20% and 23%, respectively, are also only minorly smaller than that of Ca. According to Hurlbut and Klein (1985) the uptake of Mn and Fe in carbonates is "limited and rare" but is not unfeasible.

A number of studies (e.g., Ahmad and Al-Ghais, 1997; Gauldie, 1996; and

Gauldie and Nathan, 1977), have found that both Mn and Fe are common heavy metals found in otoliths, along with Zn, Cu, Ni, Cd and Pb. The study by Ahmad and Al-Ghais (1997) found that in two- to three-year old fish, Mn concentrations were higher in the female's otoliths. At age four, however, this difference becomes small with Mn concentrations in males being slightly higher than in females. Gauldie (1996) also found concentrations of Mn and Fe (along with Sr, Mg, Na, Zn and P) in a study involving reared salmon. This study found that the chemical variation detected in the otolith was weakly related to the fish's weight and length, temperature treatment and otolith weight. Further, vaterite replacement was said to account for a large part of the observed metal ion concentration variation. The study by Gauldie and Nathan (1977) detected Fe in otoliths of tarakihi fish and found that the highest Fe concentrations were largely contained in the primordium. Gauldie and Nathan (1977) speculate that the Fe content in the tarakihi fish may be hereditary or linked to the fish's environment. In contrast to this study, the Fe concentrations in the Eden Lake otoliths were very low in the primordium and first few annuli and highest in the middle to most recent annuli. The speculated source of the Fe in the Eden Lake otoliths, however, is also the fish's environment (i.e., Fe that has entered the water from the surrounding rocks and/or diet).

Co was not expected to be present in the Eden Lake otoliths as it was not considered to substitute for Ca, yet it was detected by LAM-ICP-MS in both a cisco and a northern pike, in abundances of 23.24 and 61.58 ppm, respectively. Review of the Co concentration within the minerals of the Type 3 and 4 pegmatites found that zircon and allanite contain an abundance of this trace element (up to 1319 and 1136 ppm, respectively; Arden, 1995). Titanite also contains only a small amount of Co (up to 171 ppm). Further Co has a +2 oxidation state and an ionic radius only 25% smaller than Ca, which, according to Klein and Hurlbut (1985), makes substitution of Ca by Co "limited and rare" but not unfeasible. According to the geochemical studies by Fedikow

et al. (1993; 1994; cf. Section 2.3), the shoreline vegetation contains Co in concentrations of up to 17 ppm (cf. Appendix A, Table 1), indicating that Co is mobile in the Eden Lake environment.

Low Ba concentrations (ca. 5 ppm) were detected by LAM-ICP-MS in a white sucker and cisco while no Ba was detected in the northern pike analyzed. The ionic radius of Ba is only 20% larger than Ca and it is known to substitute for Ca in carbonates. Further, Ba is found in abundance (up to 4 wt. %) in a number of the minerals of the Type 3 and 4 pegmatites (apatite, zircon, britholite, K-feldspar and plagioclase) (cf. Arden, 1995) and was found in abundance in the shoreline vegetation (cf. Section 2.3 and Appendix A, Table 1). Due to these facts, it would be surprising if 5 ppm were representative of the maximum Ba concentration in the Eden Lake otoliths. As previously mentioned, concentrations detected by LAM-ICP-MS reflect only one spot (20 to 30 μm) on the otolith.

Clams

Clams were collected from Eden Lake and the neighboring Adam Lake to assess concentrations in other biogenic carbonates, in addition to this clams are more sessile and perhaps would be more representative of the local environment. Brilliant luminescence was observed during the CL analysis of the Eden Lake clams indicating that these organisms are also incorporating trace elements into their shells. Analysis of one clam by LAM-ICP-MS revealed the same trace elements detected in the fish (i.e., Sr, Mn, Ba, Co, Cu and Zn). Additionally, the concentrations of trace elements were comparable to that detected, by LAM-ICP-MS, in the fish, with the exception of Sr which was ~14 to 57 times higher. Consequently, the trace elements incorporated by the clams are also likely to have come from the same source as the fish (i.e., the underlying rocks and/or diet). The difference between the colours of luminescence observed in the

clams from those observed in the otoliths suggests (since the same trace elements and comparable concentrations were detected) that the local structural environment within the carbonate is different.

Studies by Crisp (1974; 1976; 1983) and Kovach (1977) on the incorporation of trace elements by freshwater clams into their hardparts, found that they incorporate Sr, Mn, Mg, Na, K, Fe, and Zn into their aragonitic shells. Of these elements, only Mn is also known to produce luminescence (Marshall, 1988). Mn concentrations vary within the shell but are consistently higher in the more recently deposited growth increments (i.e., the pearly nacreous or lamellar layer (inside of shell)); in the portion of the growth band that has the slowest growth rate (Crisp, 1974; 1976; 1983; Kovach 1977). Cathodoluminescence photographs of Eden Lake clams (cf. Figure 5.22 to 5.24) appear to support this as the more recently deposited growth increments show consistently stronger luminescence (and therefore higher Mn) when compared to the rest of the shell. It would appear that the effect of age on growth rate in freshwater clams might be a significant factor in the uptake of Mn into the shell.

Further, Crisp (1974; 1976; 1983) found that clams incorporate about 25% of the Sr/Ca and >100% of the Mn/Ca in the water with slight variation between species. Species from the family Unidonidae generally contain more Sr and Mn (>200 ppm) than species from the family Sphaeriidae (<200 ppm). Without knowing the concentrations of the trace elements in the lake, however, it is impossible to determine if the one Eden Lake clam analyzed conforms to the findings of these studies.

Clam shells from limnic environments (i.e., lakes and impounded areas of streams) also tend to exhibit higher Mn concentrations (sometimes more than twice as much) in comparison to those from "normal" riverine environments (Crisp, 1974; 1976; 1983). It is also very common for different species caught at a specific locality to show different trace element content. Unfortunately, only one family of clams was collected

and only one clam was analyzed using LAM-ICP-MS.

6.1.3 Concentration of Trace Elements between the Capture Locations

Any comparative discussion regarding the concentrations of trace elements detected at the capture locations must be done by analyzing the concentrations of trace elements in individual species from each location. This is due to the differences in the incorporation of trace elements between the species, discussed in the previous section. Further, the only trace elements whose concentrations can be compared are Mn, Zn and Sr. This is because these elements were all detected using the same analytical technique, PIXE, and the concentrations being compared are the maximum detected along a traverse across the otolith (recall LAM-ICP-MS was only spot analysis). Also, a larger sampling of the Eden Lake sample set (28 otoliths) were analyzed using PIXE while only 3 otoliths were analyzed by LAM-ICP-MS.

Mn peak concentrations detected in the different Eden Lake species that were analyzed by PIXE, ranked by capture location, are as follows (Abbreviations: NP = northern pike; WS = white sucker; C = cisco; B = burbot; YP = yellow perch; W = walleye; Wh = lake whitefish):

NP ⇒ Campsite (200 ppm) > BAK2 + Jackson L. + Adam L. (140 ppm) > BAK1 (110 ppm)
B ⇒ BAK1 = ED1 (120 ppm)
YP ⇒ KAP (160 ppm) > BAK1 (115 ppm)
Wh ⇒ KAP1 (150 ppm) > BAK2 (140 ppm) > KAP1 = BAK2 (120 ppm)
W ⇒ Pt. E (130 and 150 ppm) > Narrows (115 and 120 ppm)
WS ⇒ KAP (130 ppm)
C ⇒ KAP1 (150 ppm)

According to the above ranking, no one site in or outside of Eden Lake consistently

displays higher Mn concentrations. This is consistent with the findings of Section 5.2.1. The result of assessing the average luminescence at the different capture locations for each species, and all of the species combined, was that there is no trend to the luminescence in the lake for all of the species.

The peak Zn concentrations detected in the different species analyzed by PIXE, ranked by capture location, are as follows:

NP ⇒ Campsite (300 ppm) > Adam L. (200 ppm) > Jackson L. (190 ppm) > Adam L. (160 ppm) > BAK1 (120 ppm) > BAK2 (115 ppm) > Jackson L. (30 ppm)
B ⇒ ED1 (30 ppm) ≈ BAK1 (25 ppm)
YP ⇒ KAP = BAK1 = ED2 (35 ppm)
Wh ⇒ KAP1 (200 and 220 ppm) > BAK2 (145 and 200 ppm)
W ⇒ Pt. C (40 ppm) ≈ Pt. E (30 and 35 ppm) ≈ Narrows (25 and 35 ppm)
WS ⇒ KAP (45 and 70 ppm)
C ⇒ KAP1 (160 and 240 ppm)

According to the above ranking, there are no visible trends to the Zn concentrations at the different capture locations in and outside of Eden Lake. As was observed for Mn concentrations, no one site consistently displays higher Zn concentrations. Zn concentrations are very similar for each species between all capture locations.

The peak Sr concentrations detected in the different species analyzed by PIXE, ranked by capture location, are as follows:

NP ⇒ Campsite (900 ppm) > BAK2 (550 ppm) ≈ Jackson L. + Adam L. + BAK1 (500 ppm) > Jackson L. (300 ppm)
B ⇒ BAK1 (950 ppm) ≈ ED1 (900 ppm)
YP ⇒ BAK1 = KAP (600 ppm) ≈ ED2 (550 ppm)
Wh ⇒ BAK2 (1300 and 1400 ppm) ≈ KAP1 (1200 and 1400 ppm)
W ⇒ Pt. E (550 and 650 ppm) ≈ Pt. C + Narrows (550 ppm) ≈ Narrows (500 ppm)

WS ⇒ KAP (700 ppm)

C ⇒ KAP1 (1200 and 1400 ppm)

According to the above ranking, there are also no visible trends to the Sr concentrations at the different capture locations in and outside of Eden Lake. As was observed for Mn and Zn concentrations, no one site consistently displays higher Sr concentrations. Further, the Sr concentrations are very similar for each species between different capture locations, suggesting that the concentrations of Sr incorporated into the otoliths is species-specific; perhaps due to differences in lifestyle (i.e., diet, metabolism, movements around the lake, etc.).

That no trends in element concentration were found around Eden Lake (or in some of the neighboring lakes) may indicate that the input of trace elements from the rocks is small, relatively constant and well mixed by the high water-flow rates at the inflow points. Element concentration may not be related, therefore, to proximity to the Complex so much as to a more regional signature of yellow-green luminescence (from the incorporation of Mn), high Sr and relatively constant Zn that extends beyond the lake itself.

6.2 Distribution of Trace Elements

Using SPM and image analysis, the PIXE line-scan data was scaled and superimposed on the CL images and the element distributions were related to the annular structure of the otoliths.

All of the Eden Lake fish exhibit an oscillatory Zn distribution pattern. This pattern conforms to the optically light (wide) and dark bands (narrow) in the annuli such that the higher Zn peaks correspond to the optically light bands and lower Zn peaks correspond to the optically dark bands. As previously mentioned, these bands have

been identified as "summer" and "winter" growth periods, respectively, indicating that Zn uptake is highest in summer. The highest or most prominent Zn peaks in the pattern were further found to correspond to the primordium and first few annuli in just over half of the otoliths analyzed, suggesting that the Zn uptake in those fish is also highest when the fish are youngest. According to Halden et al. (1999), the large amount of food consumed by arctic char when they are young likely causes the prominent Zn signature in the primordium and first few annuli of the char otoliths. The similar oscillatory signal in the Eden Lake otoliths might, therefore, be a seasonal one related to nutrient availability. That some of the Eden Lake fish do not conform to this pattern (e.g., they exhibit either one or more prominent Zn peaks in their most recent annuli), suggests something different from the normal metabolic demand.

Consistently, when Zn is observed to be highest in the primordium and first few annuli in the Eden Lake otoliths, Sr is observed to be highest in the middle annuli, once Zn levels have decreased. The Sr line-scans, for every fish but one, show a relatively uniform Sr content with no oscillatory zoning. This flat distribution pattern resembles those observed in non-migratory char (cf. Figure 1.7b, c and d). The concentration variations, however, particularly where there is a significant period of elevated Sr (e.g., >200 ppm higher than rest of line-scan), would appear to indicate that the fish are moving either between lakes or are encountering areas in Eden that have significantly different Sr concentrations.

The one exceptional Sr distribution pattern is observed in a walleye caught at Point E. This walleye has Sr concentrations in the primordium and first few annuli that are similar to all of the other Eden Lake fish caught, however, after the first few annuli, the Sr concentration drops down to less than 100 ppm. The pattern exhibited by this fish indicates that it has had a very different life history. The Sr concentrations in the primordium are consistent with the Sr signal for Eden Lake suggesting that sometime in

the first few years of its life it migrated from Eden to a lake with a significantly lower Sr signal.

The Sr concentrations are not notably decreased in the optically dark bands of the annuli as they are for Zn (and Mn). This is likely because, according to Townsend et al. (1992), Sr passes more readily into the endolymph and becomes incorporated into the otolith aragonite when water temperatures are decreased and the fish's physiological processed are slowed or impaired.

The Mn distribution patterns are oscillatory, similar to the typical Zn distribution patterns observed in the Eden Lake otoliths. The Mn peaks and troughs, however, moreso than the Zn peaks and troughs, are more defined and steep. The highest Mn peaks appear to correspond directly to the brightest luminescence. Further, when present, the brightest luminescence is consistently observed in the optically light bands of the annuli.

6.3 Relationship Between Trace Element Content and Environmental Conditions and Fish Behavior and Life History

The trace element concentrations and history of absorption are either due to environmental conditions, fish behaviour and life history, or some combination of the two. In terms of environmental conditions, seasonal flood or fire events and temperature or alkalinity changes likely play a role in element uptake by the fish. In terms of fish behaviour and life history, the fish's diet, changes in its metabolism, and daily and yearly movements might also affect element uptake. For each species, the factor(s) affecting element uptake may be different.

6.3.1 Environmental Conditions

Flooding

As mentioned in Section 2.4, flooding is a relatively common occurrence in the Eden Lake area, however, many of the floods are small, only marginally increasing the water levels. There have been four "good-size" floods in the Eden Lake area before June 1997 (when the fish were caught), in 1974, 1975, 1976 and 1977. In autumn 1997, there was a flood that was substantially larger, the biggest flood on record.

Twenty-one fish in the sample set were aged to be 19 years or older and, therefore, would have been new fry up to 10 years old during the 1970s. Out of those 21, only 4 were analyzed by PIXE (KAP-B #6 (age 19), KAP1-A #3 (age 29), KAP1-D #1 (age 22) and E #6 (age 19)) and only 1 of those fish's (KAP1-A #3) line-scans were superimposed on the otolith image (cf. Figure 5.29).

The 1970s flood events were similar in size, however the 1974 (July) flood event had slightly higher water levels followed by 1977 (August), 1976 (October) and 1975 (July). In the years corresponding to the 1970s floods, the Mn and Sr concentrations appear to decrease and the Zn concentrations appear to increase in the otolith, suggesting a possible but not strong influence of flooding on element uptake (Figure 6.1).

Fire

Forest fires are much more common than flooding in the Eden Lake area (cf. Section 2.4). The area is a spruce boreal forest and at least one fire occurs somewhere between Leaf Rapids and Lynn Lake every year, with 90% occurring between the 1st of July and the beginning of August. Since the water bodies are connected, Eden Lake is likely impacted (e.g., changes in water chemistry), even in

Figure 6.1. **Mn, Sr and Zn line-scan data from a 29-year old lake whitefish (KAP1-A #3) caught at the KAP1 net site shown superimposed on the KAP1-A #3 CL otolith image. The 7 to 10 year annuli correspond to the 1970s flood events and there appears to be a decrease in the Mn and Sr concentrations and an increase in the Zn concentrations. This suggests a possible but not strong influence of flooding on element uptake. The field of view is approximately 3 mm across.**

some small way, by some or all of them. The biggest fires in the area occurred in 1989 and 1995. In 1998 (one year after sample collection), however, the Eden Lake Complex was stripped of its vegetation by a very large fire that swept through the entire area.

The ecology of the area as a whole has likely adapted to the frequent fires. For example, some of the species of flora require the fires for rejuvenation. The soil in the area is contains a lot of peat (unlike the heavy clays found in Winnipeg, Manitoba) and is largely covered by lichen and moss. The rock outcrops are also covered in lichen and moss. In general, humans or a strike of lightening cause forest fires (Don Harron, April 1999, *pers. comm.*), however, in areas like Eden Lake, many are likely due to composting. The heat generated under the many layers of leaves and other decaying organic matter can ignite and start a fire. Further, fires that have started one year can go underground into the spongy peat soil and re-emerge the following year. It is, therefore, difficult to determine the effects of fire on the Eden Lake otoliths.

For all of the Eden Lake fish, the luminescence and element concentrations (Mn, Zn, and Sr) in the fire years are no stronger or weaker than other years and there are no obvious peaks or troughs which appear to correspond to 1995 and 1989 (e.g., Figure 6.2). It is likely, because forest fires are so common in the area (occurring almost every year), that no correlations are possible.

Seasonal Influences

The majority of flooding in the area occurs between July and October and 90% of the forest fires occur between July and August (with at least one fire/year). It is, therefore, likely that at the end of summer and most of fall every year there are some changes in the water chemistry (e.g., increases or decreases in trace element concentrations in the water, alkalinity changes, etc.). These changes, however, do not appear to be greatly affecting element uptake; no corresponding signal is detected in the

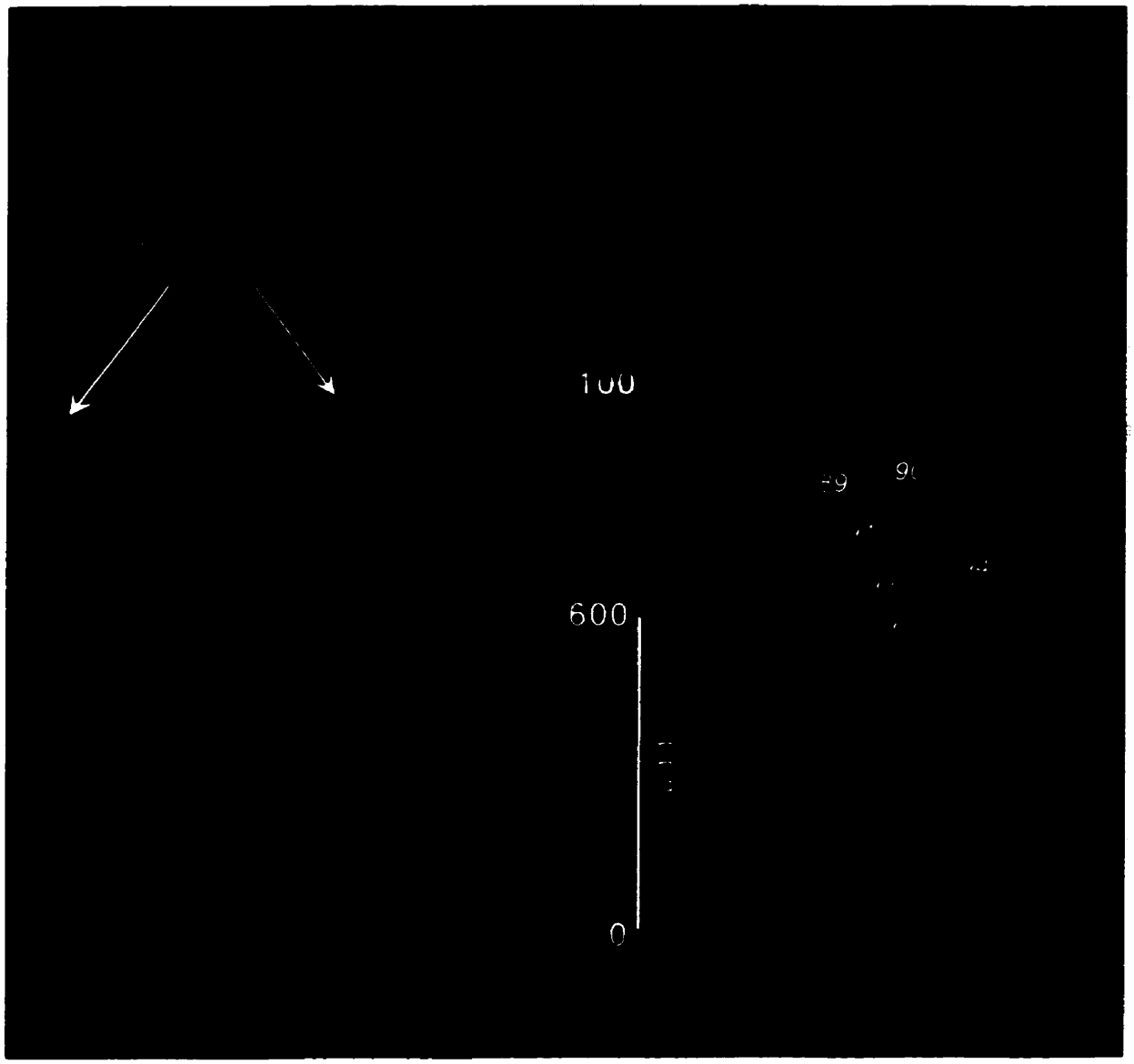

Figure 6.2. **Mn, Sr and Zn PIXE line-scans from a 9-year old yellow perch (KAP-E #3) caught at the KAP net site shown superimposed on the KAP-E #3 CL image. This yellow perch exhibits some significantly bright annuli, particularly in years 3, 4 and 8. One of these three (year 3) corresponds to the 1989 fire year. The other strongly luminescent annuli, however, correspond to 1990 and 1994 and not 1995 (the other big fire year). It is possible that 1990 and 1994 were also fire years, as at least one fire occurs in the area every year, however, they were not as big as those in 1989 and 1995 according to Manitoba Natural Resources.**

otolith chemistry. Additionally, the mean climate temperature/month has changed very little in the past 20 years in the Eden Lake area, even during the fire months and big fire years (Table 6.1). The air temperature did not jump (increase or decrease) suddenly in any month of any year, which would have caused a sudden rise or decline in surface water temperature. Something else is affecting element uptake.

Water temperature has been shown to be linked to element uptake (e.g., Kalish, 1989; Townsend et al., 1992) and the char study by Halden et al. (1999) has linked Zn incorporation to food source. The superimposition of the Mn, Zn and Sr data onto the Eden Lake CL images (cf. Section 5.5.4) further found that these elements' concentrations, particularly Mn and Zn, generally decreased (to varying degrees) during the winter period and increased during the summer. It is likely that nutrient uptake tied to fish metabolism and its dependence on water temperature (i.e., season) is a major factor influencing element uptake by the Eden Lake fish.

6.3.2 Fish Behaviour and Life History

The changes in nutrient uptake due to changes in the fish's diet and metabolism are part of fish behaviour and life history, both of which are dependent on the species of fish. The spawning, feeding and other habits typical of each species were discussed in detail in Chapter 4. What was not discussed, however, was how some of these habits over the fish's life (i.e., at particular developmental stages) may have affected their element uptake.

Diet

Halden et al. (1999) has attributed Zn concentrations in char to their dietary habits. It is likely, though, that fish incorporate a number of elements, even in very small

Table 6.1. **Mean temperature readings (rounded to nearest whole integer) for each month in the Eden Lake area over the last 21 years (1976 to 1996) (after Environment Canada, 1997).**

Year	Jan	Feb	Mar	Apr	May	Jun	Jul	Aug	Sept	Oct	Nov	Dec
1976	-25	-21	-16	2	9	13	17	15	9	1	-12	-25
1977	-24	-16	-10	1	11	13	15	10	8	1	-11	-24
1978	-25	-18	-15	-4	6	11	14	12	6	1	-14	-24
1979	-25	-30	-17	-5	4	12	17	11	6	1	-11	-15
1980	-26	-19	-15	4	9	12	15	14	5	1	-11	-26
1981	-18	-16	-9	-6	7	12	15	17	7	1	-6	-22
1982	-34	-23	-16	-5	6	10	16	12	8	1	-16	-23
1983	-22	-23	-14	-4	1	13	17	17	8	1	-6	-26
1984	-26	-14	-13	2	5	14	18	17	6	1	-16	-27
1985	-24	-26	-11	-3	7	11	14	14	6	1	-19	-22
1986	-22	-21	-12	-3	7	11	14	14	6	1	-19	-16
1987	-19	-16	-12	1	7	14	16	11	10	1	-9	-16
1988	-27	-24	-13	-4	6	15	16	15	9	1	-12	-22
1989	-25	-21	-18	-6	6	11	19	15	8	1	-19	-28
1990	-24	-25	-10	-5	6	13	16	15	8	1	-14	-26
1991	-28	-18	-12	0	8	15	17	17	7	1	-17	-21
1992	-20	-20	-11	-4	5	11	14	14	5	1	-8	-24
1993	-21	-21	-11	0	6	12	15	14	5	1	-13	-21
1994	-31	-27	-10	-5	5	15	16	14	10	1	-11	-18
1995	-20	-22	-12	-6	6	16	14	13	8	1	-17	-20
1996	-29	-19	-18	-5	5	15	17	16	8	1	-16	-24

amounts, through diet. Northern pike, for example, during the early stages of their life grow very rapidly and go through rapid dietary changes (e.g., stored yolk from their eggs to zooplankton and immature aquatic insects to fish; Scott and Crossman, 1973). Adult pike are classified as omnivorous carnivores because they eat virtually any living vertebrate animal available (from fish, frogs and crayfish to mice, muskrats and ducklings), within a size range they can engulf (i.e., anything up to 60% their own size). In contrast, white sucker fry, at about 12-mm length, begin feeding near the surface on plankton and other small invertebrates as their mouths are terminal rather than ventral (Scott and Crossman, 1973). At about 16 to 18-mm length, the mouth shifts ventrally and there is a shift to bottom feeding (other invertebrates and fish eggs). Adult suckers also consume small fish, such as logperch, sometimes in great abundance.

The northern pike contained some of the highest concentrations of many trace elements (e.g., Mn, Fe and Zn) while the suckers contained some of the lowest. Since these two species are "breathing" the same water, variations in water chemistry can not account for all of the observed differences in element uptake. Evidence appears to suggest that the abundance of trace elements is found in the hard-parts of the fauna, moreso than in the soft-parts (e.g., clams). By consuming all available vertebrate animals, northern pike may also be consuming any trace elements incorporated by those animals. In contrast, suckers consume many invertebrates. Of the small fish consumed, suckers tend to digest only their prey's soft parts. The suckers, therefore, may be incorporating the trace elements dominantly through their gills from the aqueous environment and there may be a lower concentration of trace elements in the water than in the flora and fauna.

By comparison, walleye (both juvenile and adult) are largely piscivorous (Scott and Crossman, 1973; Colby et al., 1979). Their diet shifts as they grow from invertebrates to fish. Diet for walleye is partly dominated by the degree of phototacticity

(i.e., light sensitivity) which increases with age and forces the walleye to change their habitat from the water surface to the bottom. The walleye's habitat restrictions with age might be affecting their element uptake (e.g., Mn) and might explain why some of Eden Lake walleye analyzed exhibited one or two moderate to strongly luminescent annuli that correspond to their first few years (e.g., N-B #1, Figures 5.4 and 5.35). That the walleye eat fish, just like the northern pike, later in life possibly explains some of their trace element content but it does not explain their lack of luminescence within the later annuli. Possibly they consume less fish than the northern pike, overall, because their movements are more restricted to nighttime.

The lake whitefish and ciscoes, though both coregonids, preferentially feed at opposite ends of the water column. Adult lake whitefish are bottom feeders, consuming a wide variety of bottom-dwelling invertebrates (e.g., copepods, cladocerans, clams, etc.) and small fish (Scott and Crossman, 1973). If these are in short supply, the lake whitefish have been found to feed on planktonic creatures and terrestrial insects. Ciscoes are dominantly planktonic feeders but can consume a wide variety of food (Scott and Crossman, 1973). As fry, their diet changes from dead zooplankton to algae, copepods and cladocerans. The food of adult ciscoes varies with season and location, but *Daphnia* and mayfly nymphs are a staple. Very large ciscoes will further consume small minnows. Both of these fish species exhibited singular or sets of strongly luminescent annuli within their otoliths. These annuli may reflect sudden changes in the environment experienced by the fish, such as a forced shift in diet due to shortages in their regular prey.

Burbot are voracious predators and night feeders (Scott and Crossman, 1973). Their diet changes as they grow from *Gammarus,* mayfly nymphs and crayfish (where available) to exclusively fish. The burbot occupy the same part of the water column as the lake whitefish, the hypolimnion, and, therefore, they compete for food. This

competition, combined with the lake whitefish's diet being more selective than that of the burbot, makes it even more likely that the single luminescent annuli exhibited in the lake whitefish are due to their having had to change position in the water column and, therefore, diet. Further, if the food is in shortage, the burbot will have to relocate also. This possibly explains their singular or sets of luminescent annuli observed in their otoliths.

Yellow perch consume largely immature insects, larger invertebrates and small fish (Scott and Crossman, 1973). They feed dominantly in the morning to early evening, with little to none at night. They prefer the shallow water and compete with small lake whitefish, ciscoes and some suckers. Their singular or sets of luminescent annuli are once again likely to reflect a change in diet.

Movements

If the input of trace elements from the rocks is relatively small but constant and well mixed (cf. Section 6.1.3), element uptake in the different species is likely not related to proximity to drainage from the Complex or their regular movements (e.g., spawning runs) during particular developmental stages.

The Sr concentrations in the Eden Lake fish (with two exceptions) are all relatively constant within the different species, suggesting a constant Sr uptake. The typical movements for most fish species in Eden Lake include annual spawning runs, daily or seasonal movements in response to temperature, light or food availability (Scott and Crossman, 1973). Each of these movements tends to be the same for each fish of the same species. Changes in Sr concentrations in the otoliths do not appear to change with changing Zn and Mn and, therefore, the source of Sr in the lake is not attributed to diet, but to the local geology. The concentrations of Sr in the vegetation support its mobility in the Eden Lake environment and the flat Sr distribution patterns in the otoliths

indicate that these levels are typical for the Eden Lake environment.

6.4 Atypical Luminescence

Two of the three otoliths that exhibited atypical luminescence (cf. Section 5.2.1) were analyzed to determine their trace element concentrations. The white sucker otolith caught at the ED1 net site was analyzed by LAM-ICP-MS while the walleye from Pt. E was analyzed by PIXE.

The white sucker otolith displayed a very strong red luminescence. Close examination of the otolith revealed that it was markedly larger and flatter than the other white sucker otoliths. The otolith was deformed. This deformed character may reflect an underlying chemical and/or structural difference in the calcium carbonate. Abundant trace elements (e.g., Sr, Mn, Ba, Co, Cu and Zn) were found within the otolith during LAM-ICP-MS spot analysis (cf. Table 5.4). The elements are similar to those in other white suckers but the concentrations of those elements are considerably lower (e.g., Sr and Mn). A traverse of spot analyses across the otolith by the LAM-ICP-MS further detected variations in the Mn concentration (cf. Table 5.5), but the concentrations were considerably lower (up to 100 ppm lower). It is possible that this otolith's crystal structure is different than that of other suckers due to either those organs responsible for otolith creation being malformed and/or a very different life history. If the organs were fully functioning, then a stressful event in the fish's first years might have caused the otolith deformation. Since annuli accumulate onto pre-existing annuli, the annuli created by the white sucker after the event, might have just continued the deformed growth. The addition of trace elements into the deformed crystal structure might have caused further deformation. The luminescence in this white sucker is likely cause by Mn but may be influenced by the presence or absence of another element. For example, Fe is known to hinder luminescence while Sr is a sensitizer. The Fe concentration in the otolith is

unknown but the Sr concentration, in comparison to the other Eden Lake otoliths, is considerably lower. Alternatively, as was observed in the clams, the colour might be due to a different local structural environment within the carbonate.

The walleye caught in Pt. E also displayed bright red luminescence in a few of the annuli. The luminescence has been found, by superimposing the Mn line-scan data on the CL image of the otolith, to correspond to the Mn content (though another unidentified element may also be present). PIXE analysis also detected, a Sr distribution pattern unlike that of the other Eden Lake otoliths analyzed. The Sr concentration is high (~500 ppm), but typical of the Sr levels observed in other Eden Lake walleye analyzed, in the primordium but drops off during the first few annuli to <100 ppm. No other otolith analyzed contains Sr concentrations less than ~200 ppm. One possible explanation is that this walleye hatched in Eden Lake or another nearby waterbody with a similar Sr concentration (~500 ppm) and then migrated into an area with very low Sr in the water column and little to no input from surrounding rocks. That this walleye was caught in Eden Lake might indicate that the fish was migrating back into the lake.

The similarity in luminescence color and Sr concentration observed in the white sucker and walleye suggest that both fish spent a good part of their life outside of the Eden Lake area in an environment with a very different elemental signature.

6.5 Conclusion

Many studies have focused on the concentration of various trace elements in otoliths. Most of these studies, however, have focused specifically on whether or not these bioaccumulations are a health risk due to anthropogenic activities and/or related to species, gender, temperature or age.

It is useful to understand the baseline chemistry of a system of interest and its

normal background variation over time. Environmental legislation also, now more than ever, requires that we assess baseline chemical variations in aqueous environments prior to anthropogenic influences, such as mining, in order to detect and quantify the effect these activities will have on the environment. Additionally, the knowledge gained through realistic baseline studies can be used to monitor systems that have already been impacted. This study is the first baseline study undertaken at Eden Lake. It has examined the incorporation of a broad suite of trace elements by fish in their natural setting where the only source of these trace elements currently is the local geology.

Fish are of key importance because of their involvement in the uptake of elements. Carbonate minerals are important because they can retain a historical record of the chemistry of the fluids from which they were precipitated. The use of otoliths, therefore, allows the examination of water chemistry changes over time (up to or >30 years, depending on the species). That some elements can cause luminescence in otoliths, even at the ppb level, further allows a preliminary assessment of the finely resolved spatial distribution of the elements, as well as hint at what elements might be present (since only a limited number of elements cause luminescence in carbonates). Textural information can be gained through the use of cathodoluminescence microscopy that could not be obtained by other microscopic techniques. This is the first study to analyze otoliths using cathodoluminescence microscopy and detail the concentration and distribution of its cause, which is in this case Mn.

The historical record of luminescence in the otoliths from Eden Lake and the surrounding waterbodies spans 29 years. Each fish species presents a record of seasonal environmental conditions in the lake as well as some indication of fish behaviour. Those fish exhibiting regular periodic cycles of luminescence have lived in relatively constant environments (e.g., ample food) while those that show aperiodic luminescence distribution in their otoliths have had their lives affected by singular events

(e.g., dietary changes). The majority of Eden Lake otoliths analyzed indicated that the latter is more common than the former.

Other elements detected in the fish include Sr, Zn, Fe, Cu, Co and Ba. The source of all of these elements is the local geology, however, uptake of the elements by the fish is mediated by the environmental system. Both extrinsic and intrinsic factors are involved. Aperiodic events such as fires and floods do not appear to influence element uptake and distribution or, particularly for fires, they are a continual and, therefore, undetectable influence.

No trends appear to exist overall between the element concentrations detected in each species and their capture locations within Eden Lake and the surrounding waterbodies. This indicates that the yellow-green luminescence (caused by Mn), high Sr and relatively constant Zn observed in the majority of the otoliths represents a more regional signature and are not strictly due to proximity to the Complex. The red luminescence and low Sr concentrations observed in one of the walleye and one of the white suckers suggests that these fish have had a different life history (i.e., a migratory one).

6.6 Considerations for Future Work

Exploration into a number of additional areas, not covered in this study, would lead to a more complete understanding of the nature of element uptake by the Eden Lake fauna and the normal background variation in Eden Lake and the surrounding water bodies. These are as follows:

(1) *Systematic water chemistry analysis;*

(2) *Analysis of other components of the food chain;*

(3) *Assessment of the migrating behaviour and mixing of various fish populations; and*

(4) *Systematic assessment of element content in the otoliths of fish species from other surrounding water bodies (both those connected and not connected to Eden Lake).*

In addition, long-term controlled experiments would allow a more direct assessment of element uptake by the fish fauna of Eden Lake. Controlling a number of the conditions experienced by the fish (e.g., diet, water temperature, alkalinity, movements, etc.), would aid in understanding the causative relationships underlying the otolith profiles observed in this study.

References

Ahmad, S. and Al-Ghais, S. M., 1997. Relation between age and heavy metal content in otoliths of Pomadasys stridens Forskaal 1775 collected from the Arabian Gulf. *Arch. Environ. Contam. Toxicol.* 32(3): 304-308.

Arai, N. and Sakamoto, W., 1993. PIXE Analysis of Otoliths from Reared Red Sea Bream, *Pagrus major* (Temminck et Schlegl). *International Journal of PIXE* 3(4): 275-281.

Arden, K. A., 1995. Mineral Paragenesis and Pegmatite Formation associated with the Eden Lake Syenite Complex, Northern Manitoba. MSc. Thesis, University of Manitoba, 155 pgs.

Babaluk, J. A., Halden, N. M., Reist, J. D., Kristofferson, A. H., Campbell, J. L., and Teesdale, W. J., 1997. Evidence for Non-Anadromous Behaviour of Arctic Charr (*Salvelinus alpinus*) from Lake Hazen, Ellesmere Island, Northwest Territories, Canada, based on Scanning Proton Microprobe Analysis of Otolith Strontium Distribution. *Arctic* 50(3): 224-233.

Beamish, R. J. and McFarlane, G. A., 1987. Current trends in age determination methodology, *in* R. C. Summerfelt and G. E. Hall (eds.). Age and Growth of Fish. Iowa State Univ. Press, Ames, Iowa, p. 15-41.

Bradley, R. W., Sprague, J. B., 1985. Accumulation of zinc by rainbow trout as influenced by pH, water hardness and fish size. *Env. Toxicol.* 4: 685-694.

Cameron, H. D. M., 1988. Geology of the Eden Lake Area. Manitoba Energy and Mines Geological Report GR84-2, 18 pgs.

Campana, S. E., 1983. Calcium deposition and otolith check formation during formation during periods of stress in coho salmon, *Oncorhynchus kisutch*. *Comp. Biochem. Physiol.* A75: 215-220.

Campana, S. E., Thorrold, S. R., Jones, C., Gunther, D., Turbrett, M., Longerich, H., Jackson, S., Halden, N. M., Kalish, J. M., Piccoli, P., de Pontual, H., Troadec, H., Panfilli, J., Secor, D. H., Severin, K., Sie, S. H., Thresher, R., Campbell, J. L., and Teesdale, W. J., 1997. Comparison of accuracy, precision and sensitivity in elemental analysis of fish otoliths using the electron microprobe, PIXE and laser ablation ICP-MS. *Can J. Fish. Aquat. Sci.* 54: 068-2079.

Campbell, J. L., Teesdale, W. J., and Halden, N. M., 1995. Theory, Practice and Application of Micro-PIXE Analysis and Element-Distribution Maps. *Can. Min.* 33: 279-292.

Campbell, J. L., Babaluk, J. A., Halden, N. M., Kristofferson, A. H., Maxwell, J. A., Mejia, S. R., Reist, J. D., and Teesdale, W. J., 1998. Micro-PIXE studies of char populations in Northern Canada, submitted.

Carlander, K. D., 1987. A history of scale age and growth studies of North American freshwater fish, *in* R. C. Summerfelt and G. E. Hall (eds.). Age and Growth of Fish. Iowa State Univ. Press. Ames, Iowa, p. 3-14.

Clarke, A. H., 1981. The Freshwater Molluscs of Canada. National Museums of Canada, Ottawa, Canada. 446 pgs.

Clarkson, E. N. K., 1986. Invertebrate Palaeontology and Evolution, 2nd edition. Unwin Hyman Ltd., Wincester, Mass., U.S.A. 382 pgs.

Colby, P. J., McNicol, R. E., and Ryder, R. A., 1979. Synopsis of Biological Data on the Walleye, Stizostedion v. vitreum (Mitchill 1818). FAO Fisheries Synopsis No. 119, 139 pgs.

Coote, G. E., Gauldie, R. W., and West, I. F., 1991. Application of a nuclear microprobe to the study of fish otoliths and scales. *Nucl. Inst. Methods Phys. Res.* B54: 144-150.

Crisp, E. L., 1974. Sr and Mn in freshwater bivalve shells. Abstracts with Programs, *Geological Society of America* 6(6): 503-504.

Crisp, E. L., 1976. Skeletal trace element chemistry of freshwater bivalves. Abstracts with Programs, *Geological Society of America* 8(1): 15-16.

Crisp, E. L., 1983. Shell structural, phylogenetic, and ontogenetic related variations in skeletal trace element concentrations within freshwater aragonitic bivalve shells. Abstracts with Programs, *Geological Society of America* 15(6): 550.

Dale, T., 1976. The labrinthine mechanoreceptor organs of the cod *Gadus morhua* L. (Teleostei: Gadidae). *Norwegian J. Zool.* 24: 85-128.

Degens, E. T., Deuser, W. G., and Haedrich, R. L., 1969. Molecular structure and composition of fish otoliths. *Mar. Biol.* 2: 105-113.

Dungelberger, D. G., Dean, J. M., and Watabe, N., 1980. The ultrastructure of the otolithic membrane and otolith in the juvenile mummichog, *Fundulus heteroclitus*. *J. Morphol.* 163: 367-377.

Edmonds, J. S., Moran, M. J., and Caputi, N., 1989. Trace element analysis of fish sagittae as an aid to stock identification: pink snapper (*Chrysophrys auratus*) in Western Australian waters. *Can. J. Fish. Aquat. Sci.* 46: 50-54.

Edmonds, J. S., Lenanton, R. C. J., Caputi, N., and Morita, M., 1992. Trace elements in the otoliths of yellow-eye mullet (*Aldrichetta forsteri*) as an aid to stock identification. *Fisheries Research* 13: 39-51.

Eggleston, D., 1975. Determination of age of kahawai *Arripis trutta* (Bloch and Schneider). *New Zealand J. Mar. Biol.* 2: 293-298.

Environment Canada, 1997. Information request from Climate Department: Computer disk of information on maximum, minimum and mean temperatures recorded in the Lynn Lake-Leaf Rapids region.

Fedikow, M. A., Dunn, C. E., and Kowalyk, E., 1993. A vegetation geochemical and radiometric study of part of the Eden Lake aegirine-augite syenite, northwestern Manitoba, *in* Manitoba Energy and Mines, Minerals Division, Report of Activities, 1993, p. 5-10.

Fedikow, M. A., Dunn, C. E., and Kowalyk, E., 1994. Preliminary observations from a vegetation geochemical survey over part of the Eden Lake aegirine-augite syenite, Lynn Lake areas (NTS 64C/9), *in* Manitoba Energy and Mines, Minerals Division, Report of Activities, 1994, p. 11-15.

Fenton, G. E., Short, S. A., and Ritz, D. A., 1991. Age determination of orange roughy, *Hoplostethus atlanticus* (Pisces: Trachichthyidae) using $^{210}Pb/^{226}Ra$ disequilibria. *Mar. Biol.* 109: 197-202.

Fenton, G. E. and Short, S. A., 1992. Fish age validation by radiometric analysis of otoliths. *Aust. J. Mar. Freshwater Res.* 43: 913-922.

Fowler, A. J., Campana, S. E., Jones, C. M., and Thorrold, S. R., 1995. Experimental assessment of the effect of temperature and salinity on elemental composition of otoliths using laser ablation ICPMS. *Can. J. Fish. Aquat. Sci.* 52: 1431-1441.

Fryer, B. J., Jackson, S. E. and Longerich, H. P., 1995. The design, operation and role of the laser-ablation microprobe coupled with an inductively coupled plasma – mass spectrometer (LAM-ICP-MS) in the Earth Sciences. *Can. Min.* 33(2): 303-312.

Gaemers, P. A. M., 1984. Taxonomic position of the Cichlidae (Pisces, perciformes) as demonstrated by the morphology of their otoliths. *Neth. J. Zool.* 34: 566-595.

Gauldie, R. W., 1996. Effects of temperature and vaterite replacement on the chemistry of metal ions in the otoliths of Oncorhynchus tshawytscha. *Can. J. Fish. Aquat. Sci./J. Can. Sci. Halieut Aquat.* 53(9): 2015-2026.

Gauldie, R. W. and Nathan, A., 1977. Iron content of otoliths of tarakihi (Teleosti: Cheilodactylidae). *New Zealand J. Mar. Freshwater Res.* 11(2): 179-191.

Gauldie, R. W. and Nelson, D. G. A., 1990a. Otolith growth in fishes. *Comp. Biochem. Physiol.* 97: 119-136.

Gauldie, R. W. and Nelson, D. G. A., 1990b. Interactions between crystal structure and microincrement layers in fish otoliths. *Comp. Biochem. Physiol.* 97: 475-480.

Gauldie, R. W. and West, I. F., 1992. Age determination of fish using $^{210}Pb:^{226}Ra$ disequilibria, *Mar. Biol.*

Gauldie, R. W., Graynoth, E. J., and Illingworth, J., 1980. The relationship of iron content of some fish otoliths to temperature. *Comp. Biochem. Physiol.* 66A: 19-24.

Gauldie, R. W., Coote, G., and West, I. F., 1993. The Otoliths of Senescent Kahawai, *Arripis trutta* (Arripidae). *Cybium* 17(1): 25-37.

Gauldie, R. W., West, I. F., and Coote, G., 1993. Periodic changes in the chemistry of the otolith of *Macruronus novaezelandiae*. *J. Appl. Ichthyol.* 9: 150-161.

Geological Survey of Canada, 1977. Uranium Reconnaissance Program, Map 3564G.

Giles, M. A. and Attas, E. M., 1993. Rare Earth Elements as Internal Batch marks for Rainbow Trout: Retention, Distribution, and Effects on Growth of Injected Dysprosium, Europium, and Samarium. *Trans. Am. Fish. Soc.* 122: 289-297.

Gunn, J. S., Harrowfield, I. R., Proctor, C. H., and Thresher, R. E., 1992. Electron probe microanalysis of fish otoliths - evaluation of techniques for studying age and stock discrimination. *J. Exp. Mar. Biol. Ecol.* 158: 1-36.

Gunter, R., Fedikow, M. A. F., McRitchie, W. D., and Kowalyk, E., 1995. The Eden Lake rare earth element occurrence-metallurgy, geochemical and ground scintillometer surveys (NTS 64C/9); *in* Manitoba Energy and Mines, Minerals Division, Report of Activities, 1995, p. 11-16.

Halden, N. M., Babaluk, J. A., Campbell, J. L., and Teesdale, W. J., 1995a. Scanning proton microprobe analysis of strontium in an arctic charr, *Salvelinus alpinus*, otolith: implications for the interpretation of anadromy. *Environmental Biology of Fishes.* 43: 333-339.

Halden, N. M., Campbell, J. L., and Teesdale, W. J., 1995b. PIXE Analysis in Mineralogy and Geochemistry. *Can. Min.* 33: 293-302.

Halden, N. M., Babaluk, J. A., Kristofferson, A. H., Campbell, J. L., Teesdale, W. J., Maxwell, J. A., and Reist, J. D., 1996. Micro-PIXE studies of Sr zoning in Arctic charr otoliths: migratory behaviour and stock discrimination. *Nucl. Instr. and Meth. in Phys. Res. B.* 109/110: 592-597.

Halden, N. M. and Fryer, B. J., 1999. Geochemical characteristics of the Eden Lake Complex: evidence for anorogenic magmatism in the Trans-Hudson Orogen. *Can. J. Earth Sci.* 36: 91-103.

Halden N. M., Mejia, S. R., Babaluk, J. A., Reist, J. D., Kristofferson, A. H., Campbell, J. L., and Teesdale, W. J., 1999. Oscillatory zinc distribution in Arctic char (*Salvelinus alpinus*) otoliths: the result of fish behaviour or environmental feedback? submitted.

Hederstrom, H., 1959. Observations on the age of fishes. *Rep. Inst. Freshwater Res.* 40: 161-164.

Henderson, P., 1984. Rare Earth Element Geochemistry. Elsevier Publishing, 510 pgs.

Ichii, T. and Mugiya, Y., 1983. Comparative aspects of calcium dynamics in calcified tissues in the goldfish *Carassius auratus*. *Bull. Japan. Soc. Sci. Fish.* 49: 1039-1044.

Jackson, S. E., Longerich, H. P., Dunning, G. R., and Fryer, B. J., 1992. The application of laser ablation microprobe-inductively coupled plasma-mass spectroscopy (LAM-ICP-MS) to in situ trace-element determinations in minerals. *Can. Min.* 30:1049-1064.

Jones, C., 1992. Development and Application of the Otolith Increment Technique, *in* D. K. Stevenson and S. E. Campana (eds.). Otolith Microstructure, Examination, and Analysis. *Can. Spec. Publ. Fish. Aquat. Sci.* 117: 1-11.

Kalish, J. M., 1989. Otolith microchemistry: validation of the effects of physiology, age, and environment on otolith composition. *J. Exp. Mar. Biol. Ecol.* 132: 151-178.

Kalish, J. M., 1990. Use of Otolith Microchemistry to Distinguish the Progeny of Sympatric Anadromous and Non-Anadromous Salmonoids. *Fishery Bulletin* 88(4): 657-666.

Klein, C. and Hurlbut, C. S., Jr., 1985. Manual of Mineralogy. 20th edition, John Wiley & Sons, New York, U.S.A., 596 pgs.

Kovach, J., 1977. Manganese as an environmental indicator in freshwater clam shells. Abstracts with Programs, Geological Society of America 9(5): 617.

Lapi, L. A. and Mulligan, T. J., 1981. Salmon stock identification using a microanalytic technique to measure elements present in the freshwater growth regions of scales. *Can.J. Fish. Aquat. Sci.* 38: 744-751.

Marshall, D. J. (ed.), 1988. Cathodoluminescence of Geological Materials. Unwin Hyman Publishing, Winchester, Mass., U.S.A. 243 pgs.

Maxwell, J. L., Campbell, J. L., and Teesdale, W. J., 1989. The Guelph PIXE software package. *Nucl. Inst. Methods Phys. Res.* B43: 218-230.

McRitchie, W. D., 1988. Alkaline intrusions of the Churchill Province: Eden Lake (64C/9) and Brezden Lake (64C/4); *in* Manitoba Energy and Mines, Minerals Division, Report of Activities, 1988, p. 5-11.

McRitchie, W. D., 1989. Ground scintillometer reconnaissance of the Eden Lake aegirine-augite monzonite; *in* Manitoba Energy and Mines, Minerals Division, Report of Activities, 1989, p. 7-12.

Milner, N. J., 1982. The accumulation of zinc by O-group plaice, *Pleuronectes platessa* (L.), from high concentration sea water and food. *J. Fish. Biol.* 21: 325-336.

Mugiya, Y., 1964. Calcification in fish and shellfish -III. Seasonal occurrence of a prealbumin fraction in the otolith fluid of some fish, corresponding to the period of opaque zone formation in the otolith. *Bull. Japan. Soc. Sci. Fish.* 30: 955-967.

Mugiya, Y. and Uchimura, T., 1989. Otolith resorption by anaerobic stress in the goldfish, *Carassius auratus*. *J. Fish. Biol.* 35: 813-818.

Mulligan, T. J., Lapi, L., Kieser, R., Yamada, S. B., and Duewer, D. L., 1983. Salmon stock identification based on elemental composition of vertebrae. *Can. J. Fish. Aquat. Sci.* 40: 215-229.

Mulligan, T. J., Martin, F. D., Smucker, R. A., and Wright, D. A., 1987. A method of stock identification based on elemental composition of striped bass *Morone saxatilis* (Walbaum) otoliths. *J. Exp. Mar. Biol. Ecol.* 114: 241-248.

Odum, H. T., 1951. Notes on the strontium content of sea water, celestite radiolaria, and strontianite snail shells. *Science* 114: 211-213.

Pannella, G., 1971. Fish otoliths: daily growth layers and periodical patterns. *Science* 173: 1124-1127.

Pannella, G., 1974. Otolith growth patterns: an aid in age determination in temperature and tropical fishes, *in* T. B. Bagenal (ed.). The Ageing of Fish. Unwin Bros. Ltd., Surrey, England, p. 28-39.

Paul, L. J., 1976. A study on age, growth, and population structure of the snapper, *Chrysophrys auratus* (Forster), in the Hauraki Gulf, New Zealand. *Fish. Res. Bull.* 13: 67.

Potts, P. J., 1987. A Handbook of Silicate Rock Analysis. Blackie & Son Ltd., Glasgow, England, 622 pgs.

Power, G., 1978. Fish population structure in Arctic lakes. *Journal of the Fisheries Research Board of Canada.* 35: 53-59.

Radtke, R. L., 1989. Strontium-Calcium Concentration Ratios in Fish Otoliths as Environmental Indicators. *Comp. Biochem. Physiol.* 92A(2): 189-193.

Radtke, R. L., 1995. Otolith Microchemistry of Char - Use in Life History Studies. *Nordic J. Freshwater Res.* 72: 392-395.

Radtke, R. L. and Morales-Nin, B., 1989. Mediterranean juvenile bluefin tuna: life history patterns. *J. Fish. Biol.* 35: 485-496.

Radtke, R. L. and Shafer, D. J., 1992. Environmental Sensitivity of Fish Otolith Microchemistry. *Aust. J. Mar. Freshwater Res.* 43: 935-951.

Radtke, R., Svenning, M., Malone, D., Klementsen, A., Ruzicka, J., and Fey, D., 1996. Migrations in an extreme northern population of Arctic charr *Salvelinus alpinus*: insights from otolith microchemistry. *Mar. Ecol. Prog. Ser.* 136: 13-23.

Radtke, R. L. and Targett, T. E., 1984. Rhythmic Structural and Chemical Patterns in Otoliths of the Antarctic Fish *Notothenia larseni*: Their Application to Age Determination. *Polar Biol.* 3: 203-210.

Radtke, R. L., Townsend, D. W., Folsom, S. D., and Morrison, M. A., 1990. Strontium: calcium concentration ratios in otoliths of herring larvae as indicators of environmental histories. *Environmental Biology of Fishes* 27: 51-61.

Reist, J. D., Gyselman, E., Babaluk, J. A., Johnson, J. D., and Wissink, R., 1995. Evidence for two morphotypes of Arctic Charr (*Salvelinus alpinus*) from Lake Hazen, Ellesmere Island, Northwest Territories, Canada. *Nordic J. Freshw. Res.* 71: 1-15.

Ricker, W. E., 1975. Computation and interpretation of biological statistics of fish populations. *Bull. Fish. Res. Board Can.* 191: 382.

Rieman, B. E., Myers, D. L., and Nielsen, R. L., 1994. Use of Otolith Microchemistry to Discriminate *Oncorhynchus nerka* of Resident and Anadromous Origin. *Can. J. Fish. Aquat. Sci.* 51: 68-77.

Rosenthal, H. L., Eves, M. M., and Cochran, O. A., 1970. Common strontium concentration of mineralized tissues from marine and sweet water animals. *Comp. Biochem. Physiol.* 32: 445-450.

Sadovy, Y, and Severin, K. P., 1992. Trace elements in biogenic aragonite: correlation of body growth rate and strontium levels in the otoliths of the white grunt, *Haemulon plumieri* (Pisces: Haemulidae). *Bulletin of Marine Science* 50(2): 237-257.

Sadovy, Y. and Severin, K. P., 1994. Elemental Patterns in Red Hind (*Epinephelus guttatus*) Otoliths from Bermuda and Puerto Rico Reflect Growth Rate, Not Temperature. *Can. J. Fish. Aquat. Sci.* 51: 133-141.

Schmitt, H. R., Hornbrook, E. H., and Friske, P. W. B., 1989. Geochemical results and interpretations of a lake sediment and water survey in the Lynn lake-Leaf Rapids region, northern Manitoba; Geological Survey of Canada Open File 1959.

Scott, W. B. and Crossman, E. J., 1979. Freshwater Fishes of Canada. Bulletin 184, Fisheries Research Board of Canada, Ottawa 1973, 966 pgs.

Seyama, H., Edmonds, J. S., Moran, M. J., Shibata, Y., Soma, M., and Morita, M., 1991. Periodicity in fish otolith Sr, Na, and K corresponds with visual banding. *Experientia* 47: 1193-1196.

Simkiss, K., 1974. Calcium metabolism in fish in relation to ageing, *in* T. B. Bagenal (ed.). The Ageing of Fish. Unwin Bros. Ltd., Surrey, England, p. 1-12.

Struhsaker, P. and Uchiyama, J. H., 1976. Age and growth of the nehu, *Stolephorus pupureus* (Pisces: Engraulidae), from the Hawaiian Islands as indicated by daily growth increments of sagittae. *Fish. Bull. U. S.* 74: 9-17.

Taubert, B. D. and Coble, D. W., 1977. Daily rings in otoliths of three species of *Lepomis* and *Tilapia mossambica*. *J. Fish. Res. Board Can.* 34: 332-340.

Thresher, R. E., Proctor, C. H., Gunn, J. S., and Harrowfield, I. R., 1994. An evaluation of electron-probe microanalysis of otoliths for stock delineation and identification of nursery areas in a southern temperate groundfish, *Nemadactylus macropterus* (Cheilodactylidae). *Fish. Bull.* 92:817-840.

Townsend, D. W., Radtke, R. L., Corwin, S., and Libby, D. A., 1992. Strontium: calcium ratios in juvenile Atlantic herring *Clupea harengus* L. otoliths as a function of water temperature. *J. Exp. Mar. Biol. Ecol.* 160: 131-140.

Young, J. and McRitchie, W. D., 1990. REE investigations, Eden Lake intrusive suite (NTS 64C/9); *in* Manitoba Energy and Mines, Minerals Division, Report of Activities, 1990, p. 9-19.

Appendix A: Data Tables

APPENDIX A: DATA TABLES

Table 1. Summary of neutron activation analyses for ashed (470°C) tissues collected adjacent to the allanite and britholite mineralized survey site, Eden Lake area. Analyses in ppm unless otherwise indicated. The values for REE recorded as below the limits of determination (<) have been utilized for the calculation of total REE (after Fedikow et al., 1994).

Species/ Tissues	La	Ce	Nd	Sm	Eu	Tb	Yb	Lu	ΣREE
Black Spruce (*Picea mariana*)									
Outer Bark	7	13	6	0.9	0.2	<0.5	0.4	0.06	28.5
Inner Bark	3	5	<5	0.2	<0.2	<0.5	<0.05	<0.05	13.9
Twigs	12	22	6	6	1.5	0.4	<0.5	0.12	57.2
Trunk Wood	6	8	<5	<5	0.2	<0.02	<0.5	<0.05	19.3
Needles	2	3	<5	<5	0.2	<0.01	<0.5	<0.05	10.8
Black Spruce (*Picea mariana*) Crown									
Cones	1	<3	<5	0.2	<0.03	<0.5	<0.05	<0.05	9.9
Twigs	3	6	<5	0.3	<0.03	<0.5	<0.05	<0.05	14.6
Needles	1	<3	<5	0.2	<0.02	<0.5	0.1	<0.05	10.2

Table 1 continued.

Species/ Tissues	La	Ce	Nd	Sm	Eu	Tb	Yb	Lu	ΣREE
Jack Pine (*Pinus banksiana*)									
Outer bark	33	74	49	5.6	1.3	0.6	1.2	0.19	165.0
Inner bark	3	7	<5	0.5	<0.02	<0.5	<0.05	<0.05	16.2
Twigs	2	5	<5	0.3	<0.02	<0.5	0.2	<0.05	13.0
Trunk wood	9	11	<5	0.2	<0.01	<0.5	<0.05	<0.05	25.6
Cones	1	<3	<5	0.2	<0.03	<0.5	<0.05	<0.05	9.8
Needles	2	5	<5	0.3	<0.02	<0.5	0.2	<0.05	13.0
Alder (*Alnus crispa*)									
Twigs	270	320	150	13	3.3	1.1	<0.05	<0.05	757.5
Leaves	93	120	66	5.4	1.2	<0.5	<0.05	<0.05	286.2
Birch (*Betula papyrifera*)									
Twigs	45	61	30	3.2	0.8	<0.5	<0.05	<0.05	140.6
Leaves	16	26	19	1.6	0.4	<0.5	<0.05	<0.05	63.6
Lichen (*Cladonia spp.*)	86	190	120	13	3	0.9	2.1	0.31	415.3

Table 1 continued.

Species/ Tissues	Ba	Sr	Sc	Th	U	Zn	Ash (%)	Au (ppb)	As
Black Spruce (*Picea mariana*)									
Outer Bark	3950	5100	1.4	0.9	0.4	1800	2.59	6	3
Inner Bark	4300	5800	<0.1	<0.1	<0.1	2500	3.18	<5	<0.5
Twigs	3800	5800	2.3	1.4	1.2	3100	2.08	18	5.7
Trunk Wood	3800	6400	0.1	<0.1	<0.1	3100	0.36	<5	4.2
Needles	2050	6050	0.2	<0.1	<0.1	2250	5.27	<5	<0.5
Black Spruce (*Picea mariana*) Crown									
Cones	330	780	0.4	<0.1	<0.1	1800	0.62	<5	2.7
Twigs	5700	7100	0.5	0.2	<0.1	2200	1.95	16	2.6
Needles	920	3300	0.3	<0.1	<0.1	1200	2.44	<5	2.8
Jack Pine (*Pinus banksiana*)									
Outer bark	950	1600	3.5	4.5	2.4	4200	1.61	17	6.1
Inner bark	640	1600	0.1	<0.1	<0.1	3900	2.36	13	<0.5
Twigs	120	1000	0.3	0.2	0.5	3500	1.66	5	2.2
Trunk wood	640	2100	0.1	<0.1	<0.1	6200	0.30	6	<0.5
Cones	<50	<300	0.2	0.1	<0.1	2200	0.42	<5	1.9
Needles	120	1000	0.3	0.2	0.5	3500	2.17	5	2.2

Table 1 continued.

Species/ Tissues	Ba	Sr	Sc	Th	U	Zn	Ash (%)	Au (ppb)	As
Alder (*Alnus crispa*)									
Twigs	6900	12000	0.3	<0.1	<0.2	5100	1.51	9	1.5
Leaves	1300	4700	<0.1	1.0	1.0	1500	3.84	<5	<0.5
Birch (Betula papyrifera)									
Twigs	5700	7100	0.5	<0.1	<0.1	20000	1.09	16	2.6
Leaves	1400	2400	0.1	0.4	<0.1	6000	3.23	<5	<0.5
Lichen (*Cladonia spp.*)	1000	1500	6.0	8.1	4.5	2700	1.08	22	12

Species/ Tissues	Br	Ca (%)	Co	Cr	Cs	Fe (%)	Hf	K (%)	Mo
Black Spruce (*Picea mariana*)									
Outer Bark	14	34.5	5	9	1.6	0.48	1.5	1.9	2
Inner Bark	24	30.0	4	<1	2.6	0.06	<0.5	11.2	<2
Twigs	27	23.8	7	16	4.4	0.84	1.7	10.9	<2
Trunk Wood	190	33.9	8	50	2.7	0.07	<0.5	7.4	<2
Needles	38	29.9	2	3	1.2	0.06	<0.5	5.6	<2

Table 1 continued.

Species/ Tissues	Br	Ca (%)	Co	Cr	Cs	Fe (%)	Hf	K (%)	Mo
Black Spruce (*Picea mariana*)									
Crown									
Cones	36	4.0	10	5	22	0.23	<0.5	24.7	<2
Twigs	23	21.5	17	8	1.9	0.23	<0.5	22.3	<2
Needles	48	20.9	2	6	8.2	0.12	<0.5	14.4	<2
Jack Pine (*Pinus banksiana*)									
Outer bark	11	24.2	8	23	4.0	1.16	2.1	4.0	<2
Inner bark	46	24.6	3	<1	4.2	0.07	<0.5	18.5	<2
Twigs	55	15.2	5	3	2.1	0.16	<0.5	18.9	<2
Trunk wood	32	27.1	4	3	3.9	0.05	<0.5	13.3	<2
Cones	51	2.0	6	<1	19.0	0.24	<0.5	21.4	<2
Needles	55	15.2	5	3	2.1	0.16	<0.5	18.9	<2
Alder (*Alnus crispa*)									
Twigs	12	26.1	10	3	7.0	0.15	<0.5	14.3	6
Leaves	30	17.2	9	4	17	0.20	<0.5	25.1	<2
Birch (Betula papyrifera)									
Twigs	23	21.5	17	8	1.9	0.23	<0.5	22.3	<2
Leaves	21	15.4	8	<1	3.2	0.13	<0.5	28.9	<2

Table 1 continued.

Species/ Tissues	Br	Ca (%)	Co	Cr	Cs	Fe (%)	Hf	K (%)	Mo
Lichen (*Cladonia spp.*)	130	7.0	13	51	14	1.67	4.2	20.6	5

Species/ Tissues	Na	Ni	Rb	Sr
Black Spruce (*Picea mariana*)				
Outer Bark	1750	<50	56	0.8
Inner Bark	401	<50	200	0.1
Twigs	2550	<50	170	0.7
Trunk Wood	296	<50	220	0.5
Needles	145	<50	70	0.1
Black Spruce (*Picea mariana*) Crown				
Cones	758	160	940	0.6
Twigs	746	<50	320	0.5
Needles	347	64	320	0.3
Jack Pine (*Pinus banksiana*)				
Outer bark	4530	190	66	1.5
Inner bark	2600	<50	230	0.4

Table 1 continued.

Species/ Tissues	Na	Ni	Rb	Sr
Twigs	377	<50	180	0.3
Trunk wood	304	<50	220	0.3
Cones	261	120	780	0.6
Needles	377	<50	180	0.3
Alder (*Alnus crispa*)				
Twigs	492	<50	310	0.4
Leaves	253	<50	1000	0.4
Birch (Betula papyrifera)				
Twigs	746	<50	320	0.5
Leaves	184	80	530	<0.1
Lichen (*Cladonia spp.*)	7310	<50	500	1.6

Table 2. Select sample set. Abbreviations are as follows: NP = northern pike; W = walleye; WS = white sucker; B = burbot; LNS = long-nose sucker; P = yellow perch; Wh = lake whitefish; C = cisco; LogP = log perch; MSc = mottled sculpin; ES = emerald shiner; (TL) = total length; F = female; M = male; and ? = did not determine. The term "immature" means the fish has not spawned yet and the term "spent" means the fish has spawned.

Sample number	Species	Fork Length (mm)	Weight (g)	Sex	Maturity	Otolith collected	Location
F1	NP	591	1270	F	Spent	Yes	See map
F2	NP	623	1440	F	Spent	Yes	Narrows
F3	W	459	1030	F	Spent	Yes	Narrows
F4	W	361	470	F	Immature	Yes	See map
F5	W	493	1370	F	Immature	Yes	See map
F6	WS	439	1180	F	Spent	Yes	ED1
F9	W	333	404	M	Immature	Yes	Narrows
F10	W	462	1038	F	Immature	Yes	Narrows
F11	NP	580	1264	F	Spent	Yes	Narrows
F12	W	438	917	M	Spent	Yes	Narrows
F13	WS	443	1254	M	Spent	Yes	Narrows
F14	NP	589	1148	F	Spent	Yes	Narrows
F15	NP	516	917	M	Spent	Yes	Narrows
F16	WS	439	1274	M	Spent	Yes	ED2
F17	WS	468	1437	F	Spent	Yes	ED2
F18	LNS	518	2295	F	Spent	Yes	KAP
F19	W	508	1424	F	Spent	Yes	KAP
F20	W	562	1762	F	Spent	Yes	KAP
F21	B	495	819	F	Immature	Yes	ED1
F22	WS	482	1561	F	Spent	Yes	ED2
F23	WS	463	1645	F	Spent	Yes	ED2
F24	WS	464	1528	F	Spent	Yes	ED2
F25	WS	423	1122	F	Spent	Yes	KAP
F26	WS	448	1468	F	Spent	Yes	KAP
F27	WS	441	1309	F	Spent	Yes	KAP
F28	WS	414	1158	M	Immature	Yes	KAP
F29	WS	432	1308	F	Spent	Yes	KAP
F30	WS	432	1274	M	Spent	Yes	KAP
F31	WS	474	1533	F	Spent	Yes	ED1
F32	WS	450	1485	F	Spent	Yes	ED1
F33	WS	453	1468	F	Spent	Yes	ED1
F34	WS	501	2085	F	Spent	Yes	ED1
F35	WS	462	1460	F	Spent	Yes	ED1
F42	NP	558	1153	F	Immature	Yes	Campsite
F43	W	334	420	F	Immature	Yes	Narrows
F44	W	340	427	F	Immature	Only one	Narrows

Table 2 continued.

Sample number	Species	Fork Length (mm)	Weight (g)	Sex	Maturity	Otolith collected	Location
F45	W	337	466	F	Immature	Yes	ED1
F46	W	333	420	F	Immature	Yes	ED1
F47	W	335	376	M	Immature	Yes	ED1
F48	W	558	1723	F	Spent	Yes	BAK2
F49	W	467	1088	M	Spent	Yes	BAK2
F55	NP	568	1199	F	Spent	Broken	Adam Lake
F56	NP	520	1024	M	Spent	Yes	Adam Lake
F57	W	493	1532	M	Spent	Yes	ED2
F58	W	521	1523	F	Spent	Yes	ED2
F59	W	350	471	F	Immature	Yes	ED2
F60	W	311	301	M	Immature	Only one	ED2
F61	W	376	615	F	Immature	Yes	ED2
F62	NP	808	4622	F	Spent	Yes	ED1
F63	NP	768	3607	M	Spent	Yes	ED1
F64	NP	792	4037	M	Spent	Yes	Narrows
F65	NP	440	583	M	Immature	Yes	Narrows
F66	W	530	1440	F	Spent	Yes	BAK1
F67	W	559	1674	M	Spent	Yes	BAK1
F68	W	532	1578	F	Spent	Yes	BAK1
F69	W	513	1364	M	Spent	Yes	KAP1
F70	W	382	708	F	Immature	Yes	KAP1
F71	W	361	548	M	Immature	Yes	KAP1
F72	NP	352	433	M	Immature	Yes	Jackson L.
F73	NP	581	1581	M	Spent	Yes	Jackson L.
F74	NP	522	911	F	Spent	Yes	Jackson L.
F75	W	592	1580	M	Spent	Yes	Pt. E
F82	W	345	448	M	Immature	Yes	Pt. D
F83	NP	520	1135	M	Spent	Yes	Pt. F
F84	NP	534	905	F	Spent	Yes	Pt. A
F85	NP	540	1163	M	Spent	Yes	Pt. A
F97	WS	378	949	M	Spent	Yes	KAP1
F98	WS	427	1076	F	Spent	Yes	KAP1
F99	WS	438	1424	M	Spent	Yes	KAP1
F100	WS	416	1016	M	Spent	Yes	KAP1
F101	WS	431	1228	M	Spent	Yes	KAP1
F102	WS	419	1066	M	Spent	Yes	KAP
F103	NP	607	1344	M	Spent	Yes	KAP
F104	NP	574	1351	F	Spent	Yes	KAP
F105	P	removed from stomach of NP (F104)				Yes	KAP
F106	NP	577	1292	M	Spent	Yes	ED1
F107	NP	678	2256	F	Spent	Yes	ED1
F108	NP	639	1913	M	Spent	Yes	ED1

Table 2 continued.

Sample number	Species	Fork Length (mm)	Weight (g)	Sex	Maturity	Otolith collected	Location
F109	NP	685	2549	F	Spent	Yes	ED1
F110	NP	559	1197	F	Spent	Yes	KAP
F111	NP	563	1198	M	Spent	Yes	KAP
F112	NP	597	1822	F	Spent	Yes	KAP
F113	NP	551	1233	F	Spent	Yes	KAP1
F114	NP	515	971	M	Spent	1 broken	KAP1
F115	NP	588	1046	F	Spent	Yes	KAP1
F116	NP	272	149	M	Immature	Yes	KAP1
F117	NP	253	124	F	Immature	Yes	KAP1
F118	NP	567	1109	F	Spent	Yes	KAP1
F119	NP	535	1037	M	Spent	Yes	KAP1
F120	B	505	848	F	Immature	Yes	BAK1
F121	WS	432	1280	F	Spent	Yes	BAK1
F122	WS	452	1414	F	Spent	Yes	BAK1
F123	NP	511	1069	M	Spent	Yes	BAK2
F124	NP	766	3209	M	Spent	Yes	BAK2
F125	WS	486	1790	F	Spent	Yes	BAK2
F126	WS	480	2095	M	Spent	Yes	BAK2
F127	NP	615	1493	F	Spent	Yes	BAK1
F128	NP	812	4471	F	Spent	Yes	BAK1
F129	NP	581	1156	F	Spent	Yes	ED2
F130	NP	531	1127	M	Spent	Yes	ED2
F131	P	removed from stomach of NP (F130)				Yes	ED2
F132	NP	571	1232	F	Spent	Yes	ED2
F133	NP	595	1271	M	Spent	Yes	ED2
F134	NP	523	1075	M	Spent	Yes	ED2
F141	C	436	1035	F	Unknown	Yes	KAP1
F142	C	388	687	F	Unknown	Yes	KAP1
F143	P	140	34	?	?	Yes	ED2
F144	P	132	33	?	?	Yes	ED2
F145	P	134	26	?	?	Yes	ED2
F146	P	135	34	?	?	Yes	BAK2
F147	P	138	31	?	?	Yes	BAK2
F148	P	170	64	?	?	Yes	KAP
F149	P	154	49	?	?	Yes	KAP
F150	P	157	48	?	?	Yes	KAP
F151	P	149	39	?	?	Yes	KAP
F152	P	150	43	?	?	Yes	KAP
F153	P	171	67	?	?	Yes	BAK1
F154	P	154	43	?	?	Yes	BAK1
F155	C	353	578	F	Unknown	Yes	KAP1
F156	C	333	594	M	Unknown	Yes	KAP1

Table 2 continued.

Sample number	Species	Fork Length (mm)	Weight (g)	Sex	Maturity	Otolith collected	Location
F157	C	169	66	F	Unknown	Yes	KAP1
F158	C	190	75	F	Immature	Yes	KAP1
F159	C	161	42	F	Immature	Yes	KAP1
F160	C	147	36	F	Immature	Yes	KAP1
F161	Wh	446	1452	F	Immature	Yes	KAP
F162	Wh	484	1731	F	Spent	Yes	BAK1
F163	Wh	477	2120	F	Spent	Yes	BAK1
F164	Wh	430	1333	M	Spent	Yes	BAK2
F165	Wh	436	1483	M	Spent	Yes	BAK2
F166	Wh	373	747	M	Immature	Yes	KAP1
F167	Wh	410	1169	M	Immature	Yes	KAP1
F168	Wh	458	1664	F	Spent	Yes	KAP1
F169	W	102	8.6	?	?	Yes	KAP
F170	W	105	10.1	?	?	Yes	KAP
F171	W	106	9.5	?	?	Yes	KAP
F176	Wh	92	7.2	?	?	Yes	BAK1

Table 3. Additional fish heads acquired from sport fishermen. Abbreviations are as follows: NP = northern pike and W = walleye.

Sample number	Species	Fork Length (mm)	Weight (g)	Sex	Maturity	Otolith collected	Location
F7	NP	Had heads only				Yes	See map
F8	NP	Had heads only				Yes	See map
F36	W	Had heads only				Yes	Narrows
F37	W	Had heads only				Broken	Narrows
F38	W	Had heads only				Yes	Narrows
F39	W	Had heads only				Yes	Narrows
F40	W	Had heads only				Yes	Narrows
F41	W	Had heads only				Yes	Narrows
F50	W	Had heads only				Yes	Pt. B
F51	W	Had heads only				Yes	Pt. B
F52	W	Had heads only				Yes	Pt. B
F53	W	Had heads only				Yes	Pt. B
F54	W	Had heads only				Yes	Pt. B
F76	W	Had heads only				Yes	Pt. E
F77	W	Had heads only				Yes	Pt. E
F78	W	Had heads only				Yes	Pt. E
F79	W	Had heads only				Yes	Pt. E
F80	W	Had heads only				Yes	Pt. E
F81	W	Had heads only				Yes	Pt. E
F86	W	Had heads only				Yes	Pt. C
F87	W	Had heads only				Yes	Pt. C
F88	W	Had heads only				Yes	Pt. C
F89	W	Had heads only				Yes	Pt. C
F90	W	Had heads only				Yes	Pt. C
F91	W	Had heads only				Yes	Pt. C
F92	W	Had heads only				No	Pt. C
F93	W	Had heads only				Yes	Pt. C
F94	W	Had heads only				Yes	Pt. C
F95	W	Had heads only				Yes	Pt. C
F96	W	Had heads only				Yes	Pt. C
F135	W	Had heads only				Yes	KAP
F136	W	Had heads only				Yes	KAP
F137	W	Had heads only				Yes	KAP
F138	W	Had heads only				Yes	KAP
F139	W	Had heads only				Yes	Narrows
F140	W	Had heads only				Yes	Narrows

Table 4. **List of the disks of otoliths (segregated by location and species).**

SITE	DISK NAME	SPECIES	CAPTURE METHOD	NUMBER OF OTOLITHS	SAMPLE NUMBERS
KAP	KAP-A	Walleye	Angled and Netted	6	F135, F136, F137, F138, F19, and F20
	KAP-B	White suckers and one Long-nose sucker	Netted	7	F25, F26, F27, F28, F29, F30, AND F18
	KAP-C	Northern Pike	Netted	6	F110, F111, F112, F103, F104, and F106
	KAP-D	Lake whitefish and three baby Walleye	Netted	4	F161, F171, F170, and F169
	KAP-E	Yellow Perch	Netted	6	F105, F148, F149, F150, F151, F151, and F152
KAP1	KAP1-A	Lake whitefish and Walleye	Netted	6	F166, F167, F168, F71, F72, and F69
	KAP1-B	White suckers	Netted	5	F98, F99, F100, F101, and F102
	KAP1-C	Northern Pike	Netted	7	F118, F113, F117, F119, F116, F114, and F115
	KAP1-D	Cisco	Netted	4	F142, F155, F156, and F141
	KAP1-E	Cisco	Netted	4	F160, F157, F158, and F159
ED1	ED1-A	Walleye and one Burbot	Netted	4	F45, F46, F47, and F21
	ED1-B	White suckers	Netted	6	F31, F6, F32, F35, F33, and F34
	ED1-C	Northern Pike	Netted	5	F62, F109, F108, F107, and F63

Table 4 continued.

LOCATION	DISK NAME	SPECIES	CAPTURE METHOD	NUMBER OF OTOLITHS	SAMPLE NUMBERS
ED2	ED2-A	Walleye	Netted	5	F57, F58, F59, F60, and F61
	ED2-B	White suckers	Netted	5	F17, F16, F24, F23, and F22
	ED2-C	Northern Pike	Netted	5	F134, F129, F130, F132, and F133
	ED2-D	Yellow Perch	Netted	3	F143, F144, and F145
BAK1	BAK1-A	Walleye, White suckers, and Northern Pike	Netted	7	F66, F67, F68, F121, F122, F127, and F128
	BAK1-B	Lake whitefish and one Burbot	Netted	3	F163, F162, and F120
	BAK1-C	Yellow Perch	Netted	2	F153 and F154
BAK2	BAK2-A	Walleye, White suckers, and Northern Pike	Netted	6	F48, F49, F123, F124, F125, and F126
	BAK2-B	Lake whitefish and Yellow Perch	Netted	4	F164, F146, F147, and F165
Narrows	N-A	Walleye	Angled	5	F12, F10, F9, F37, and F36
	N-B	Walleye	Angled	5	F3, F39, F38, F40, and F41
	N-C	Walleye and one White sucker	Angled	5	F140, F13, F43, F44, and F139
	N-D	Northern Pike	Angled	6	F15, F14, F11, F65, F64, and F2
Campsite, Adam Lake, and Jackson Lake	C+A+J	Northern Pike	Angled	6	F74, F73, F72, F42, F55, and F56
Pt. A and Pt. B	A+B	Walleye and Northern Pike	Angled	7	F54, F53, F85, F84, F51, F50, and F52

Table 4 continued.

LOCATION	DISK NAME	SPECIES	CAPTURE METHOD	NUMBER OF OTOLITHS	SAMPLE NUMBERS
Pt. C	C	Walleye	Angled	6	F91, F86, F87, F88, F89, and F90
Pt. C and Pt. D	C+D	Walleye	Angled	5	F93, F94, F95, F96, and F82
Pt. E	E	Walleye	Angled	7	F75, F76, F78, F77, F79, F80, and F81
Pt. F and "See Map"	F+MAP	Walleye and Northern Pike	Angled	6	F5, F43, F1, F7, F83, and F8

Table 5. Ages of the Eden Lake fish. Abbreviations are as follows: RM = reflection microscopy; CL = cathodoluminescence microscopy; BB = "break and burn" method; and ND = no data (i.e. otolith damaged, fish could not be aged).

DISK NAME	DISK #	SAMPLE #	SPECIES	LOCATION	METHOD USED FOR AGING	AGE (years)
KAP-A	1	F135	Walleye	KAP	RM	14
	2	F136	Walleye	KAP	RM	15
	3	F137	Walleye	KAP	RM	15
	4	F138	Walleye	KAP	RM	15
	5	F19	Walleye	KAP	RM	14
	6	F20	Walleye	KAP	RM	15
KAP-B	1	F25	White sucker	KAP	BB	12
	2	F26	White sucker	KAP	BB	18
	3	F27	White sucker	KAP	BB	17
	4	F28	White sucker	KAP	BB	14
	5	F29	White sucker	KAP	BB	15
	6	F30	White sucker	KAP	BB	19
	7	F18	White sucker	KAP	RF	>15
KAP-C	1	F110	N. pike	KAP	CL	13
	2	F111	N. pike	KAP	CL	11
	3	F112	N. pike	KAP	CL	9
	4	F103	N. pike	KAP	CL	13
	5	F104	N. pike	KAP	CL	8
	6	F106	N. pike	KAP	CL	15
KAP-D	1	F161	Whitefish	KAP	RM	15
	2	F171	Walleye	KAP	RM	3
	3	F170	Walleye	KAP	RM	3
	4	F169	Walleye	KAP	RM	4
KAP-E	1	F105	Yellow perch	KAP	RM	5
	2	F148	Yellow perch	KAP	RM	7
	3	F149	Yellow perch	KAP	RM	9
	4	F150	Yellow perch	KAP	RM	6
	5	F151	Yellow perch	KAP	RM	8
	6	F152	Yellow perch	KAP	RM	5
KAP1-A	1	F166	Whitefish	KAP1	RM	11
	2	F167	Whitefish	KAP1	RM	18
	3	F168	Whitefish	KAP1	RM	29
	4	F71	Walleye	KAP1	RM	13
	5	F70	Walleye	KAP1	RM	11
	6	F69	Walleye	KAP1	RM	18

Table 5 continued.

DISK NAME	DISK #	SAMPLE #	SPECIES	LOCATION	METHOD USED FOR AGING	AGE (years)
KAP1-B	1	F98	White sucker	KAP1	BB	12
	2	F99	White sucker	KAP1	BB	15
	3	F100	White sucker	KAP1	BB	11
	4	F101	White sucker	KAP1	BB	10
	5	F102	White sucker	KAP1	BB	16
KAP1-C	1	F118	N. pike	KAP1	CL	12
	2	F113	N. pike	KAP1	CL	9
	3	F117	N. pike	KAP1	BB	4
	4	F119	N. pike	KAP1	BB	7
	5	F116	N. pike	KAP1	BB	4
	6	F114	N. pike	KAP1	BB	8
	7	F115	N. pike	KAP1	CL	10
KAP1-D	1	F142	Cisco	KAP1	RM	22
	2	F155	Cisco	KAP1	RM	10
	3	F156	Cisco	KAP1	RM	9
	4	F141	Cisco	KAP1	RM	20
KAP1-E	1	F160	Cisco	KAP1	RM	4
	2	F157	Cisco	KAP1	RM	5
	3	F158	Cisco	KAP1	RM	6
	4	F159	Cisco	KAP1	RM	7
ED1-A	1	F45	Walleye	ED1	RM	9
	2	F46	Walleye	ED1	RM	11
	3	F47	Walleye	ED1	RM	11
	4	F21	Burbot	ED1	RM	10
ED1-B	1	F31	White sucker	ED1	BB	17
	2	F6	White sucker	ED1	BB	12
	3	F32	White sucker	ED1	ND	ND
	4	F35	White sucker	ED1	BB	23
	5	F33	White sucker	ED1	BB	22
	6	F34	White sucker	ED1	BB	24
ED1-C	1	F62	N. pike	ED1	CL	19
	2	F109	N. pike	ED1	CL	14
	3	F108	N. pike	ED1	CL	10
	4	F107	N. pike	ED1	CL	12
	5	F63	N. pike	ED1	CL	18

Table 5 continued.

DISK NAME	DISK #	SAMPLE #	SPECIES	LOCATION	METHOD USED FOR AGING	AGE (years)
ED2-A	1	F57	Walleye	ED2	RM	11
	2	F58	Walleye	ED2	RM	18
	3	F59	Walleye	ED2	RM	12
	4	F60	Walleye	ED2	RM	10
	5	F61	Walleye	ED2	RM	14
ED2-B	1	F17	White sucker	ED2	BB	16
	2	F16	White sucker	ED2	BB	25
	3	F24	White sucker	ED2	BB	20
	4	F23	White sucker	ED2	BB	17
	5	F22	White sucker	ED2	BB	21
ED2-C	1	F134	N. pike	ED2	CL	15
	2	F129	N. pike	ED2	BB	11
	3	F130	N. pike	ED2	BB	8
	4	F132	N. pike	ED2	CL	10
	5	F133	N. pike	ED2	CL	11
ED2-D	1	F143	Yellow perch	ED2	RM	8
	2	F144	Yellow perch	ED2	RM	7
	3	F145	Yellow perch	ED2	RM	10
BAK1-A	1	F66	Walleye	BAK1	RM	23
	2	F67	Walleye	BAK1	RM	19
	3	F68	Walleye	BAK1	RM	18
	4	F121	White sucker	BAK1	RM	10
	5	F122	White sucker	BAK1	BB	17
	6	F127	N. pike	BAK1	CL	9
	7	F128	N. pike	BAK1	CL	11
BAK1-B	1	F163	Whitefish	BAK1	RM	25
	2	F162	Whitefish	BAK1	RM	24
	3	F120	Burbot	BAK1	RM	9
BAK1-C	1	F153	Yellow perch	BAK1	RM	8
	2	F154	Yellow perch	BAK1	RM	5
BAK2-A	1	F48	Walleye	BAK2	RM	17
	2	F49	Walleye	BAK2	RM	17
	3	F123	N. pike	BAK2	CL	11
	4	F124	N. pike	BAK2	CL	13
	5	F125	White sucker	BAK2	BB	21
	6	F126	White sucker	BAK2	BB	16

Table 5 continued.

DISK NAME	DISK #	SAMPLE #	SPECIES	LOCATION	METHOD USED FOR AGING	AGE (years)
BAK2-B	1	F164	Whitefish	BAK2	RM	16
	2	F146	Yellow perch	BAK2	RM	6
	3	F147	Yellow perch	BAK2	RM	5
	4	F165	Whitefish	BAK2	RM	17
N-A	1	F12	Walleye	Narrows	RM	16
	2	F10	Walleye	Narrows	RM	12
	3	F9	Walleye	Narrows	RM	9
	4	F37	Walleye	Narrows	RM	11
	5	F36	Walleye	Narrows	RM	17
N-B	1	F3	Walleye	Narrows	RM	12
	2	F39	Walleye	Narrows	RM	10
	3	F38	Walleye	Narrows	RM	12
	4	F40	Walleye	Narrows	RM	11
	5	F41	Walleye	Narrows	RM	18
N-C	1	F140	Walleye	Narrows	RM	16
	2	F13	White sucker	Narrows	BB	19
	3	F43	Walleye	Narrows	RM	12
	4	F44	Walleye	Narrows	RM	11
	5	F139	Walleye	Narrows	RM	22
N-D	1	F15	N. pike	Narrows	CL	12
	2	F14	N. pike	Narrows	CL	10
	3	F11	N. pike	Narrows	CL	13
	4	F65	N. pike	Narrows	BB	6
	5	F64	N. pike	Narrows	CL	10
	6	F2	N. pike	Narrows	CL	13
C+A+J	1	F74	N. pike	Jackson L.	CL	12
	2	F73	N. pike	Jackson L.	CL	10
	3	F72	N. pike	Jackson L.	CL	13
	4	F42	N. pike	Campsite	GB	7
	5	F55	N. pike	Adam Lake	CL	13
	6	F56	N. pike	Adam Lake	CL	8

Table 5 continued.

DISK NAME	DISK #	SAMPLE #	SPECIES	LOCATION	METHOD USED FOR AGING	AGE (years)
A+B	1	F54	Walleye	Pt. B	RM	14
	2	F53	Walleye	Pt. B	RM	12
	3	F85	N. pike	Pt. A	CL	8
	4	F84	N. pike	Pt. A	CL	11
	5	F51	Walleye	Pt. B	RM	10
	6	F50	Walleye	Pt. B	RM	10
	7	F52	Walleye	Pt. B	RM	11
C	1	F91	Walleye	Pt. C	RM	9
	2	F86	Walleye	Pt. C	RM	10
	3	F87	Walleye	Pt. C	RM	8
	4	F88	Walleye	Pt. C	RM	9
	5	F89	Walleye	Pt. C	RM	10
	6	F90	Walleye	Pt. C	RM	10
C+D	1	F93	Walleye	Pt. C	RM	10
	2	F94	Walleye	Pt. C	RM	10
	3	F95	Walleye	Pt. C	RM	12
	4	F96	Walleye	Pt. C	RM	10
	5	F82	Walleye	Pt. D	RM	11
E	1	F75	Walleye	Pt. E	RM	13
	2	F76	Walleye	Pt. E	RM	17
	3	F78	Walleye	Pt. E	RM	9
	4	F77	Walleye	Pt. E	RM	9
	5	F79	Walleye	Pt. E	RM	12
	6	F80	Walleye	Pt. E	RM	19
	7	F81	Walleye	Pt. E	RM	14
F+MAP	1	F5	Walleye	See Map	RM	11
	2	F4	Walleye	See Map	RM	10
	3	F1	N. pike	See Map	CL	12
	4	F7	N. pike	See Map	CL	22
	5	F83	N. pike	Pt. F	BB	8
	6	F8	N. pike	See Map	CL	16

Table 6. Qualitatively determined cathodoluminescence ratings (on a scale from 0 to 10) of all of the Eden Lake fish. E.g., "0" indicates no luminescence was observed; "5" indicates moderate luminescence overall was observed; and "10" indicates a very strong luminescence overall was observed.

DISK NAME	DISK #	SAMPLE #	SPECIES	LOCATION	AGE (years)	CL RATING
KAP-A	1	F135	Walleye	KAP	14	0
	2	F136	Walleye	KAP	15	0
	3	F137	Walleye	KAP	15	0
	4	F138	Walleye	KAP	15	1
	5	F19	Walleye	KAP	14	0
	6	F20	Walleye	KAP	15	1
KAP-B	1	F25	White sucker	KAP	12	0
	2	F26	White sucker	KAP	18	0
	3	F27	White sucker	KAP	17	1
	4	F28	White sucker	KAP	14	0
	5	F29	White sucker	KAP	15	0
	6	F30	White sucker	KAP	19	0
	7	F18	White sucker	KAP	>15	0
KAP-C	1	F110	N. pike	KAP	13	5
	2	F111	N. pike	KAP	11	5
	3	F112	N. pike	KAP	9	5
	4	F103	N. pike	KAP	13	5
	5	F104	N. pike	KAP	8	5
	6	F106	N. pike	KAP	15	5
KAP-D	1	F161	Whitefish	KAP	15	5
	2	F171	Walleye	KAP	3	0
	3	F170	Walleye	KAP	3	0
	4	F169	Walleye	KAP	4	0
KAP-E	1	F105	Yellow perch	KAP	5	5
	2	F148	Yellow perch	KAP	7	5
	3	F149	Yellow perch	KAP	9	10
	4	F150	Yellow perch	KAP	6	6
	5	F151	Yellow perch	KAP	8	5
	6	F152	Yellow perch	KAP	5	6
KAP1-A	1	F166	Whitefish	KAP1	11	10
	2	F167	Whitefish	KAP1	18	7
	3	F168	Whitefish	KAP1	29	10
	4	F71	Walleye	KAP1	13	1
	5	F70	Walleye	KAP1	11	1
	6	F69	Walleye	KAP1	18	1

Table 6 continued.

DISK NAME	DISK #	SAMPLE #	SPECIES	LOCATION	AGE (years)	CL RATING
KAP1-B	1	F98	White sucker	KAP1	12	1
	2	F99	White sucker	KAP1	15	1
	3	F100	White sucker	KAP1	11	1
	4	F101	White sucker	KAP1	10	1
	5	F102	White sucker	KAP1	16	1
KAP1-C	1	F118	N. pike	KAP1	12	6
	2	F113	N. pike	KAP1	9	6
	3	F117	N. pike	KAP1	4	4
	4	F119	N. pike	KAP1	7	4
	5	F116	N. pike	KAP1	4	5
	6	F114	N. pike	KAP1	8	8
	7	F115	N. pike	KAP1	10	4
KAP1-D	1	F142	Cisco	KAP1	22	8
	2	F155	Cisco	KAP1	10	7
	3	F156	Cisco	KAP1	9	7
	4	F141	Cisco	KAP1	20	6
KAP1-E	1	F160	Cisco	KAP1	4	8
	2	F157	Cisco	KAP1	5	6
	3	F158	Cisco	KAP1	6	5
	4	F159	Cisco	KAP1	7	7
ED1-A	1	F45	Walleye	ED1	9	0
	2	F46	Walleye	ED1	11	0
	3	F47	Walleye	ED1	11	0
	4	F21	Burbot	ED1	10	7
ED1-B	1	F31	White sucker	ED1	17	0
	2	F6	White sucker	ED1	12	10
	3	F32	White sucker	ED1	ND	0
	4	F35	White sucker	ED1	23	0
	5	F33	White sucker	ED1	22	0
	6	F34	White sucker	ED1	24	0
ED1-C	1	F62	N. pike	ED1	19	6
	2	F109	N. pike	ED1	14	7
	3	F108	N. pike	ED1	10	7
	4	F107	N. pike	ED1	12	7
	5	F63	N. pike	ED1	18	7

Table 6 continued.

DISK NAME	DISK #	SAMPLE #	SPECIES	LOCATION	AGE (years)	CL RATING
ED2-A	1	F57	Walleye	ED2	11	1
	2	F58	Walleye	ED2	18	2
	3	F59	Walleye	ED2	12	2
	4	F60	Walleye	ED2	10	2
	5	F61	Walleye	ED2	14	1
ED2-B	1	F17	White sucker	ED2	16	0
	2	F16	White sucker	ED2	25	0
	3	F24	White sucker	ED2	20	0
	4	F23	White sucker	ED2	17	1
	5	F22	White sucker	ED2	21	1
ED2-C	1	F134	N. pike	ED2	15	10
	2	F129	N. pike	ED2	11	10
	3	F130	N. pike	ED2	8	8
	4	F132	N. pike	ED2	10	8
	5	F133	N. pike	ED2	11	10
ED2-D	1	F143	Yellow perch	ED2	8	7
	2	F144	Yellow perch	ED2	7	6
	3	F145	Yellow perch	ED2	10	8
BAK1-A	1	F66	Walleye	BAK1	23	0
	2	F67	Walleye	BAK1	19	1
	3	F68	Walleye	BAK1	18	1
	4	F121	White sucker	BAK1	10	0
	5	F122	White sucker	BAK1	17	0
	6	F127	N. pike	BAK1	9	6
	7	F128	N. pike	BAK1	11	8
BAK1-B	1	F163	Whitefish	BAK1	25	8
	2	F162	Whitefish	BAK1	24	8
	3	F120	Burbot	BAK1	9	8
BAK1-C	1	F153	Yellow perch	BAK1	8	8
	2	F154	Yellow perch	BAK1	5	5
BAK2-A	1	F48	Walleye	BAK2	17	0
	2	F49	Walleye	BAK2	17	1
	3	F123	N. pike	BAK2	11	8
	4	F124	N. pike	BAK2	13	7
	5	F125	White sucker	BAK2	21	1
	6	F126	White sucker	BAK2	16	2

Table 6 continued.

DISK NAME	DISK #	SAMPLE #	SPECIES	LOCATION	AGE (years)	CL RATING
BAK2-B	1	F164	Whitefish	BAK2	16	8
	2	F146	Yellow perch	BAK2	6	9
	3	F147	Yellow perch	BAK2	5	8
	4	F165	Whitefish	BAK2	17	5
N-A	1	F12	Walleye	Narrows	16	0
	2	F10	Walleye	Narrows	12	0
	3	F9	Walleye	Narrows	9	0
	4	F37	Walleye	Narrows	11	1
	5	F36	Walleye	Narrows	17	1
N-B	1	F3	Walleye	Narrows	12	2
	2	F39	Walleye	Narrows	10	1
	3	F38	Walleye	Narrows	12	1
	4	F40	Walleye	Narrows	11	0
	5	F41	Walleye	Narrows	18	0
N-C	1	F140	Walleye	Narrows	16	1
	2	F13	White sucker	Narrows	19	0
	3	F43	Walleye	Narrows	12	1
	4	F44	Walleye	Narrows	11	1
	5	F139	Walleye	Narrows	22	0
N-D	1	F15	N. pike	Narrows	12	7
	2	F14	N. pike	Narrows	10	6
	3	F11	N. pike	Narrows	13	6
	4	F65	N. pike	Narrows	6	7
	5	F64	N. pike	Narrows	10	8
	6	F2	N. pike	Narrows	13	8
C+A+J	1	F74	N. pike	Jackson L.	12	4
	2	F73	N. pike	Jackson L.	10	6
	3	F72	N. pike	Jackson L.	13	5
	4	F42	N. pike	Campsite	7	9
	5	F55	N. pike	Adam Lake	10	10
	6	F56	N. pike	Adam Lake	8	10

Table 6 continued.

DISK NAME	DISK #	SAMPLE #	SPECIES	LOCATION	AGE (years)	CL RATING
A+B	1	F54	Walleye	Pt. B	14	2
	2	F53	Walleye	Pt. B	12	1
	3	F85	N. pike	Pt. A	8	9
	4	F84	N. pike	Pt. A	11	10
	5	F51	Walleye	Pt. B	10	0
	6	F50	Walleye	Pt. B	10	1
	7	F52	Walleye	Pt. B	11	1
C	1	F91	Walleye	Pt. C	9	0
	2	F86	Walleye	Pt. C	10	1
	3	F87	Walleye	Pt. C	8	1
	4	F88	Walleye	Pt. C	9	2
	5	F89	Walleye	Pt. C	10	1
	6	F90	Walleye	Pt. C	10	1
C+D	1	F93	Walleye	Pt. C	10	0
	2	F94	Walleye	Pt. C	10	0
	3	F95	Walleye	Pt. C	12	1
	4	F96	Walleye	Pt. C	10	1
	5	F82	Walleye	Pt. D	11	1
E	1	F75	Walleye	Pt. E	13	0
	2	F76	Walleye	Pt. E	17	0
	3	F78	Walleye	Pt. E	9	0
	4	F77	Walleye	Pt. E	9	0
	5	F79	Walleye	Pt. E	12	0
	6	F80	Walleye	Pt. E	19	0
	7	F81	Walleye	Pt. E	14	8
F+MAP	1	F5	Walleye	See Map	11	0
	2	F4	Walleye	See Map	10	0
	3	F1	N. pike	See Map	12	6
	4	F7	N. pike	See Map	22	7
	5	F83	N. pike	Pt. F	8	8
	6	F8	N. pike	See Map	16	8

Appendix B: Fish and Clam Descriptions and Illustrations

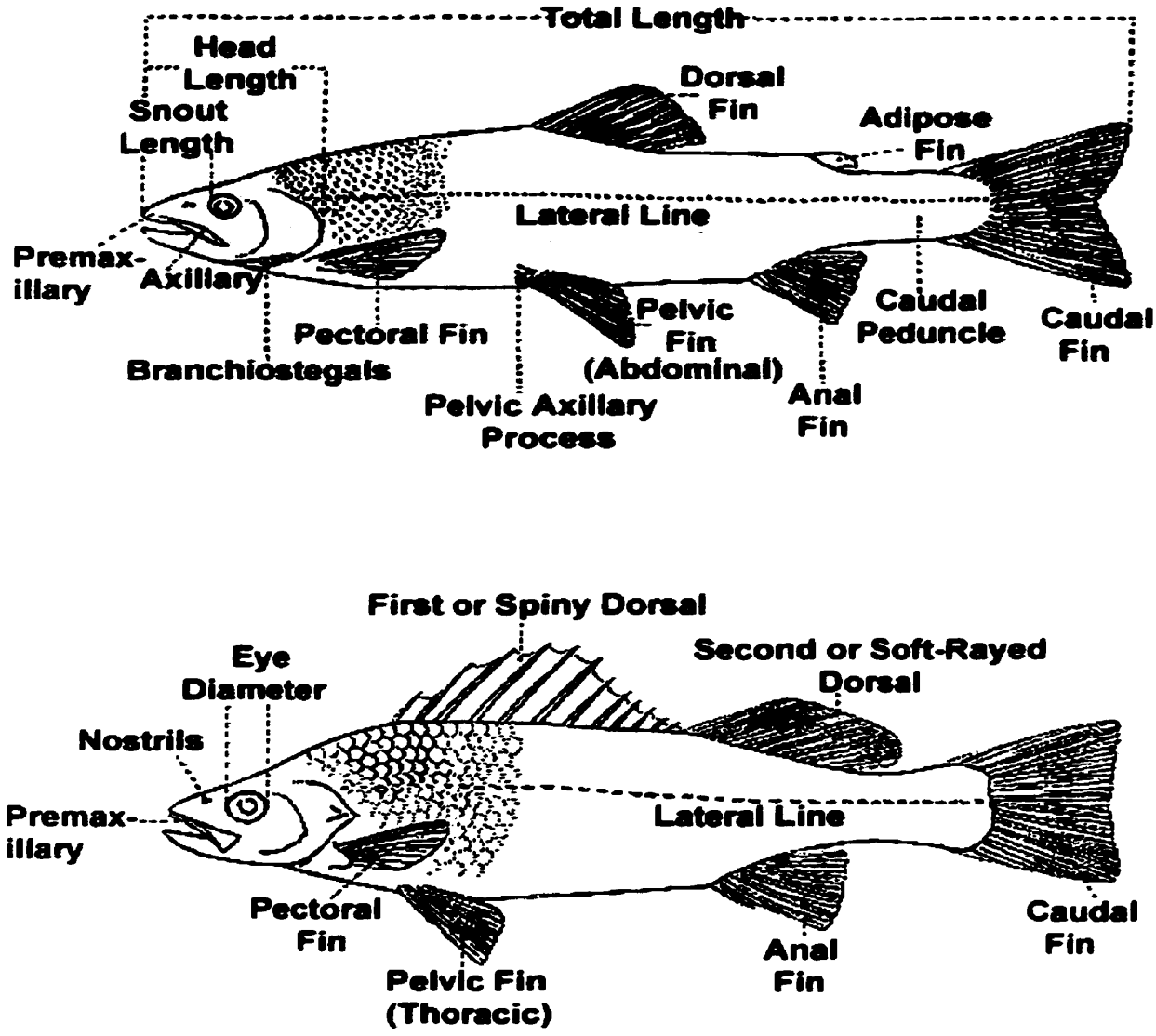

Figure 1. General anatomical features of two fish illustrating different possibilities of dorsal fins and different locations of the pelvic fin to aid with the following descriptions (after Scott andCrossman, 1973).

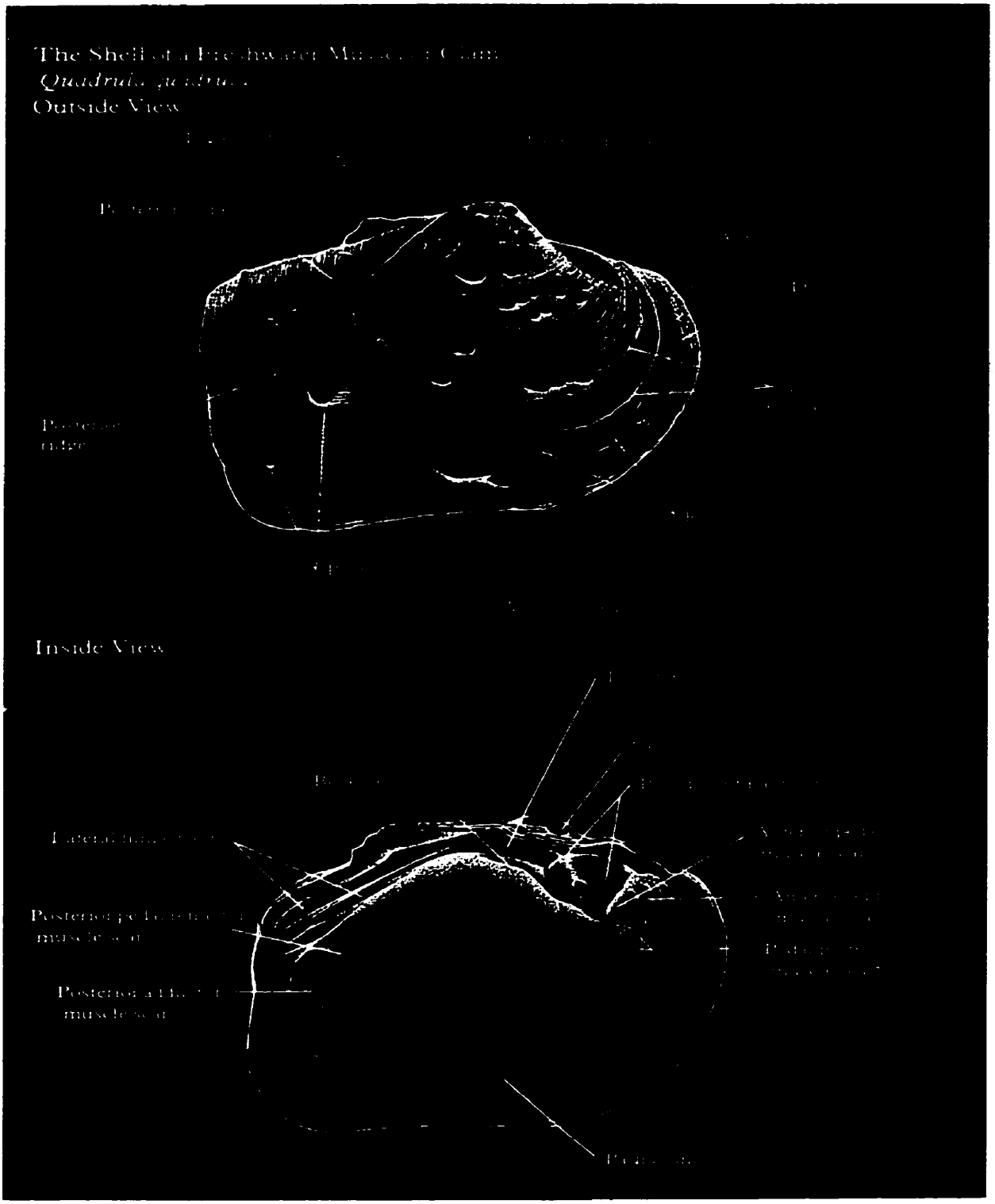

Figure 2. **General anatomical features of a freshwater clam to aid with the following descriptions (after Clarke, 1981).**

FISH DESCRIPTIONS

Walleye (Stizostedion vitreum)

The variability of meristics and proportions within walleye populations is possibly as great as that between populations. In general, the adult walleye from Eden Lake have an elongate body, ranging in length from 333 to 592 millimetres with the length of the head ranging from 23.8 to 28.4% of the total length (Figure 3a). The gill membranes extend forward and are not broadly joined. The preopercle bone is strongly serrate with the serrae curving forward. The eyes are large, having a diameter approximately 16.1 to 26.7% of the head length, and silvery; hence the genus name *vitreum* which means glassy. Eden Lake walleye have a long snout, bluntly pointed, and a large, almost horizontal mouth. Walleye characteristically have 8 fins in total: 2 dorsal, 1 caudal, 1 anal, 2 pelvic (thoracic), and 2 pectoral. The two dorsal fins are obviously separated. The first dorsal fin is spiny (12 to 16 strong spines), high, long, and rounded. The second dorsal fin is square to slightly emarginate and as high or higher than the first, with 1 fine spine and 18 to 22 rays. The caudal fin is not very broad but long and well forked with well rounded tips. The anal fin has 2 spines and 11 to 14 rays and its base is shorter than its height. This fin is square, like the second dorsal fin, but not as long. The pelvic (thoracic) fins are the same length as the pectoral fins, have 1 spine and 5 rays, and the tips are rounded. the pectoral fins are only moderately broad, have 13 to 16 rays, and also have rounded tips. Walleye have strongly ctenoid scales.

Walleye coloring is highly variable with habitat and to a lesser extent with size (Scott and Crossman, 1973). The walleye found in turbid water, such as that of Eden Lake, are paler and less marked with obvious black pattern than those found in clear water. Their background color ranges from olive-brown to yellow with darker patches on the dorsal surface of the head and back. Some young Eden Lake walleye, (102-356 millimetres) in contrast to the adults, exhibit dark vertical bands across their back and

down their sides.

Northern pike (Esox lucinius)

Northern pike characteristically have a very long body that is laterally compressed and only moderately deep (11.0 to 16.7% of its total length; Figure 3b). Eden Lake individuals that were caught during sample collection ranged in length from 253 to 812 millimetres. They have a long head, 25.2 to 30.4% of their total length, which is flat and very broad on top. They have large, bright yellow eyes (diameter 10.7 to 20.6% of their head length) located high and at the center of the head and a very long snout (42.5 to 46.8% of their head length) that is moderately broad and rounded on top. The mouth of a northern pike is large and horizontal, with the maxillary usually reaching at least to midpupil. Their teeth are short, very sharp, and recurved, which are located along the premaxillary and in patches along the tongue. The lower jaw often extends well beyond the snout and 10 pores (5 on each side) usually pierce the underside of the lower jaw. Northern pike characteristically have 7 fins: 1 dorsal, 1 caudal, 1 anal, 2 pelvic (abdominal), and 2 pectoral. The dorsal fin is soft rayed (15 to 19 principal rays) and far back on the body. This fin has a rounded upper edge and the base is shorter than the height, about equal to the snout length. The caudal fin is long and moderately forked. The anal fin has 12 to 15 principal rays and is located slightly behind that of the dorsal fin. This fin's base length is less than its height and less than that of the dorsal fin. The pelvic (abdominal) fins are low, long, and paddle-like with 10 or 11 rays. The pectoral fins are also low, arising under the edge of the opercular flap. These fins are rounded and also paddle-like with 14 to 17 rays. Northern pike have moderately small cycloid scales.

The basic color arrangement of the northern pike is a pattern of light spots on a dark ground coat (Scott and Crossman, 1973). The dorsal surface, upper sides, and the

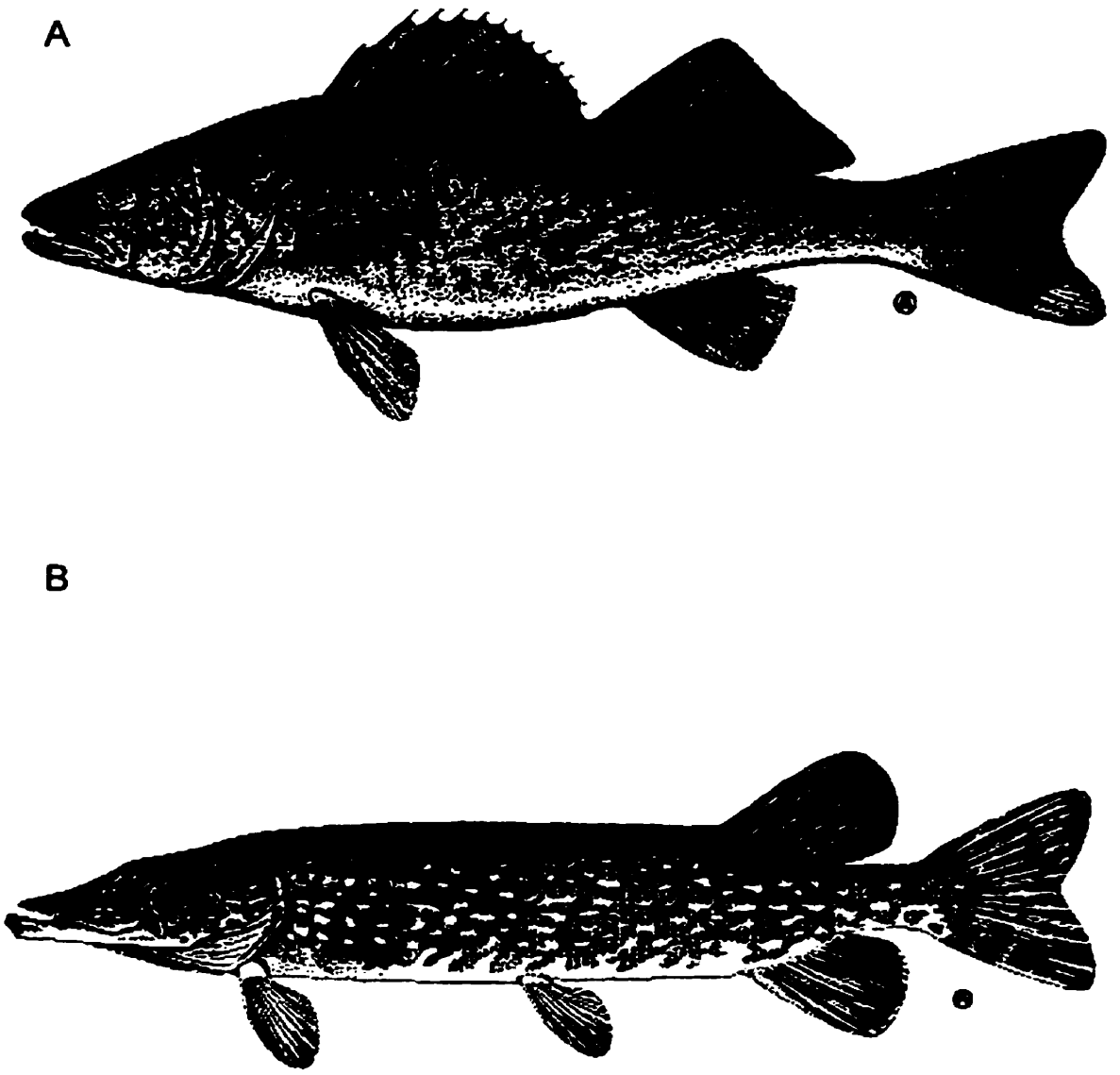

Figure 3. (A) Illustration of a walleye and (B) Illustration of a northern pike (after Scott and Crossman, 1973).

top and upper parts of the head range in color from brilliant green to almost brown. The ground color of the flanks is lighter, and in pike over 381 millimetres long, conspicuously marked with 7 to 9 irregular longitudinal rows of yellow to whitish, bean-shaped spots, some as long as the eye diameter. The body has the appearance of being flecked with gold, resulting from a tiny gold spot on the tip of the exposed edge of most scales. The ventral surface of the body and head is cream to white in color with fingers projecting up into the ground coat of the flanks. These fingers are all that remain of the characteristic juvenile pattern of this species. Due to the striped, rather than spotted, nature of juvenile northern pike, they are often misidentified.

White suckers (Catostomus commersoni)

Adult Eden Lake white suckers are robust, cylindrical, torpedo-shaped fish, ranging in length between 378-501 millimetres (Figure 4a). They are oval to round in cross-section and slightly compressed laterally, with their greatest depth at the origin of their dorsal fin (14.1 to 20.0% of their total length). The head of a white sucker is moderately long (about 20% of the total length), bluntly pointed, rounded on top, and moderately wide. They have small eyes, 41.3 to 66.6% of the snout length, which are located high but at the center of the head length. White suckers also have a rounded snout and a ventrally located mouth that is toothless, suctorial and relatively small. White suckers characteristically have 7 fins: 1 dorsal, 1 caudal, 1 anal, 2 pelvic (abdominal), and 2 pectoral. The dorsal fin is soft-rayed (10 to 13 principal rays) and located almost at the midpoint of the total length. This fin is slightly emarginate and has a short base, 10.7 to 15% of the total length. The caudal fin is deeply forked, its tips are roundly pointed, and it usually has 18 rays. The anal fin is long with a height at least two times the base, is more or less pointed, and has 6 to 8 large principal rays. The pelvic (abdominal) fins are low, located under the middle of the dorsal fin, and are short and

square, with a moderately broad base. These fins have 10 or 11 rays. The pectoral fins are also low and long (almost equal to the head length). These fins are pointed and have 16 to 18 prominent rays. White suckers have moderately small scales, larger on peduncle than near operculum.

In adults, the back, top of the head, upper sides, and sides of the head to below the eyes are gray through to almost black (Scott and Crossman, 1973). The lower sides and ventral surface of the head and body are cream to white. Young white suckers, 51 to 152 mm long, usually have 3 prominent black spots on their sides. The lower body of spawning white suckers turns a more golden color while the dark patches on the upper body and head become more intense.

Longnose suckers (Catostomus catostomus)

Longnose suckers characteristically have an elongate, cylindrical, torpedo-shaped body that is almost round in cross-section, but not deep (the maximum is only 14.2 to 18.3% of the total length; Figure 4b). They generally range from 305 to 356 millimetres in length, though the Eden Lake individual was 518 millimetres long. Their head is moderately long, about 20% of their total length, moderately broad, and rounded on top. Their snout is long, about 38.4 to 48.2% of their head length and is bulbous, ending in a rounded point. Their eyes, located high and beyond the midpoint of the head, have a diameter that is 38.4 to 66.6% of the snout length. The mouth of a longnose sucker is protrusible, suctorial, toothless, and rather small. It is located ventrally, well behind the tip of the snout. Their lips are very large with coarse, long, oval papillae. Longnose suckers characteristically have 7 fins: 1 dorsal, 1 caudal, 1 anal, 2 pelvic (abdominal), and 2 pectoral. The dorsal fin is soft-rayed (9 to 11 principal rays) and originates slightly ahead of the midpoint of the body. Its height is slightly greater than the base and its edges are somewhat emarginate. The caudal fin is only

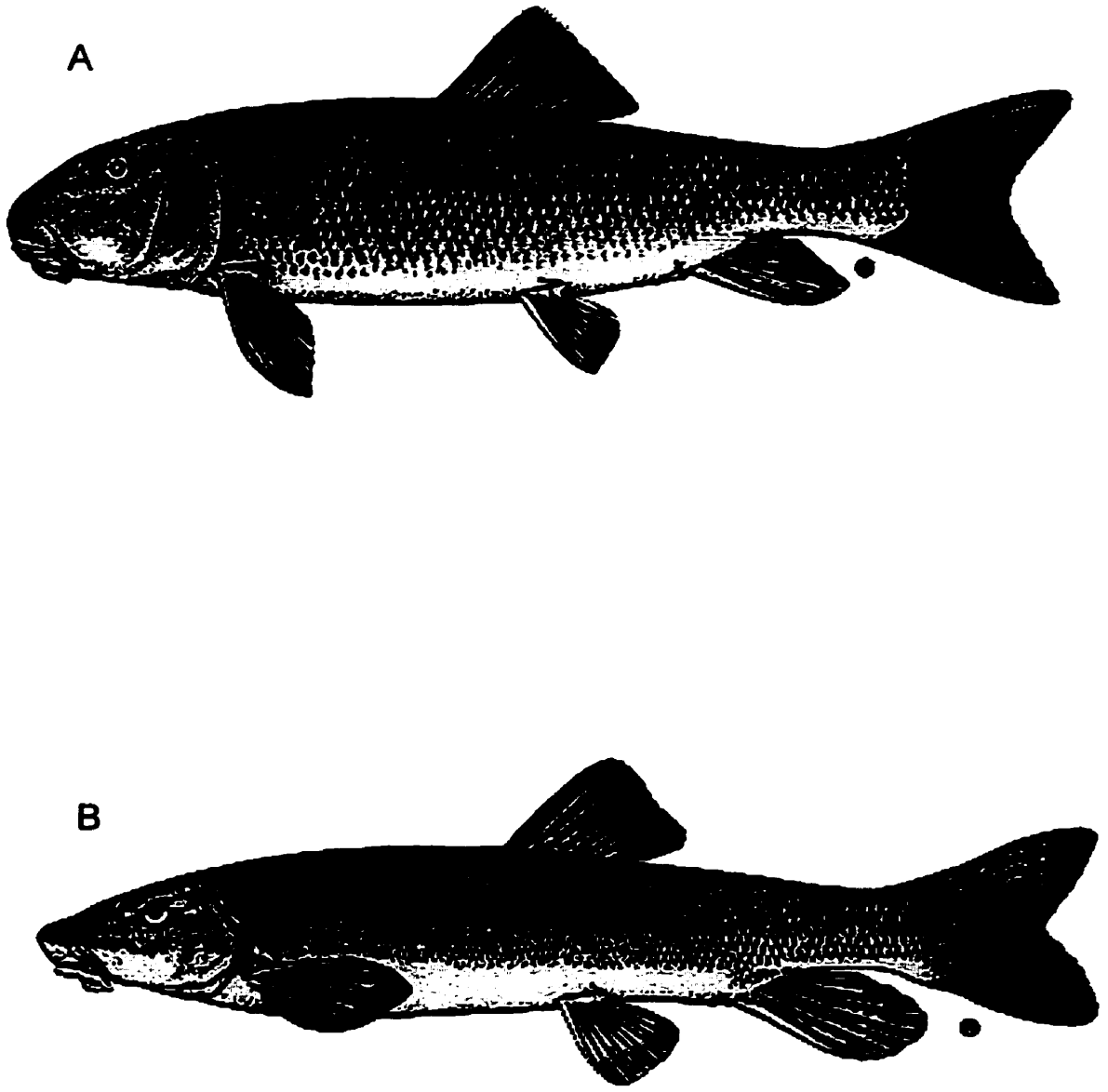

Figure 4. (A) Illustration of a white sucker and (B) Illustration of a longnose sucker (after Scott and Crossman, 1973).

moderately long, moderately forked, with rounded tips. The anal fin is long, its height about 2.5 times the length of the base and it has 7 principal rays. The pelvic (abdominal) fins are only moderate in length and their base is fairly wide. These fins are square to rounded and have 9 to 11 principal rays. The pectoral fins are low, horizontal, and somewhat stiff. They have 16 to 18 principal rays and their tips are broadly pointed. The scales on the longnose sucker are small, cycloid, and crowded towards the head.

The coloring of adult longnose suckers is generally dark, with strong countershading (Scott and Crossman, 1973). Their back, upper sides, and head to below the eyes are gray to almost black while the lower sides and ventral surface of the head and body are cream to white. The males for the most part are darker in color than the females. At the time of spawning, both the males and females have a broad, horizontal, midlateral band of vivid pink to dark red that continues on to the snout. This band is also darker and more vivid on the males than the females. The young are very dark in color and somewhat mottled on the back.

Lake whitefish (Coregonus clupeaformis)

Eden Lake adult whitefish have an elongate body, ranging in length from 373 to 484 millimetres (Figure 5a). The smaller lake whitefish are usually slender, however, the large ones are somewhat ovate in lateral view. Body depth varies greatly but is generally greatest in females and increases with increasing weight. The head of a lake whitefish is short, only 20-23% of their total length. Their eyes are small, with a diameter 19.5 to 25% of the head length, and they have a snout (27 to 35% of the head length) that projects beyond their inferior and weak-toothed mouth. Lake whitefish characteristically have 8 fins: 1 dorsal, 1 dorsal adiopse, 1 caudal, 1 anal, 2 pelvic (abdominal), and 2 pectoral. The dorsal fin is roughly triangular, has 11 to 13 prominent rays, and is located near the midpoint of the total length. The dorsal adiopse fin is small

and located near the caudal fin, across and slightly back from the anal fin. The caudal fin is distinctly forked with pointed tips.

The anal fin is slightly triangular and has 10 to 14 rays. The pelvic (abdominal) fins usually have 11 rays and a pelvic axillary process located at the front of each fin. The pectoral fins are long and paddle-like and have 14 to 17 rays. The scales on the lake whitefish are large and cycloid.

The overall coloration of lake whitefish is silvery (Scott and Crossman, 1973). At Eden Lake, the lake whitefish exhibit darkened scale margins that result in an overall crosshatch pattern overlaying the silvery background. The fins are often dark colored or black-tipped.

Cisco (Coregonus artedii)

Eden Lake Ciscoes have an elongate body, ranging in length from 147 to 353 millimetres (Figure 5b). The body is compressed laterally and its greatest body depth (in front of dorsal fin) is variable, usually 20 to 30% of its total length. The head length of a cisco is about 20 to 24% of the total length. The eye diameter is 21 to 26% of the head length while the snout is even longer. Ciscoes have a terminal mouth and the lower jaw often projects slightly beyond the upper jaw. Ciscoes characteristically have 8 fins: 1 dorsal, 1 dorsal adipose, 1 caudal, 1 anal, 2 pelvic (abdominal), and 2 pectoral. The dorsal fin is moderately long, with the front height being much larger than the back, and has 10 to 15 rays. The dorsal adipose is small and located near the back of the fish, by the caudal fin, which is distinctly forked. The anal fin has 11 to 15 rays and is a similar shape to the dorsal fin but considerably smaller. The pelvic (abdominal) fins are moderately long, have a pelvic axillary process, and 11 or 12 rays each. The pectoral fins are long, paddle-like, and have 14 to 18 rays each. the scales on a cisco are large and cycloid.

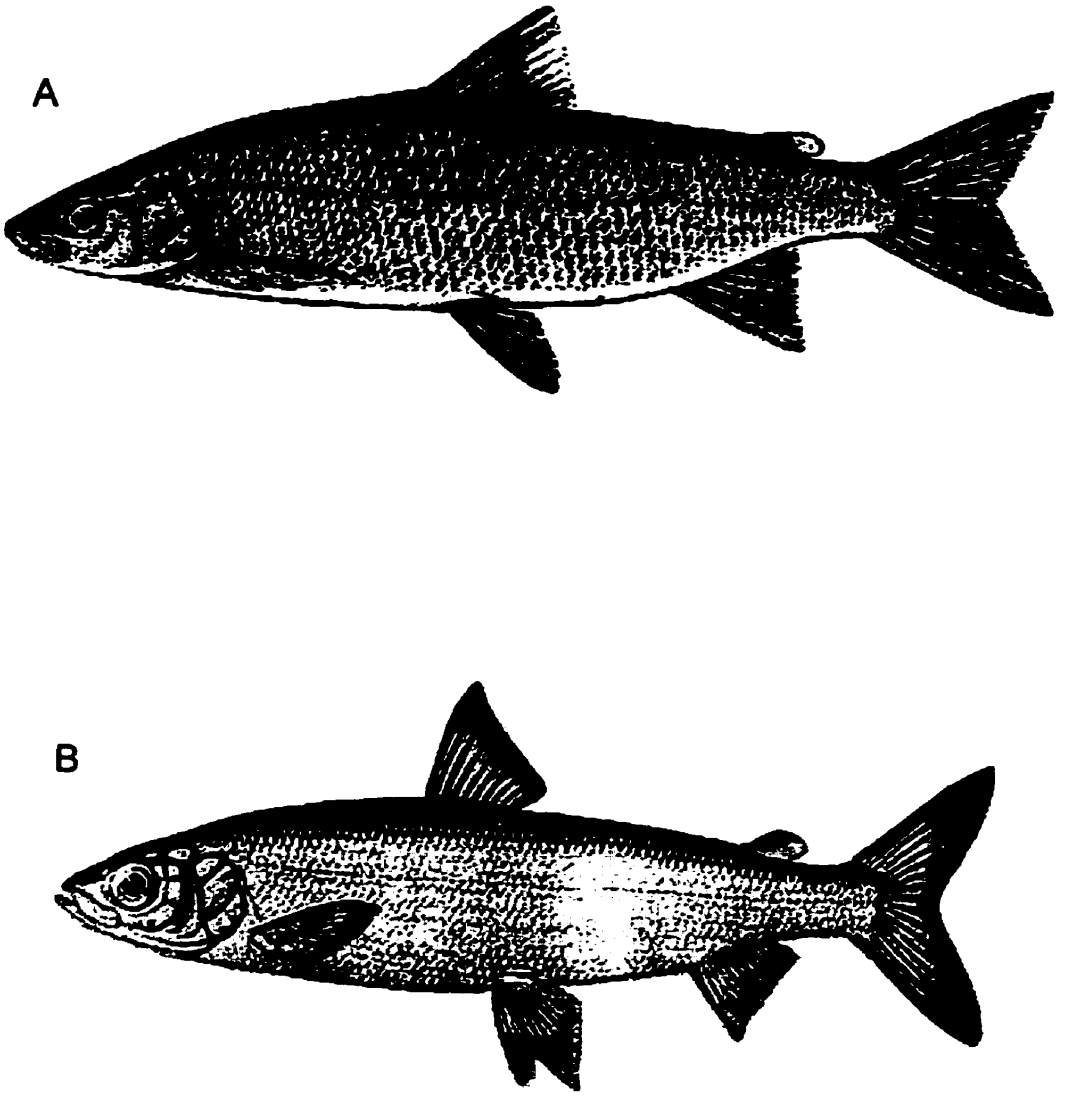

Figure 5. (A) Illustration of a lake whitefish and (B) Illustration of a cisco (after Scott and Crossman, 1973).

The overall coloration is silvery with pink to purple iridescence (Scott and Crossman, 1973). The color of the cisco's back varies greatly from lake to lake (or population to population in large lakes), from almost black to nearly any shade of blue-green to gray or light tan. The sides and ventral side of the cisco are silvery and white, respectively. All of the fins are more or less transparent but pelvic and anal fins can be milky to opaque in adults and usually lightly speckled with black pigment. The dorsal and caudal fins in adults are also sometimes black-tipped.

Burbot (Lota lota0

Burbot have an elongate and robust body with an average length of about 381 millimetres (Figure 6a). They have a nearly round cross section from anterior to anus and the body width to body depth ratio is about 1:1. Burbot have a broad, depressed, triangular head that totals about 19.2 to 19.9% of its length. They have a relatively large mouth; small eyes, with a diameter that is 11.2 to 16.4% of the head length; and a projecting snout, approximately 27.5 to 32.5% of head length. Burbot also have a long chin barbel and smaller barbel-like extensions from each nostril (each about a 1/4 the length of the chin barbel). Burbot have 8 fins: 2 dorsal, 1 caudal, 1 anal, 2 pelvic (thoracic), and 2 pectoral. The first dorsal fin is low and short, with 8 to 16 rays. The second dorsal fin is low, with a long base that extends onto the caudal peduncle and is joined to the caudal fin. This dorsal fin has 60 to 79 rays. The height of the first and second dorsal fins is about 25% of the head length.

The caudal fin is very rounded. It is joined to the second dorsal and anal fins, but separated by a deep notch. The anal fin is long and low, like the second dorsal fin, and has 59 to 76 rays. The pelvic (thoracic) fins are jugular, inserted in advance to the pectoral fins, and have 5 to 8 rays (the 2nd ray is prolonged). The pectoral fins are short, rounded, and paddle-like, with 17 to 21 rays. The scales on the burbot are cycloid,

small, and embedded.

Their color ranges from yellow to light brown, becoming darker northward (Scott and Crossman, 1973). This background color is overlaid by a lace-like pattern of dark brown or black. The two burbot caught in Eden Lake were adults and very dark in color.

Yellow perch (Perca flavescens)

Eden Lake yellow perch have an elongate body that is oval, rather than subcylindrical, and laterally compressed (greatest body depth 16.3 to 28.1% of the total length; Figure 6b). They range in length, on average, from 102 to 254 millimetres. Their head constitutes 23.1 to 29.3% of their total length and is moderately deep and rounded at the tip. The yellow-green eyes of the yellow perch have a diameter that is 15.8 to 30.4% of the head length (greatest in the young), while their snout is 23.4 to 34.2% of the head length and is moderately long and blunt. The upper jaw does not extend past the lower jaw and the mouth is moderately large, terminal, and slightly oblique. The teeth of the yellow perch are in brush-like bands on the jaws, palatines, and vomer. They are small and decrease in size posteriorly. Yellow perch have 8 fins: 2 dorsal, 1 caudal, 1 anal, 2 pelvis (thoracic), and 2 pectoral. The two dorsal fins are obviously separated. The first is spiny (13 to 15 strong spines), high, and rounded, while the second is smaller, but about the same height, with 1 or 2 spines and 12 to 15 rays. The caudal fin is long, narrow, and shallowly forked, with rounded tips. The anal fin has 2 spines and 6 to 8 rays. This fin is square to rounded and about half the size of the second dorsal. The pelvic (thoracic) fins have a space between them that is less than half of the base of one fin. These fins are moderate in length (a little longer than the pectoral fins), square, and have 1 spine and 5 rays each. The pectoral fins are broad, rounded, and have 13 to 15 rays. Yellow perch have small ctenoid scales.

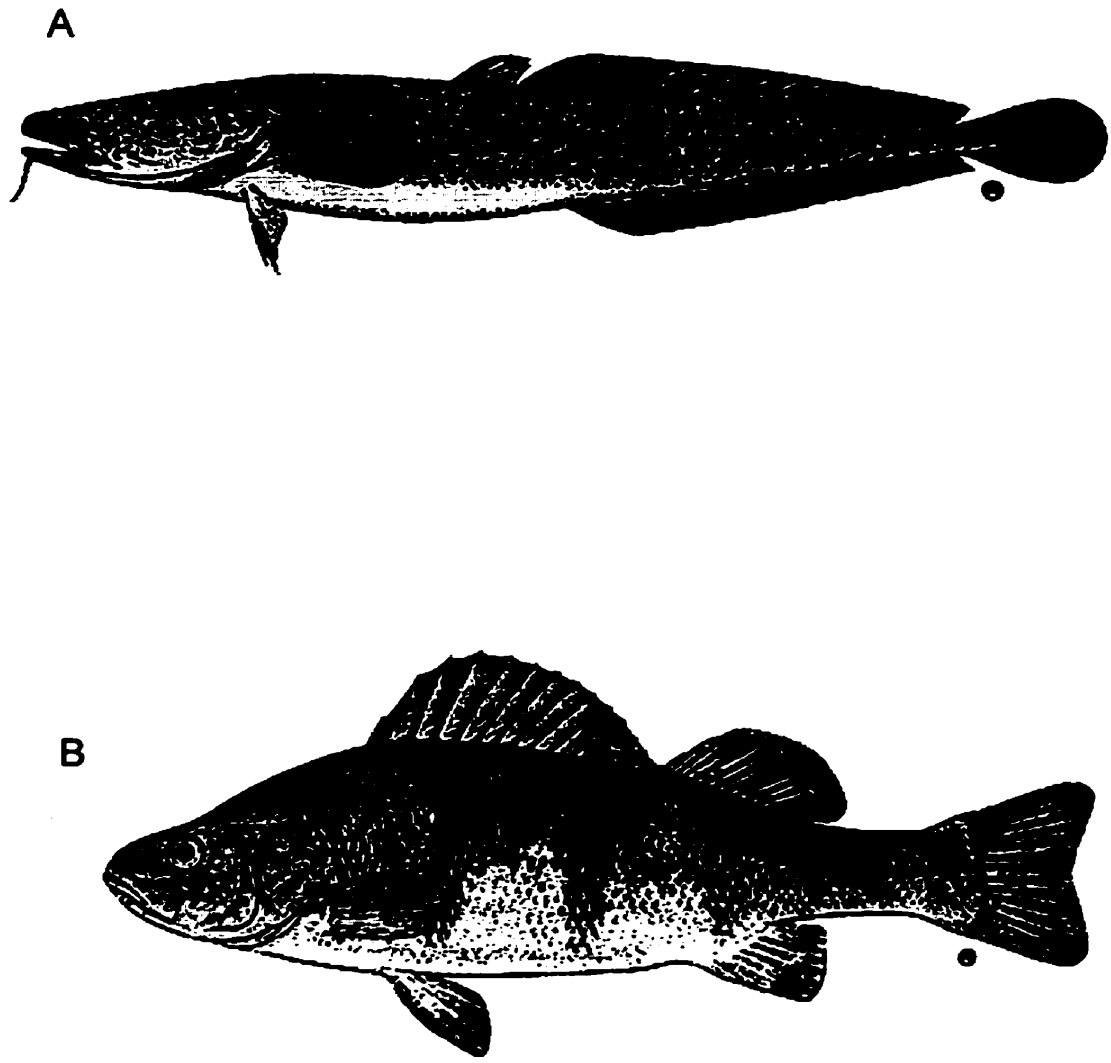

Figure 6. (A) Illustration of a burbot and (B) Illustration of a yellow perch (after Scott and Crossman, 1973).

In general, the color of yellow perch is variable with size and habitat (Scott and Crossman, 1973). The Eden Lake yellow perch are olive-green to golden brown on the dorsal surface of the back and head while their sides, to below the pectoral fins, are yellow-green. The color on their back extends down their sides in about 7 tapering bars. The ventral side of a yellow perch is milky-white to cream, their dorsal and caudal fins are yellow, and their pectoral fins are amber and translucent. The tips of all their fins are often black. The coloration of spawning males is often more intense than that of the females and the lower fins of a spawning male turn orange to bright red.

CLAM DESCRIPTIONS

Pyganodon grandis (northern floater)

P. grandis shells can be up to about 125 millimetres long, 55 millimetres high, and 45 millimetres wide (Figure 7a). The shell wall is thin and fragile, only 2 millimetres thick at mid-anterior. The shape of the shell is commonly elliptical, as was observed in all the specimens collected, and is roundly pointed posteriorly. The surface of each valve is roughened by fine concentric wrinkles and prominent growth rests. The periostracum on the Eden Lake specimens was brown, with concentric darker and paler bands, and the nacre was silvery-white. Northern floaters characteristically have beaks which are located closer to the anterior than posterior, and that are low, but clearly project above the hinge line. The beak sculpture is composed of 4 to 6 single-looped or faintly double-looped curved bars that are not nodulous. Hinge teeth are absent in this species.

Lampsilis radiata siliquoidea (fat mucket)

L. radiata siliquoidea shells can be up to 140 millimetres long, 70 millimetres

high, and 45 millimetres wide, though most are much smaller (Figure 7b). The anterior ventral shell wall can be extremely thick, up to 12 millimetres, near the palial line. They have an heavy, strong, elliptical shell that is posteriorly expanded at the ventral margin only in females. The sexual dimorphism of the Eden Lake specimens was easily distinguishable (cf. Table 4.1). The surface of this species' shell is also roughened by concentric wrinkles and growth lines. The periostracum on the Eden Lake specimens was yellow-brown and most specimens were covered by extensive, sharply defined, narrow rays. The nacre on the Eden Lake specimens was iridescent at the posterior and white at the anterior. Fat muckets characteristically have low beaks that project only slightly above the hinge line and their beak cavities are shallow. The beak sculpture is coarse, consisting of numerous bars that have a shallow central sinuation or are centrally broken. Hinge teeth are well developed and fairly strong. There are two pseudocardinal teeth in each valve and these are medium-sized, erect, serrated, compressed, and directed forward. There is one lateral tooth in the right valve and two lateral teeth in the left and these are narrow, prominent, and straight to slightly curved.

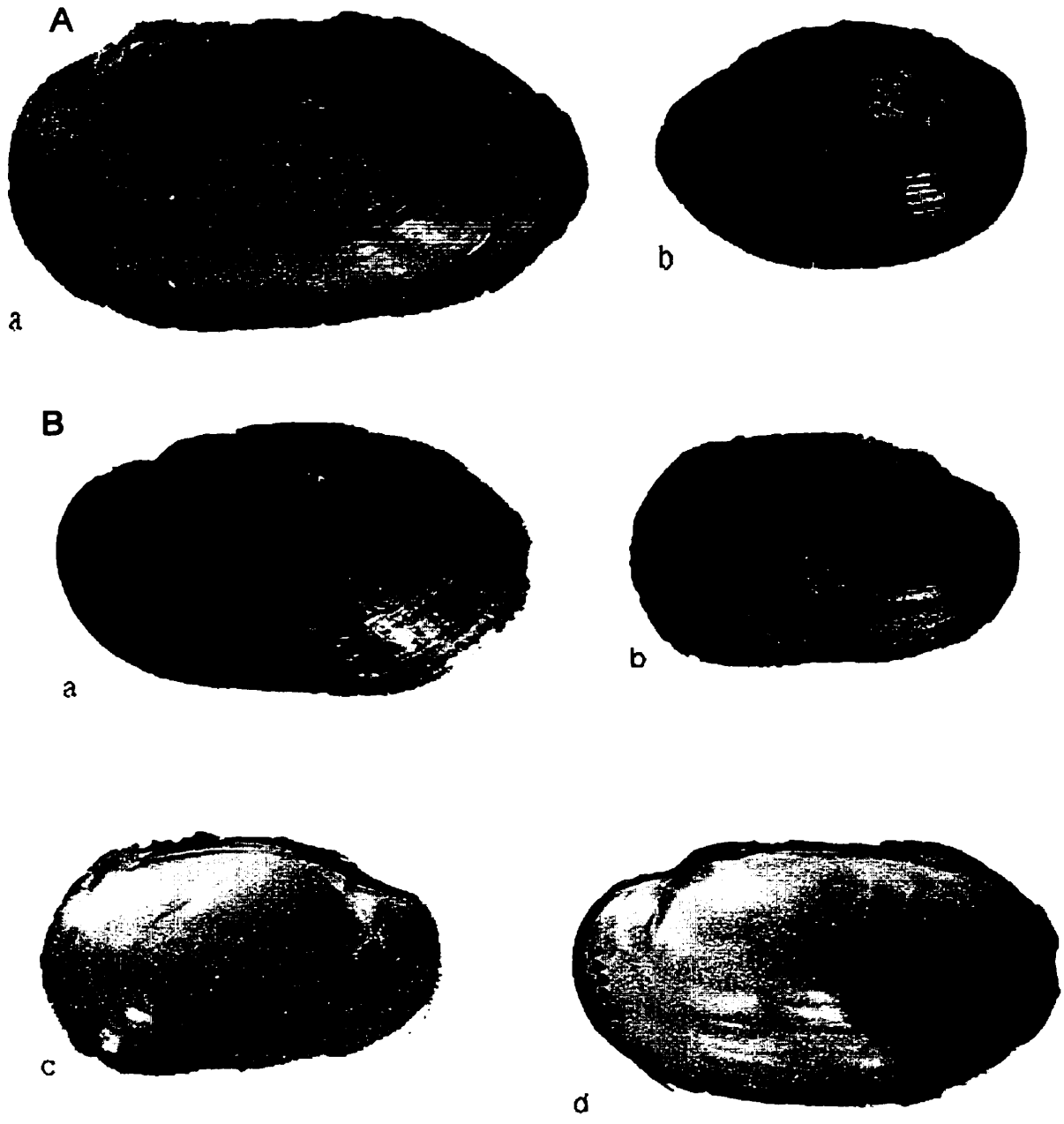

Figure 7. (A) Illustrations of *Pyganodon grandis.* (A) is a specimen from Lake St. Joseph near Rat Rapids, Ontario and (B) is from Lake Cache near Chibougamau, Quebec and (B) Illustrations of *Lampsilis radiata siliquoidea.* (A) and (D) are specimens from the Assiniboine River, Manitoba and (B) and (C) are from the mouth of Hay River, Northwest Territories (after Clarke, 1981).

Appendix C: PIXE Line-scan Data

ED2-D #3 YELLOW PERCH

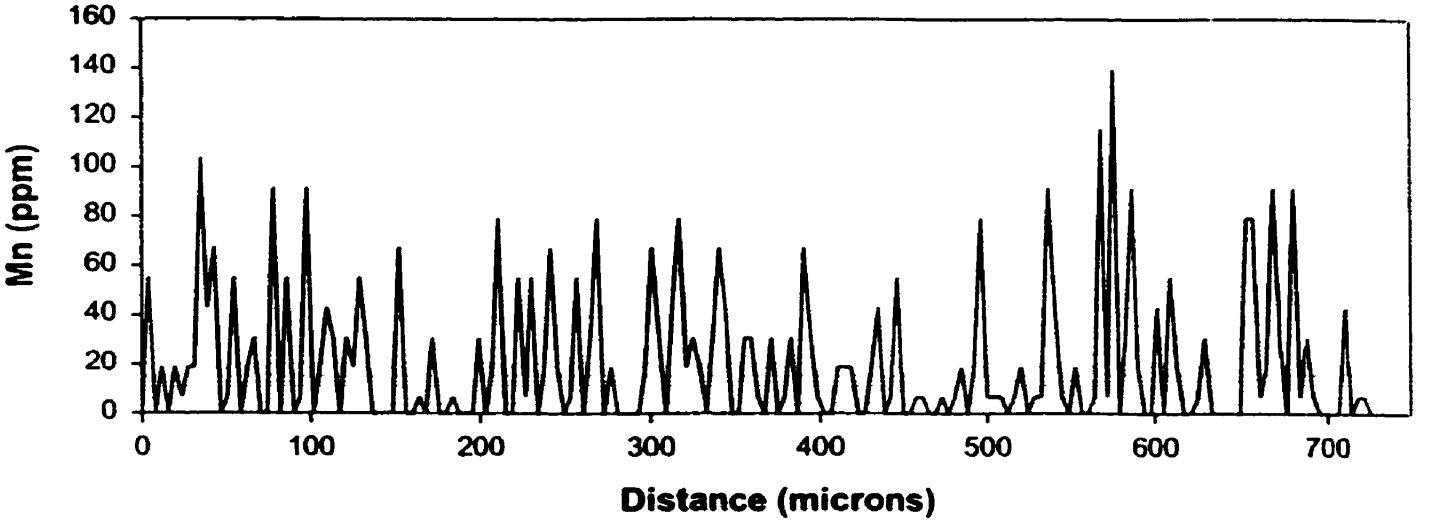

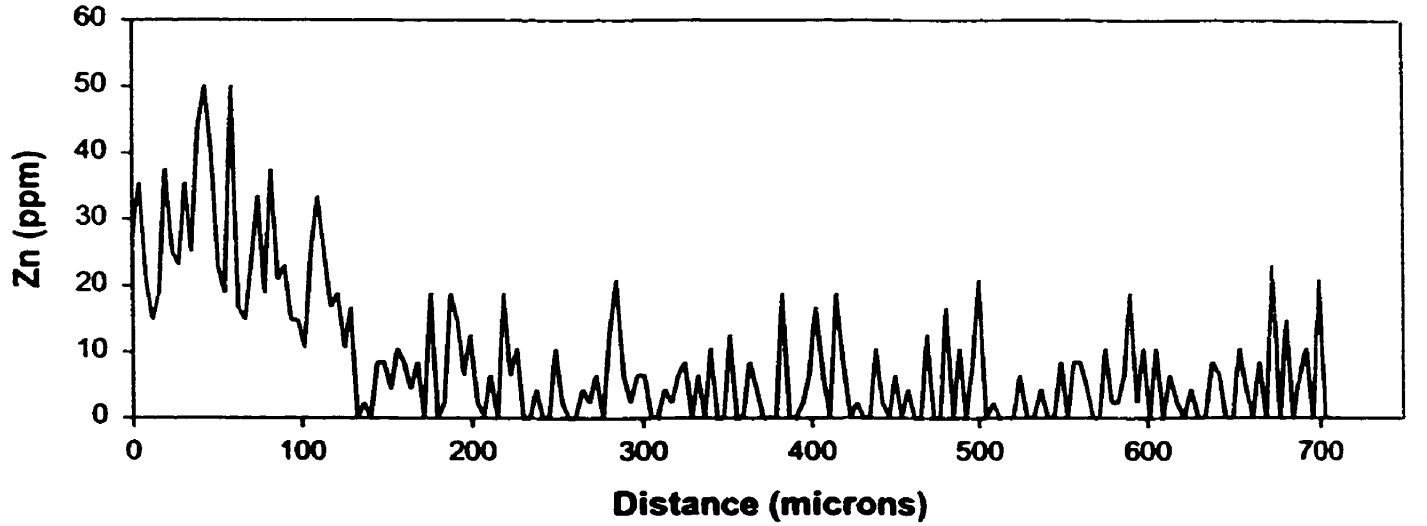

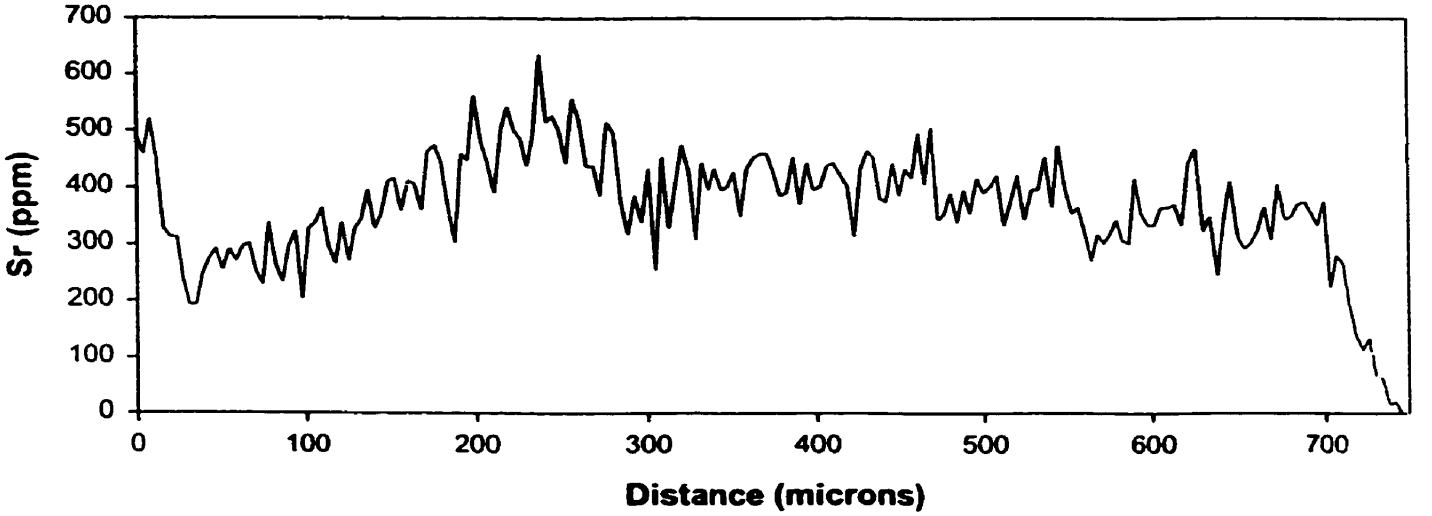

BAK1-A #7 NORTHERN PIKE

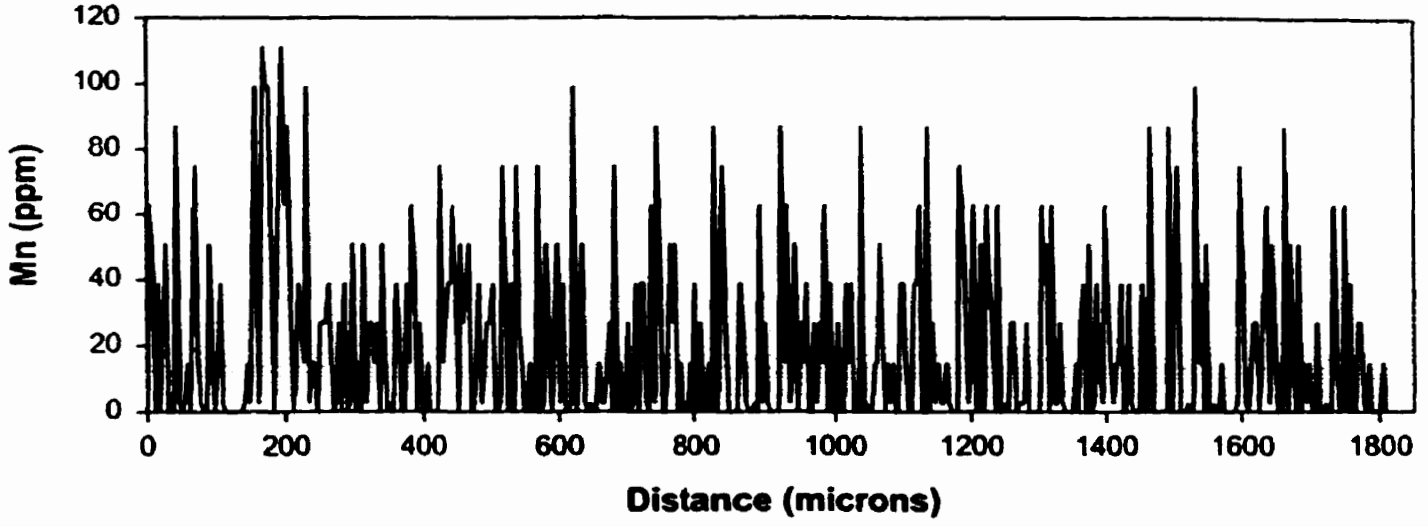

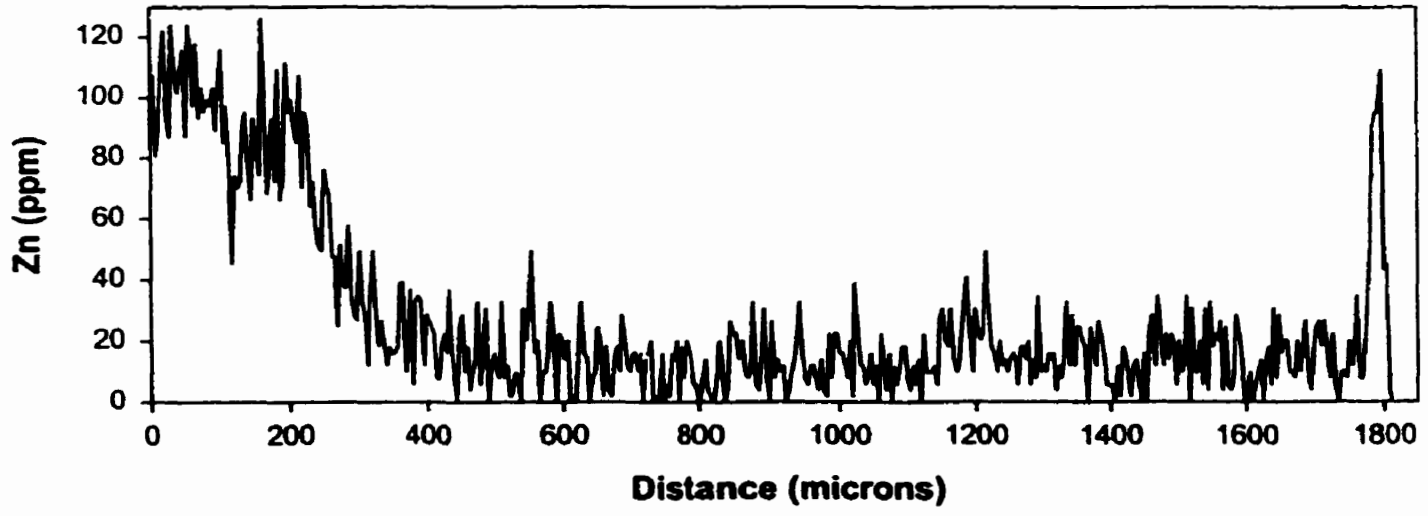

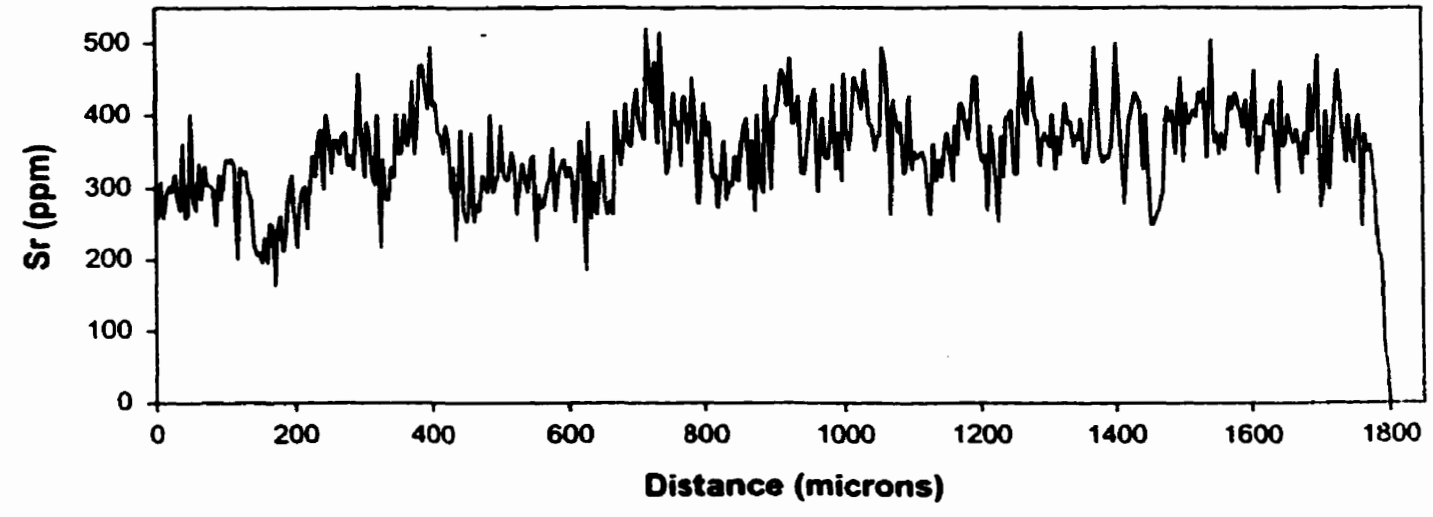

BAK1-B #3 BURBOT

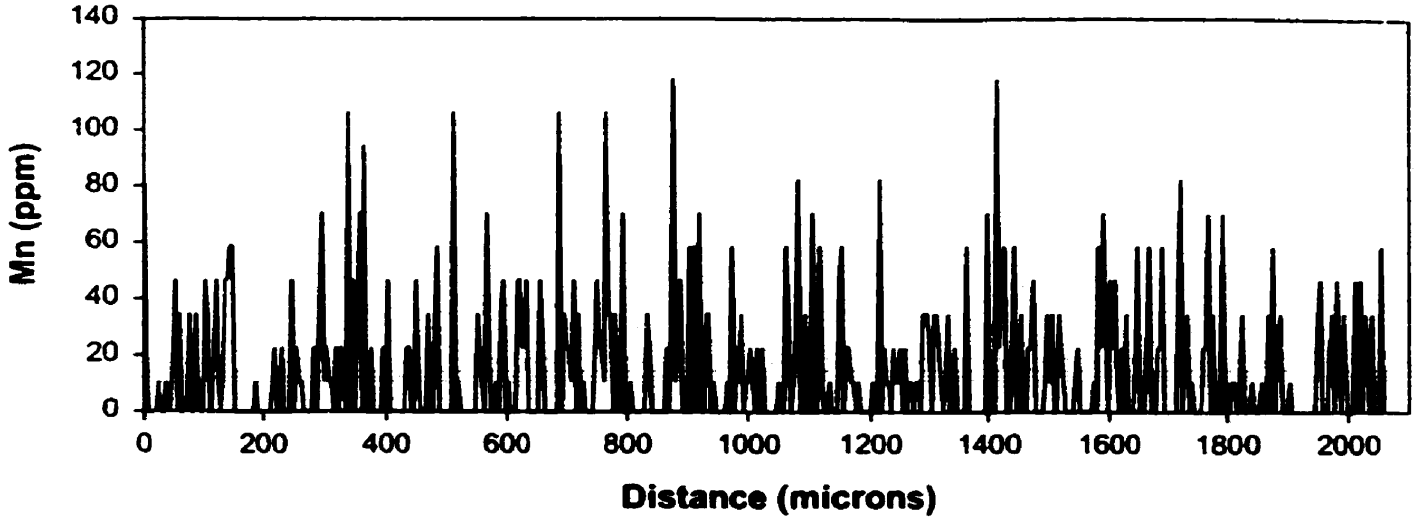

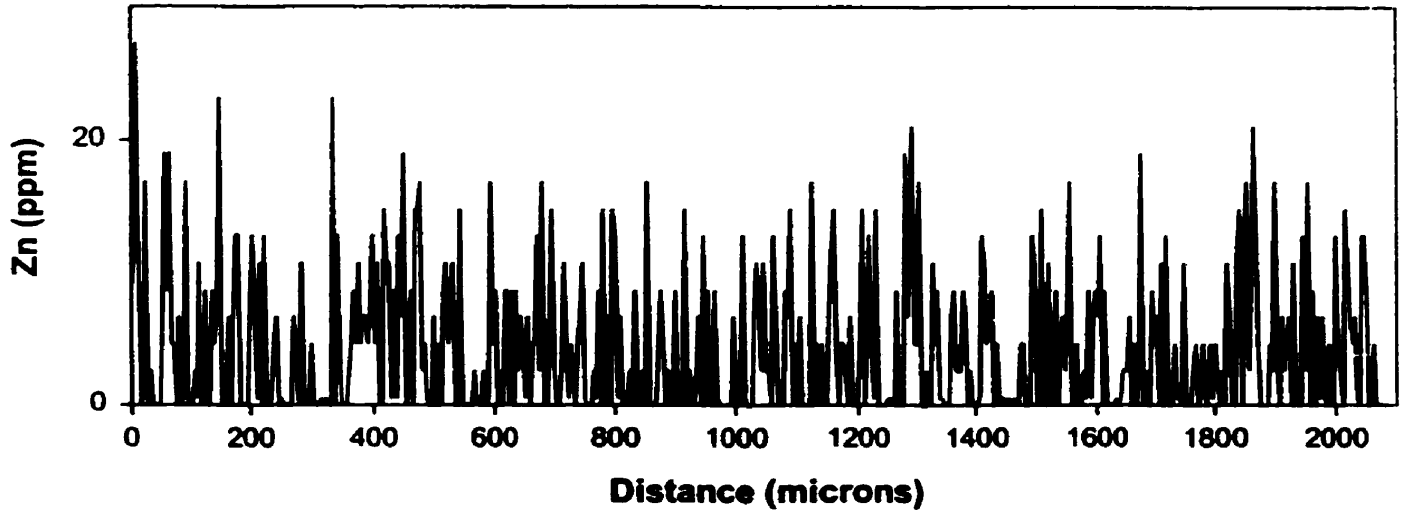

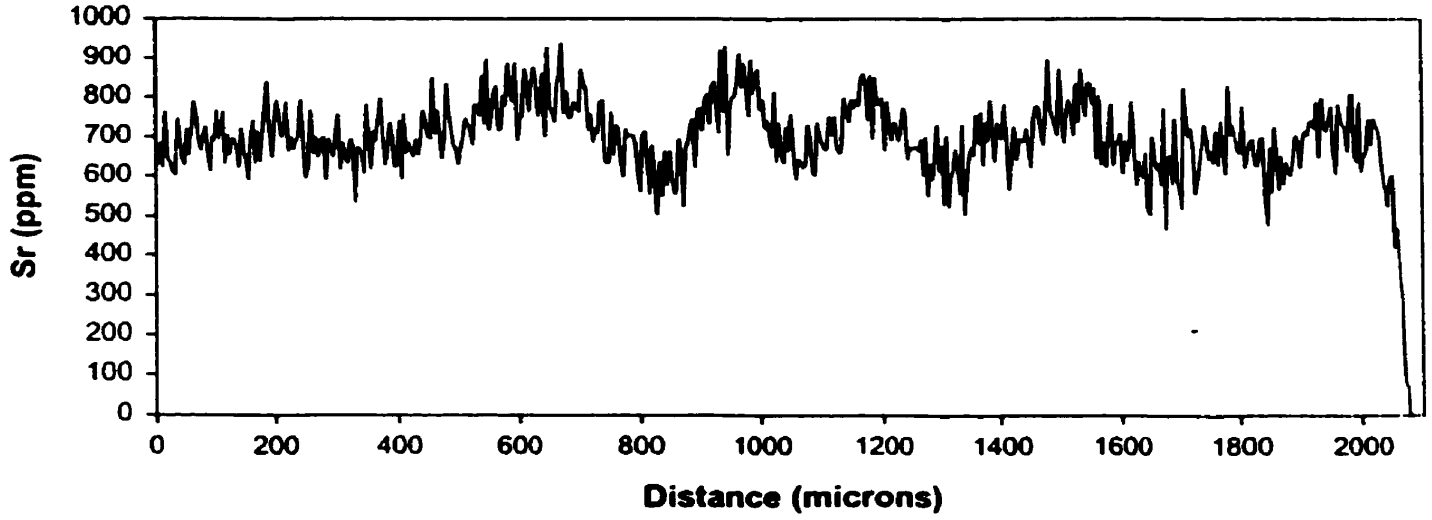

BAK1-C #1 YELLOW PERCH

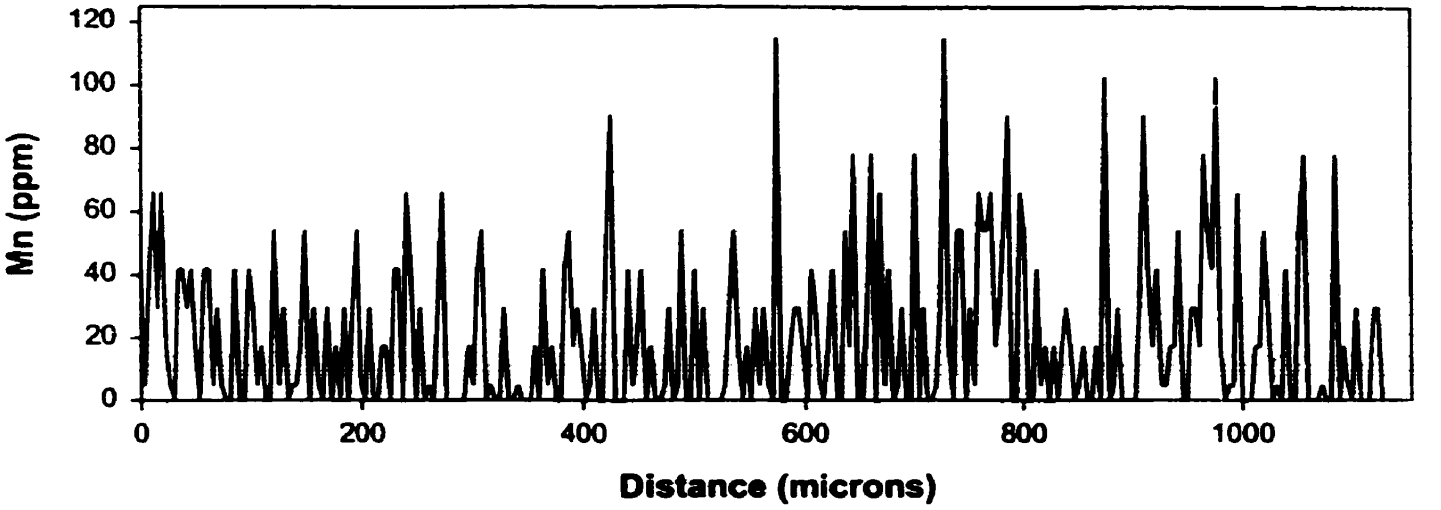

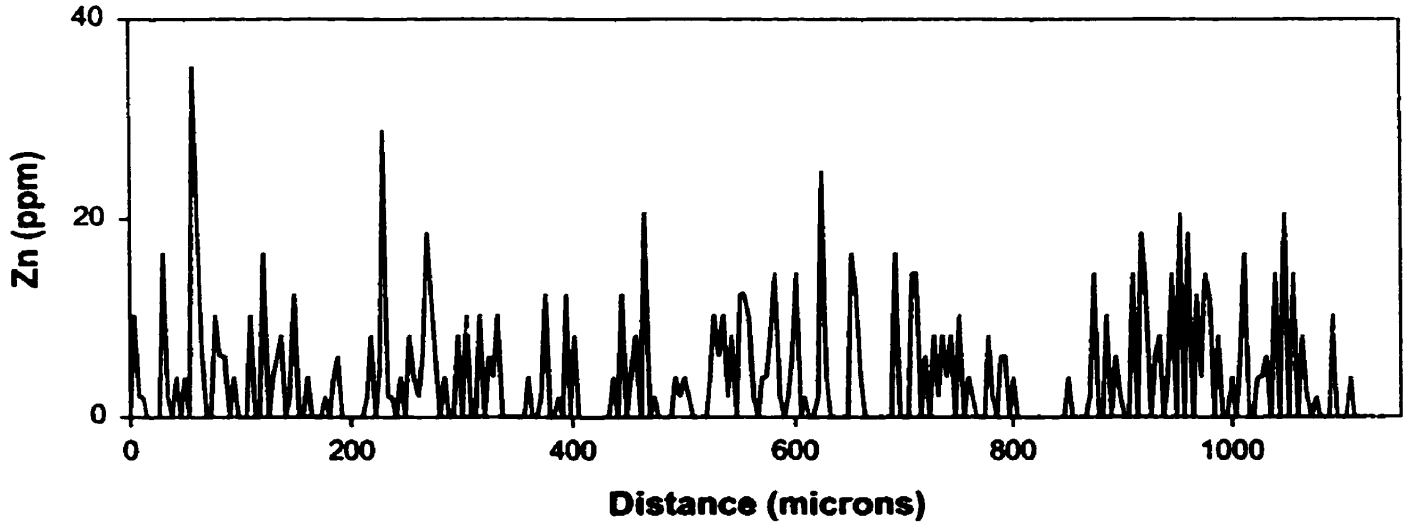

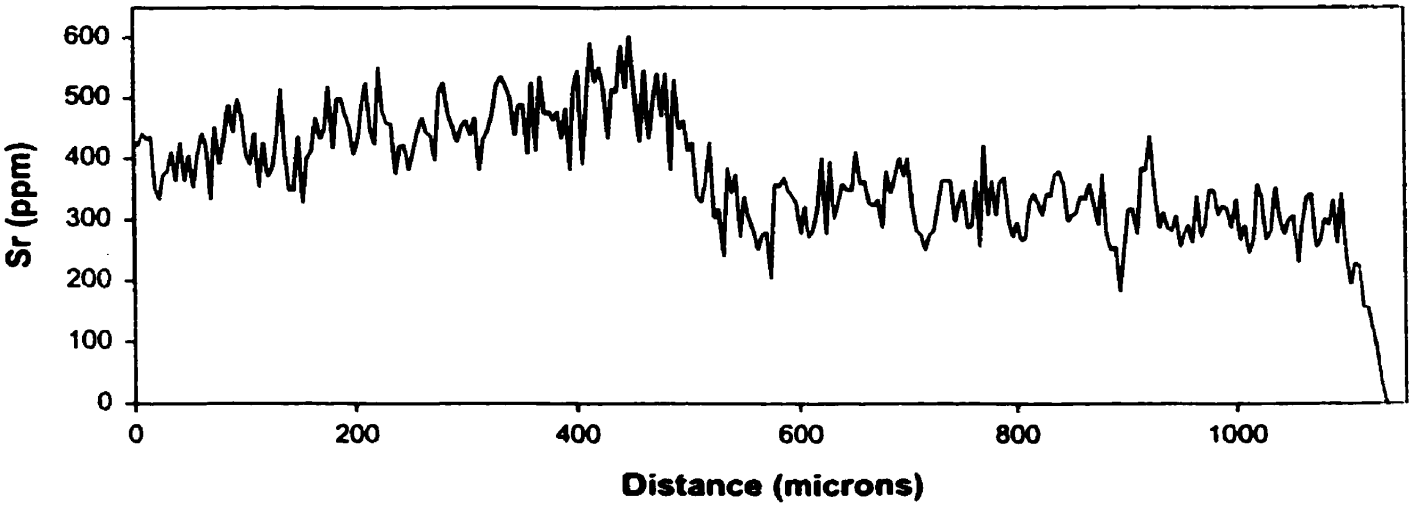

BAK2-A #3 NORTHERN PIKE

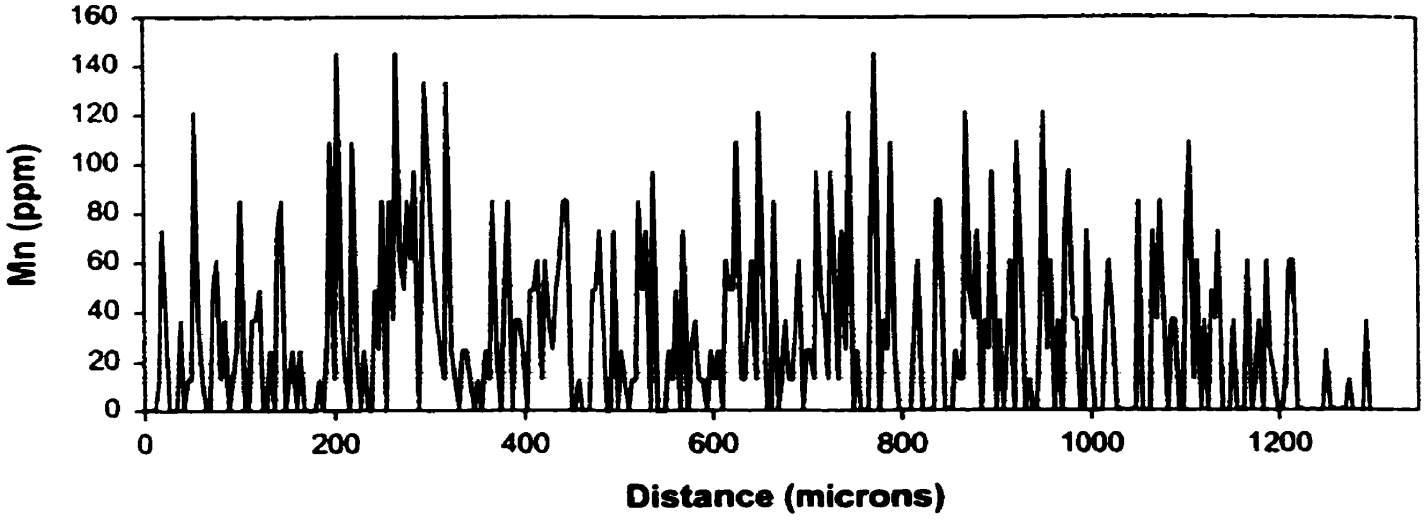

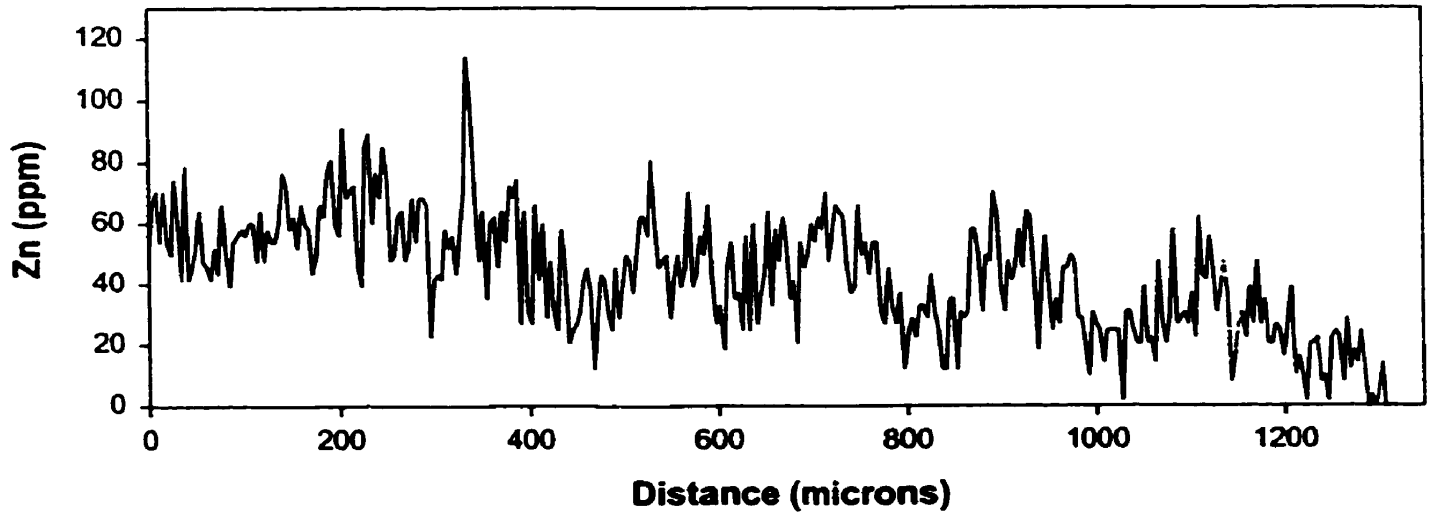

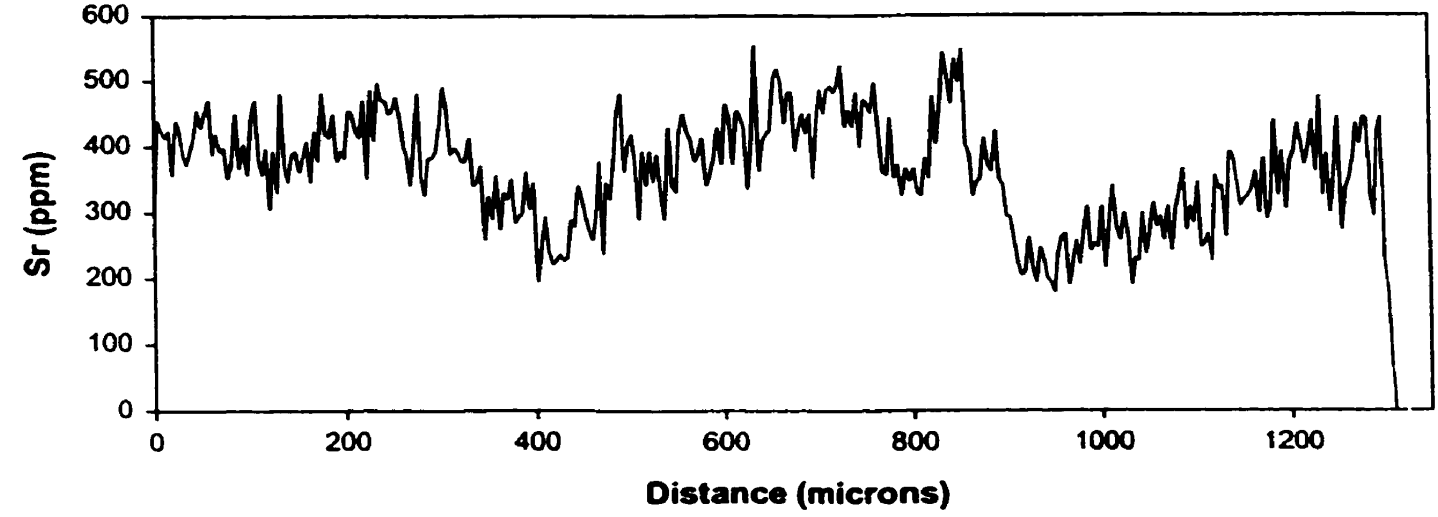

BAK2-B #1 LAKE WHITEFISH

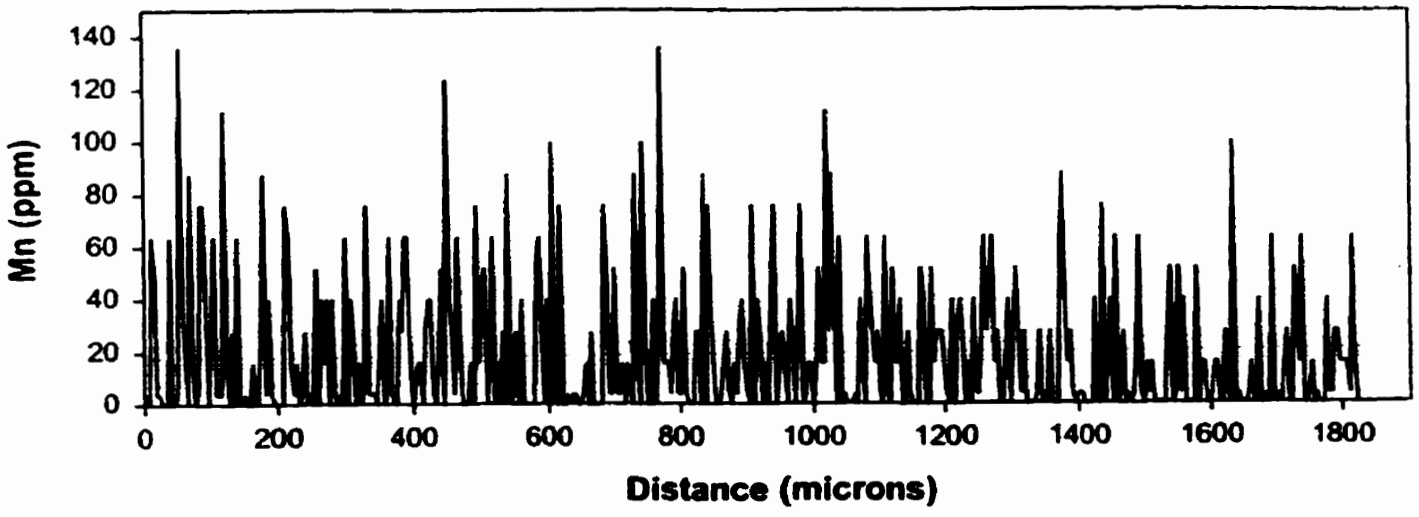

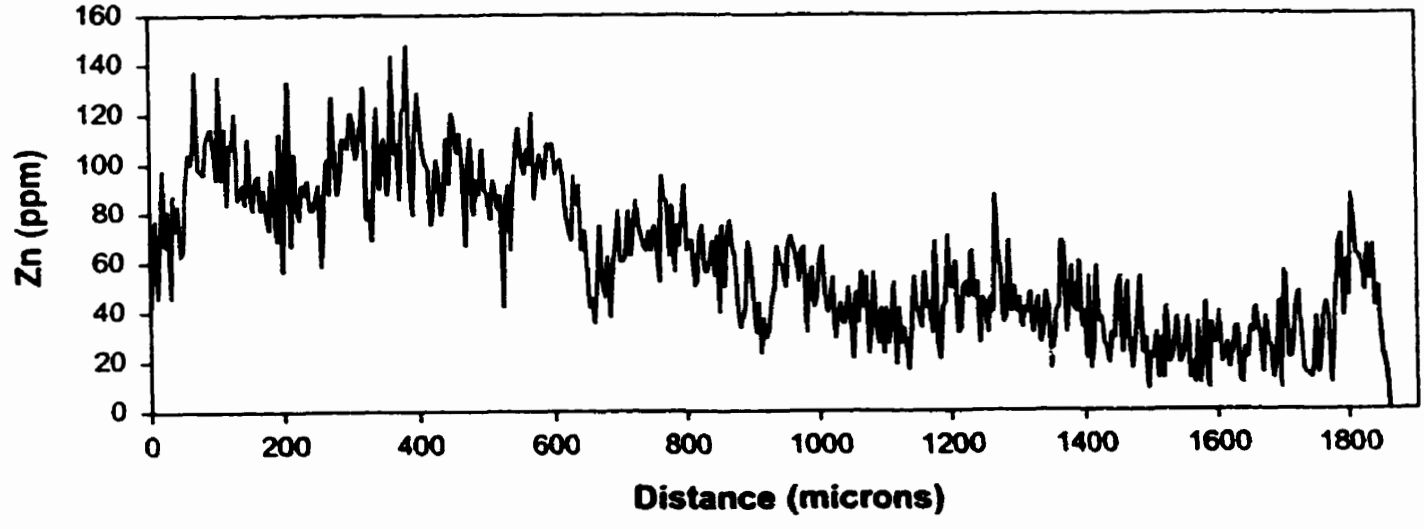

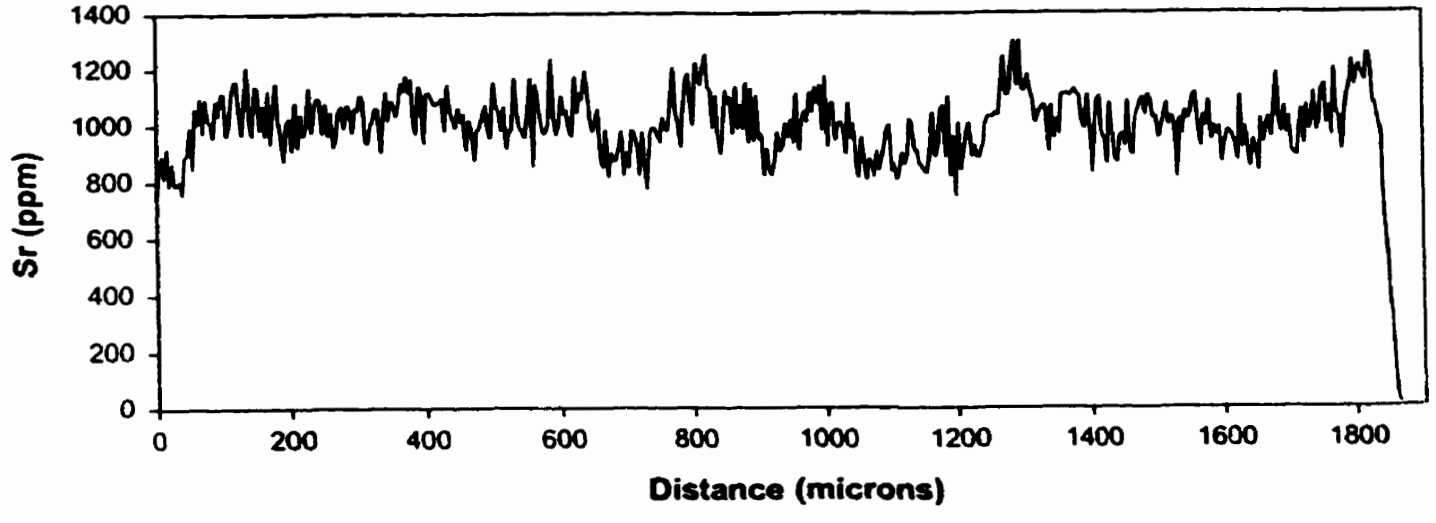

BAK2-B #4 LAKE WHITEFISH

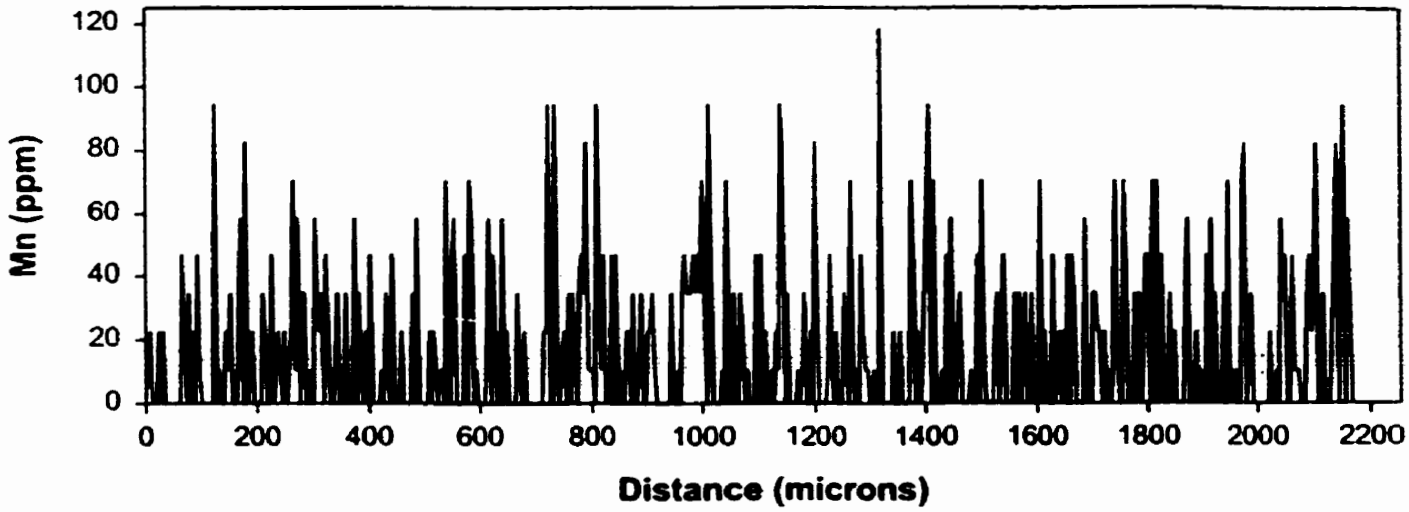

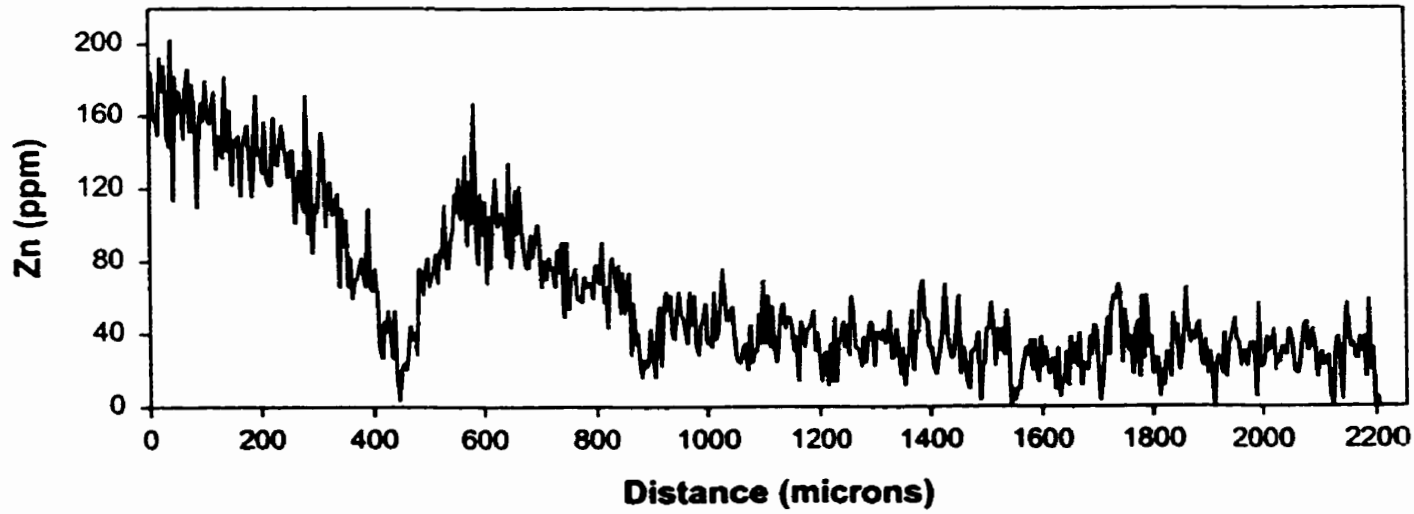

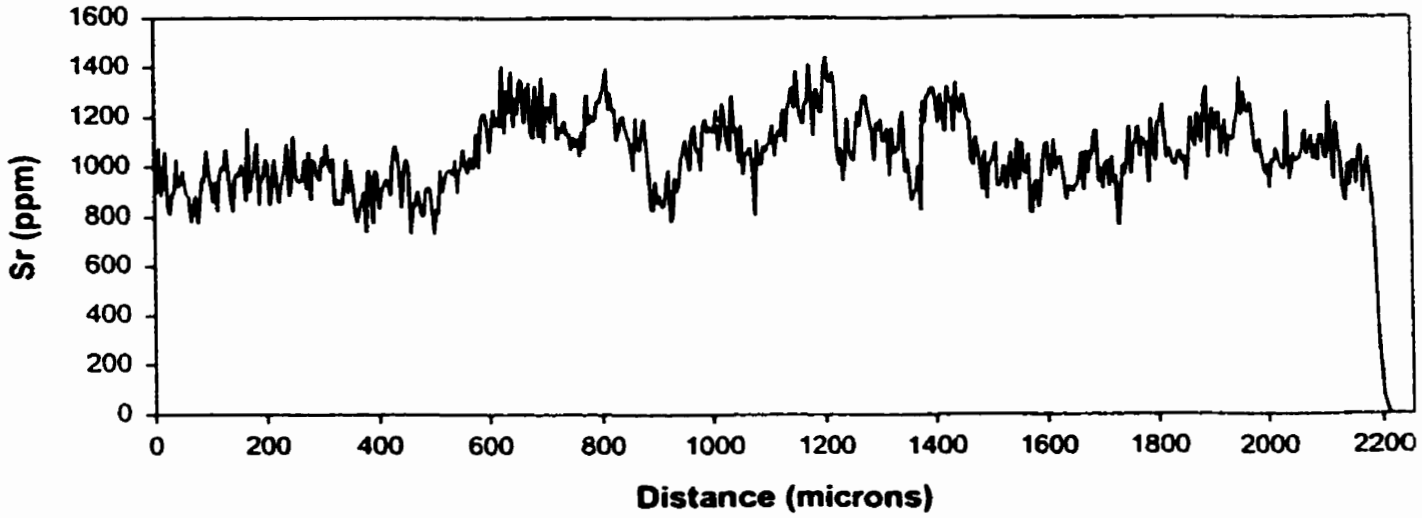

C #4 WALLEYE

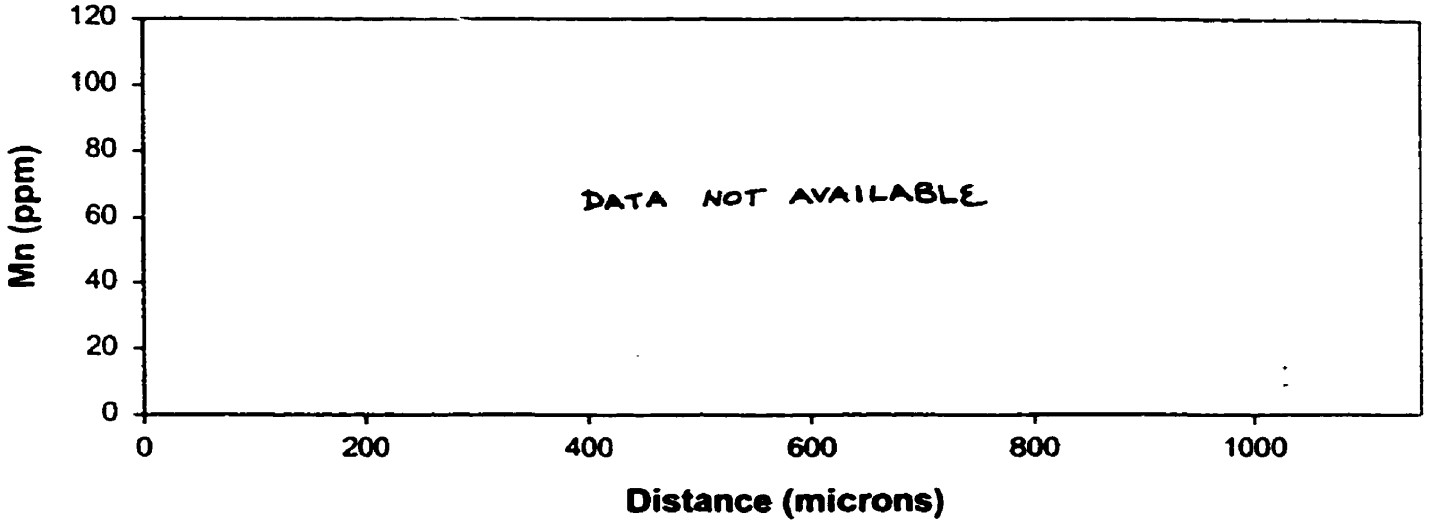
Mn (ppm)
120
100
80
60
40
20
0
DATA NOT AVAILABLE
0
200
400
600
800
1000
Distance (microns)

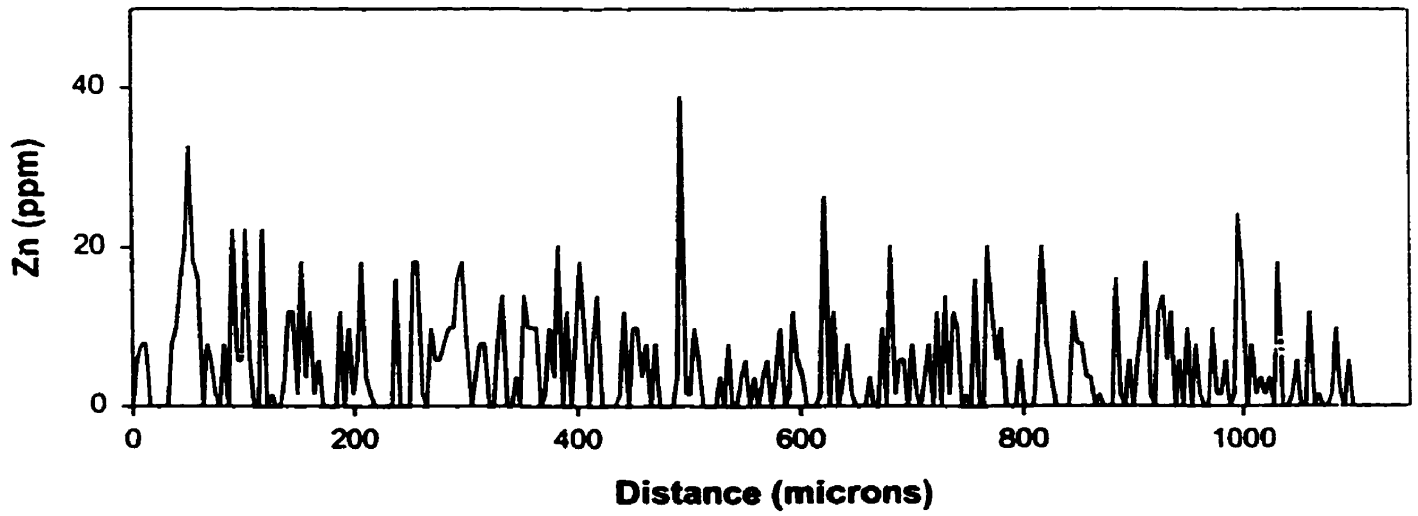
Zn (ppm)
40
20
0
0
200
400
600
800
1000
Distance (microns)

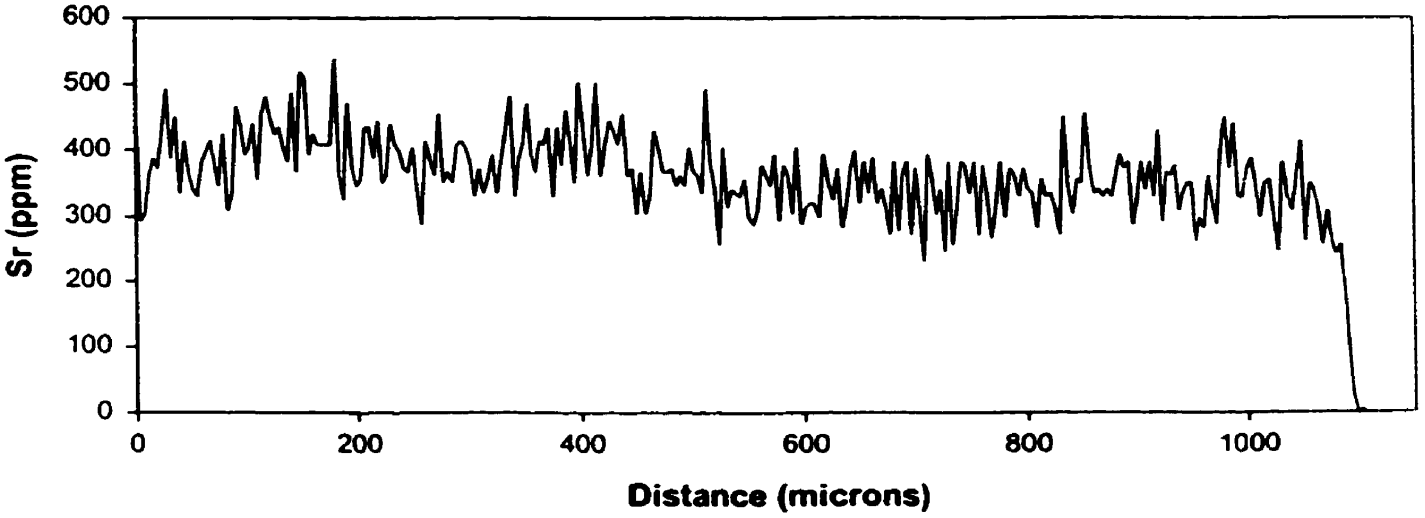
Sr (ppm)
600
500
400
300
200
100
0
0
200
400
600
800
1000
Distance (microns)

CAJ #1 NORTHERN PIKE

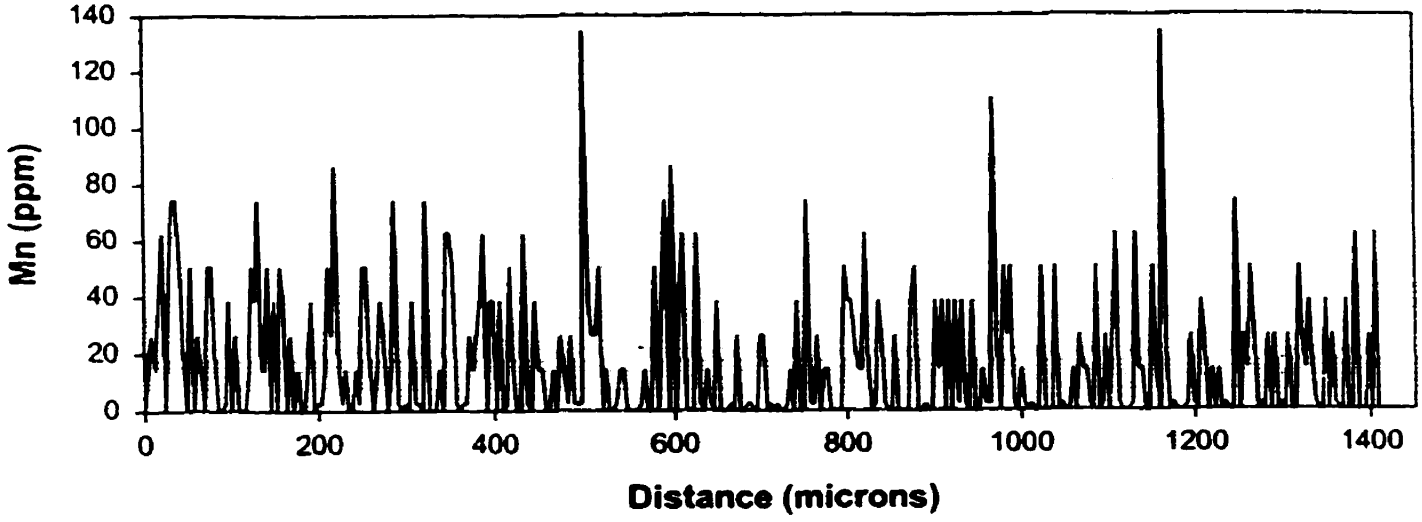

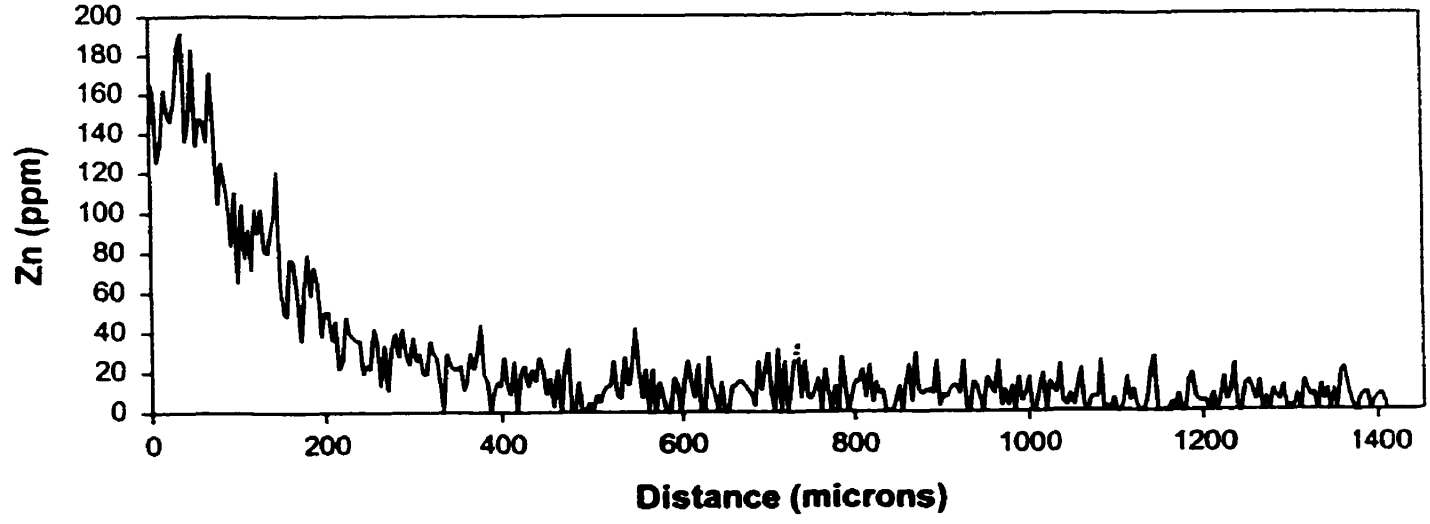

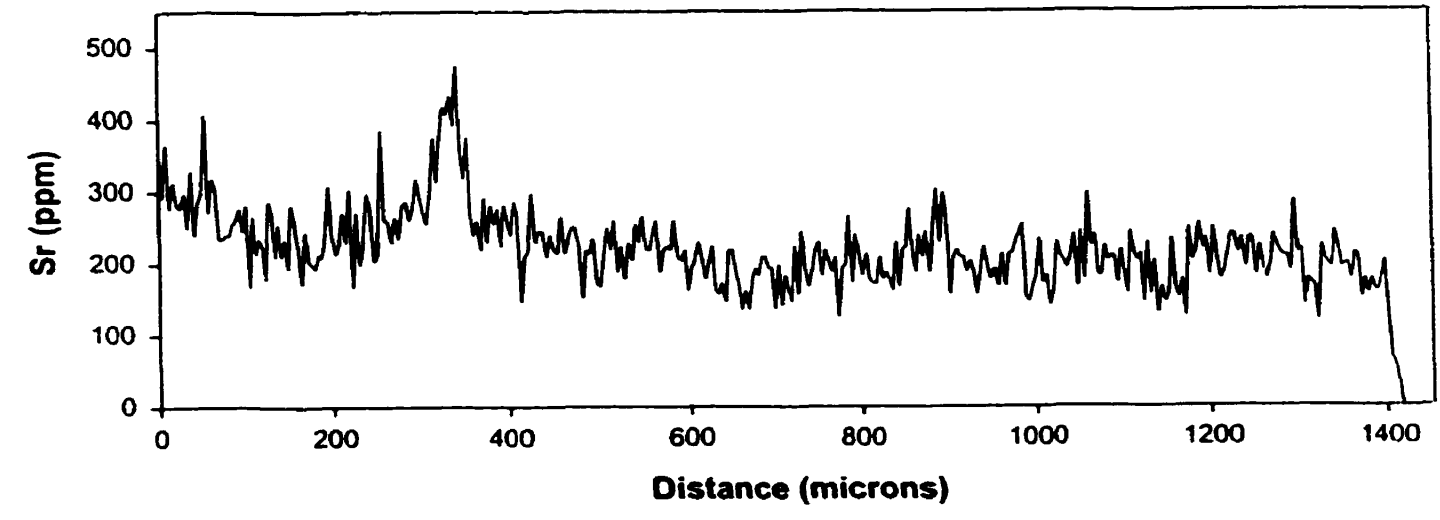

CAJ #3 NORTHERN PIKE

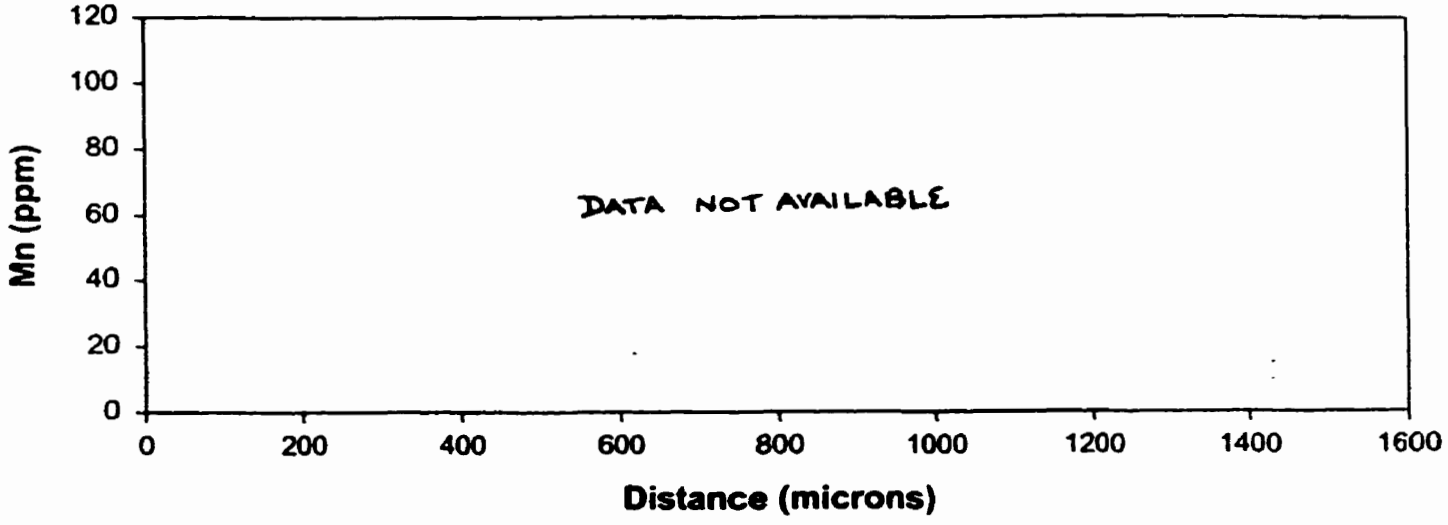

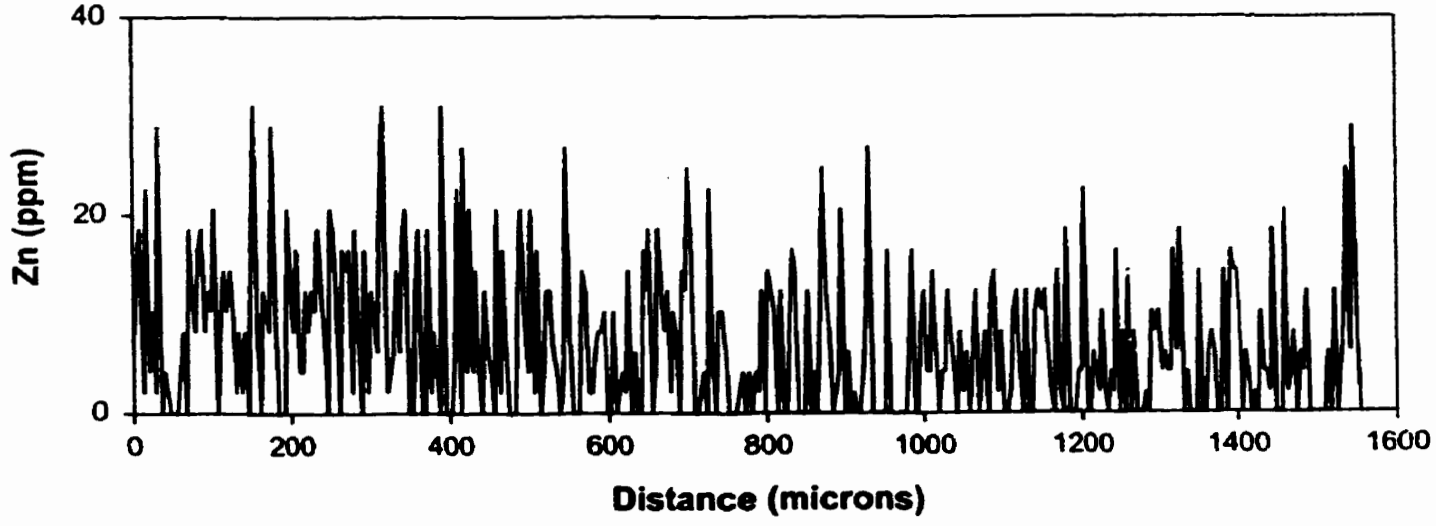

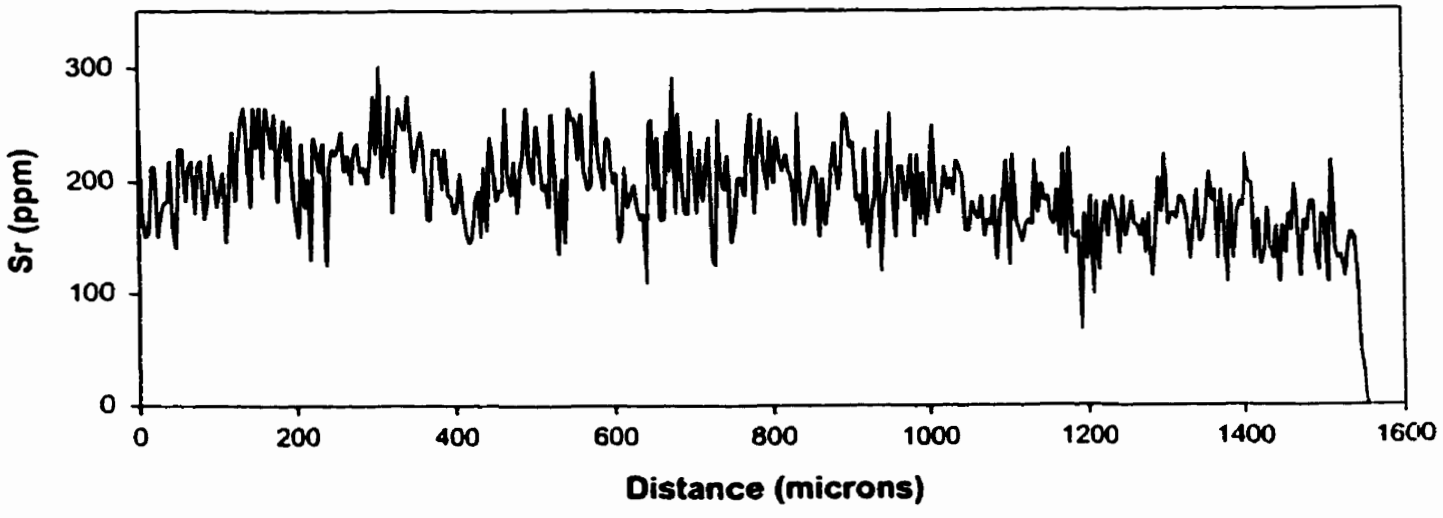

CAJ #4 NORTHERN PIKE

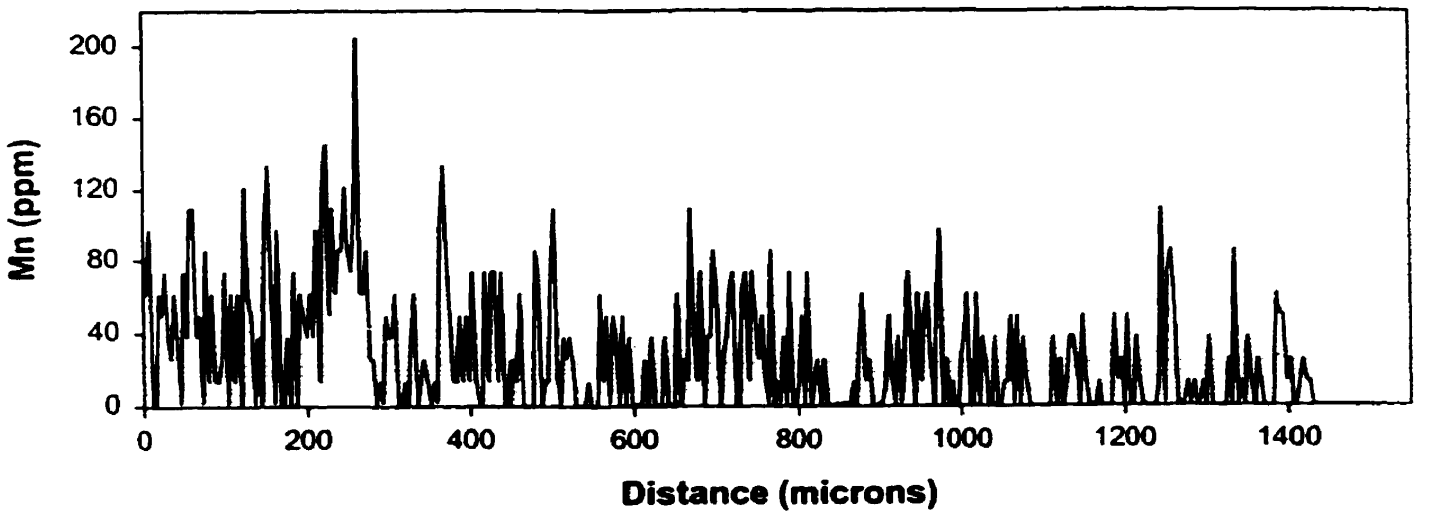

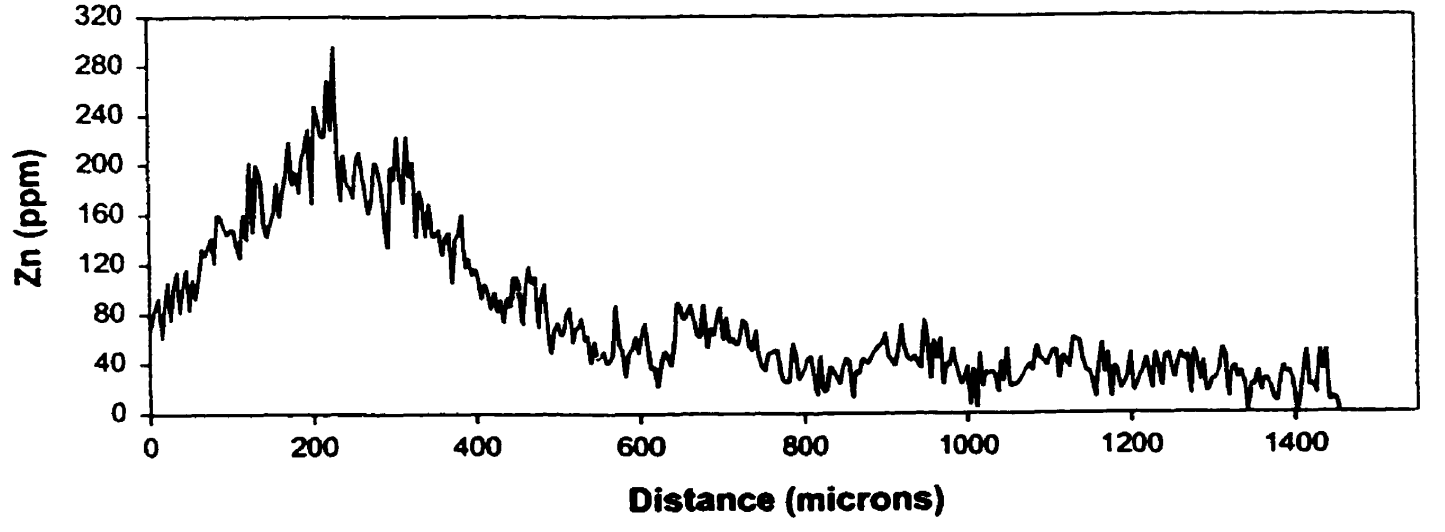

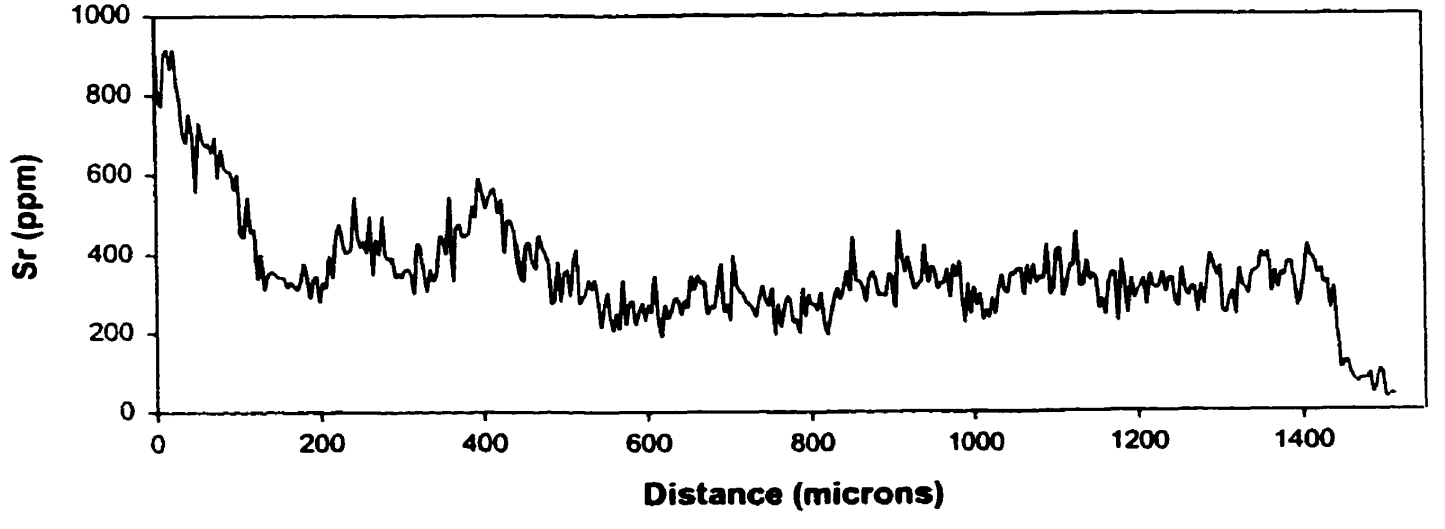

CAJ #5 NORTHERN PIKE

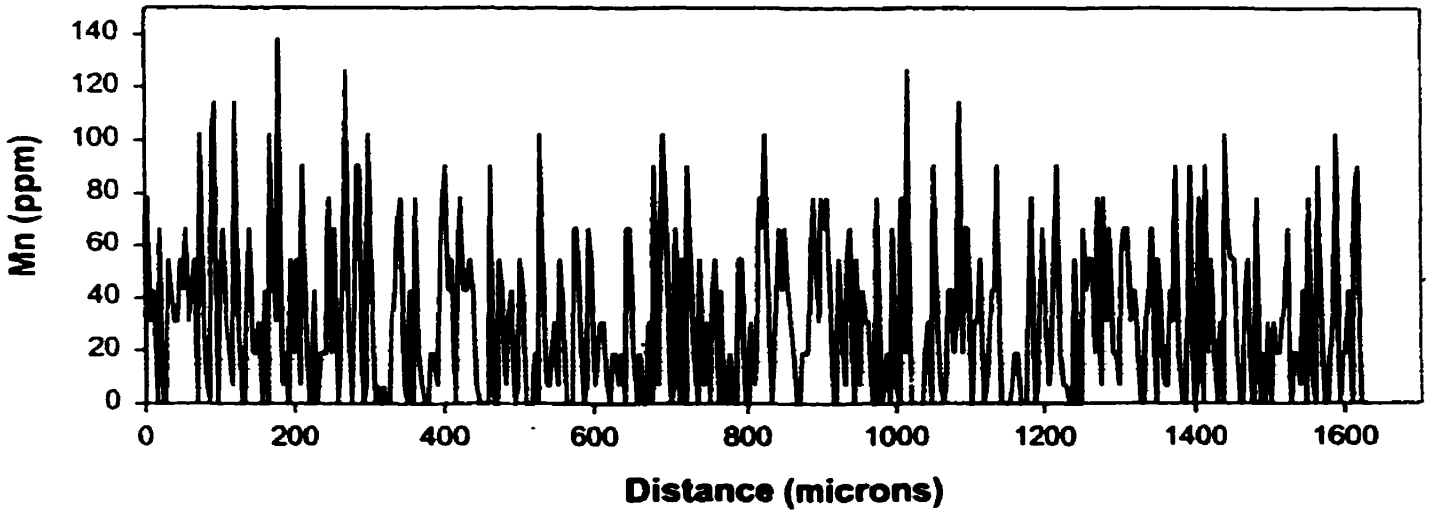

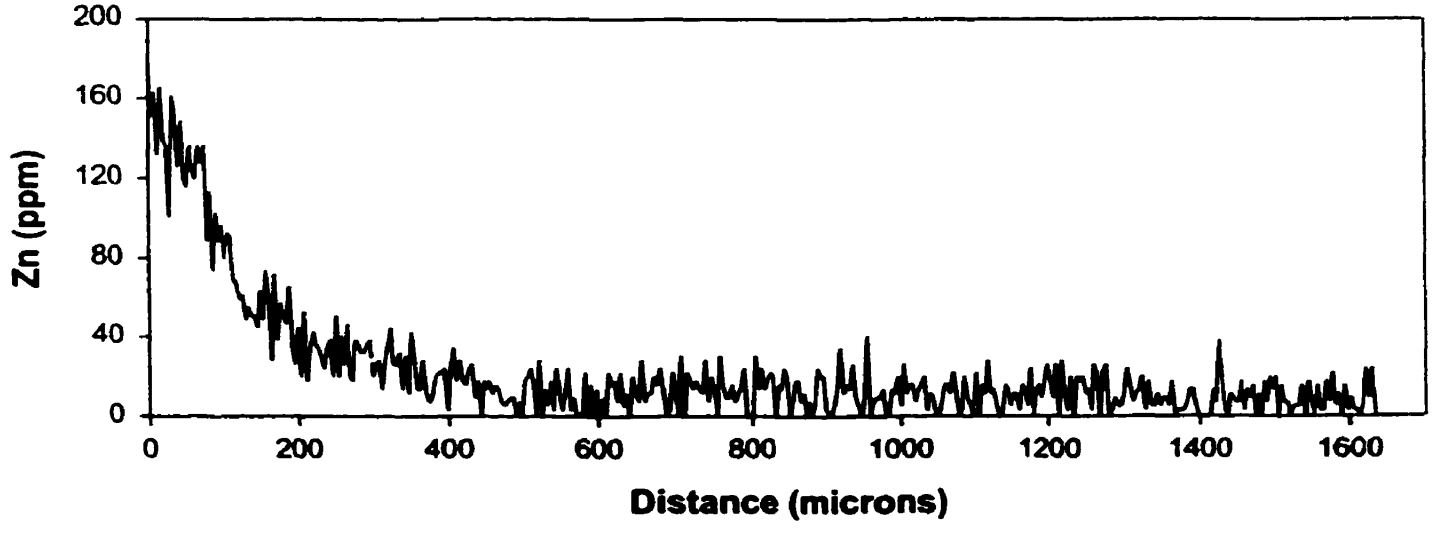

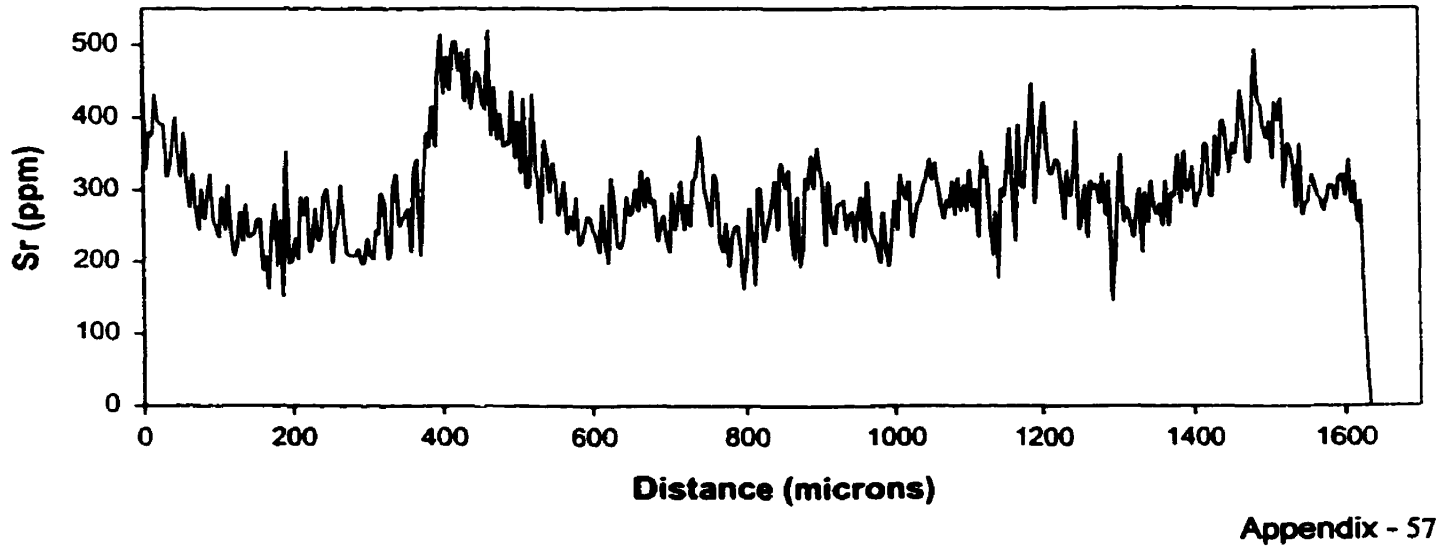

CAJ #6 NORTHERN PIKE

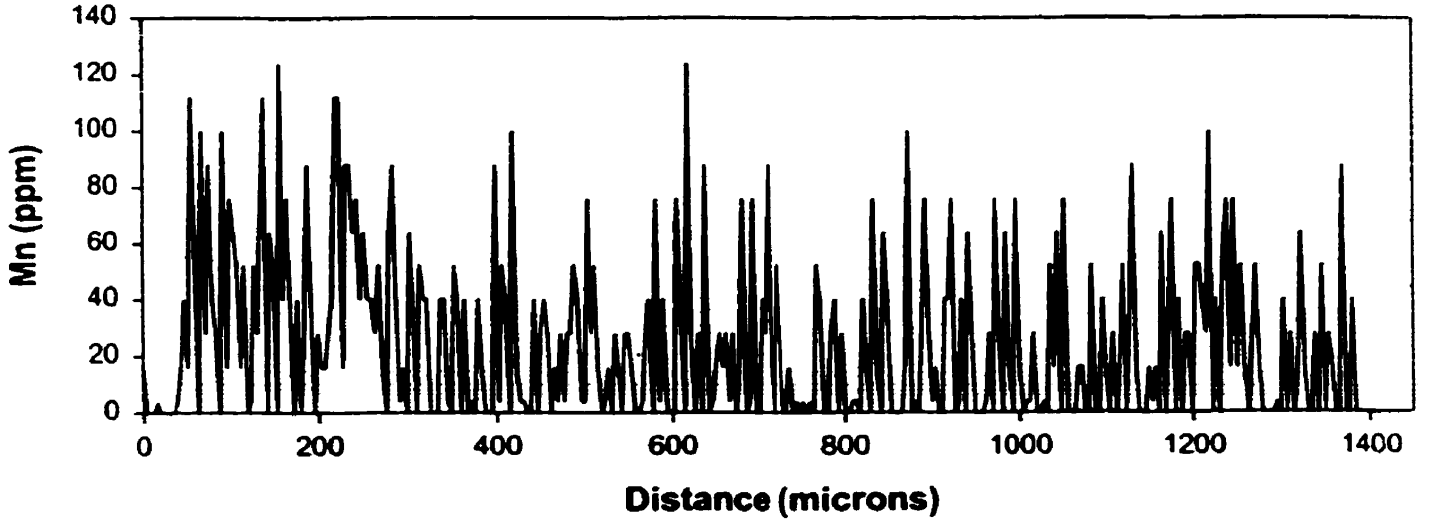

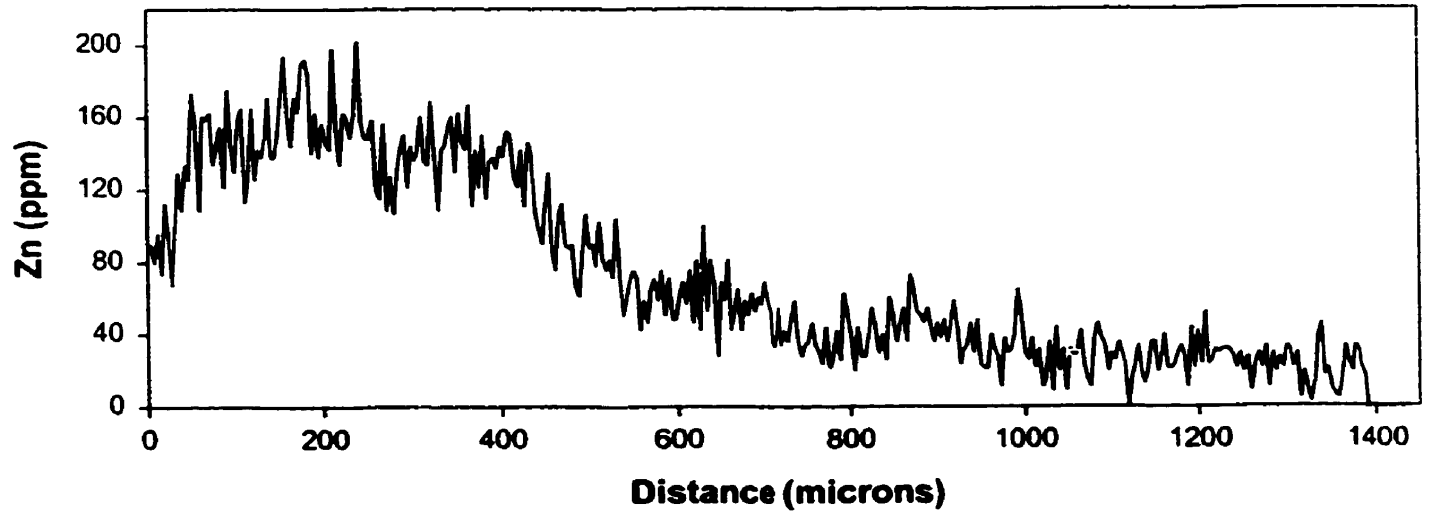

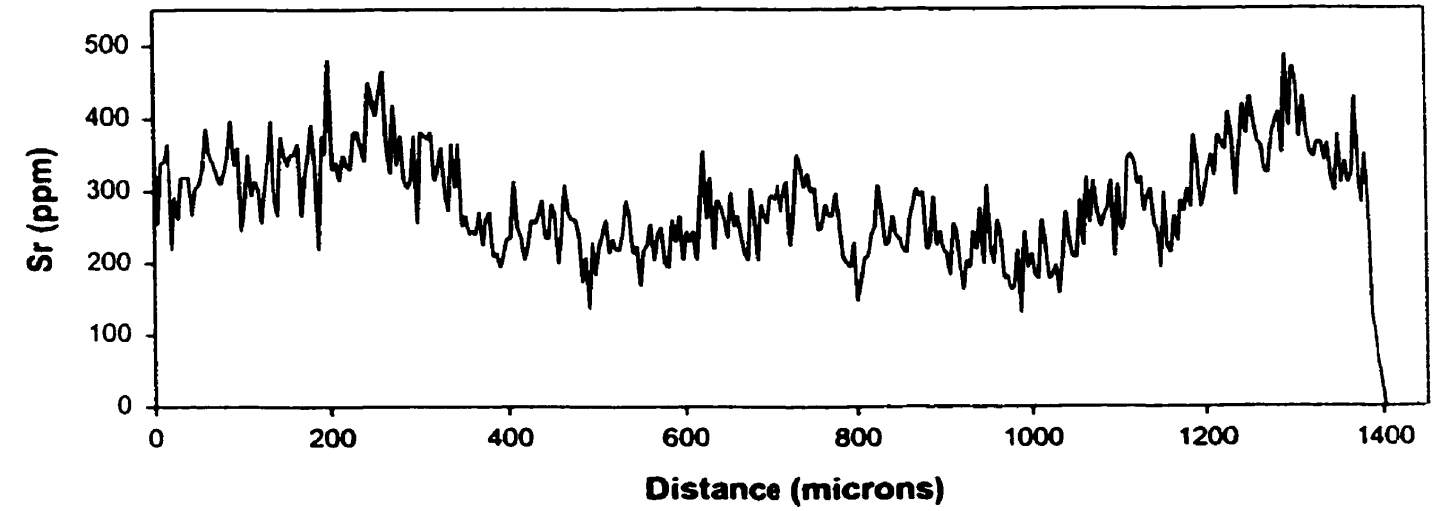

KAP1-A #1 LAKE WHITEFISH

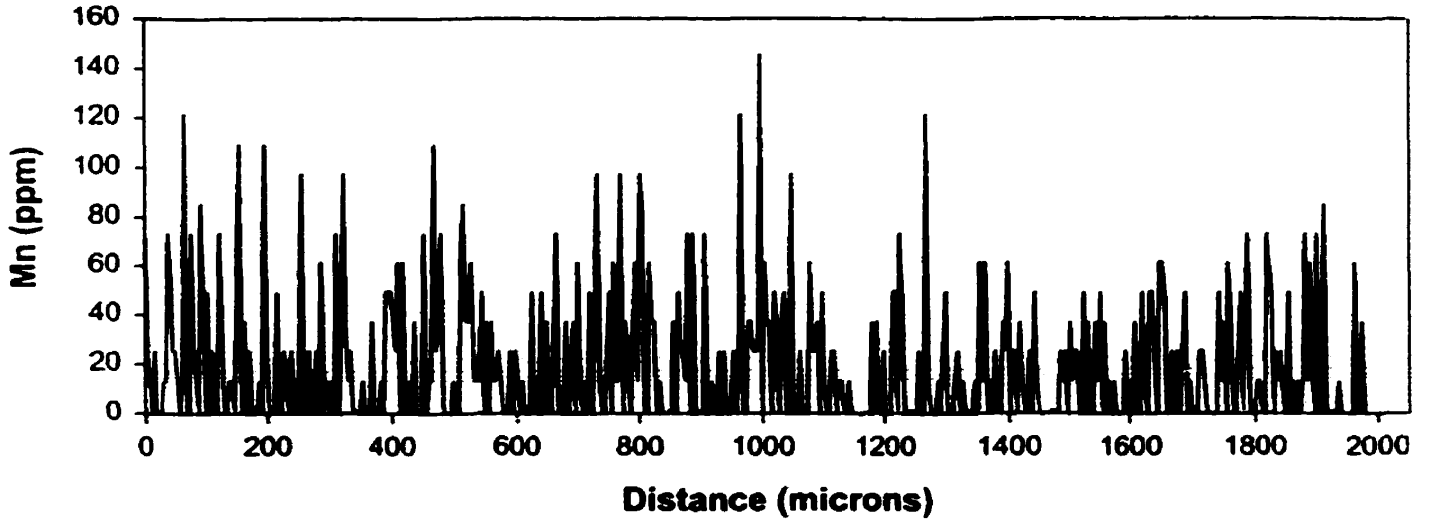

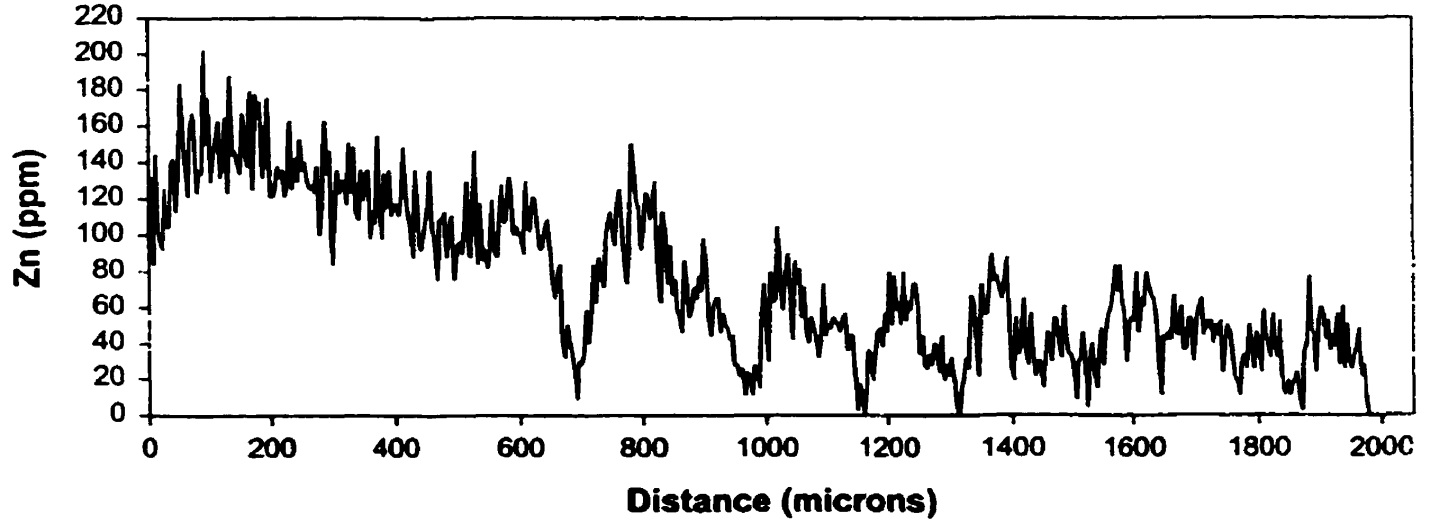

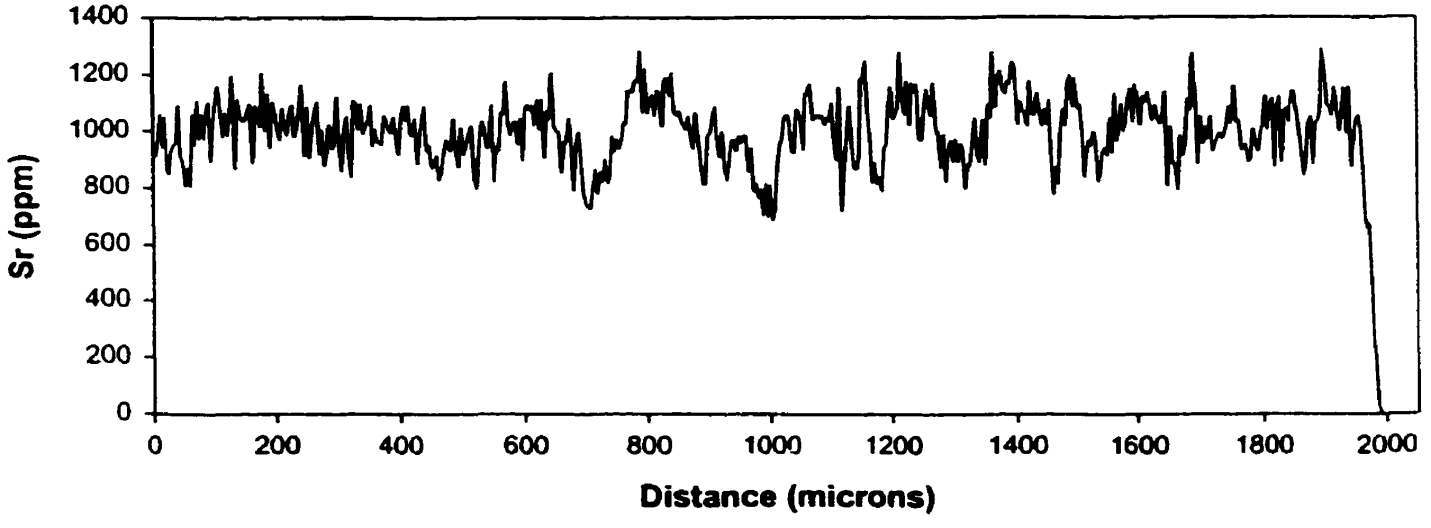

KAP1-A #2 LAKE WHITEFISH SCAN A

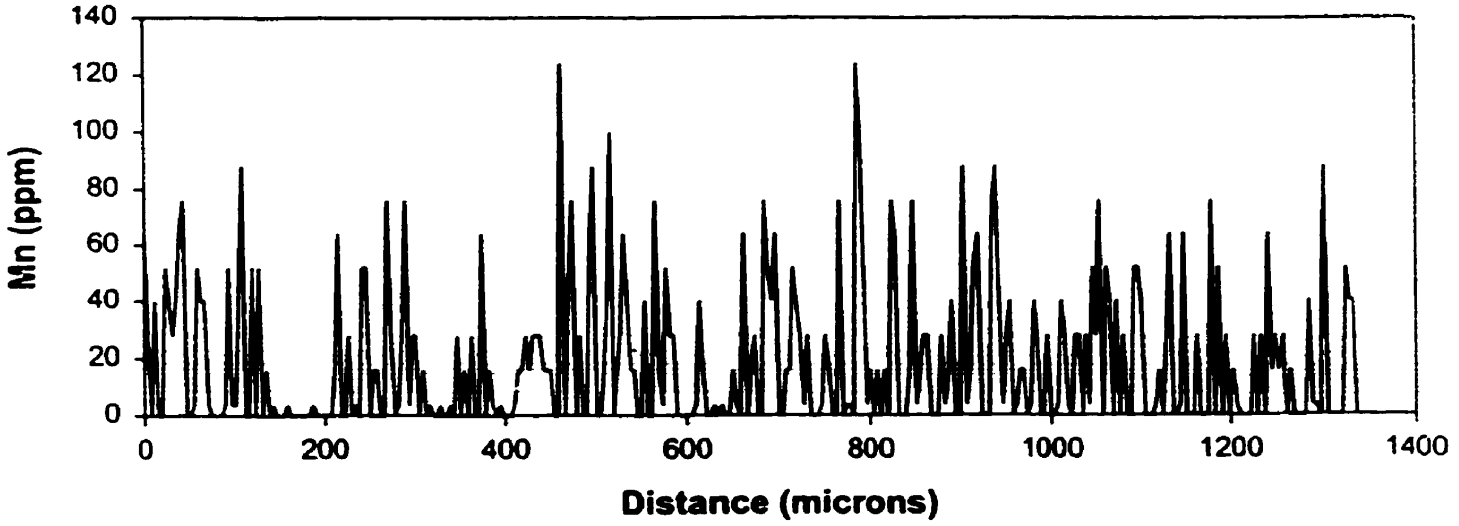

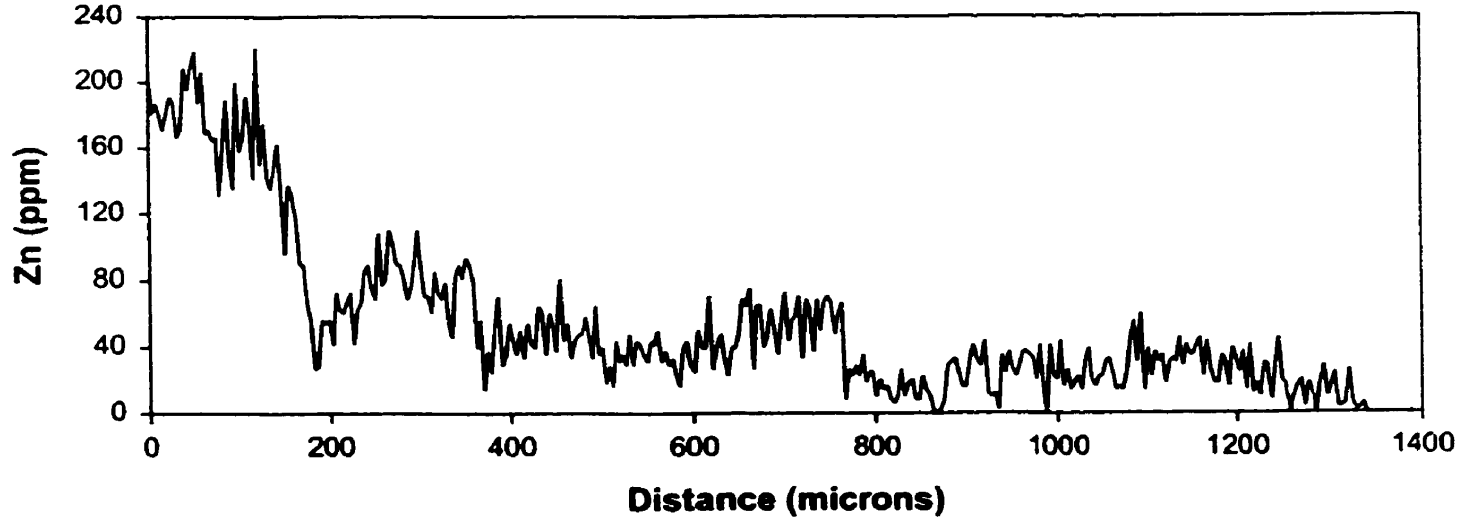

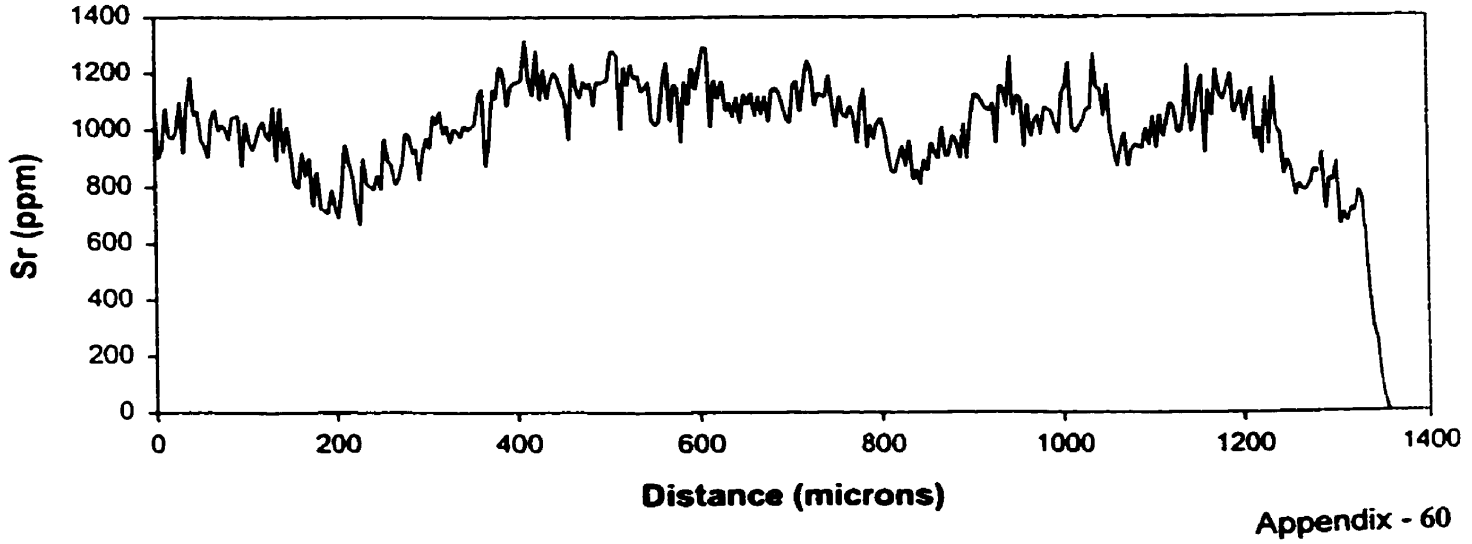

KAP1-A #2 LAKE WHITEFISH SCAN B

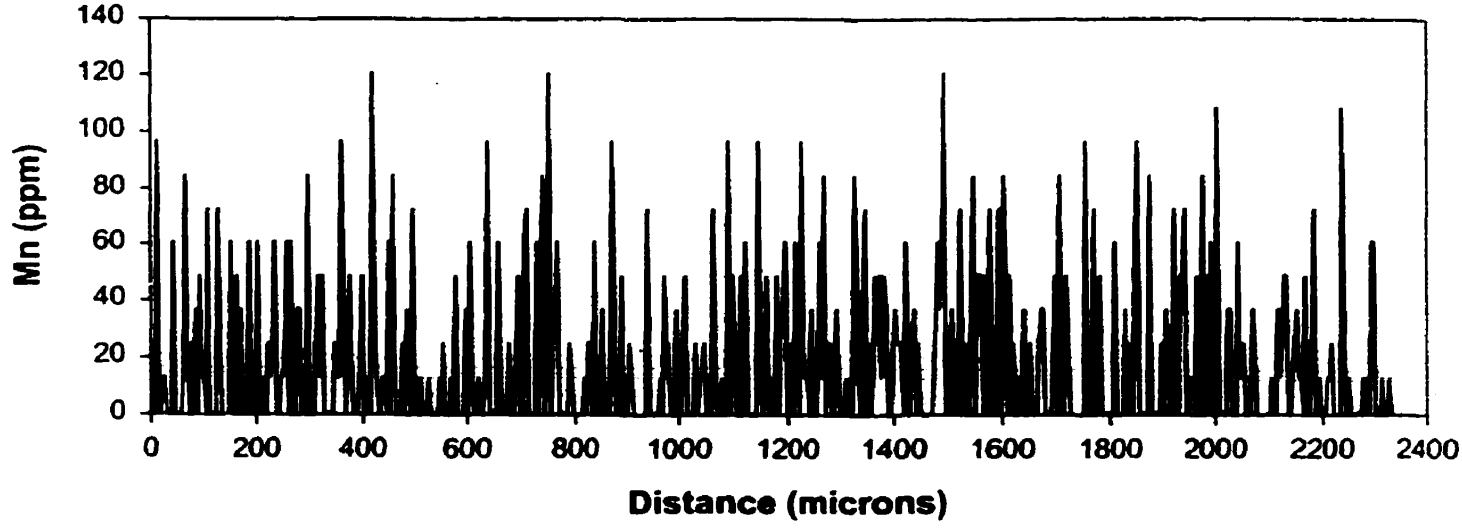

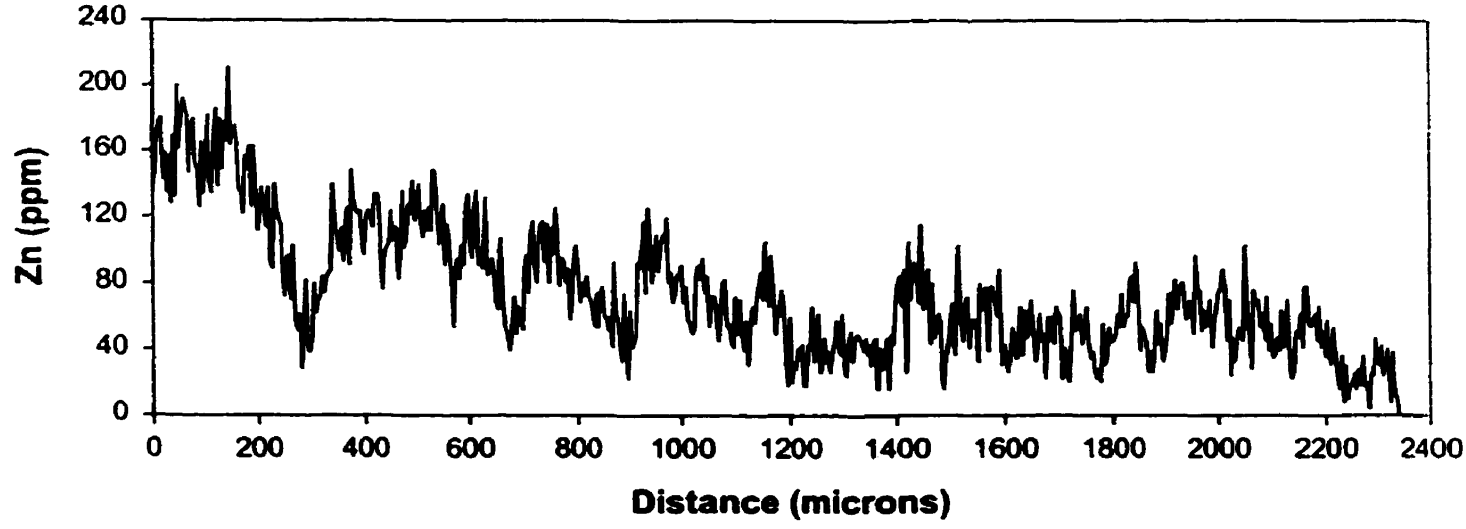

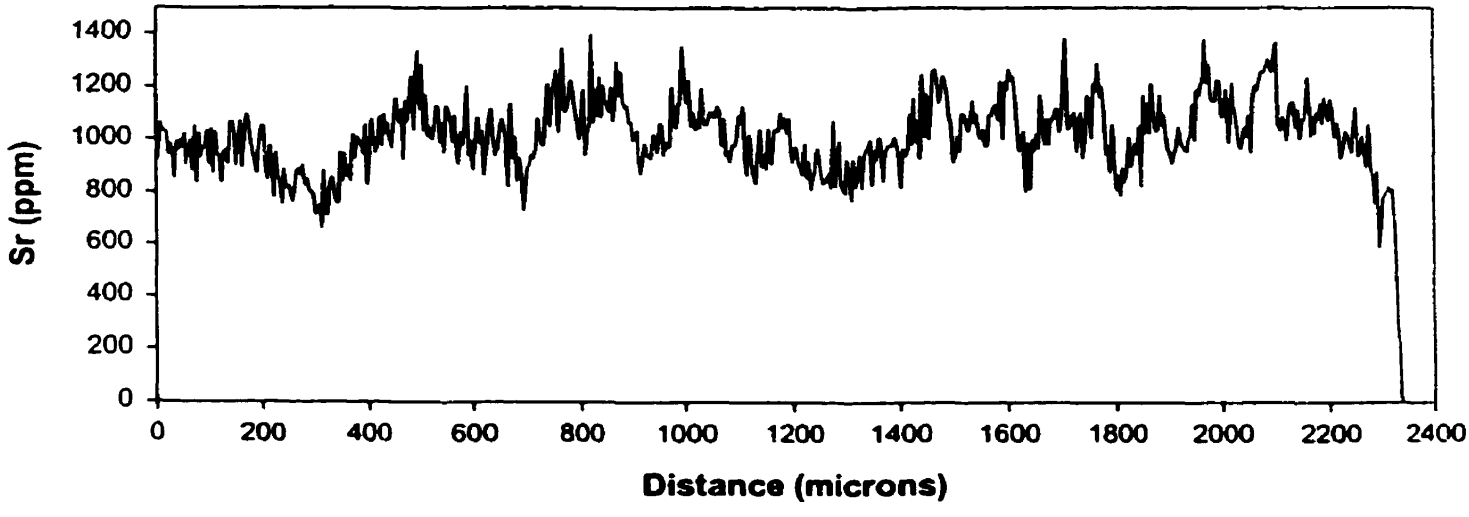

KAP1-A #3 LAKE WHITEFISH

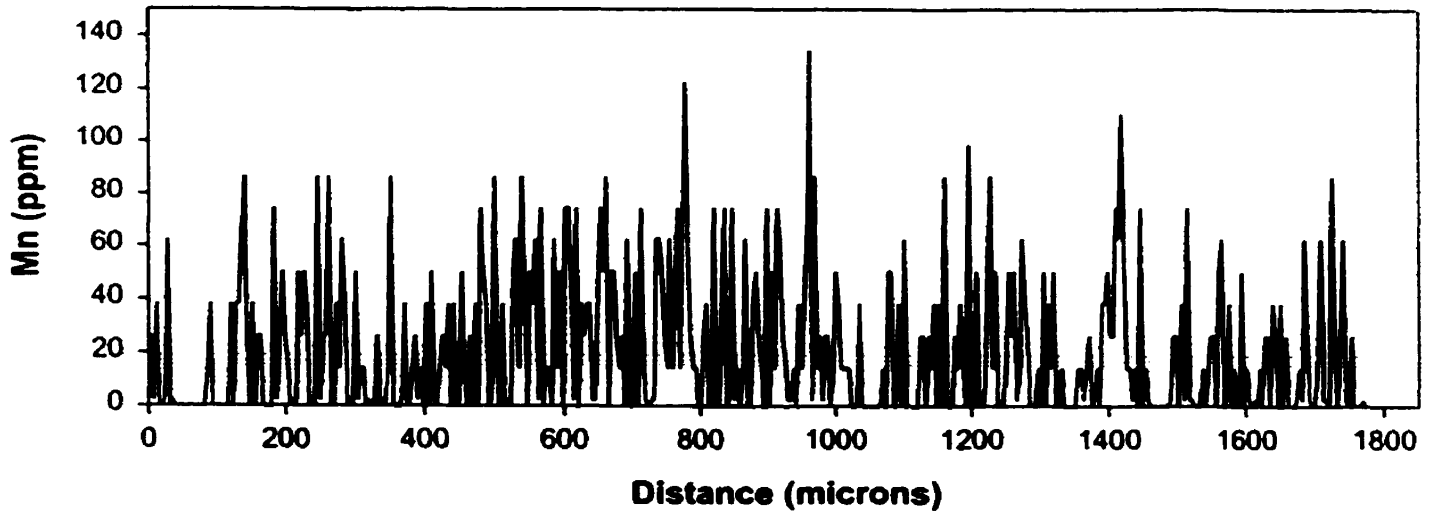

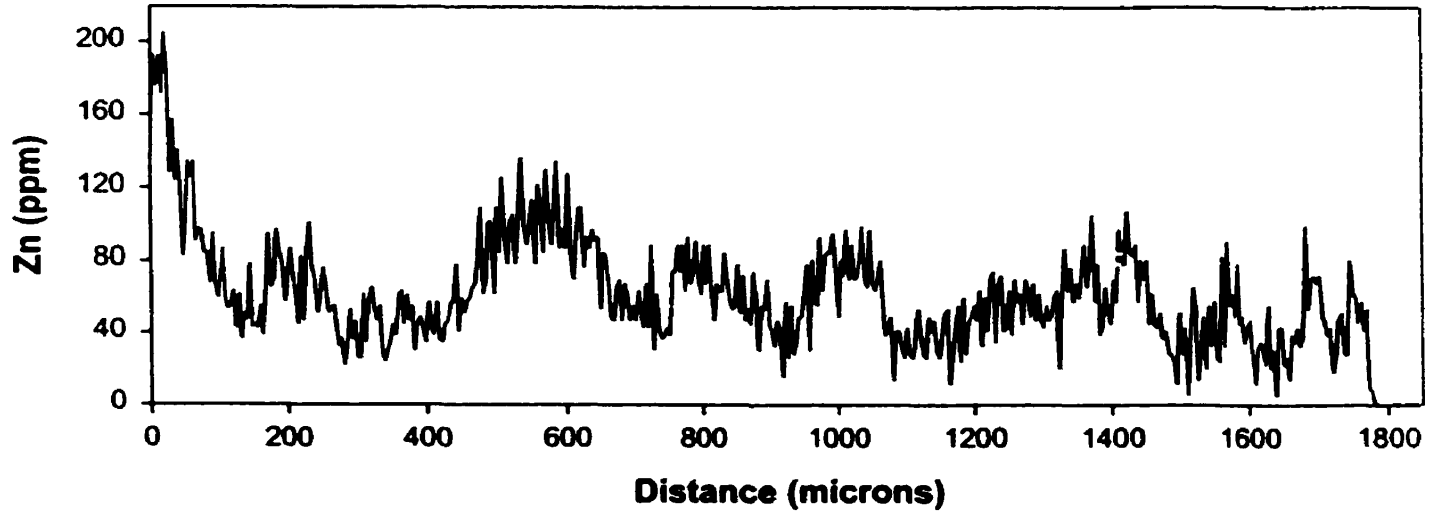

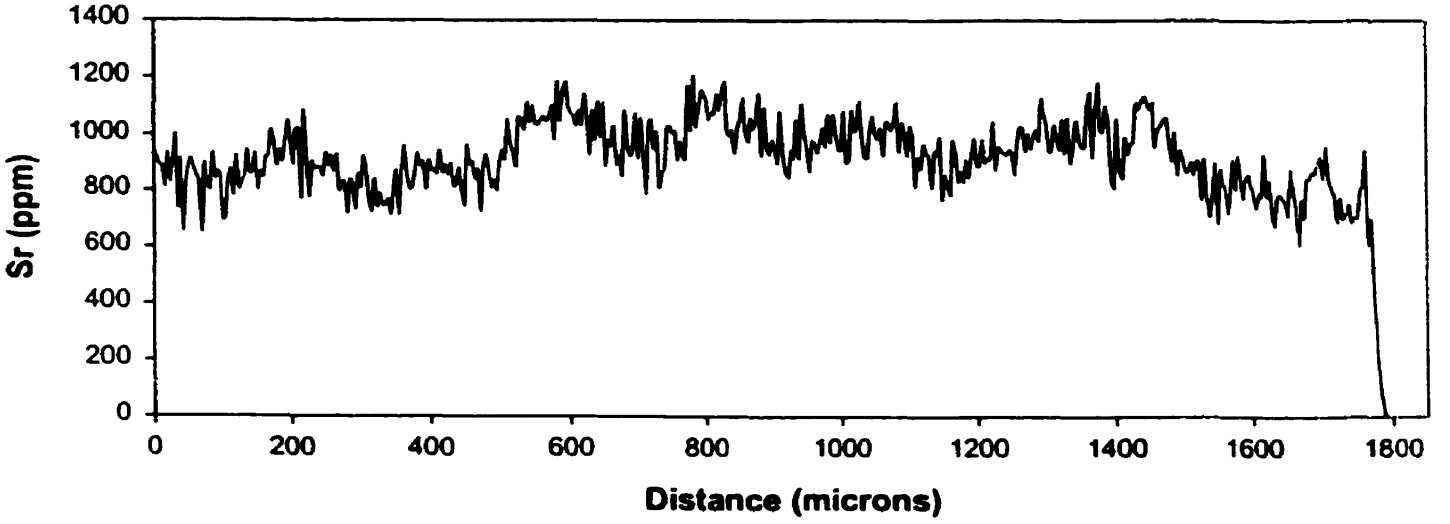

KAP1-D #1 CISCO SCAN A

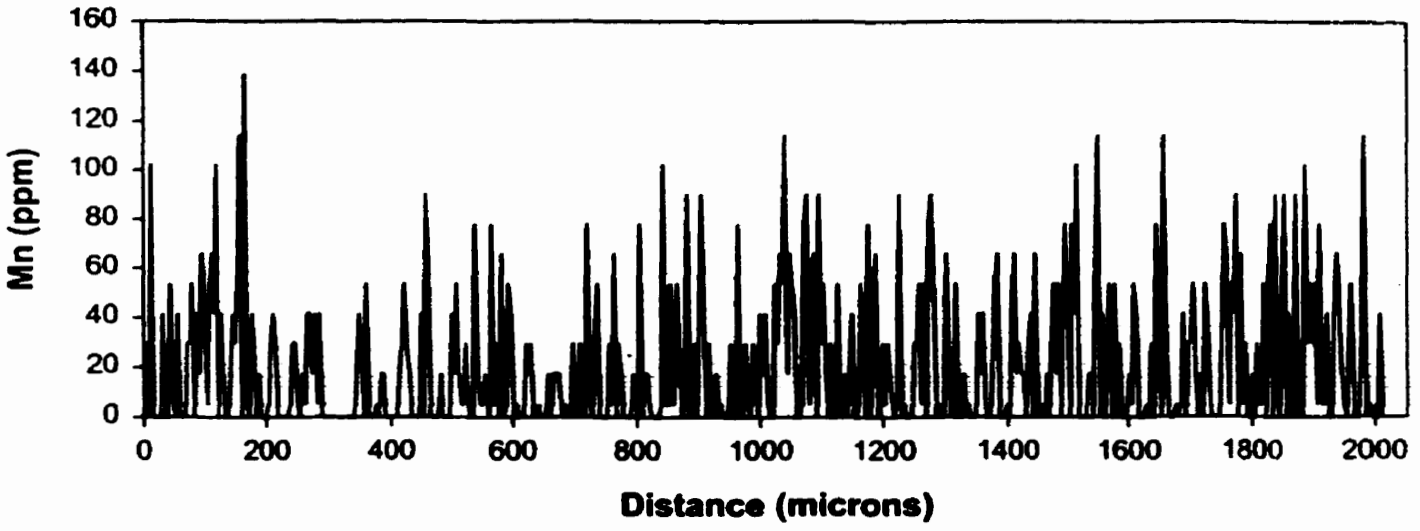

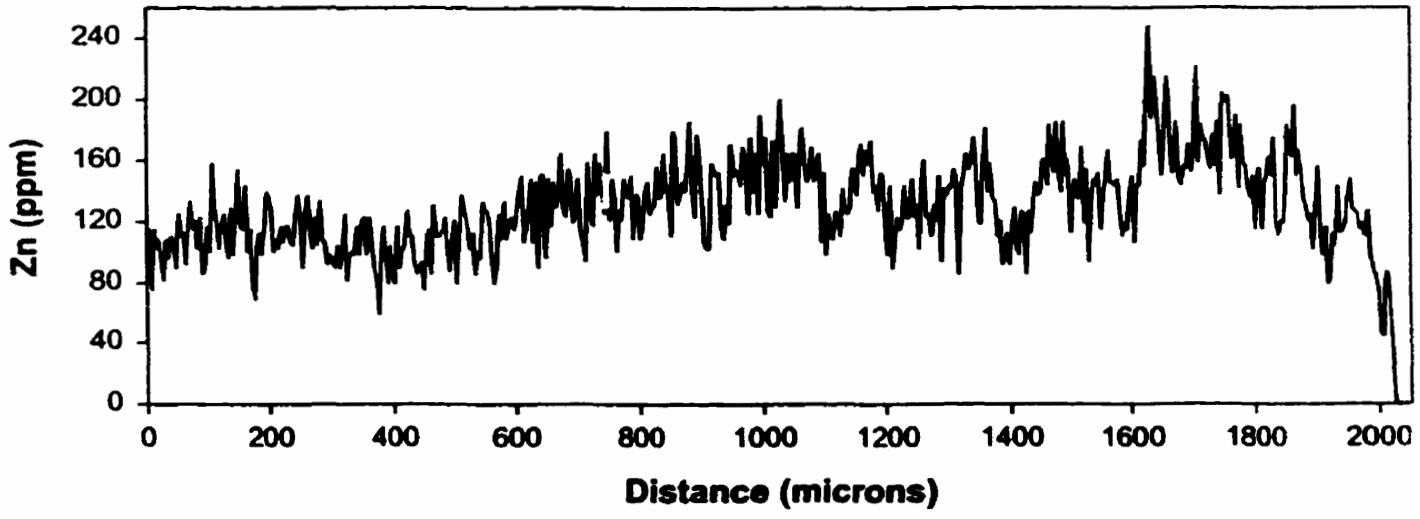

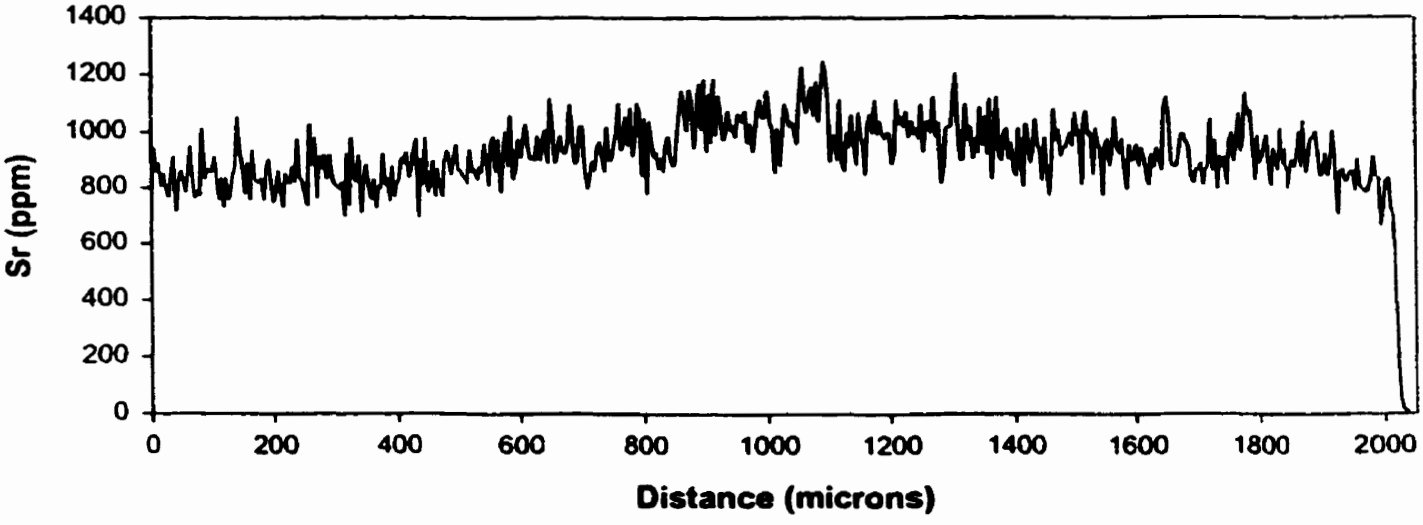

KAP1-D #1 CISCO SCAN B

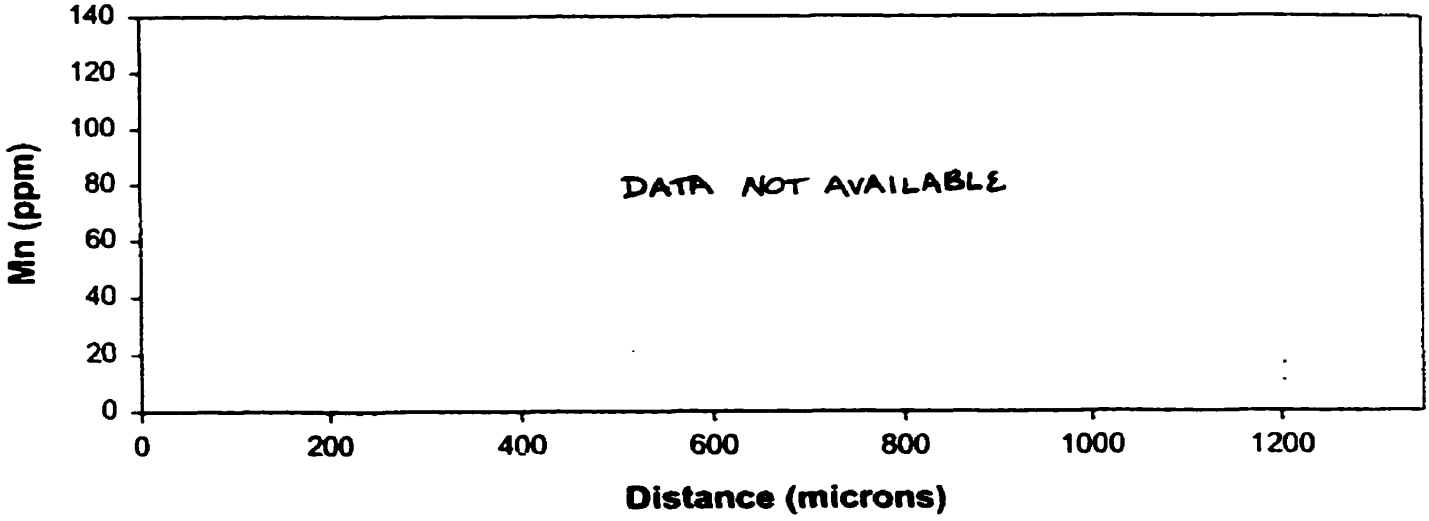

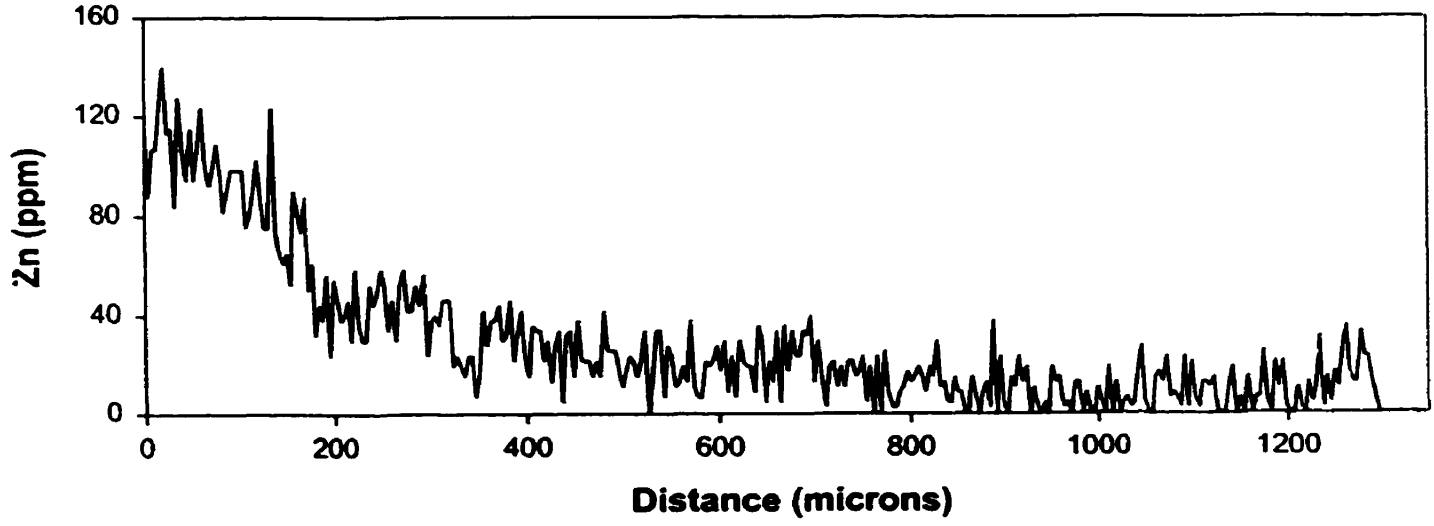

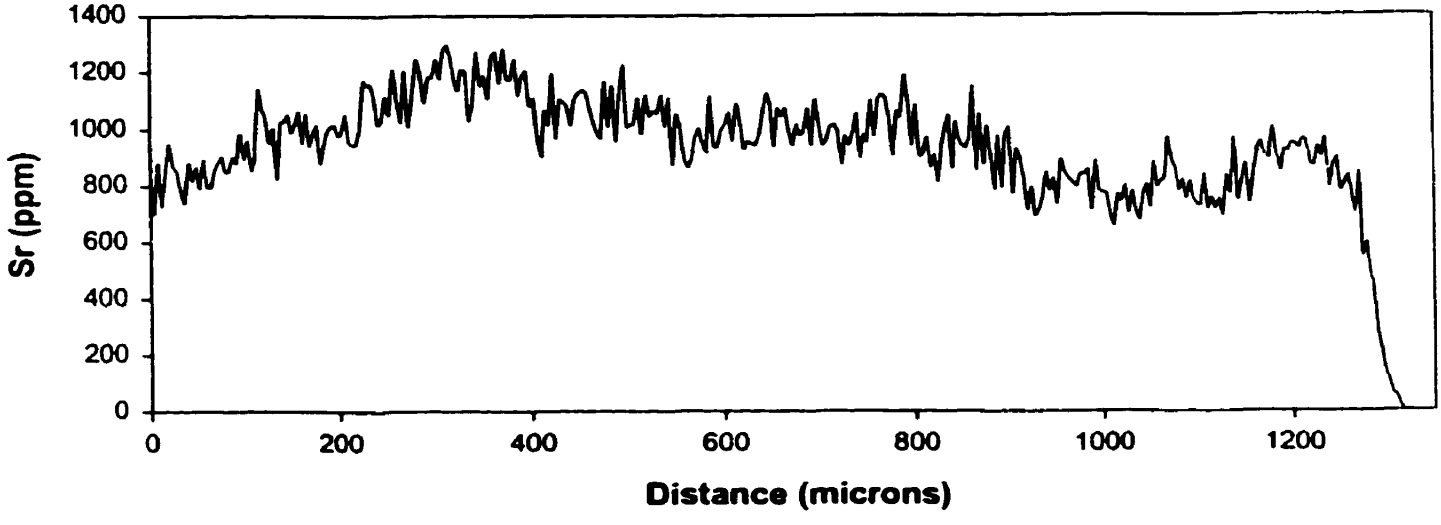

KAP1-D #2 CISCO

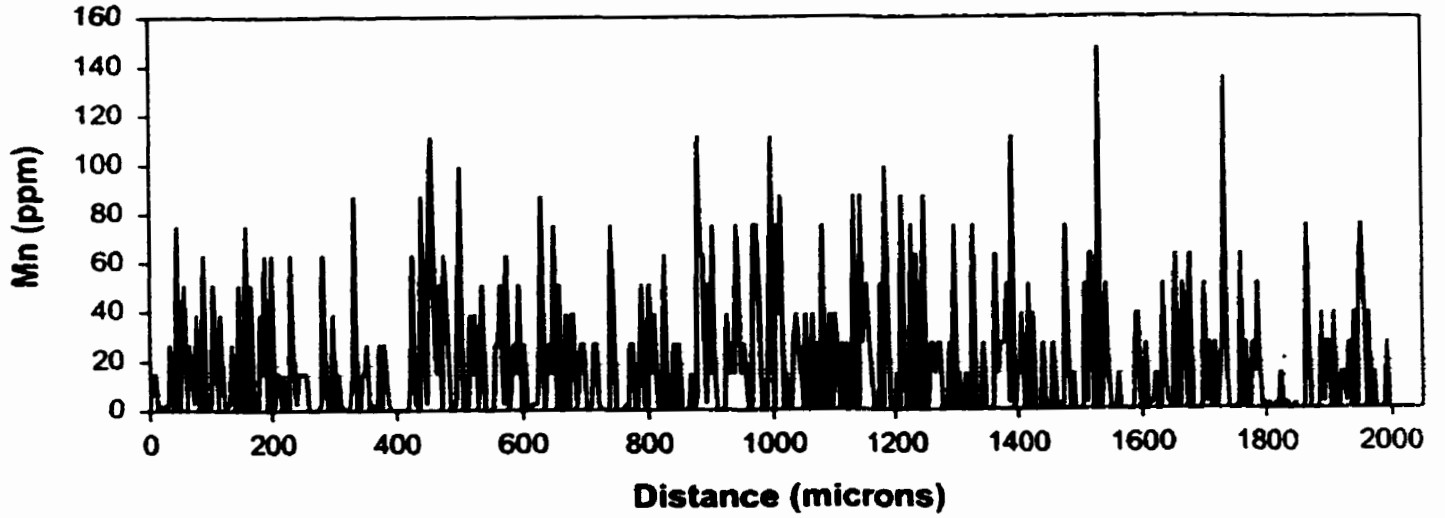

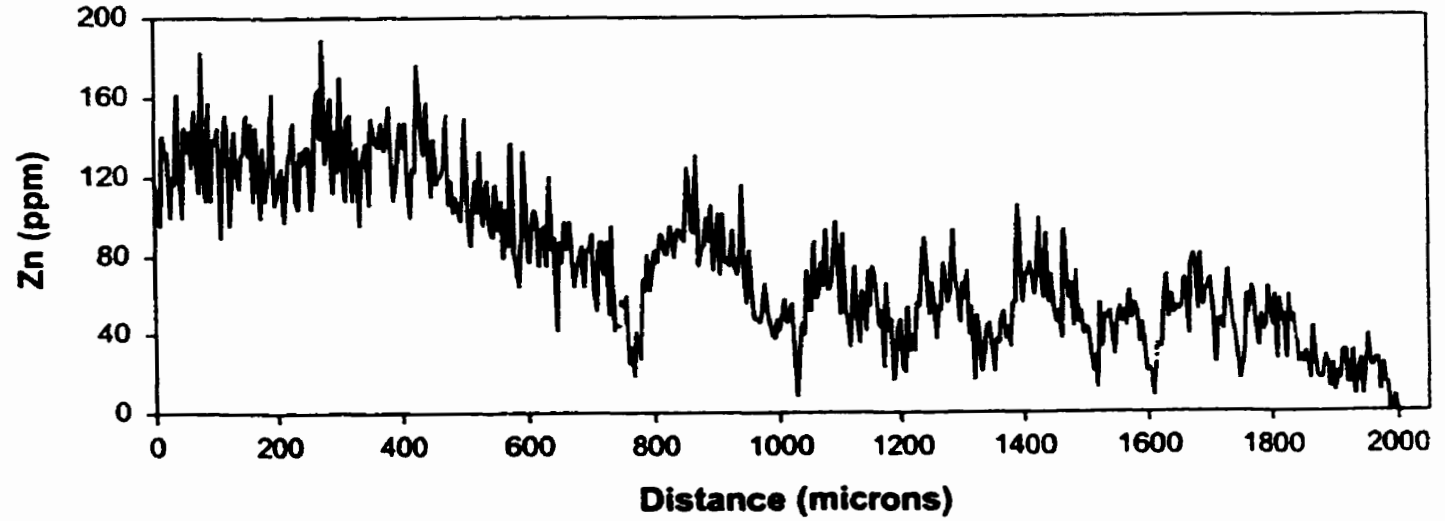

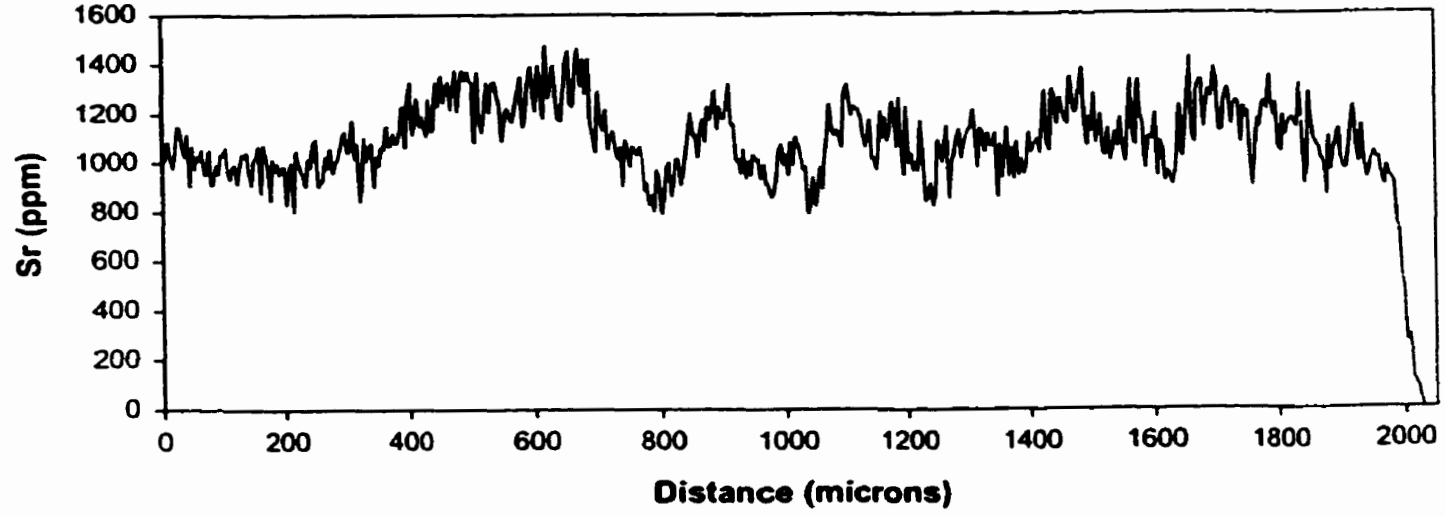

KAP1-D #3 CISCO SCAN A

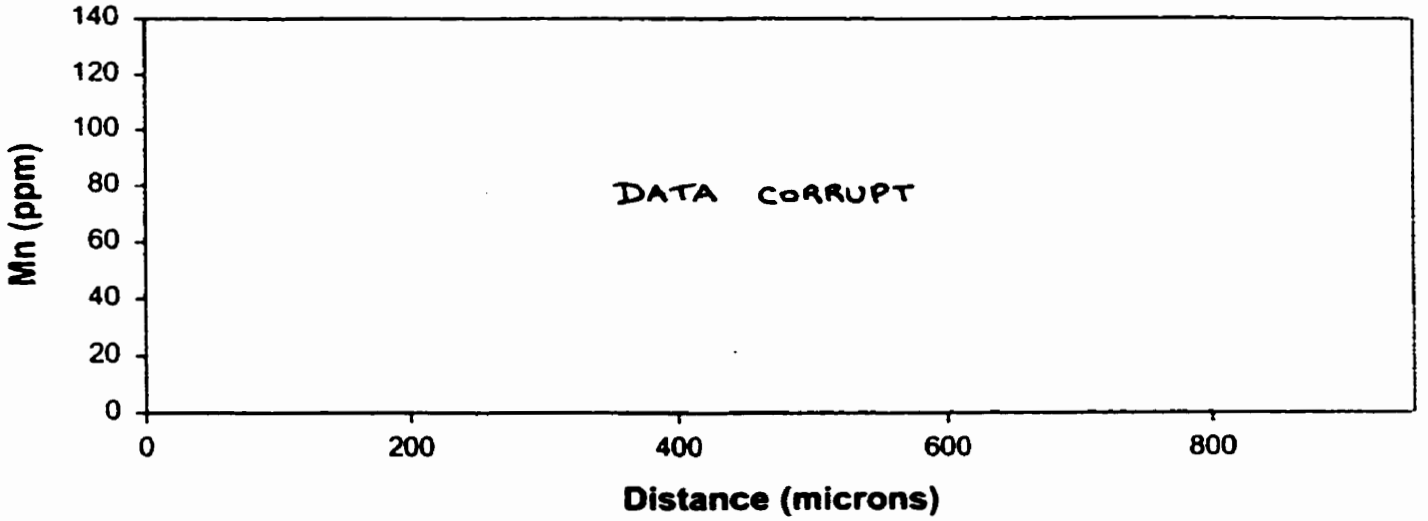

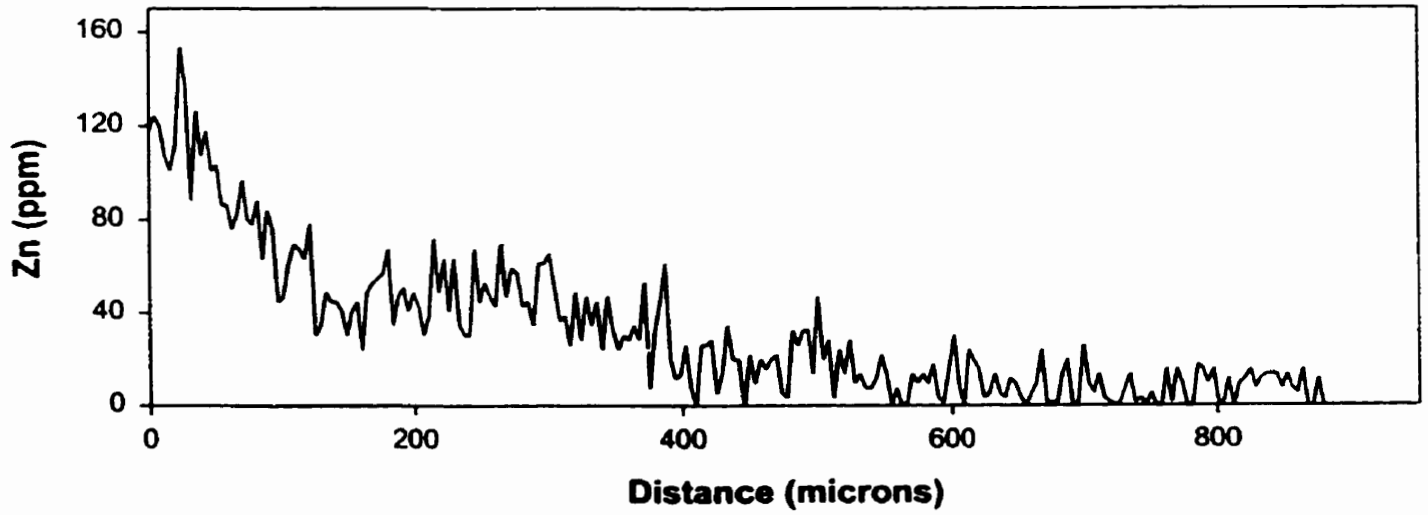

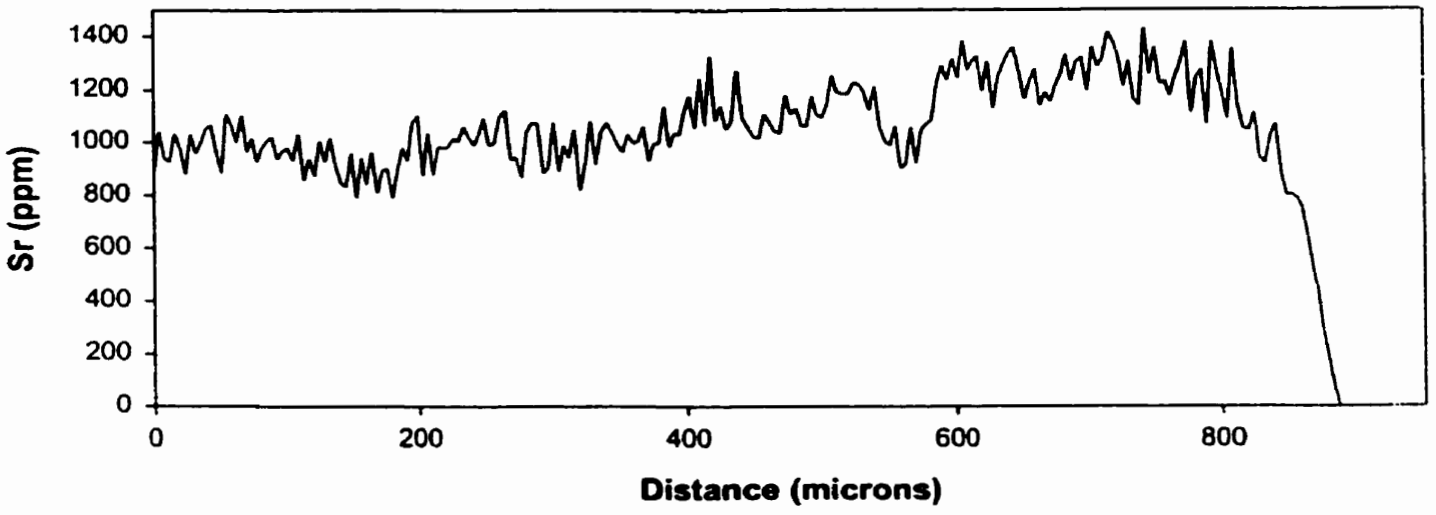

KAP1-D #3 CISCO SCAN B

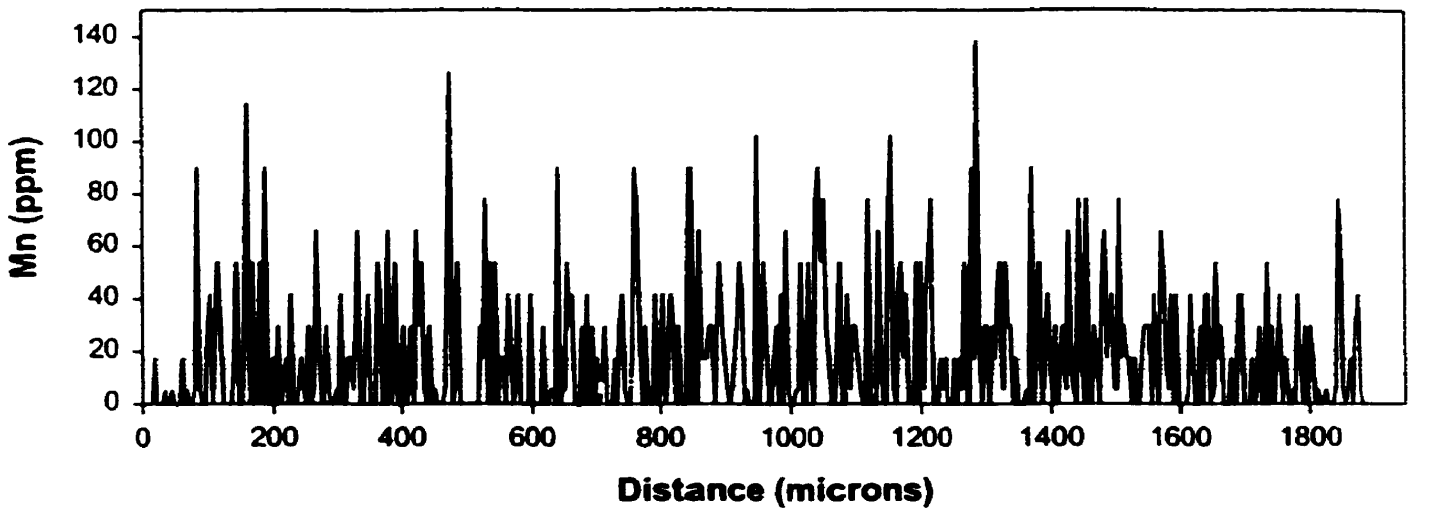

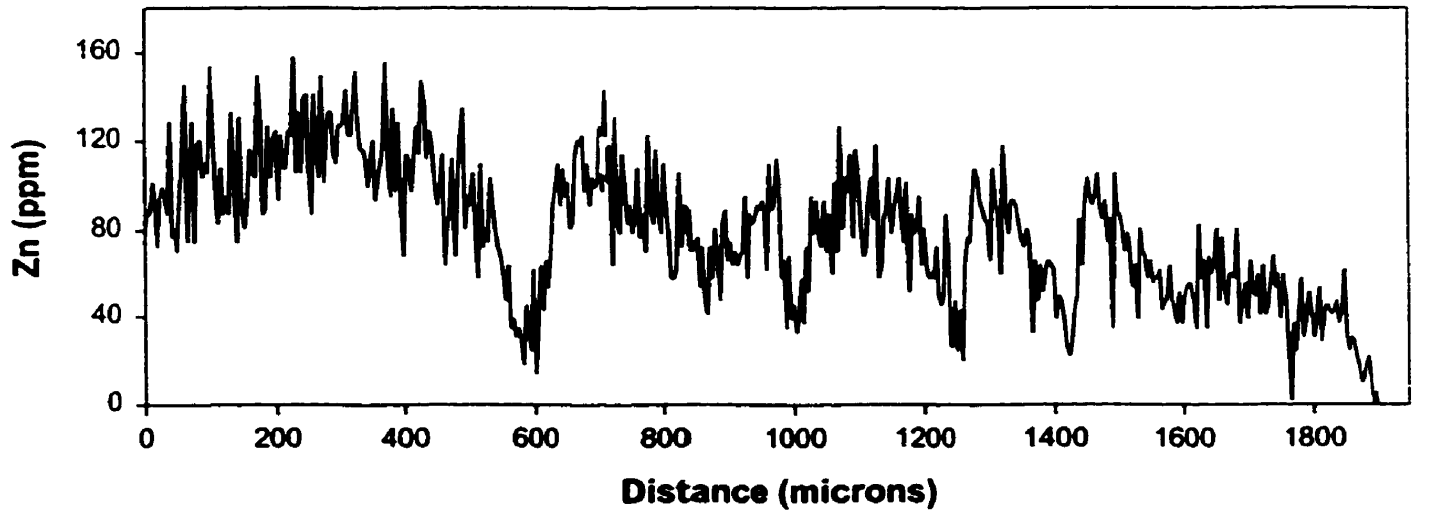

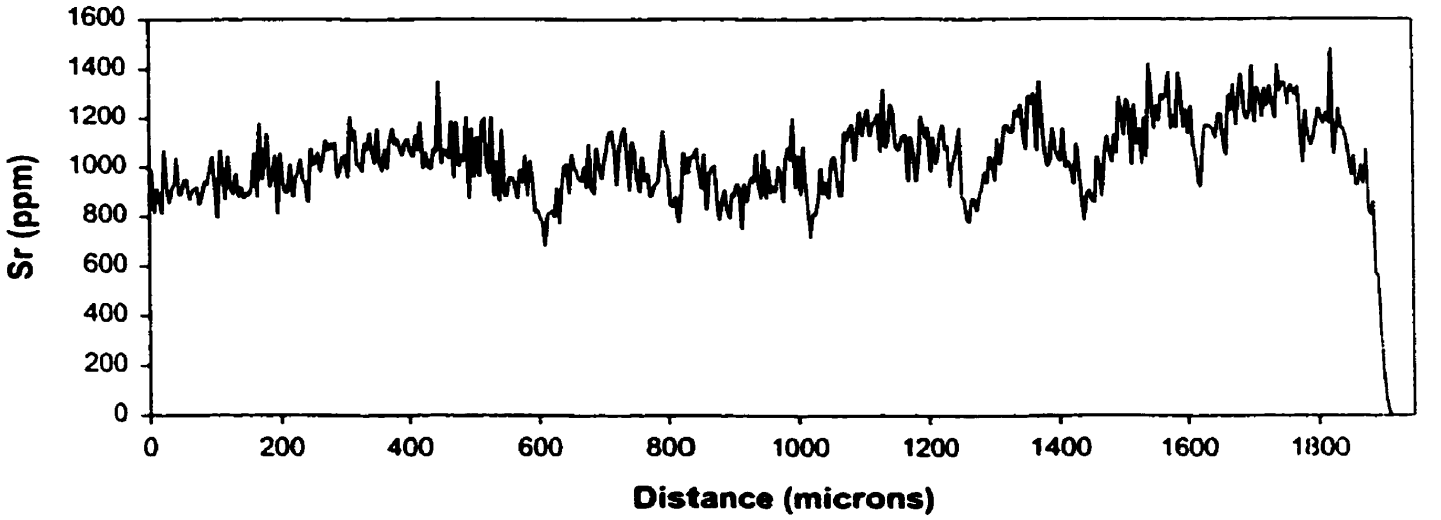

KAP-B #3 WHITE SUCKER

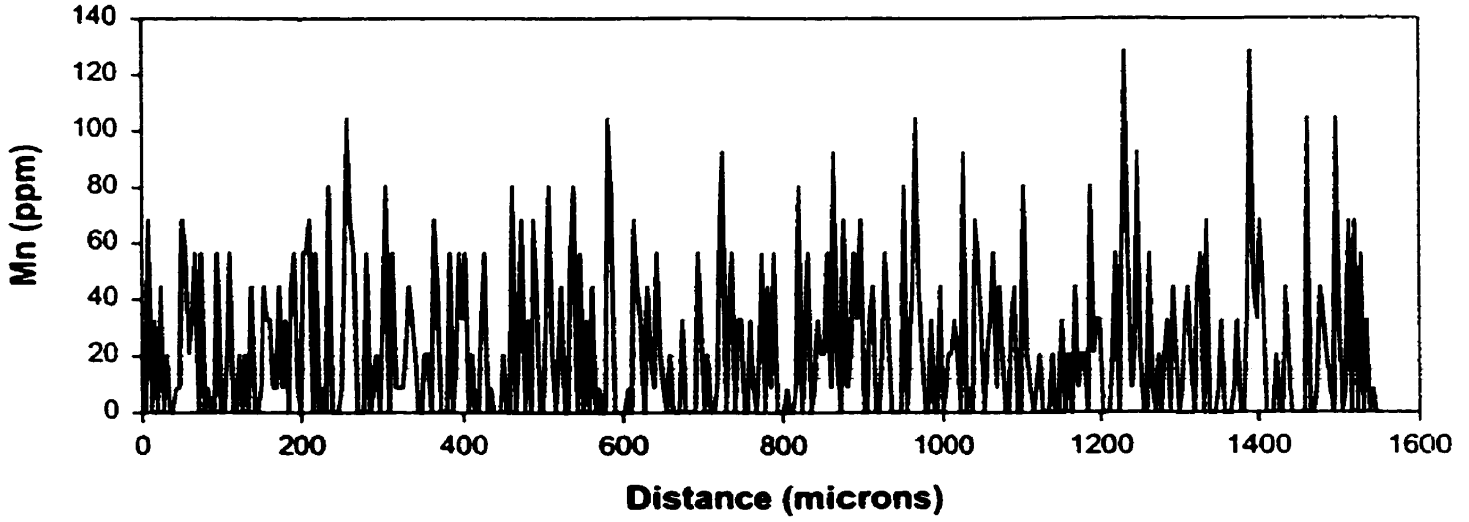

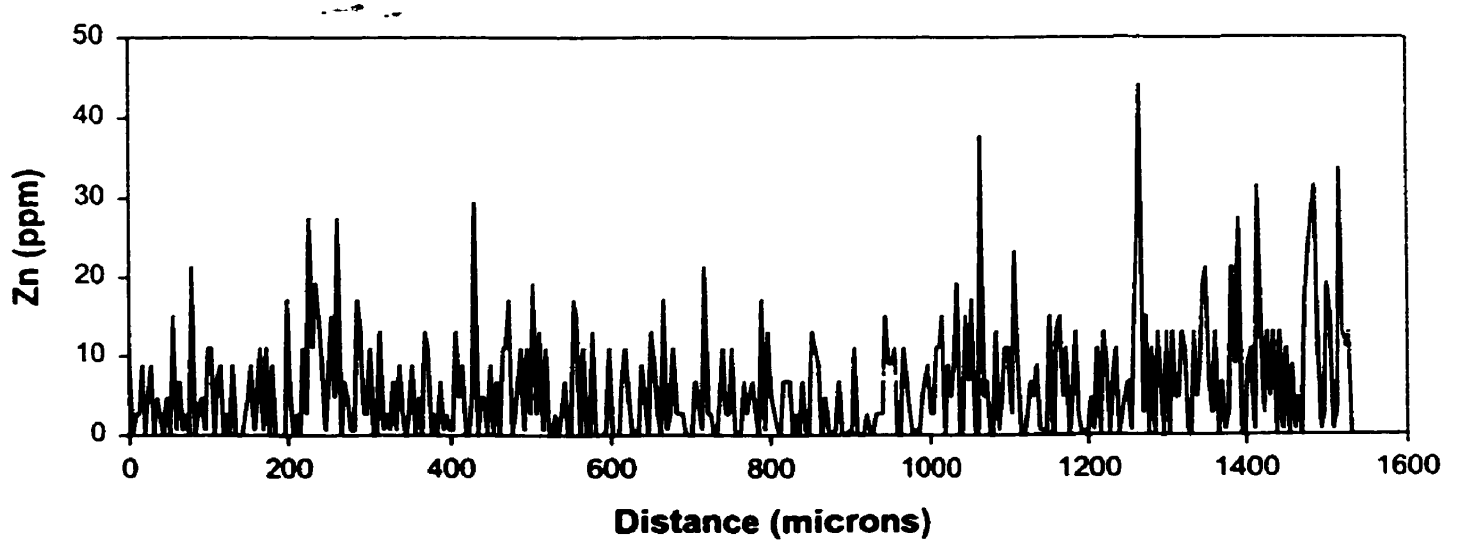

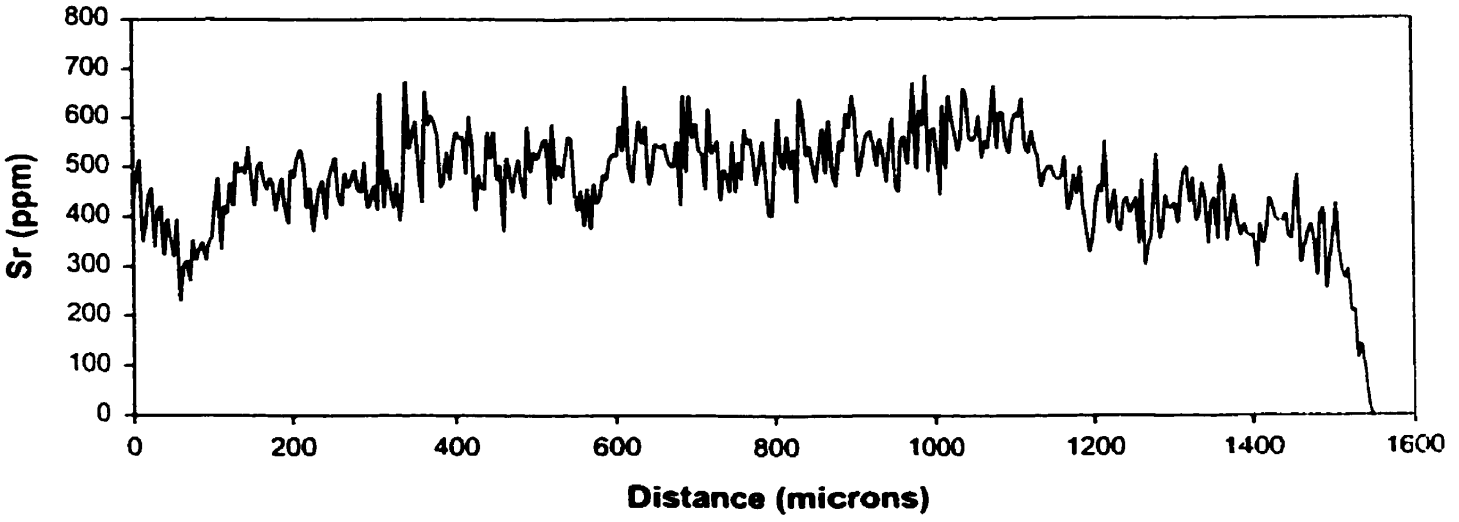

KAP-B #6 WHITE SUCKER

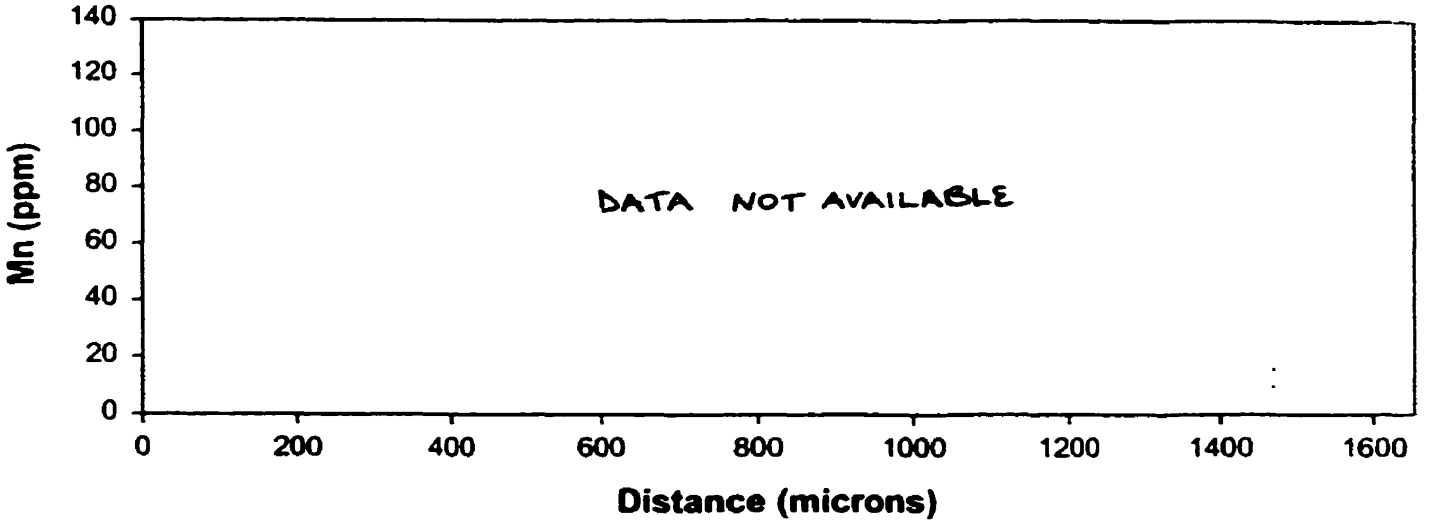

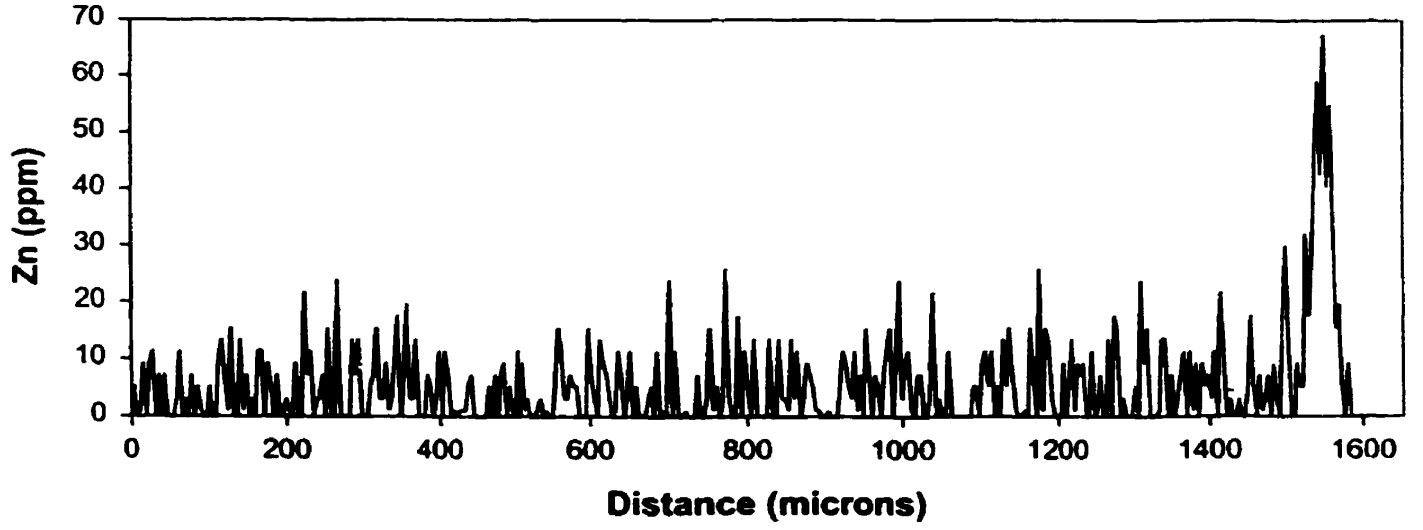

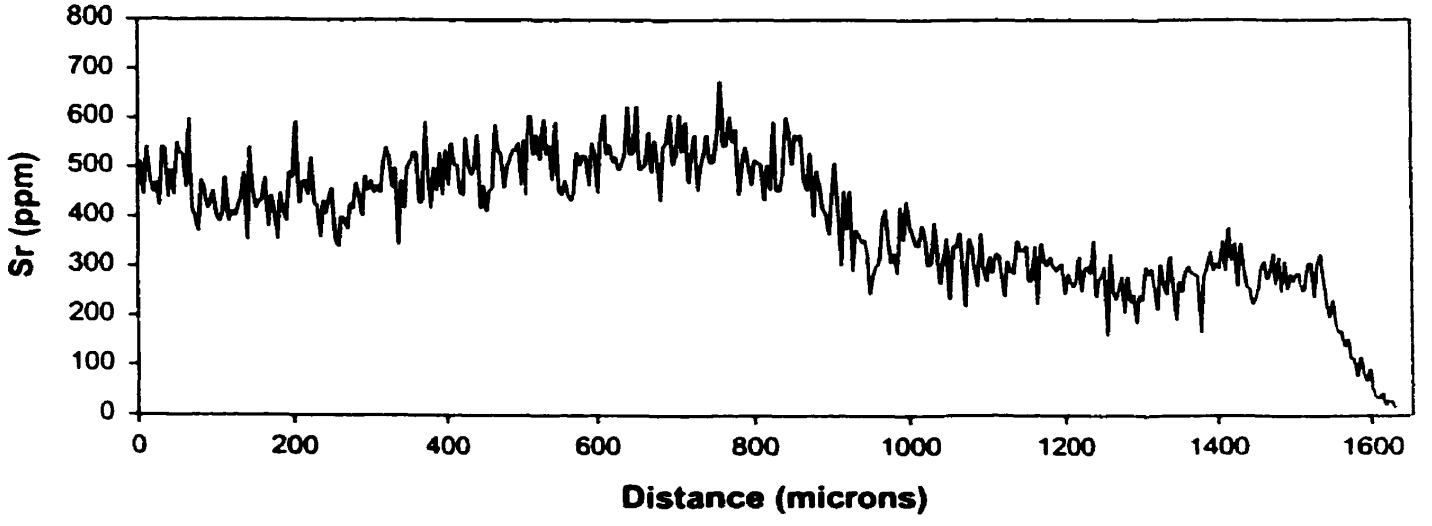

KAP-E #3 YELLOW PERCH

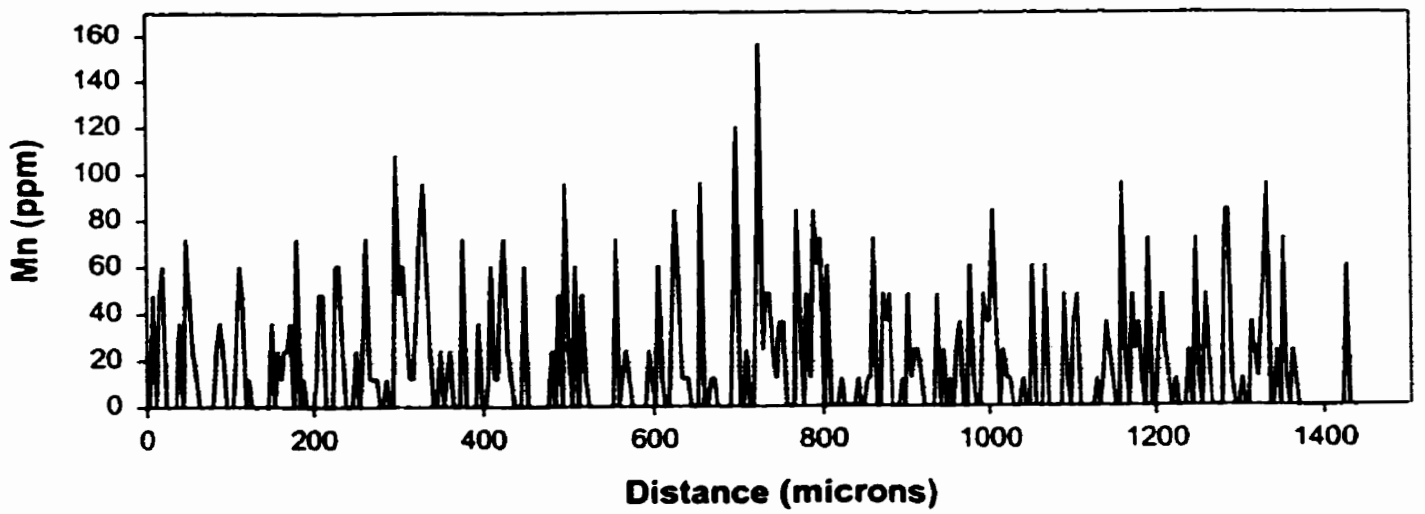

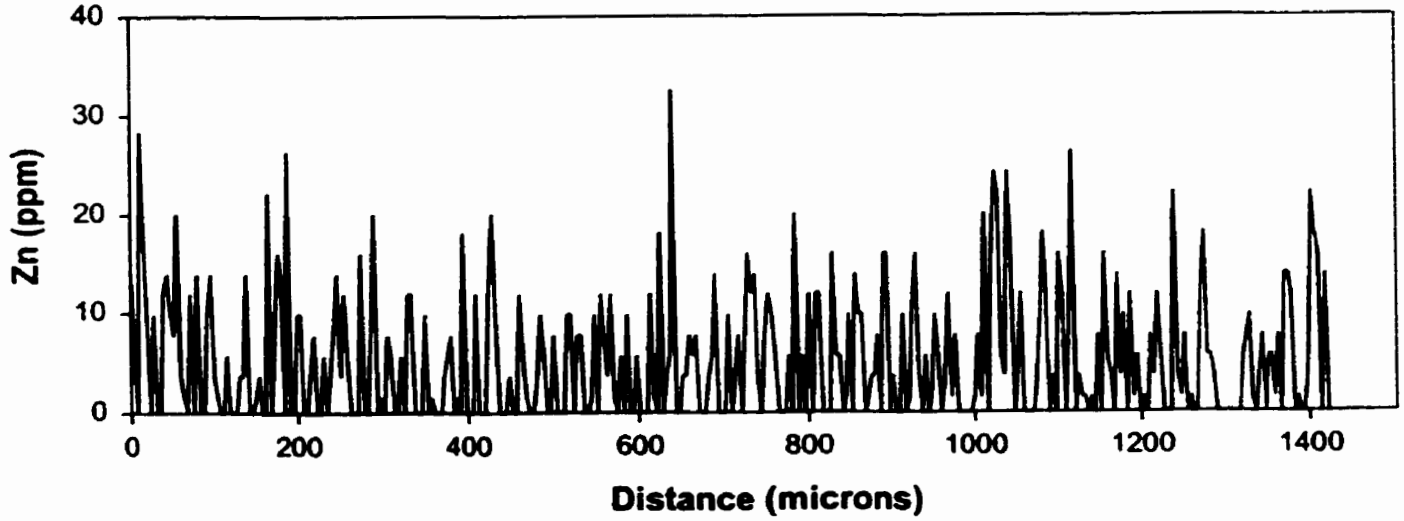

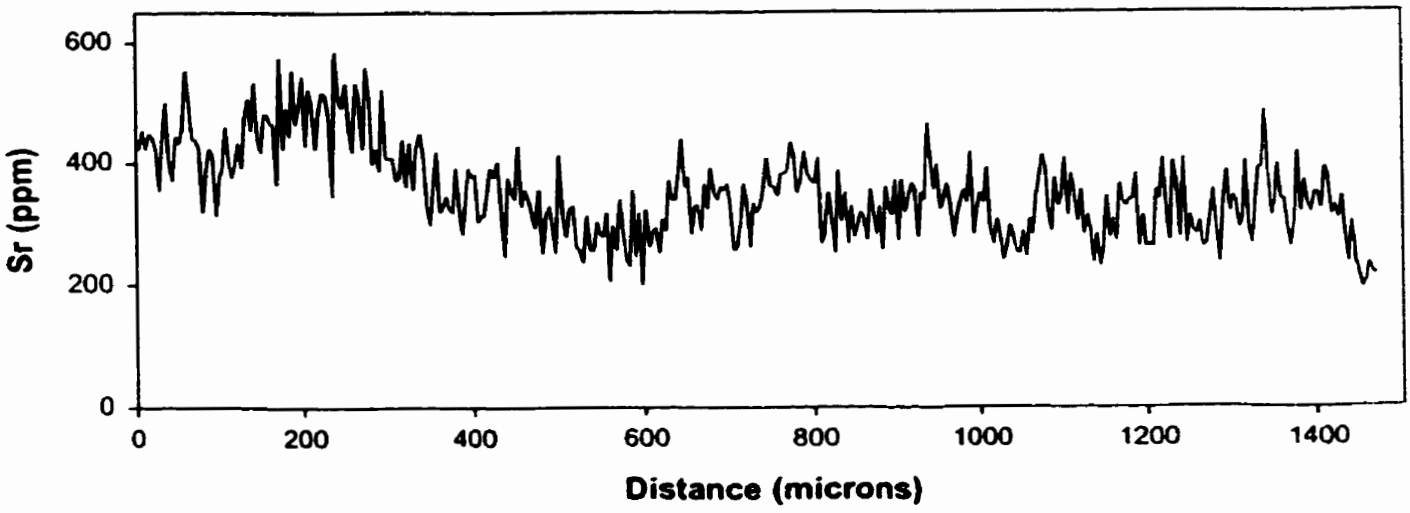

E #6 WALLEYE

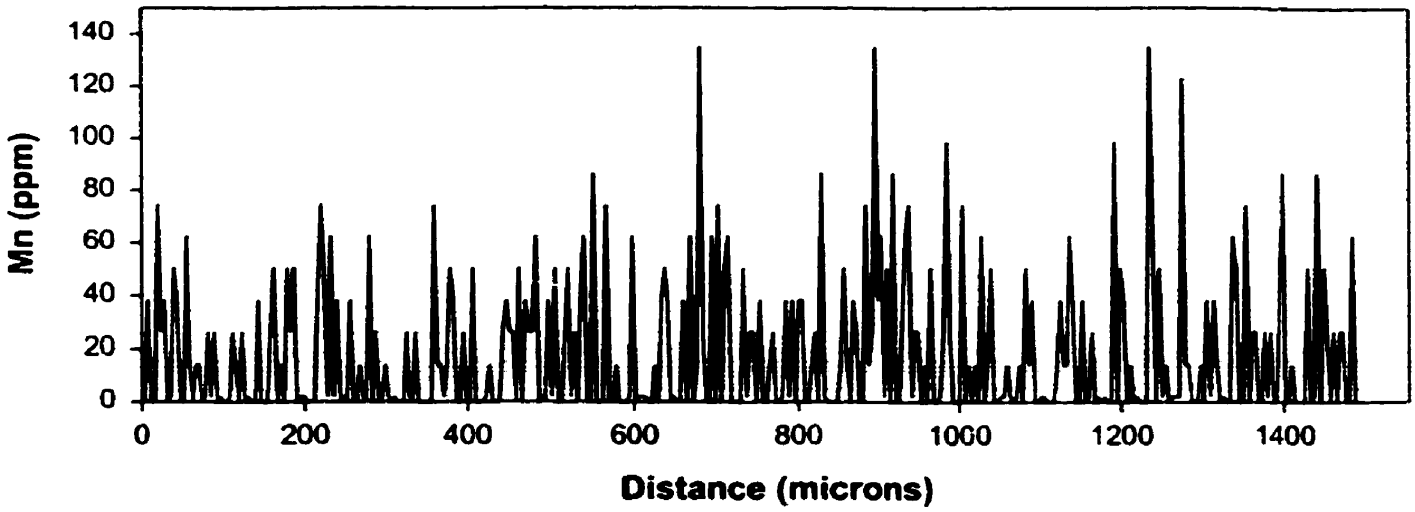
Mn (ppm)
140
120
100
80
60
40
20
0
0
200
400
600
800
1000
1200
1400
Distance (microns)

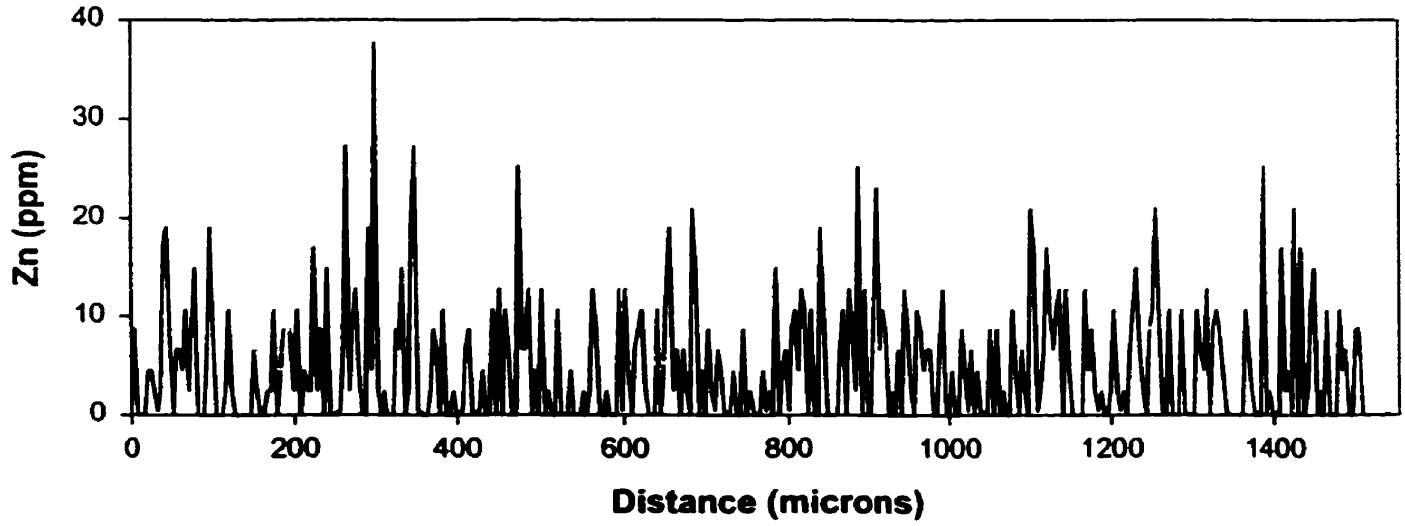
Zn (ppm)
40
30
20
10
0
0
200
400
600
800
1000
1200
1400
Distance (microns)

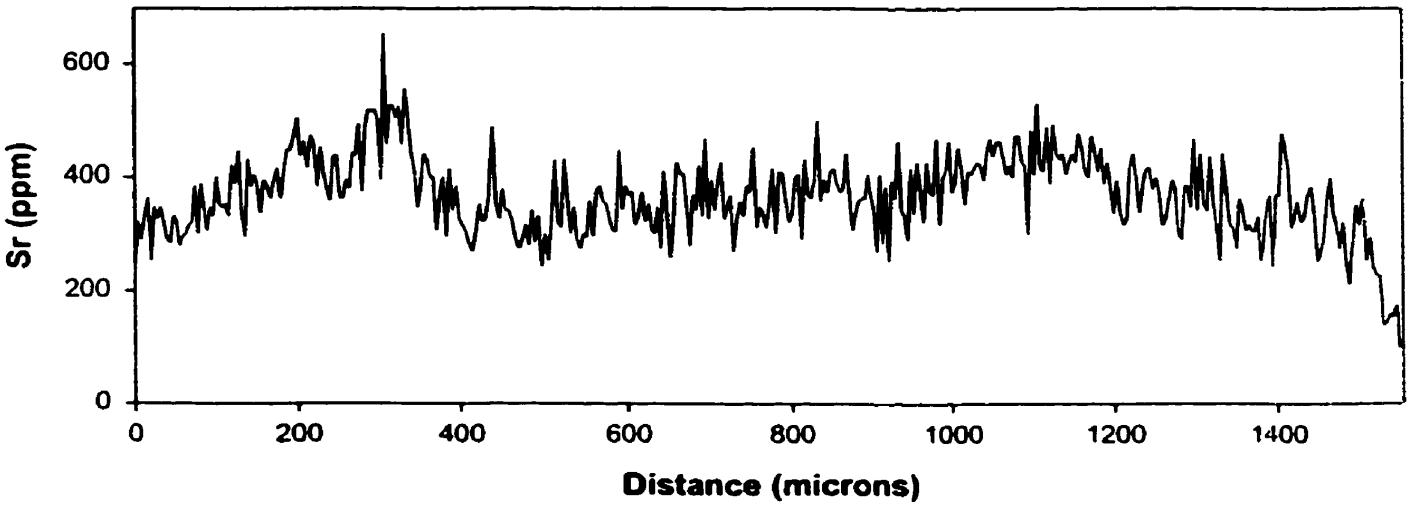
Sr (ppm)
600
400
200
0
0
200
400
600
800
1000
1200
1400
Distance (microns)

E #7 WALLEYE SCAN A

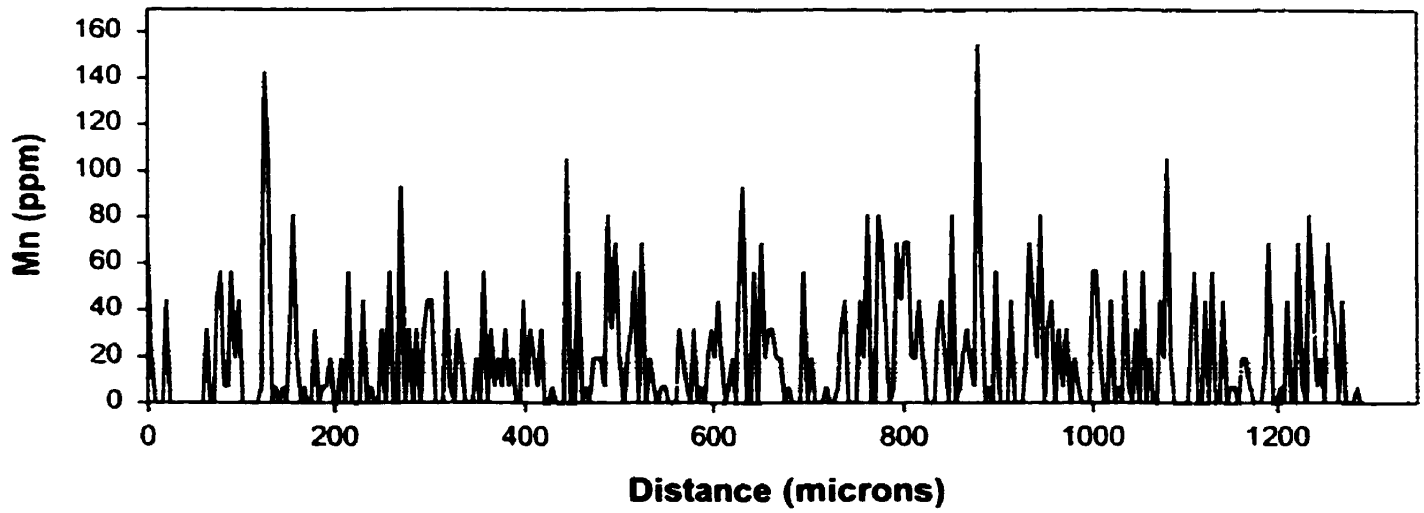

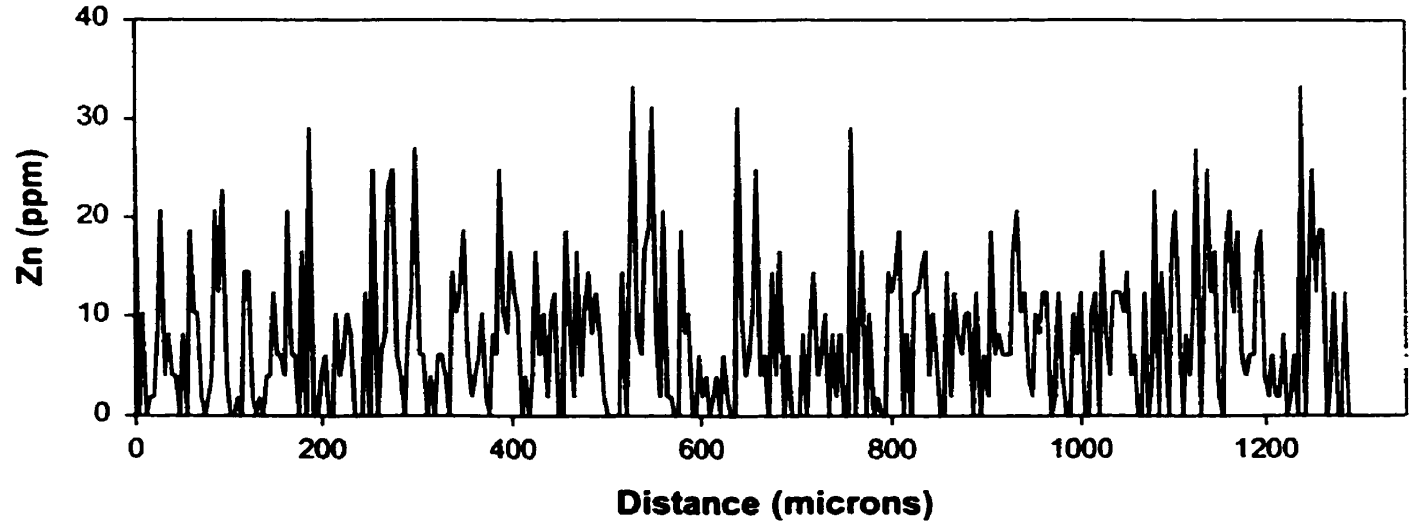

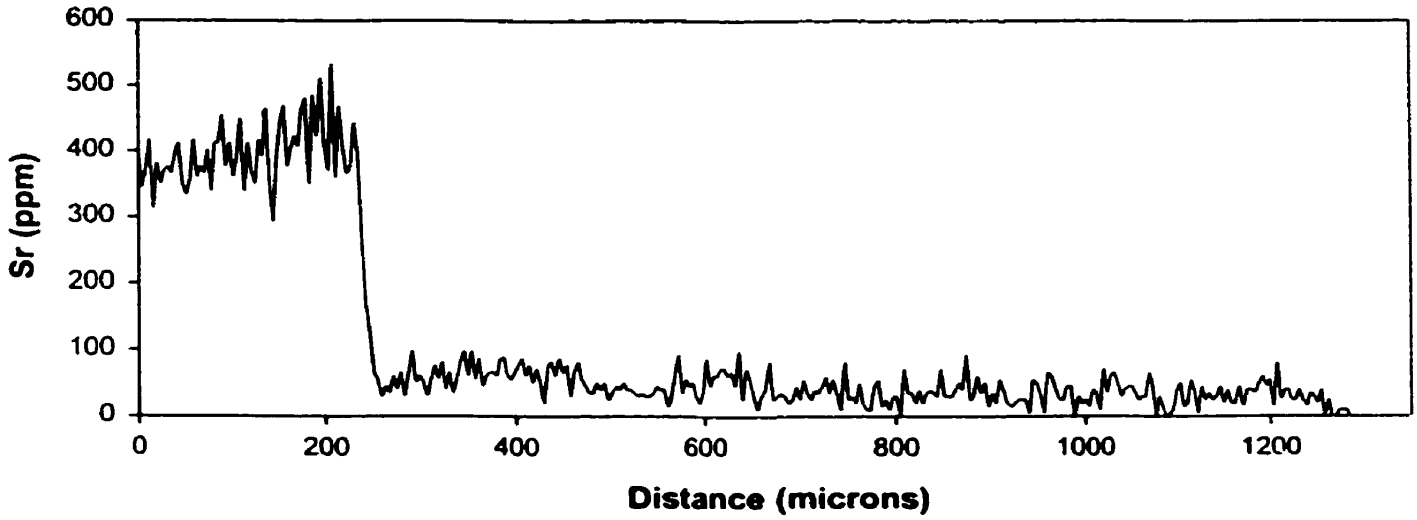

E #7 WALLEYE SCAN B

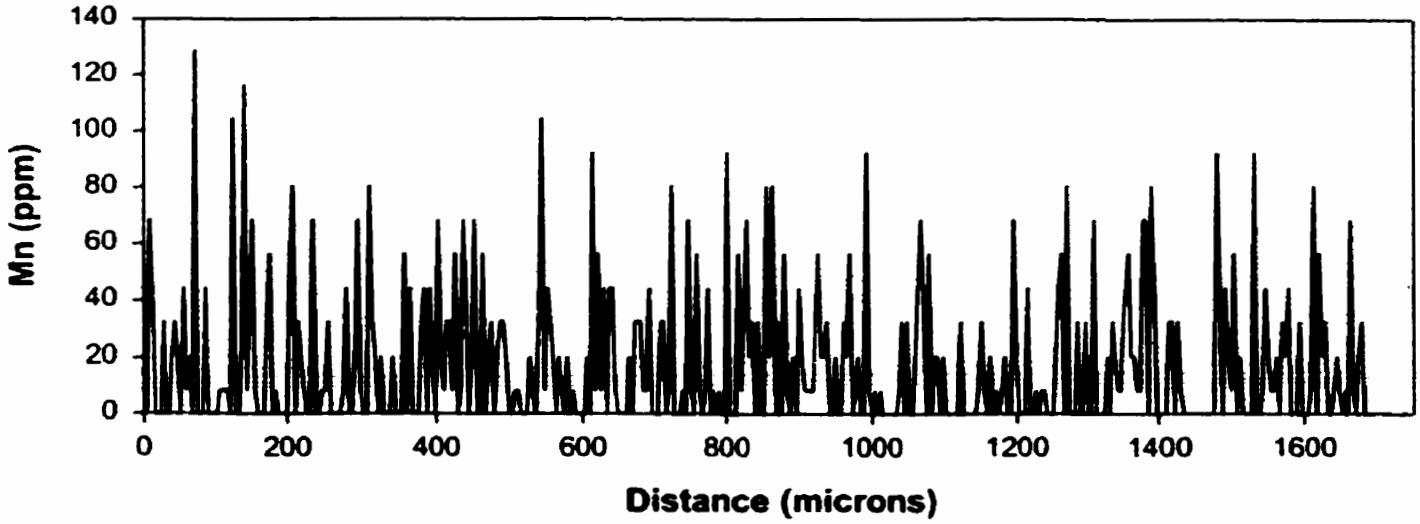

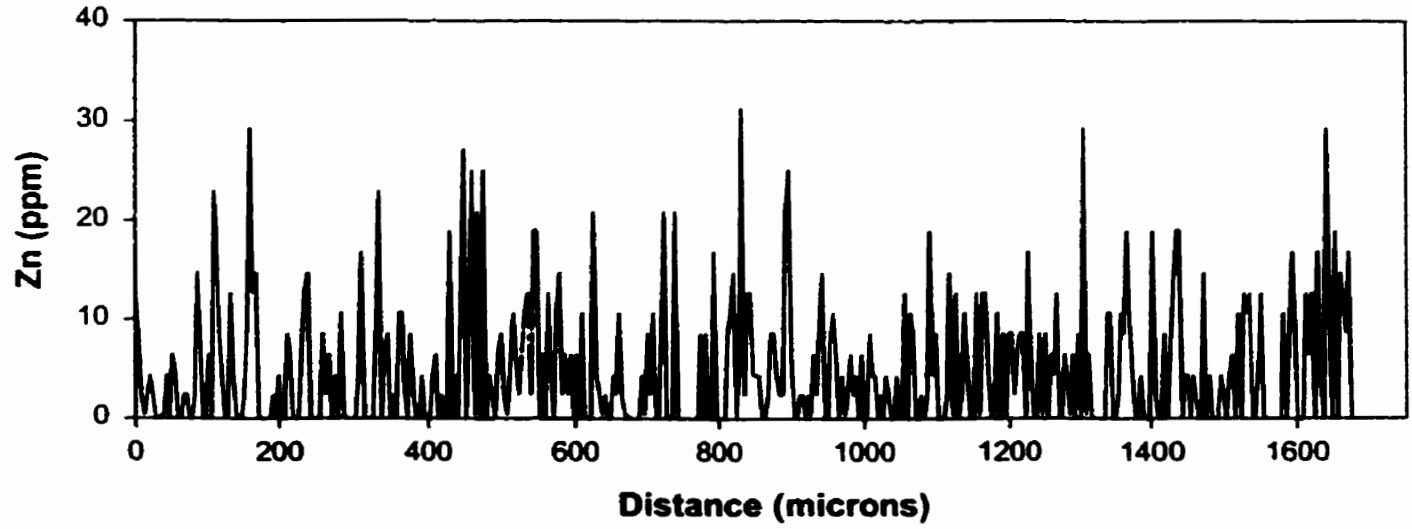

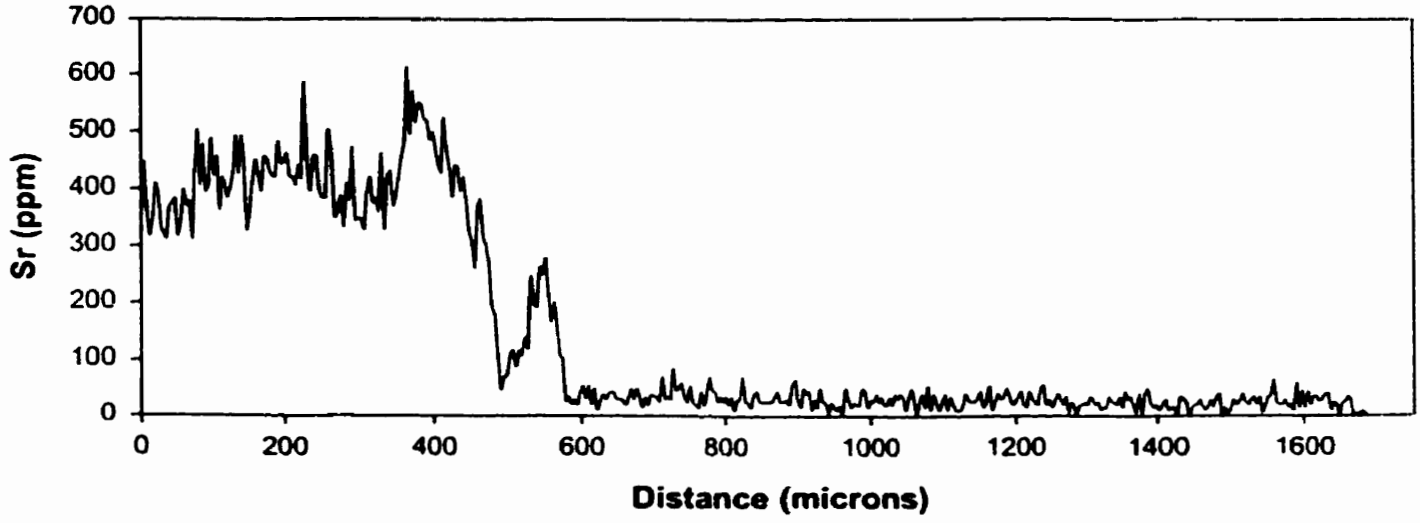

ED1-A #4 BURBOT

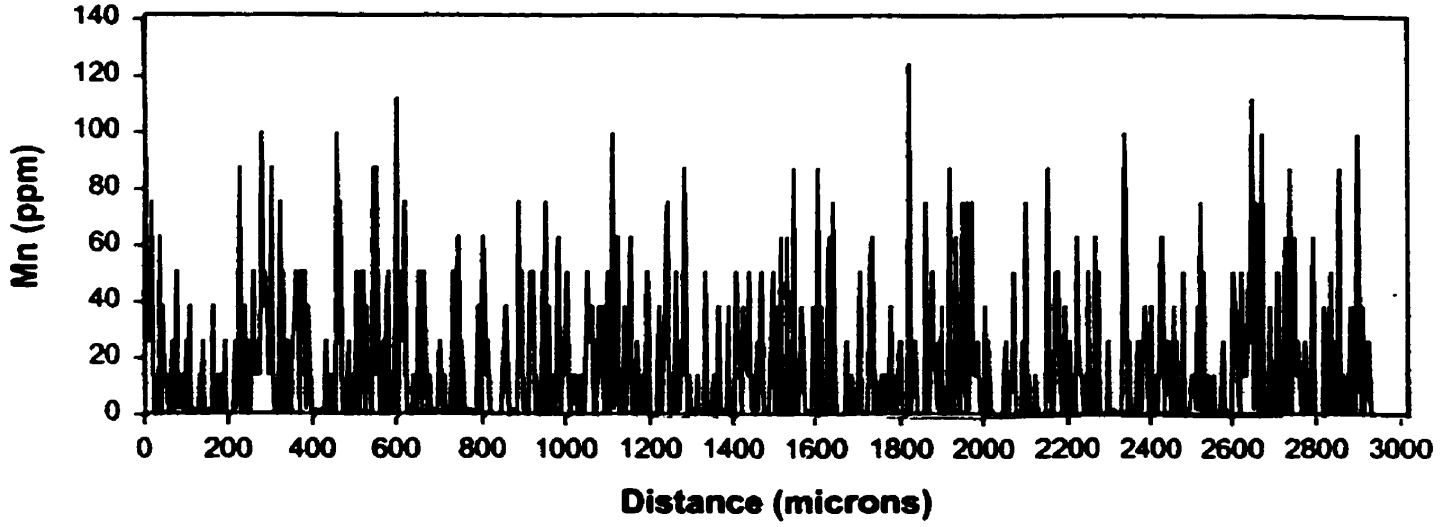

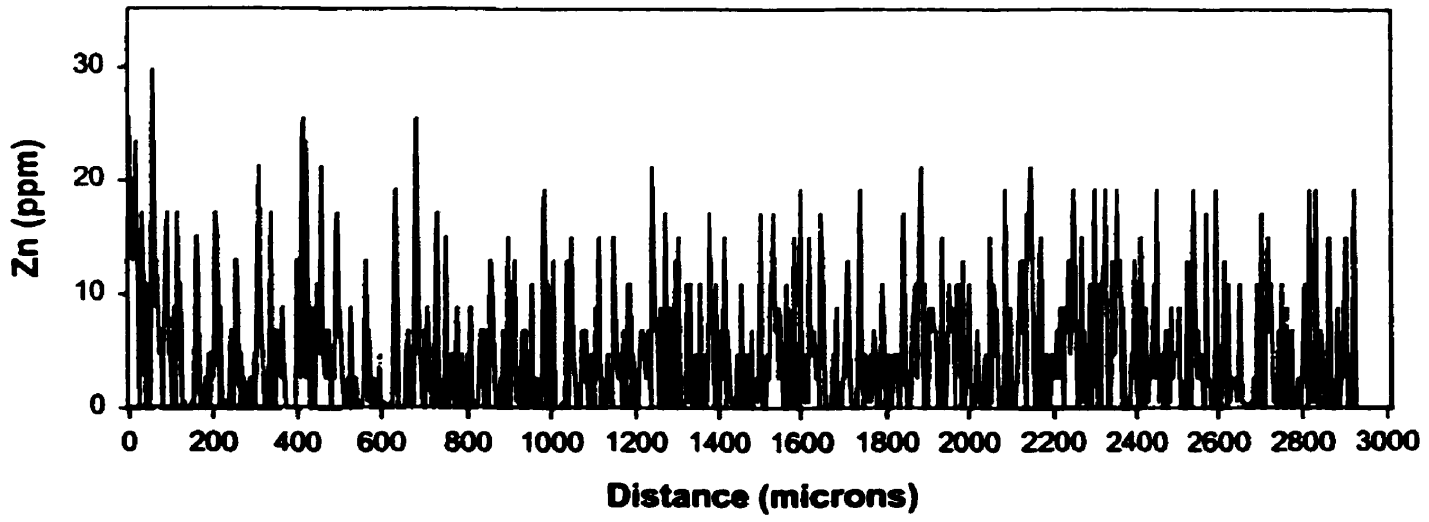

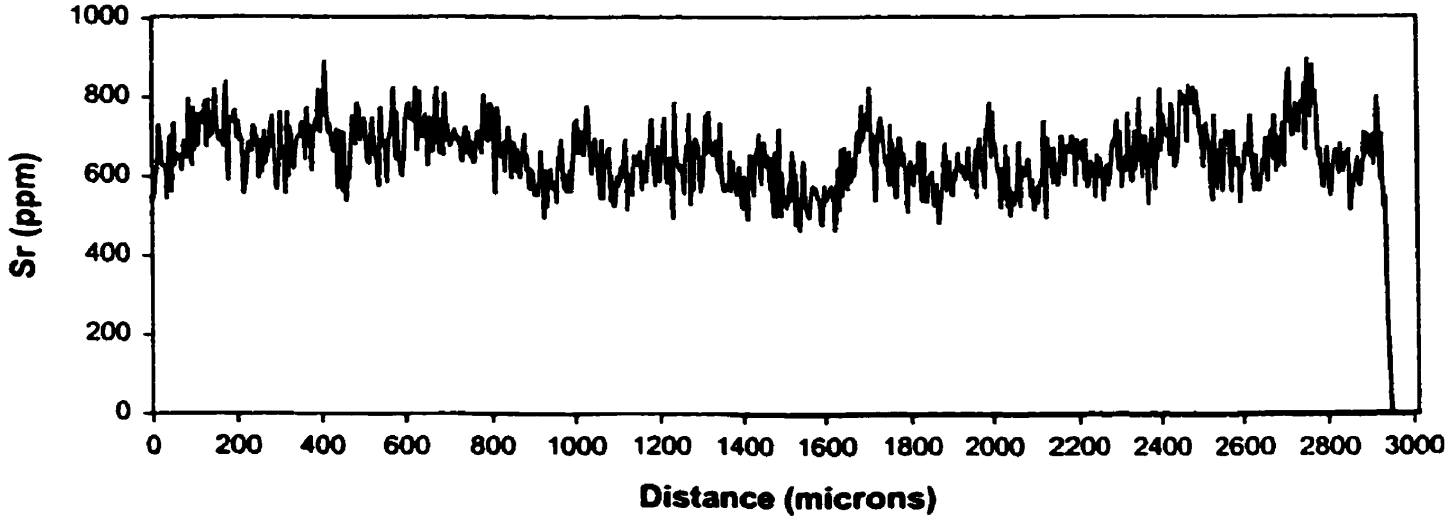

ED2-D #1 YELLOW PERCH

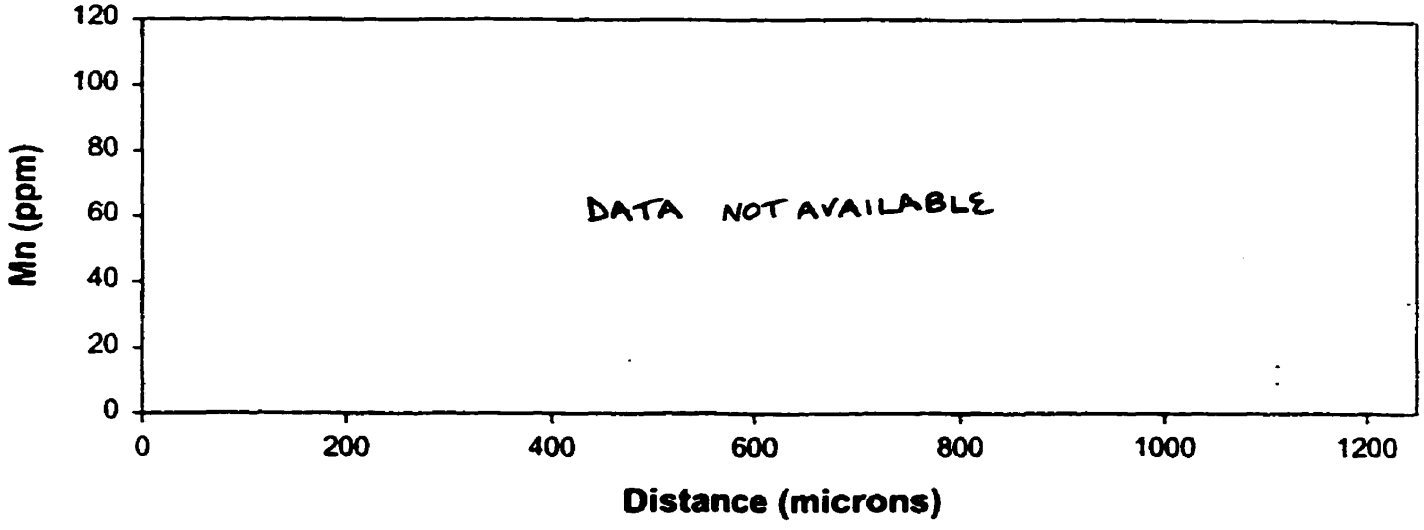

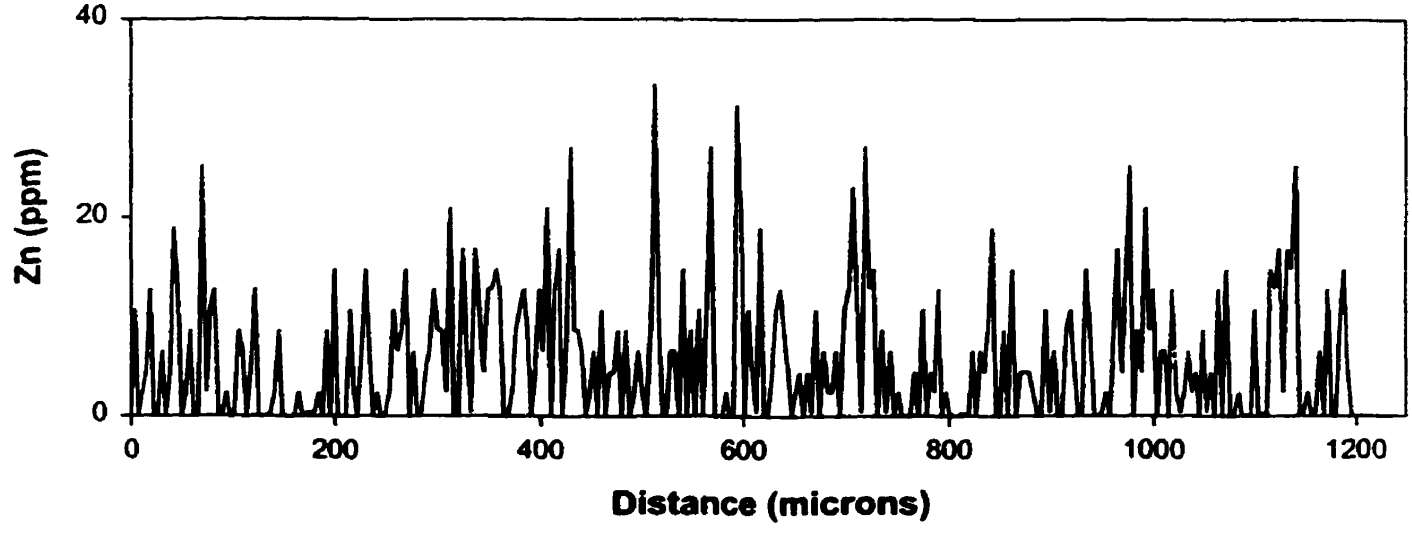

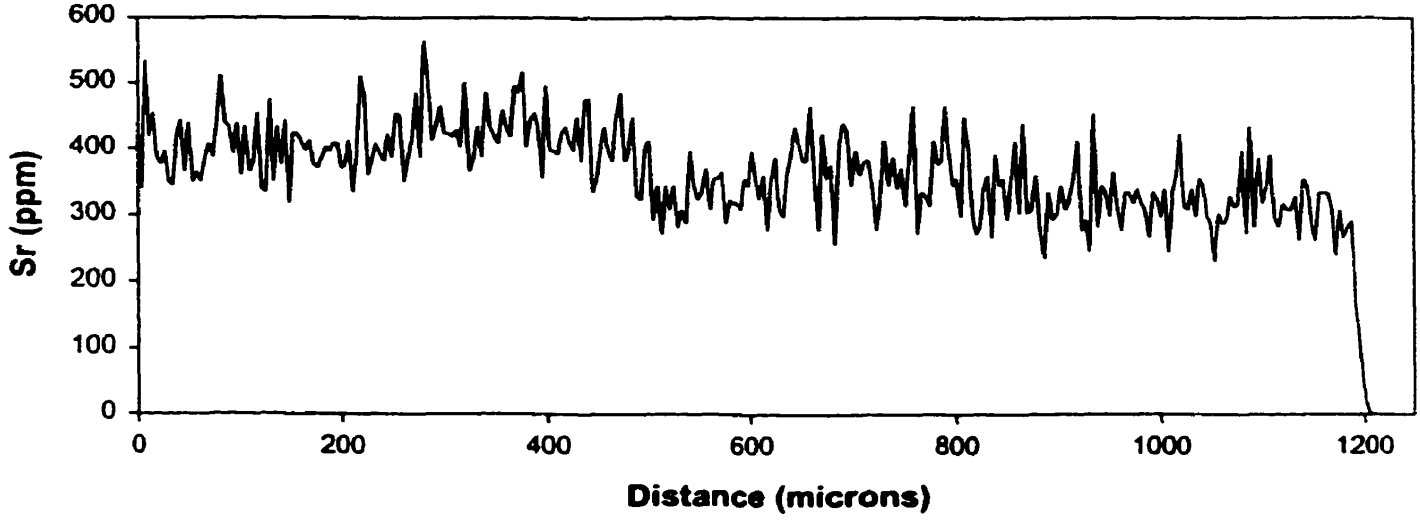

N-B #1 WALLEYE SCAN A

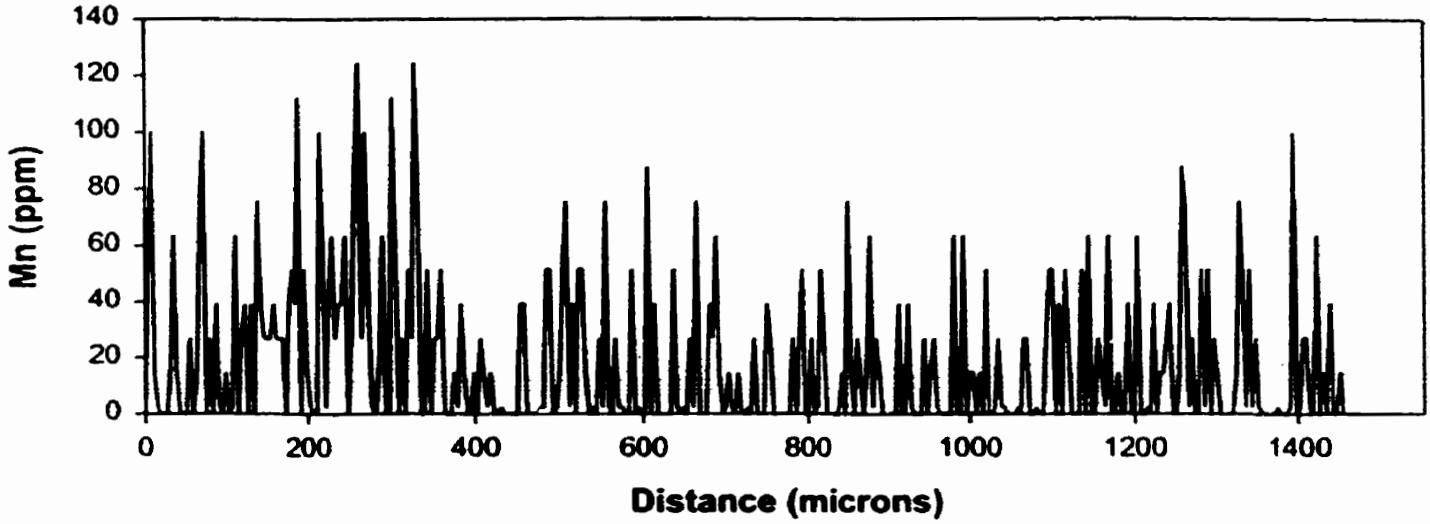

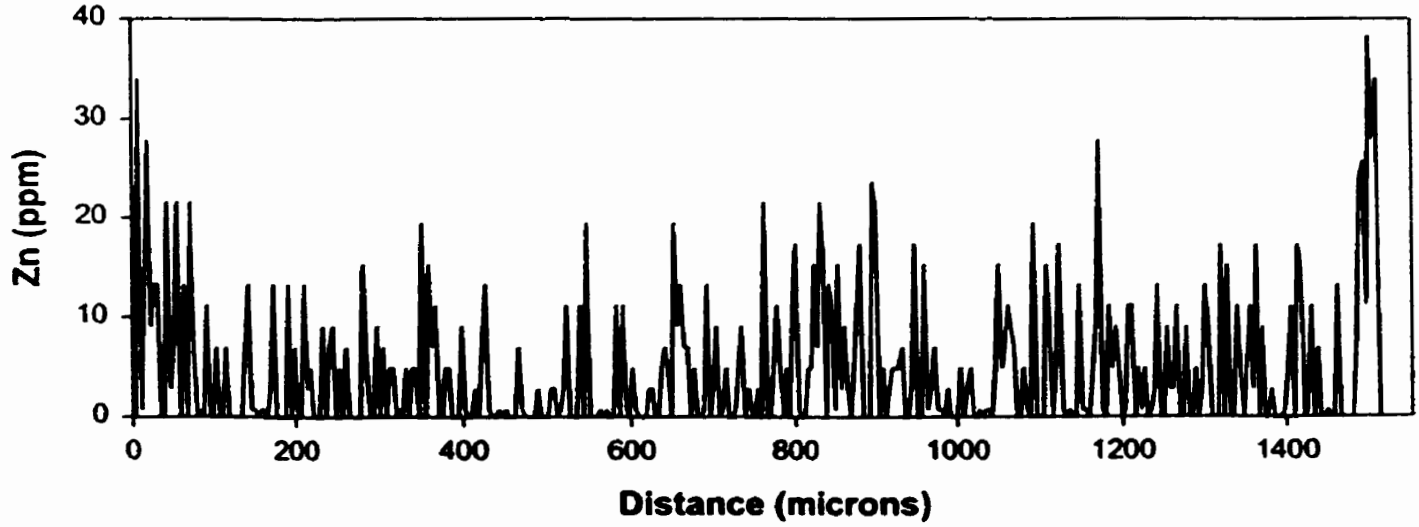

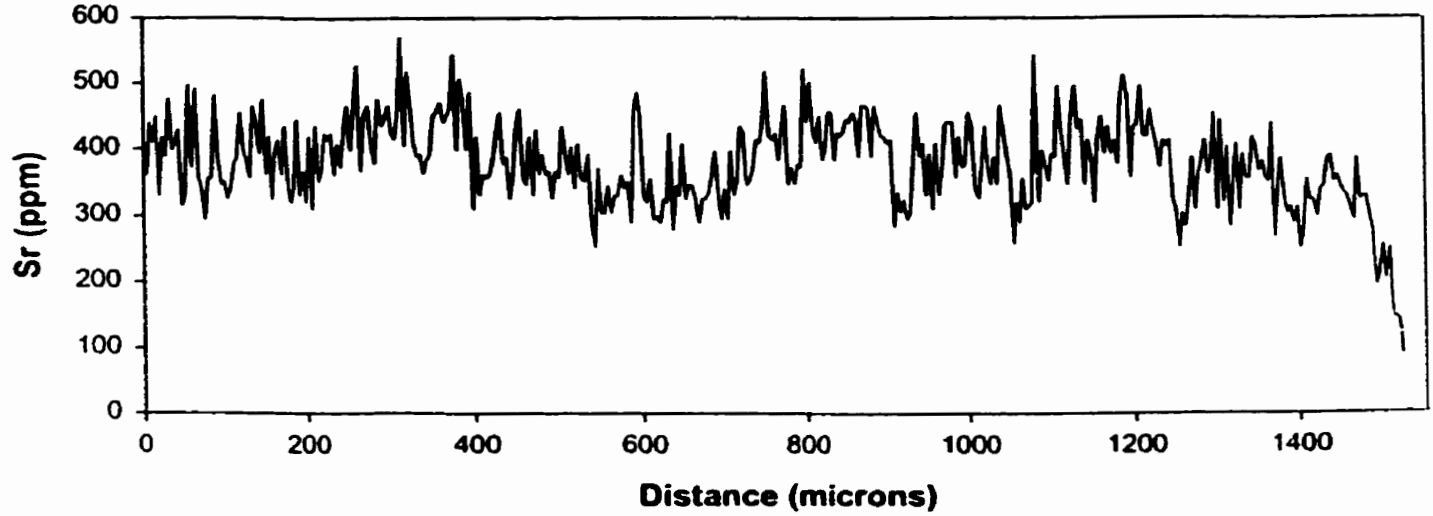

N-B #1 WALLEYE SCAN B